



City Research Online

City, University of London Institutional Repository

Citation: Hart, R. (1987). The potential use of synthetic faujasite zeolites as slow release ammonium and potassium fertilizers. (Unpublished Doctoral thesis, The City University)

This is the accepted version of the paper.

This version of the publication may differ from the final published version.

Permanent repository link: <https://openaccess.city.ac.uk/id/eprint/35658/>

Link to published version:

Copyright: City Research Online aims to make research outputs of City, University of London available to a wider audience. Copyright and Moral Rights remain with the author(s) and/or copyright holders. URLs from City Research Online may be freely distributed and linked to.

Reuse: Copies of full items can be used for personal research or study, educational, or not-for-profit purposes without prior permission or charge. Provided that the authors, title and full bibliographic details are credited, a hyperlink and/or URL is given for the original metadata page and the content is not changed in any way.

THE POTENTIAL USE OF SYNTHETIC FAUJASITE ZEOLITES AS
SLOW RELEASE AMMONIUM AND POTASSIUM FERTILIZERS.

By Richard Hart.

A Thesis Submitted for The Degree of Doctor of Philosophy.

The City University, London.

Department of Chemistry.

January 1987.



IMAGING SERVICES NORTH

Boston Spa, Wetherby

West Yorkshire, LS23 7BQ

www.bl.uk

**BEST COPY AVAILABLE.
VARIABLE PRINT QUALITY**

PAGE NUMBERING AS ORIGINAL

Dedicated to the [REDACTED] [REDACTED] [REDACTED] [REDACTED] [REDACTED].

TABLE OF CONTENTS.

TABLE OF CONTENTS.	1
LIST OF TABLES.	4
LIST OF FIGURES.	6
ACKNOWLEDGEMENTS.	10
ABSTRACT.	11
1. INTRODUCTION.	12
1.1. Plant Nutrition.	12
1.2. Elements Required in Plant Nutrition.	18
1.2.1. Nitrogen.	18
1.2.2. Potassium.	19
1.2.3. Phosphorus.	20
1.2.4. Calcium.	21
1.2.5. Magnesium.	22
1.2.6. Sulphur.	22
1.3. Soil Fertility and Fertilizers.	24
1.4. The Use of Zeolites as Soil Amendments and Fertilizers.	26
1.5. Zeolites.	35
1.6. Applications of Zeolites.	38
1.6.1. Sorption on Zeolites.	38
1.6.2. Catalysis.	39
1.6.3. Ion-exchange Applications.	40
1.7. Zeolite Structures.	44
1.7.1. Zeolite A.	44
1.7.2. Cation Sites in Zeolite A.	45
1.7.3. Zeolites X and Y.	47
1.7.4. Cation Sites in Zeolites X and Y.	49
1.8. Justification of this Work.	52

2.	THEORY OF ION-EXCHANGE.	53
2.1.	Ion-Exchange Equilibria.	53
2.1.1.	The Ion-Exchange Isotherm.	53
2.1.2.	Classification of Binary Isotherms.	57
2.1.3.	Thermodynamics of Ion-Exchange.	61
2.1.3.1.	The Gapon Mole Fraction Formulation.	64
2.1.3.2.	The Cationic Mole Fraction Approach.	72
2.1.3.3.	The Gaines and Thomas Approach.	75
2.1.3.4.	Comparison of the Thermodynamic Formulations.	77
2.1.3.5.	Thermodynamic Procedure for Partial Exchange.	81
2.1.3.6.	The Solution Phase Correction.	82
3.	EXPERIMENTAL.	85
3.1.	Chemical Reagents.	85
3.2.	Synthesis of Zeolite A.	86
3.3.	Preparation of Homoionic Zeolites.	87
3.3.1.	Sodium Zeolites.	87
3.3.2.	Potassium Zeolites.	87
3.4.	Investigation of Hydronium Exchange.	88
3.4.1.	Design of Computer Interface.	88
3.4.2.	Calibration of the pH Electrode.	91
3.4.3.	Calibration of the Ion-Selective Electrode.	92
3.4.4.	The Interface Program.	95
3.4.5.	Original Experimental Apparatus.	96
3.4.6.	Preparation of "Ultra-Pure" Water.	98
3.4.7.	Measurement of dissolved Carbon Dioxide.	99
3.4.8.	Elimination of Evaporation from the Reaction Cell.	100
3.4.8.1.	Design of the Diffusion Cell.	101
3.4.8.2.	Theory of the Diffusion Cell.	102
3.4.8.3.	Calculation of the Diffusion Cell Parameters.	108
3.4.9.	Re-design of Experimental Apparatus.	109
3.4.10.	Calculation of Hydronium Exchange.	110
3.5.	Measurement of Ion-Exchange Isotherms.	113
3.6.	Analysis of Zeolites.	115
3.6.1.	Water Analysis.	115
3.6.2.	Silicon Analysis.	115
3.6.3.	Aluminium Analysis.	117
3.6.4.	Cation Analysis.	119

3.6.4.1.	Analysis for Sodium and Potassium.	119
3.6.4.2.	Analysis for Calcium.	119
3.6.4.3.	Analysis for Ammonium.	119
3.7.	Thermodynamic Treatment of Equilibrium Ion-Exchange Data.	121
3.7.1.	Thermodynamic Reversibility.	121
3.7.2.	The Solution Phase Correction.	121
3.7.3.	Calculation of the Equilibrium Constant for Exchange.	125
3.7.4.	Calculation of the Standard Free Energy of Exchange.	128
4.	RESULTS AND DISCUSSION.	130
4.1.	Analysis of Zeolites.	130
4.2.	Hydronium Exchange in Zeolites.	137
4.3.	Ion-Exchange Equilibria.	182
4.3.1.	Sodium-Potassium Exchange in Zeolite Y.	182
4.3.2.	Sodium-Potassium Exchange in Zeolite X.	191
4.3.3.	Sodium-Ammonium and Potassium-Ammonium Exchange in Zeolite Y.	193
4.3.4.	Potassium-Calcium Exchange in Zeolite Y (Grace).	198
4.3.5.	Sodium-Hydronium and Potassium-Hydronium Exchange in Zeolite Y (Grace).	199
4.3.6.	Sodium-Aluminium Exchange in Zeolite Y (Grace).	202
4.4.	^{27}Al and ^{29}Si MASNMR Studies of Hydronium Exchange in Zeolite Y.	245
5.	CONCLUSION.	258
6.	REFERENCES.	262
	APPENDIX 1.	
	Equilibrium Ion-Exchange Data.	271
	APPENDIX 2.	
	Computer Programs.	298

LIST OF TABLES.

1.1.	Essential Elements Found in Higher Plants.	14
1.2.	Composition of Knop's Solution.	15
1.3.	Composition of Von der Crone's Solution.	16
1.4.	Composition of Hoagland's Solution.	17
3.1.	Addition of Standard Solutions in the Calibration Procedure.	93
3.2.	Values of the Constants a and b in the Extended Debye-Huckel Equation.	124
4.1.	Compositions (wt%) of Zeolite A Samples.	133
4.2.	Compositions (wt%) of Zeolite X Samples.	133
4.3.	Compositions (wt%) of Zeolite Y Samples.	134
4.4.	Oxide Compositions of Zeolite Samples.	135
4.5.	Unit Cell Compositions of Zeolite Samples.	136
4.6.	NaA (Charnell) Contacted with Distilled Water for three hours. Under Nitrogen.	154
4.7.	NaA (Charnell) Contacted with Distilled Water for three hours. In Air.	155
4.8.	Zeolites NaA and NaX (4 g dm^{-3}) Contacted With Distilled Water for three hours. Under Nitrogen.	156
4.9.	Zeolites NaA and NaX (4 g dm^{-3}) Contacted With Distilled Water for three hours. In Air.	157
4.10.	Zeolites CaA and CaX (4 g dm^{-3}) Contacted With Distilled Water for three hours. Under Nitrogen	158
4.11.	Zeolites CaA and CaX (4 g dm^{-3}) Contacted With Distilled Water for three hours. In Air.	159
4.12.	Zeolites NaA, NaX and NaY (4 g dm^{-3}) contacted with Distilled Water. Under Nitrogen.	160
4.13.	Zeolite NaY (Grace) Contacted With Distilled Water for 15 minutes. Under Nitrogen.	161

4.14.	Zeolite NaY (Grace) - 4 g dm ⁻³ , Contacted with Sodium Nitrate Solutions for 15 minutes. Under Nitrogen.	162
4.15.	Zeolite NaY (Grace) - 4 g dm ⁻³ , 4 contacts with Distilled Water for 15 minutes.	163
4.16.	Zeolite NaY (Grace) - 4 g dm ⁻³ , 5 contacts with Distilled Water for 15 minutes.	164
4.17.	Zeolite NaY (Grace) - 4 g dm ⁻³ , 11 contacts with Distilled Water for 15 minutes.	165
4.18.	Hydrolysis Data for Na-K Exchange in Zeolite (Grace) at pH 2 and pH 2.3.	188
4.19.	Hydrolysis Data for Na-K Exchange in Zeolite Y (Laporte) at pH 2.3.	192
4.20.	Hydrolysis Data for Na-H and K-H Exchange in Zeolite Y(Grace) at pH 2 and pH 2.3.	201
4.21.	²⁷ Al and ²⁹ Si MASNMR Data for Acid-Treated NaK Zeolite Y (Grace).	252
4.22.	Chemical and ²⁷ Al MASNMR Data for Acid-Treated NaK Zeolite Y (Grace).	253
4.23.	Chemical Analyses of Zeolite Y (Grace) ²⁹ Si MASNMR Samples.	254
4.24.	²⁹ Si MASNMR Data for Acid-Treated Na-K Zeolite Y (Grace).	255

LIST OF FIGURES.

1.1.	Nitrogen Recovered in Seriatim Cuttings of Sudangrass Grown in Cisne Loam Treated with either $(\text{NH}_4)_2\text{SO}_4$ or NH_4 -Saturated Clinoptilolite.	30
1.2.	Secondary Building Units.	37
1.3.	The Structure of Zeolite A.	46
1.4.	The Structure of Zeolites X and Y.	51
2.1.	Binary Ion-Exchange Isotherm Showing Graphical Determination of Selectivity Coefficient α .	56
2.2.	Classification of Binary Ion-Exchange Isotherms.	60
3.1.	Circuit Diagram of Computer Interface.	90a
3.2.	Original Experimental Apparatus.	97
3.3.	Design of the Diffusion Cell.	102
4.1.	8 g dm^{-3} NaA (Charnell). Under Nitrogen.	166
4.2.	8 g dm^{-3} NaA (Charnell). In Air.	166
4.3.	4 g dm^{-3} NaA (Charnell). Under Nitrogen.	167
4.4.	4 g dm^{-3} NaA (Charnell). In Air.	167
4.5.	1 g dm^{-3} NaA (Charnell). Under Nitrogen.	168
4.6.	1 g dm^{-3} NaA (Charnell). In Air.	168
4.7.	0.2 g dm^{-3} NaA (Charnell). Under Nitrogen.	169
4.8.	0.2 g dm^{-3} NaA (Charnell). In Air.	169
4.9.	NaA (Charnell). Under Nitrogen.	170
4.10.	NaA (Charnell). Under Nitrogen.	170
4.11.	NaA (Charnell). In Air.	171
4.12.	NaA (Charnell). In Air.	171
4.13.	4 g dm^{-3} NaA (Laporte). Under Nitrogen.	172
4.14.	4 g dm^{-3} NaA (Laporte). In Air.	172
4.15.	4 g dm^{-3} NaX (BDH). Under Nitrogen.	173
4.16.	4 g dm^{-3} NaX (BDH). In Air.	173

4.17.	4 g dm ⁻³ CaA (Laporte). Under Nitrogen.	174
4.18.	4 g dm ⁻³ CaA (Laporte). In Air.	174
4.19.	4 g dm ⁻³ CaX (Laporte). Under Nitrogen.	175
4.20.	4 g dm ⁻³ CaA (Laporte). In Air.	175
4.21.	4 g dm ⁻³ CaA (Laporte). Under Nitrogen.	176
4.22.	4 g dm ⁻³ CaA (Laporte). In Air.	176
4.23.	4 g dm ⁻³ NaA (Charnell). Under Nitrogen.	177
4.24.	4 g dm ⁻³ NaA (Laporte). Under Nitrogen.	177
4.25.	4 g dm ⁻³ NaX (Laporte). Under Nitrogen.	178
4.26.	4 g dm ⁻³ NaX (BDH). Under Nitrogen.	178
4.27.	4 g dm ⁻³ NaY (Unilever-2.70). Under Nitrogen.	179
4.28.	4 g dm ⁻³ NaY (Unilever-2.75). Under Nitrogen.	179
4.29.	4 g dm ⁻³ NaY (Grace). Under Nitrogen.	180
4.30.	4 g dm ⁻³ NaY (Grace). Under Nitrogen.	180
4.31.	4 g dm ⁻³ NaY (Grace). Under Nitrogen.	181

Na-K Exchange in Y (Laporte).
1 week Exchange, Normal Initial pH.

4.32.	Isotherm.	204
4.33.	Selectivity Plot.	205
4.34.	Corrected Selectivity Plot.	206
4.35.	Zeolite Phase Activity Coefficients.	206

Na-K Exchange in Y (Grace).
1 week Exchange, Normal Initial pH.

4.36.	Isotherm.	207
4.37.	Selectivity Plot.	208
4.38.	Corrected Selectivity Plot.	209
4.39.	Zeolite Phase Activity Coefficients.	209

Na-K Exchange in Y (Grace).
24 Hour Exchange, Normal Initial pH.

4.40.	Isotherm.	210
4.41.	Selectivity Plot.	211
4.42.	Corrected Selectivity Plot.	212
4.43.	Zeolite Phase Activity Coefficients.	212

Na-K Exchange in Y (Grace).	
24 Hour Exchange, Initial pH 4.	
4.44. Isotherm.	213
4.45. Selectivity Plot.	214
4.46. Corrected Selectivity Plot.	215
4.47. Zeolite Phase Activity Coefficients.	215
Na-K Exchange in Y (Grace).	
24 Hour Exchange, Initial pH 3.	
4.48. Isotherm.	216
4.49. Selectivity Plot.	217
4.50. Corrected Selectivity Plot.	218
4.51. Zeolite Phase Activity Coefficients.	218
Na-K Exchange in Y (Grace).	
24 Hour Exchange, Initial pH 2.3.	
4.52. Isotherm.	219
4.53. Selectivity Plot.	220
Na-K Exchange in Y (Grace).	
24 Hour Exchange, Initial pH 2.	
4.54. Isotherm.	221
4.55. Selectivity Plot.	222
Na-K Exchange in Y (Grace) at 2°C.	
4.56. Isotherm.	223
4.57. Selectivity Plot.	224
4.58. Corrected Selectivity Plot.	225
4.59. Zeolite Phase Activity Coefficients.	225
Na-K Exchange in X (Laporte)	
24 Hour Exchange, Normal Initial pH.	
4.60. Isotherm.	226
4.61. Selectivity Plot.	227
4.62. Corrected Selectivity Plot.	228
4.63. Zeolite Phase Activity Coefficients.	228
Na-K Exchange in X (Laporte)	
24 Hour Exchange, Initial pH 2.3.	
4.64. Isotherm.	229
4.65. Selectivity Plot.	230
Na-NH ₄ Exchange in Y (Grace).	
4.66. Isotherm.	231
4.67. Selectivity plot.	232
4.68. Corrected Selectivity Plot.	233
4.69. Zeolite Phase Activity Coefficients.	233

K-NH ₄ Exchange in Y (Grace).	
4.70.	Isotherm. 234
4.71.	Selectivity plot. 235
4.72.	Corrected Selectivity Plot. 236
4.73.	Zeolite Phase Activity Coefficients. 236
K-Ca Exchange in Y (Grace).	
4.74.	Isotherm. 237
4.75.	Selectivity plot. 238
4.76.	Corrected Selectivity Plot. 239
4.77.	Zeolite Phase Activity Coefficients. 239
Na-H Exchange in Y (Grace).	
15 Minute Exchange.	
4.78.	Isotherm. 240
4.79.	Selectivity Plot. 240
K-H Exchange in Y (Grace).	
15 Minute Exchange.	
4.80.	Isotherm. 241
4.81.	Selectivity Plot. 241
Na-Al Exchange in Y (Grace).	
4.82.	Isotherm. 242
4.83.	Selectivity Plot. 243
4.84.	Distribution of Aluminium Species in Solution With pH. 244
4.85.	²⁷ Al and ²⁹ Si MASNMR Spectra of Acid-Treated Zeolite Y (Grace) Samples. 256
4.86.	Variation in the (Si/Al) Ratio of Acid-Treated Zeolite Y (Grace) Samples With Final Solution pH. 256a
4.87.	²⁹ Si MASNMR Spectra of NaKH-Y and NaH-Y Samples. Zeolite Y (Grace). 257

ACKNOWLEDGEMENTS.

I would like to express my thanks to my original supervisor, Dr. R. P. Townsend for his help and guidance throughout the course of this study. Thanks are also due to Mr B. O. Field who provided supervision and support at City University during the final year of the work.

I would also like to thank the members of the Chemistry Department, both past and present, for the technical assistance received, and for their friendship during my period of study at The City University.

Finally, I would like to take this opportunity to thank my family: ■■■■■ ■■■■■ ■■■■■ ■■■■■, for their love and support throughout my University education, and ■ ■■■■■ ■■■■■ ■■■■■, for his companionship and encouragement over the years.

ABSTRACT.

The suitability of the synthetic faujasite zeolites X and Y as slow release ammonium and potassium fertilizers has been researched by examining their ion-exchange properties.

The resistance of the zeolites to hydrolysis in water with a neutral or only mildly acidic pH has been investigated. The change in pH and cation concentration of solutions into which zeolite was added, was monitored using pH and ion-selective electrodes. The role of atmospheric carbon dioxide in determining the final solution pH and the level of hydronium exchange was examined by conducting experiments both in air and under a nitrogen blanket. The design and construction of a computer interface, which enabled the rapid and accurate measurement of pH and cation concentrations in solution, and a diffusion cell, which allowed the solution to be blanketed by a flowing stream of nitrogen whilst preventing the mass transfer of water into or out of the reaction cell, is described. A discrepancy between the total number of equivalents of cation released from the zeolite and the number of equivalents of hydronium ion exchanged has been observed and is discussed.

Ion-exchange reactions between the fertilizer elements and ions likely to be present in the soil solution have been investigated. Sodium - potassium ion-exchange isotherms in zeolites X and Y were measured using different background pH's of between 5.5 and 2. Levels of hydronium exchange and hydrolysis of the zeolites under these conditions were measured and the results are presented and discussed. Ion-exchange isotherms for the systems ammonium - sodium, potassium - ammonium and potassium - calcium in zeolite Y were also measured and the isotherms, and the thermodynamic interpretation of the results, are presented here.

Hydronium ion-exchange and hydrolysis in zeolite Y was investigated further by the measurement of sodium - hydronium, potassium - hydronium and sodium - aluminium isotherms. The selectivity of zeolite Y for hydronium ions was found to be extremely high at lower exchange levels and these results help to explain the relatively high levels of hydronium exchange found when zeolite Y is contacted with water with a neutral or only mildly acidic pH. It is suggested that evidence of the initial dealumination of the faujasite lattice by acid solutions is masked by exchange of cationic aluminium species into exchange sites in the zeolite. Aluminium is only released into solution when the pH falls below a certain critical value, or when the total number of hydronium and aluminium ions in the zeolite exceeds the exchange capacity in the large pore sites.

²⁷Al and ²⁹Si MASNMR studies of partially hydrolysed zeolite Y samples, carried out in conjunction with Unilever Research and the Karl Marx University in Leipzig, are used to support this hypothesis.

"I hereby grant to the University Librarian
the authority to allow this thesis to be
copied in whole or in part, at his discretion,
without further reference to the author."

Richard Hart. January, 1987.

1. INTRODUCTION.

1.1. Plant Nutrition.

The uptake, conduction and transpiration of water are fundamental processes in the life of a plant. A controlled water balance, by creating an internal environment in which the various metabolic processes can go to completion, is essential for normal physiological activity. The next most important processes are those concerned with nutrition. As an organism grows and develops, its increasing mass requires the supply and incorporation of the necessary structural materials, and these in turn must be taken up and synthesised from the food supply.

With the exception of a few families and specialised forms, the green plants are autotrophic; they obtain the energy necessary for the maintenance of life directly from the sun. All green plants contain the pigment chlorophyll, and with its help the radiant energy of the sun is utilised for the synthesis of organic molecules which are sources of high energy.

The discovery that the carbon of the organic mass generated by plants was derived from carbon dioxide in the atmosphere was made in 1779 by the Dutch doctor Jan Ingen-Housz, and it was subsequently investigated further by Theodore de Saussure (Bell and Coombe, 1965). This conclusion did not

meet with immediate acceptance by the scientific community of the time, and it was still widely believed that plants drew their nourishment from humus substances in the soil, well into the nineteenth century. Sir Humphry Davy, in a work entitled "The Elements of Agricultural Chemistry", published around 1813, stated that although some plants may receive their carbon from the air, the major portion was taken in through the roots. Davy was so enthusiastic in this belief that he recommended the use of oil as a fertilizer because of its carbon and hydrogen content (Tisdale, Nelson and Beaton, 1985).

A major breakthrough in the knowledge of plant nutrition was made with the work of the German chemist Justus von Liebig. Liebig stated unequivocally that most of the carbon in plants came from the carbon dioxide of the atmosphere and that hydrogen came from water. He also drew several conclusions as to the mineral essentiality of plants and although this was based more on speculation and observation rather than sound experimentation, nevertheless it opened the way for a greater understanding of the role of mineral nutrition in plants (Follet, Murphy and Donahue, 1981). Over the next one hundred years the list of essential mineral nutrients grew, progress often being linked to developments in analytical chemistry, and there are fourteen elements recognised today as being universally essential.

Three criteria of mineral essentiality have been defined by Arnon and Stout (1939):

- a) If the element is removed from the growth medium of the plant it is unable to complete its vegetative life cycle.
- b) The function is specific and cannot be replaced by other elements.
- c) Essentiality is confirmed if the element is a necessary component of an essential metabolite.

Table 1.1 lists the levels of essential elements known to be critical for multicellular plants.

Table 1.1: Essential Elements Found in Higher Plants.

<u>Element</u>	<u>*$\mu\text{mol g}^{-1}$</u>	<u>ppm</u>	<u>Relative atoms w.r.t. Mo</u>
Mo	0.001	0.1	1
Cu	0.1	6	100
Zn	0.3	20	300
Mn	1	50	1 000
Fe	2	100	2 000
B	2	20	2 000
Cl	3	100	3 000
S	30	1 000	30 000
P	60	2 000	60 000
Mg	80	2 000	80 000
Ca	125	5 000	125 000
K	250	10 000	250 000
N	1 000	15 000	1 000 000
O	30 000	450 000	30 000 000
C	35 000	450 000	35 000 000
H	60 000	60 000	60 000 000

*Concentration average in dry matter sufficient for adequate growth.

From Bonner and Varner (1976).

In addition, sodium, cobalt, vanadium and silicon have been found to be essential to some but not all plants.

There is a large difference in the concentration levels between chlorine and sulphur. The elements in the upper half of the table are used by plants in relatively small amounts and are termed micronutrients, whereas the elements in the lower half of the table are used by plants in relatively large amounts and are therefore termed the macronutrients. Although the relative concentrations of mineral elements found in plant ash are not necessarily the same as those required in the soil solution for optimum growth, they serve as a good indication of the levels required. A large number of mineral solutions capable of supporting the normal growth of green plants have been discovered by trial and error.

Tables 1.2 and 1.3 show examples of such solutions.

Table 1.2: Composition of Knop's Solution.

$\text{Ca}(\text{NO}_3)_2$	1.0g	
$\text{MgSO}_4 \cdot 7\text{H}_2\text{O}$	0.25g	
KH_2PO_4	0.25g	
FeSO_4	trace	...in 1 dm ³ of distilled water.

Element	Concentration/	
	ppm	mmol dm ⁻³
Ca	244	6.09
N	170	12.18
K	71	1.01
P	57	1.01
S	32	1.84
Mg	25	1.84

Reference: Bell and Coombe (1965).

Table 1.3: Composition of Von der Crone's solution.

KNO_3	1.0g	
$\text{MgSO}_4 \cdot 7\text{H}_2\text{O}$	0.5g	
$\text{CaSO}_4 \cdot 2\text{H}_2\text{O}$	0.5g	
$\text{Ca}_3(\text{PO}_4)_2$	0.25g	
$\text{Fe}_3(\text{PO}_4)_2$	0.25g	... in 1 dm ³ of distilled water.

Element	Concentration/	
	ppm	mmol dm ⁻³
K	387	9.89
Ca	227	5.68
S	150	4.93
N	139	9.89
Fe	117	2.10
Mg	99	2.03
P	92	3.25

Reference: Bell and Coombe (1965).

With a greater understanding of the importance of trace elements it was found necessary to add a drop of the so-called Hoagland's solution (A-Z solution of Hoagland) to the nutrient solution. The composition of Hoagland's solution is given in table 1.4.

Table 1.4: Composition of Hoagland's solution.

Element	Concentration/	
	*ppm	mmol dm ⁻³
Mn	107	1.97
B	107	9.93
Ti	33	0.688
Zn	22	0.341
I	21	0.169
Br	19	0.235
Sn	15	0.124
Cu	14	0.203
Ni	14	0.237
Co	11	0.189
Al	9	0.322
Li	5	0.661

*after dilution in the nutrient solution these concentrations will be reduced by a factor of several thousand.

Reference: Bell and Coombe (1965).

It has been found that these salts will only support growth in the proportions as given. A solution of a single one of these salts by itself may even be poisonous. When present in the above proportions an "ionic antagonism" is set up.

1.2. Elements Required in Plant Nutrition.

Carbon, hydrogen, oxygen, nitrogen, phosphorus and sulphur are the elements of which proteins, and hence protoplasm, are composed. In addition to these six there are ten other elements essential to the growth of all higher plants: potassium, calcium, magnesium, iron, manganese, molybdenum, copper, boron, zinc and chlorine.

The roles of the various elements in plant growth are covered briefly in the following sections.

1.2.1. Nitrogen.

Nitrogen is a vitally important plant nutrient, the supply of which can be controlled by the addition of fertilizers. Plants normally contain between 1 and 5% by weight of nitrogen. It is absorbed by plants in the form of nitrate or ammonium ions, or as urea. In moist, well aerated soils the NO_3^- form predominates. Once absorbed by the plant, nitrate is reduced to ammonium using energy derived from photosynthesis. The ammonium nitrogen so produced combines with organic molecules to build up amino acids and proteins.

In addition to its role in the formation of proteins, nitrogen is an integral part of chlorophyll. The basic unit of the chlorophyll structure is the porphyrin ring

system, comprising four pyrrole rings, each containing one nitrogen and four carbon atoms. A single magnesium atom is bonded to the centre of each porphyrin ring.

An adequate supply of nitrogen is associated with vigorous vegetative growth and a dark green colour. When plants are deficient in nitrogen they become stunted and yellow in appearance. This yellowing, or chlorosis of the leaves will cause the death of the plant in cases of severe nitrogen shortage.

1.2.2. Potassium.

The concentration of potassium in plants ranges typically between 1 and 4% but it can be somewhat higher. Much of this potassium, however, is not bound in organic compounds and it seems that one of the most important functions of this element is in water relations. Potassium enables the plant to develop an osmotic pressure which draws water into the roots. Potassium deficient plants are less able to withstand water stress, mainly because of their inability to make full use of the available water.

Potassium has also been found to be important to many of the metabolic processes of the plant. Over 60 enzymes have been identified that require potassium for their activation (Marschner, 1983) and these enzymes are involved in a great many of the plant's physiological processes. Plants also require potassium for the production of high energy

phosphate molecules, ATP (adenosine triphosphate) which are produced in both photosynthesis and respiration. Nitrogen uptake, protein synthesis and starch synthesis also rely on potassium and are inhibited in potassium deficient plants. Potassium deficiency is also associated with decreased resistance to certain plant diseases (Tisdale, Nelson and Beaton, 1985).

1.2.3. Phosphorus.

Phosphorus occurs in plants in concentrations between 0.1 and 0.4%, a range considerably lower than that found for nitrogen and potassium. Plants absorb phosphorus either as the primary H_2PO_4^- ion or in smaller amounts as the secondary HPO_4^{2-} orthophosphate ion.

The single most important function of phosphorus in plant physiology is in its role in energy storage and transfer. The two most common phosphorus compounds which take place in this process are adenosine di- and triphosphate (ADP and ATP). Energy obtained from photosynthesis and the metabolism of carbohydrates is stored in these compounds for subsequent use in growth and reproductive processes.

In addition to its vital metabolic role, phosphorus is an important structural component of a wide variety of biochemicals, including nucleic acids, coenzymes, nucleotides, phosphoproteins, phospholipids and sugar

phosphates. Phosphorus has been shown to be particularly important in the development of a plant's reproductive and root systems. Large quantities of phosphorus are also found in seeds and fruits; it is considered essential for seed formation.

Phosphorus deficiency has a marked effect on retarding overall growth and leads to delays in grain ripening. The quality of certain fruit, forage, vegetable and grain crops is said to be improved, and disease resistance is increased when these crops have adequate phosphorus nutrition (Marschner, 1983).

1.2.4. Calcium.

Calcium is known to be a structural component of plant cells and as a cofactor for certain enzymes. Its normal concentration in plants ranges between 0.2 to 1.0%.

Calcium pectate is one of the components of the middle lamellae of plant cells, binding together the cell walls. Calcium is involved in cell membrane functions and influences the affinity of membrane constituents for certain cations, thereby influencing the selectivity of ion-transport processes (Bonner and Varner, 1976). Calcium is also used to protect plants from acidity, high salinity and other potentially toxic effects when it is introduced to the soil through liming.

A deficiency in calcium manifests itself in the failure of terminal buds of plants to develop. The same applies to the apical tips of roots.

1.2.5. Magnesium.

This element is present in concentrations of 0.1 to 0.4% in plants. It is the only inorganic constituent of chlorophyll and its importance from this point of view is obvious. Also, like calcium, magnesium is a structural component of cells, is involved as a cofactor in many enzyme transfers and appears to stabilise the ribosomal particles in the configuration necessary for protein synthesis. Magnesium is also commonly associated with transfer reactions involving phosphate reactive groups.

Magnesium deficiency causes chlorosis in plant leaves due to the depletion of chlorophyll.

1.2.6. Sulphur.

Sulphur is the last of the six macronutrient elements. It is absorbed by plants as the sulphate anion. Typical concentrations of sulphur in plants range between 0.1 and 0.4%. Sulphur is required for the synthesis of many biomolecules including the sulphur-containing amino acids, coenzyme A, vitamin B1 and the ferredoxins. Deficiency of sulphur has a pronounced retarding effect on plant growth characterised by chlorosis.

The remaining minerals (the micronutrients) are required by plants in much smaller quantities. The concentrations range typically from up to a few percent in the case of chlorine (although much lower levels satisfy the physiological requirements of most plants) to less than 0.5 ppm of cobalt. In general the micronutrients are required as constituents of certain biomolecules or as enzyme cofactors. The specific function of these elements is not known always but deficiency symptoms can be recognised in most cases when their concentrations drop below a critical level.

1.3. Soil Fertility and Fertilizers.

Soil fertility is supported naturally by river flooding, breakdown of animal and plant waste and deposition of volcanic ash. When man first began cultivating crops for food he depended on the natural fertility of the land, moving on when the soil was depleted of the necessary nutrients. As man became less of a wanderer and more of a settler, settlements and villages were established and with these came the development of agricultural skills. In time it was discovered that certain soils would fail to produce satisfactory yields when cropped continuously. The practice of adding animal manure and vegetable compost to the soil to restore fertility probably developed from such observations.

Although the use of mineral fertilizers or soil amendments was not completely unknown in history (specifically the use of potash and lime) farm manure remained as practically the only source of fertilizer nitrogen until the late nineteenth century. Ammonium sulphate from coal carbonization then became available and, with supplies of sodium nitrate from Chile and phosphates from mineral deposits in Germany, the use of high analysis mineral fertilizers became more widespread. However, the rapid development of the chemical industry in the late nineteenth and early twentieth centuries, which led (for example) to the discovery of the Haber process for ammonia manufacture,

enabled the large scale production and use of synthetic inorganic fertilizers (Kent, 1983).

1.4. The Use of Zeolites as Soil Amendments and Fertilizers.

Farmers in Japan have long used crushed zeolitic rock to control moisture content and malodour of animal wastes, and to increase the pH of acidic volcanic soils (Mumpton, 1984). Natural zeolites (mainly clinoptilolite) have been used extensively in Japan as amendments for sandy soils. The beneficial effects of zeolites used in agriculture stem from both their ion-exchange and water retention properties. Used as soil amendments zeolites increase the cation-exchange capacity of the soil and thereby reduce nutrient losses due to leaching.

Clinoptilolite is important because of its stability towards weathering and because of its selectivity for both ammonium (Howery and Thomas, 1965) and potassium ions (Chelischev et al, 1974). Using clinoptilolite-rich tuff the Agricultural Improvement Sector of Yamagata Prefectural Government in Japan reported significant improvements in yields of wheat (13-15%), aubergine (19-55%), apples (13-38%) and carrots (63%). 4-8 tonnes of the zeolitic tuff were added per acre of land (Sand and Mumpton, 1978).

Torii (1978) reported a consumption of 400 to 500 tonnes of clinoptilolite tuff per month as a soil amendment in Japan in 1976. Small tonnages were also exported to Taiwan for the same purpose.

The natural zeolites used in Japan are predominantly in the sodium form. The disadvantage of using sodium zeolite as a soil amendment is that there can be a toxicity effect arising from the sodium released during ion-exchange. In some cases, addition of zeolites to the growing medium can actually suppress plant growth (Nishita and Haug, 1972). In field trials in America, Pirela and his co-workers found that application of sodium clinoptilolite at rates of 0.5 and 2 tons ha^{-1} had no significant effect on corn yields but at 8 tons ha^{-1} the yield actually decreased. This was attributed either to sodium poisoning or to a suppression of ammonium availability (Pirela et al, 1984).

Results obtained when a zeolite soil amendment is applied in combination with nitrogen fertilizers are very promising. Clinoptilolite adsorbs ammonium ion, thus reducing the leaching of nitrogen. The zeolite also prevents microbial oxidation of ammonium to the highly leachable nitrate ion. The nitrosomonas bacterium is typically 8,000 Å in size (Lewis et al, 1984) whereas the free apertures of the main channels in clinoptilolite are only 4.4 x 7.2 Å, 4.1 x 4.7 Å and 4.0 x 5.5 Å in size (Alberti, 1975).

Clinoptilolite can act as a protection against excessive amounts of ammonium when nitrogen is added as urea. This is especially true when the soil clay level is low and cannot itself provide protection. Lewis, Moore and

Goldsberry (1984) reported approximately 100% improvements in leaf area, plant and root weight, and nitrogen uptake by plant tops when mixtures of clinoptilolite and urea were added to radishes in a coarse textured soil, compared to additions of urea alone.

In greenhouse trials, Pirela et al (1984) found that sodium clinoptilolite added at 0.5, 2 and 8 tons per hectare with nitrogen fertilizer did not significantly affect yields of corn, soya bean or cucumber. When applied at 0, 8, 16 and 32 tonnes per hectare with nitrogen fertiliser and using multiple cropping production, the clinoptilolite increased yields on the third harvest.

Several workers have shown that clinoptilolite exchanged into the ammonium form can supply nitrogen to the soil over relatively long periods of time, thus acting as a slow release fertilizer.

Bartz and Jones (1983) have looked at the availability of nitrogen to sudangrass from ammonium clinoptilolite. In greenhouse trials, clinoptilolite from Buckhorn, New Mexico was exchanged into the ammonium form and added to the soil so as to provide 71, 236, 353 and 706 mg of nitrogen per pot. Two different soils were used, one highly fertile (0.19% total nitrogen) the other of low fertility (0.09% total nitrogen). Control treatments of no added nitrogen and a comparison treatment of ammonium sulphate (236 mg N

per pot) were also investigated. Six cuttings of the sudangrass were made over a period of 242 days.

The yields of sudangrass were significantly increased by additions of ammonium clinoptilolite but this was much more marked in the case of the low fertility soil. For those treatments where ammonium sulphate and ammonium zeolite were at the same level (236 mg N per pot) there were no significant differences between means for yield with the high fertility soil. However, on the less fertile soil, the same comparison showed significant differences in yields for the first and third cuttings. For the first cutting the ammonium sulphate treatment gave greater yields. For the third and subsequent cuttings the zeolite treatment produced the greater yield.

The cumulative recovery of added nitrogen was calculated from the nitrogen content of the sudangrass. The recovery was lower for the high fertility soil and similar for each treatment. The nitrogen recovery in the less fertile soil is illustrated in figure 1.1. The highest nitrogen recovery (over 70%) occurred when zeolite was added at a rate of 71 mg N per pot. Nitrogen uptake from ammonium clinoptilolite applied at 71 and 236 mg N per pot was complete by the third cutting on the low fertility soil, and the same was true for the ammonium sulphate treatment. Similar recovery was complete by the fourth cutting of grass from the 353 mg N / pot treatment. However, at a

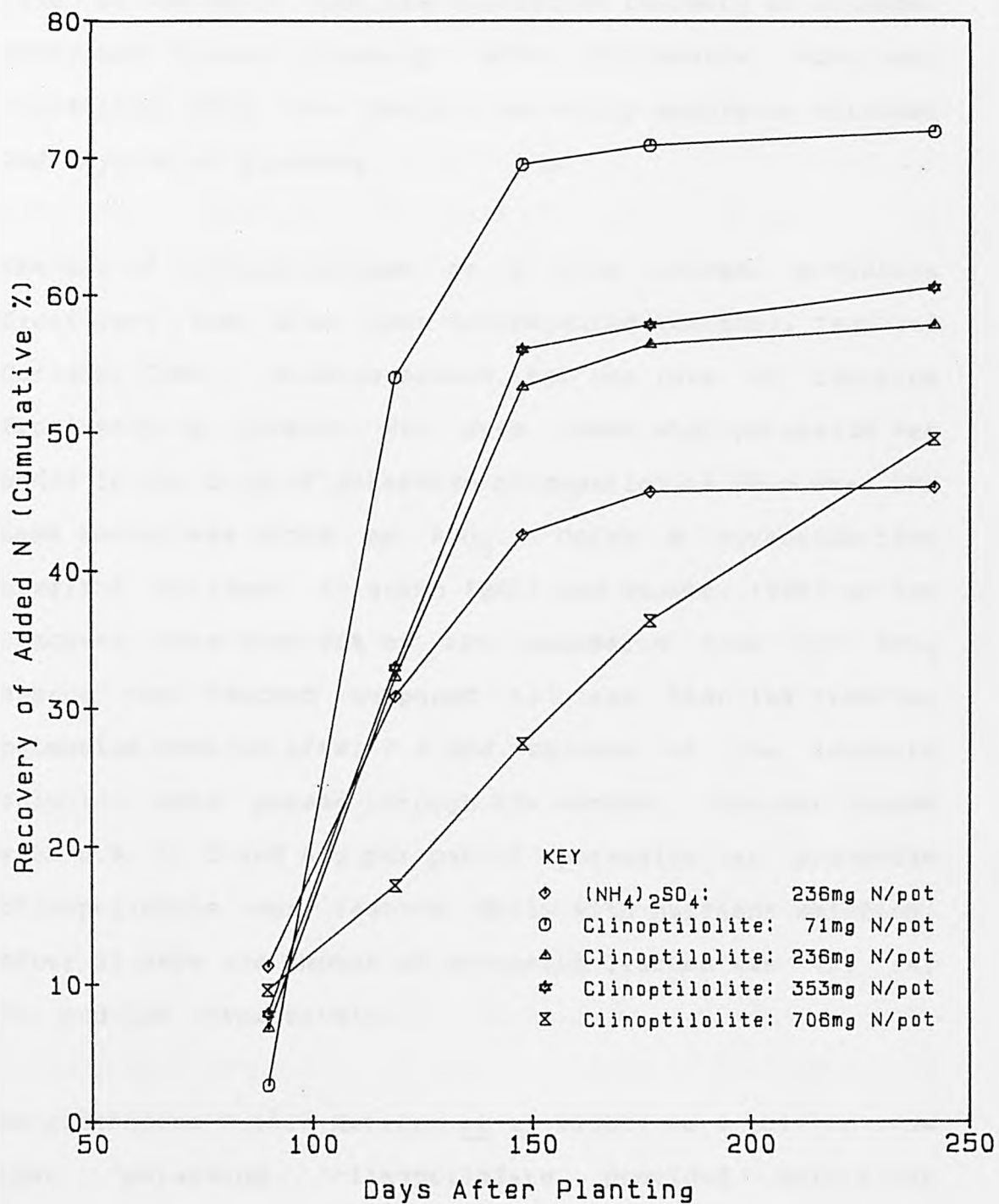


Figure 1.1:

Nitrogen recovered in seriatim cuttings of sudangrass grown in Cisne loam treated with either (NH₄)₂SO₄ or NH₄-saturated clinoptilolite.

Reference: Bartz and Jones (1983).

rate of 706 mg N / pot the cumulative recovery of nitrogen increased almost linearly with successive cuttings, indicating that the zeolite was still supplying nitrogen 242 days after planting.

The use of clinoptilolite as a slow release potassium fertilizer has also been investigated (Hershey, Paul and Carlson, 1980). Studies showed that the rate of leaching from potting compost was much lower when potassium was added in the form of potassium clinoptilolite than when the same amount was added as KNO_3 . Using a potassium-free Hoagland nutrient solution (Bell and Coombe, 1965) as the leachate, more than 90% of the potassium from the KNO_3 source was leached compared to less than 10% from the potassium zeolite after 2.1 bed volumes of the leachate solution were passed through the compost. Compost loaded with 0.5, 1, 3 and 6 g per pot of potassium as potassium clinoptilolite was leached daily with nutrient solution. After 25 days the amount of potassium leached was 48, 44, 20, and 13% respectively.

In greenhouse trials Hershey et al (1980) were able to show that potassium clinoptilolite provided sufficient quantities of potassium for normal growth of chrysanthemums for up to three months. Chrysanthemums were grown in compost and irrigated with potassium-free nutrient solution. When potassium was supplied as potassium clinoptilolite at rates equal to or greater than 3 g per

1.5 litres of compost, plant yields were not significantly different to controls containing no soil potassium but which had been irrigated with Hoagland's solution containing 234 ppm K. The zeolite used was a natural potassium zeolite from The Anaconda Minerals Company. The analysis of the exchangeable cations was $160.1 \text{ meq hg}^{-1} \text{ K}$; $33.5 \text{ meq hg}^{-1} \text{ Na}$; $18.7 \text{ meq hg}^{-1} \text{ Ca}$; and $0.4 \text{ meq hg}^{-1} \text{ Mg}$.

Valente et al (1982) made a comparative study of the use of three minerals as soil conditioners in tomato growing. The materials used were Lipari pumice, zeolite N36 (a 2:1 mixture of faujasite and hydroxy sodalite) prepared by hydrothermal synthesis from pumice, and commercial zeolite 4A. The zeolites were used in the sodium form and the pumice and the zeolites were added with fertilizers to tomato plants in field trials. The yield of tomatoes, compared to control experiments, was about 60% higher when zeolite N36 was used, slightly higher when pumice was present and significantly lower in the case of the zeolite A treatment. The authors concluded from this that the ion-exchange properties of zeolites could not explain the results obtained because pumice shows a greater beneficial effect in comparison with the commercial zeolite, the latter having the best ion-exchange properties. However, the potentially toxic effects of exchangeable sodium and of aluminium released from the zeolite lattice through hydrolysis under relatively mild acid conditions (Cook et al, 1982) are not taken into consideration at all. It

would appear that the more stable zeolite N36 is able to maintain levels of soil nitrogen by preventing losses arising from nitrification and leaching, by exchanging ammonium ions into the zeolite lattice. The beneficial effects of the pumice are probably due to the presence of elements such as potassium and iron. Potassium is particularly important in the formation of fruits (Marschner, 1983).

The application of zeolites in spinach growing has been investigated by Burriesci et al (1983). The zeolites used were hydroxysodalite, faujasite and zeolite Pc all produced by hydrothermal synthesis from Lipari pumice. The zeolites were used in the sodium form and added on their own or with fertilizers during sowing. The presence of zeolite on its own gave rise to an increase in the germination rate of the spinach seeds of over 100% compared to control experiments. This has been attributed to the water retention properties of the zeolite increasing the humidity in the location of the seeds. In general crop yields increased when increasing amounts of zeolite were applied with fertilizers. However, when zeolite was added without fertilizer at increasing rates, the spinach yield first increased, being higher when zeolite was added at a rate of 100 g m^{-2} than at 50 g m^{-2} , but then decreased when the rate was increased to 150 g m^{-2} . The explanation of these observations is that there are two separate effects. The zeolite increased the cation exchange capacity of the soil,

thus acting as a fixing agent for nutrient elements, preventing elution by rain and irrigation water, and allowing slow release to the roots. Adding sodium zeolite will however cause salinity problems if the concentration rises to too high a value and this will have a deleterious effect on crop yield.

1.5. Zeolites.

As found in nature, or when synthesised, zeolites are crystalline, hydrated aluminosilicates of group I and II elements. Natural zeolites are found principally in the sodium, potassium, calcium, magnesium and barium-exchanged forms (Breck, 1974). A wide range of other ions can be introduced by ion-exchange. The zeolite framework structure consists of corner linked tetrahedra in which small (T) atoms lie at the centres of tetrahedra with oxygens at the corners. The tetrahedral sites of natural zeolites are dominated by aluminium and silicon, but chemically related elements such as gallium, germanium and phosphorus have been incorporated into synthetic zeolites.

A useful, loose definition of zeolites has been made by Smith (1963): "a zeolite is an aluminosilicate with a framework structure enclosing cavities occupied by large ions and water molecules, both of which have considerable freedom of movement, permitting ion-exchange and reversible dehydration".

Zeolites may be represented by the empirical formula $M_{2/n}O \cdot Al_2O_3 \cdot xSiO_2 \cdot yH_2O$, where n is the valency of cation M , x is a number greater than or equal to 2 (Loewenstein, 1954), and y is a function of the porosity.

The crystallographic unit cell structure is best

represented by $M_{x/n} \cdot [(AlO_2)_x (SiO_2)_y] \cdot wH_2O$, where $(x+y)$ is the number of tetrahedral atoms in the unit cell and the formula within the square brackets represents the framework composition.

Meier (1968) presented a classification of zeolites for which the structure is known, based on their framework topologies. The structures are broken down into eight groups characterised by a common sub-unit of structure which is a specific array of SiO_4 and AlO_4 tetrahedra. The primary building units are the silicon and aluminium tetrahedra. The secondary building units, as proposed by Meier (1968), are illustrated in figure 1.2.

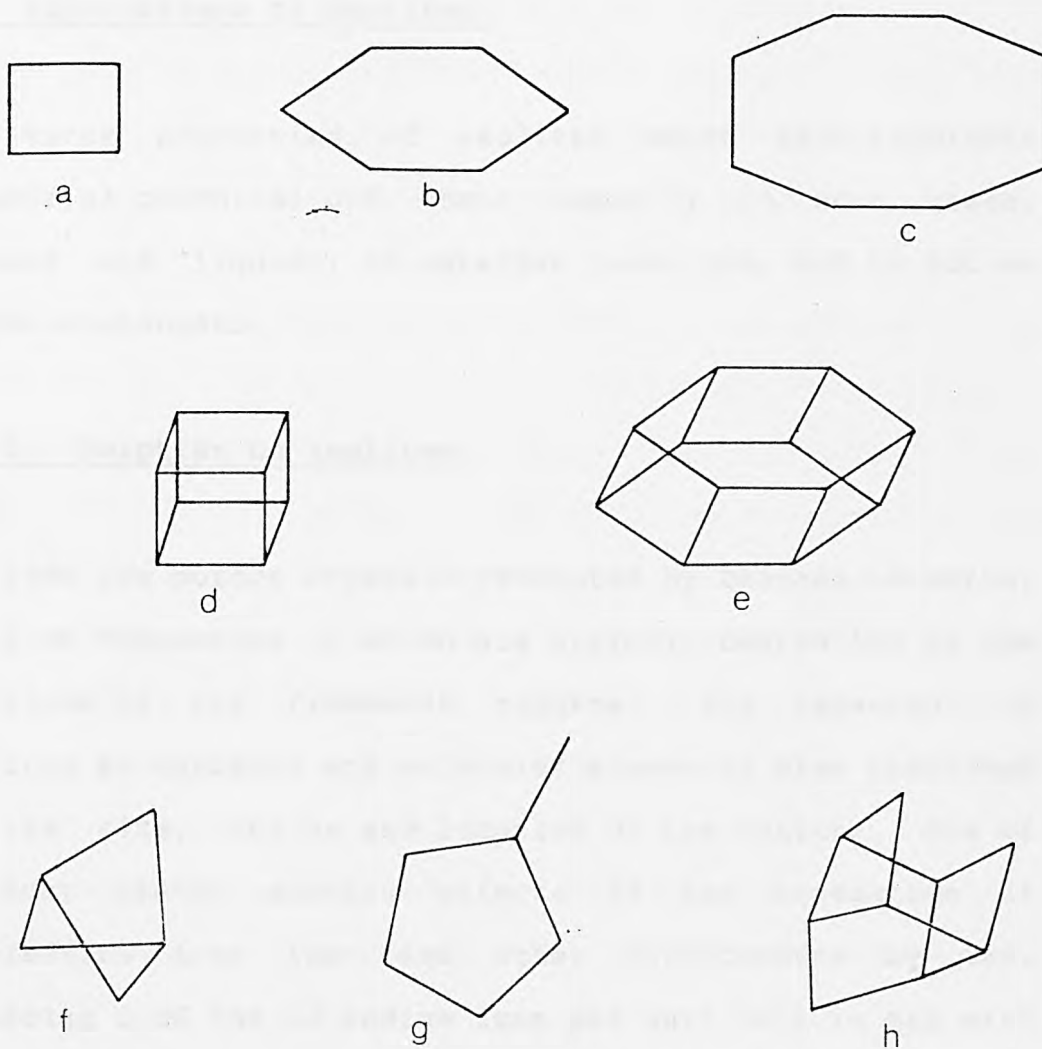


Figure 1.2:

Secondary Building Units in Zeolite Structures:

- (a) Single 4-ring
- (b) Single 6-ring
- (c) Single 8-ring
- (d) Double 4-ring
- (e) Double 6-ring
- (f) Complex 4-1 unit
- (g) Complex 5-1 unit
- (h) Complex 4-4-1 unit

Reference: Meier (1968).

1.6. Applications of Zeolites.

The three properties of zeolites which have important industrial potential are their capacity to sorb gases, vapours and liquids; to catalyse reactions; and to act as cation exchangers.

1.6.1. Sorption on Zeolites.

Zeolites are porous crystals permeated by channel networks, the free dimensions of which are strictly controlled by the positions of the framework oxygens. The behaviour of zeolites as sorbents and molecular sieves is also regulated by the size, charge and location of the cations. One of the most useful sieving effects is the separation of n-paraffins from iso- and other hydrocarbons by CaA. Replacing 8 of the 12 sodium ions per unit cell in NaA with calcium increases the free diameter of the 8-oxygen windows from 4 to 5 Å. This allows the n-paraffin molecules to be sorbed whilst excluding branched chain hydrocarbons (Breck, Eversole, Milton, Reed and Thomas, 1956; Rees, 1984).

Air separation is achieved using pressure swing adsorption (PSA) processes (Breck, 1974; Kenney and Kirkby, 1984). Nitrogen, but not oxygen, possesses a considerable molecular quadrupole moment, enhancing its energy of sorption on the zeolite. Beds of zeolite pellets are subjected to adsorption, depressurisation, desorption and

repressurisation steps. By simple mechanical switching it is possible to obtain a steady flow of one highly purified product. Many tonnes of oxygen are produced in this way for medical and industrial processes (Rees, 1984).

Pressure swing parametric pumping processes are mechanically less complex than PSA processes, and oxygen productivity is about five times that of PSA for similar feed pressures. In addition, gas mixtures other than N_2/O_2 can be separated. For example H_2/CH_4 mixtures from the steam cracking of ethane and propane; nitrogen/ CH_4 ; and N_2 /ethene mixtures have been separated using pressure swing parametric pumping (Rees, 1984; Keller and Jones, 1980).

Other applications include intensive drying of liquids, industrial gases, air and natural gas, and the removal of sulphur compounds from petroleum (Barrer, 1978).

1.6.2. Catalysis.

Zeolite catalysts have been applied to the following four areas of industrial processes: petroleum processing, petrochemicals, synthesis of chemicals, and pollution control (Vaughan, 1980). The most important applications are in catalytic cracking, hydroisomerisation, selective forming, hydrocracking and transformation of aromatic hydrocarbons.

Cracking catalysts (mainly employing zeolite Y) account for more than 95% of the market both in terms of catalyst and value of products. The main objective of catalytic cracking is to convert heavy feeds (i.e. crude gas oil) into lighter and more valuable fractions in the gasoline and middle distillate ranges.

Zeolite cracking catalysts need to have a large number of acid sites in order to be catalytically active. These are introduced into the synthetic sodium zeolites by ion-exchange with ammonium, followed by thermal deammoniation (Kerr, 1973). Alternatively, the catalysts are prepared by ion-exchange with rare-earth elements, such as lanthanum, which stabilise the zeolite to high temperatures and produce acid sites through reaction with water.

1.6.3. Ion-Exchange Applications.

The isomorphous replacement of silicon atoms by aluminium within the zeolite lattice results in a net negative charge being found on the framework. The charge is neutralised by the presence of cations occluded within the channels and cages of the zeolite. The mobility of these cations gives rise to the ion-exchange properties of zeolites.

The direct use of zeolites as ion-exchangers has been

somewhat limited as they have often proved inferior in many respects to ion-exchange resins. One major drawback is that their solution stability is rather limited, many zeolites being open to acid attack even in mildly acidic solutions such as pH 4 to 5, (Cook et al, 1982). Also when pelletised for use in columns, zeolites exhibit much slower exchange kinetics than their resin counterparts (Townsend, 1984).

Despite these drawbacks zeolites have found a number of specialised but nonetheless important applications as ion-exchangers in recent years. Zeolites prove ideal in particular situations where large quantities of exchanger are required and where recovery is not a priority, because of their relative cheapness. Commercially the most important use of zeolites as ion-exchangers is in detergency. Sodium tripolyphosphate, used as a sequestering agent in detergents to remove the hardness ions calcium and magnesium, gives rise to serious pollution problems when discharged into rivers and streams (Kroes, 1980). Considerable quantities of zeolites A and X are now used as an alternative water softener to sodium tripolyphosphate in detergent formulations without any of the associated environmental problems (Kuhl and Sherry, 1980; Schwuger and Smolka, 1977).

Clinoptilolite is used extensively in the treatment of sewage and agricultural effluents (Dyer, 1984). Its high

selectivity for ammonium ion (Townsend and Loizidou, 1984) enables the removal of around 99% of ammonium from tertiary sewage in plants capable of handling several million gallons of water per day (Ames, 1960). Regeneration of the zeolite does present some problems due to the very high selectivity of clinoptilolite for ammonium, but a novel biological method has been suggested to improve the regeneration efficiency (Semmens, 1980; Murphy, Hyrck and Gleason, 1978).

Natural zeolites have been used since the 1960's for the treatment of radioactive waste. Clinoptilolite has been used to remove ^{90}Sr and ^{137}Cs selectively from low level waste water created by nuclear reactors. Zeolites are also used in the removal of ^{137}Cs from high level radioactive wastes and in the fixation of fission products prior to long term storage (Dyer, 1984). In the early 1980's zeolites were used in the clean-up of "hot" water resulting from the Three Mile Island nuclear reactor accident in the U.S.A. (King et al, 1984).

The use of zeolites as soil amendments and slow release fertilizers has already been reviewed in section 1.4. In the agricultural context natural zeolites are also finding increasing applications as dietary supplements for pigs, chickens and ruminants. Beneficial effects include increased growth rates and higher disease resistance (Barbarick and Pirela, 1984).

In addition to these direct applications, the principles of ion-exchange in zeolites are very important in the preparation of molecular sieve sorbents and catalysts. The size and charge of exchanged ions determines the free dimensions of the openings to the zeolite pores, and hence the molecular sieving characteristics of the sorbent (Breck et al, 1956). Zeolite Y is the most widely used cracking catalyst (Vaughan, 1980) and this is synthesised in the sodium form. As even small amounts of sodium may reduce the stability and effectiveness of this zeolite as a catalyst it must be exhaustively exchanged before use (McDaniel and Maher, 1976; Ward, 1983). The cation forms most commonly used as cracking catalysts are hydrogen Y, rare earth Y, rare earth hydrogen Y and rare earth magnesium Y (Vaughan, 1980; Magee and Blazek, 1976). "Hydrogen Y" cannot be prepared directly by hydronium exchange due to the limited stability of zeolite Y in acid media. Instead it is prepared by deammoniation of the ammonium-exchanged form (Kerr, 1973). The preparation of hydrocracking catalysts requires further ion-exchange with various transition metals such as Ni, Co, Mo, W, Pt, Ru and Rh (Vaughan, 1980; Ward, 1983).

1.7. Zeolite Structures.

1.7.1 Zeolite A.

The synthetic zeolite A was first synthesised in the laboratories of the Linde Air Products Company in the 1950's (Breck, Eversole, Milton, Reed and Thomas, 1956) and has no natural analogue.

Zeolite A can be represented by the formula $\text{Na}_{12}[(\text{AlO}_2)_{12}(\text{SiO}_2)_{12}]\cdot 27\text{H}_2\text{O}$. The framework can be described in terms of two polyhedra, the double 4-ring (D4R) and the β -cage or sodalite unit. The zeolite has a cubic structure, the D4R units occurring in the centres of the edges of a cube of edge 12.3 Å. The β -cages are centred at the corners of the cube. The centre of the unit cell is a large cavity of free diameter 11.4 Å with circular openings 4.2 Å in diameter (the 26-hedra type I, or α -cage). The α -cages enclose a cavity of free diameter 6.6 Å.

In A the Si/Al ratio is 1.0 and the electrostatic valence rule as modified by Loewenstein (1956) requires a rigorous alternation of AlO_4 and SiO_4 tetrahedra. To achieve this the true unit cell size of A must be 24.6 Å rather than the "pseudo-cell" which contains 24 tetrahedra and has a dimension of 12.3 Å.

1.7.2. Cation Sites in Zeolite A.

Despite the relatively simple structure of zeolite A, Barrer (1978) has identified seven possible ion sites:

Site S1: in the 8-ring.

Site S2: in the 6-ring.

Site S2': in the sodalite cage adjacent to the 6-rings.

Site S2^{*}: in the α -cage adjacent to the 6-rings.

Site S3: against the 4-ring.

Site SU: in the centre of the sodalite cage.

Site S4: in the centre of the α -cage.

In hydrated zeolite NaA it is generally accepted that 8 of the 12 sodium ions per pseudo unit cell are located near the centre of the 6-rings in the α -cages (site S2^{*}) while the other 4 are located in the highly hydrated state in the 8-rings (site S1) (Breck, 1974).

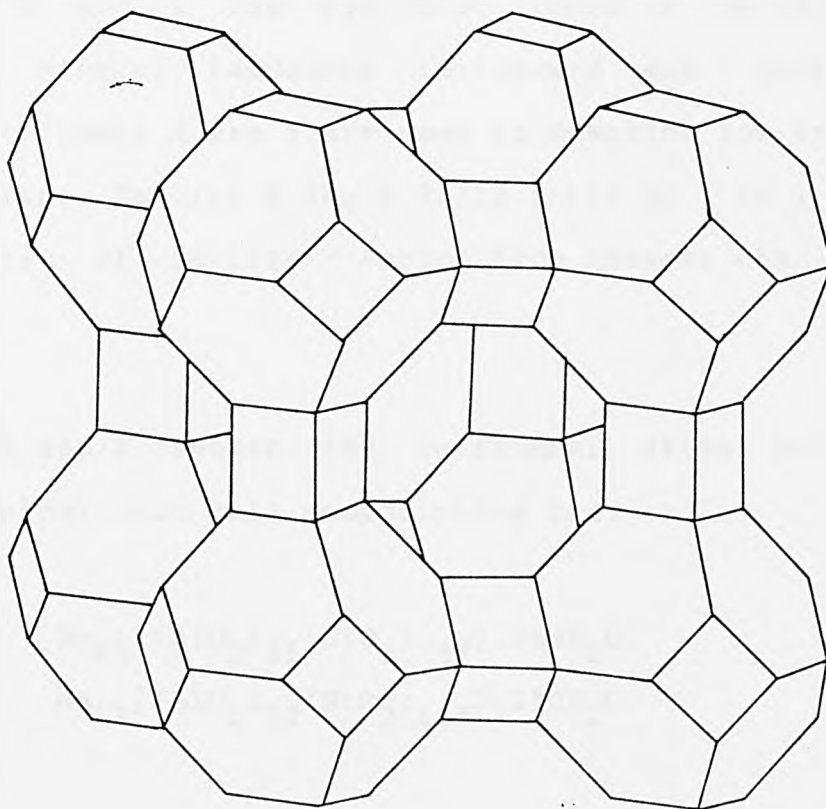
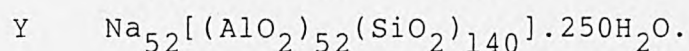
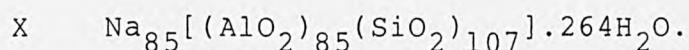


Figure 1.3: The Structure of Zeolite A.

1.7.3. Zeolites X and Y.

Zeolites X and Y are synthetic forms of the naturally occurring mineral faujasite (Broussard and Shoemaker, 1960). The names X and Y are used to describe low and high silica forms. Zeolite X has a Si/Al ratio of 1 to 1.5, the Si/Al ratio of zeolite Y varies from greater than 1.5 to about 3.

Zeolites X and Y contain 192 tetrahedral atoms per unit cell. Typical unit cell compositions are:



The structure of X and Y is analogous to that of diamond, with sodalite cages in positions corresponding to carbon atoms. Each sodalite unit is linked to four others through double 6-rings, forming a series of smaller hexagonal prism cages (Broussard and Shoemaker, 1960). This method of linking also results in the formation of a series of large cavities (the 26-hedra type II, or supercages). The free diameter of the supercages is about 12 Å whilst the 12-rings, through which the supercages are connected, have a free diameter of about 8 Å. Entrance to the small cages is through the 6-rings of the sodalite cages, which have a free diameter of about 2.5 Å (Pekarek and Vasely, 1972).

The ordering of the silicon and aluminium atoms in X and Y is complicated and obviously varies with the Si/Al ratio (Klinowski, Ramsdas, Thomas, Fyfe and Hartman, 1982).

1.7.4. Cation Sites in Zeolites X and Y.

Two major classifications of cation sites in faujasite zeolites are found in the literature. Breck (1974) identified 6 sites:

Site I: in the centre of the hexagonal prism.

Site I': in the sodalite cage near the hexagonal prism.

Site II': in the sodalite cage near the 6-ring leading to the supercage.

Site II: near site II' but inside the supercage.

Site III: in the 4-rings around the wall of the supercage.

Site IV: in the 12-ring of the supercage.

Barrer (1978) however identified nine sites:

Site I: as Breck site I.

Site I': as Breck site I'.

Site U: in the centre of the sodalite cage.

Site II: in the 6-ring linking the sodalite cage to the supercage.

Site II': as Breck site II'.

Site II*: as Breck site II.

Site III: as Breck site III.

Site IV: in the centre of the supercage.

Site V: as Breck site IV.

For the interpretation of ion-exchange phenomena it is useful to group the sites into two types: those in the supercage system and those in the small cage system.

Various studies have suggested that in hydrated sodium and potassium zeolites X and Y, between 15 and 19 of the ions per unit cell are located in the small cage system (Broussard and Shoemaker, 1960; Olson, 1970; Mortier and Bosman, 1971; Beagley, Dwyer and Ibrahim, 1978; Barrer, 1978). From the point of view of exchange the siting of these ions is of particular interest since their position has been used to explain the observed incomplete exchange of some cations such as Cs, Ba and La in both zeolites X and Y (Sherry, 1966; Sherry, 1968a; Sherry 1968b). It has been proposed that these ions are unable to pass through the six-oxygen windows and therefore cannot exchange with the ions in the small cage system. The ions are unable to pass through the 6-rings either because the non-hydrated ions are too large or because the hydrated ions are too large and dehydration would be energetically unfavourable. It has also been shown that some ions, which at room temperature are unable to enter the small cages can, at elevated temperatures, pass through the 6-rings and then become irreversibly "locked" in the sodalite cages (Sherry, 1968b; Sherry, 1976).

A complete review of cation site locations and occupancies in zeolites A, X and Y is given by Mortier (1982).

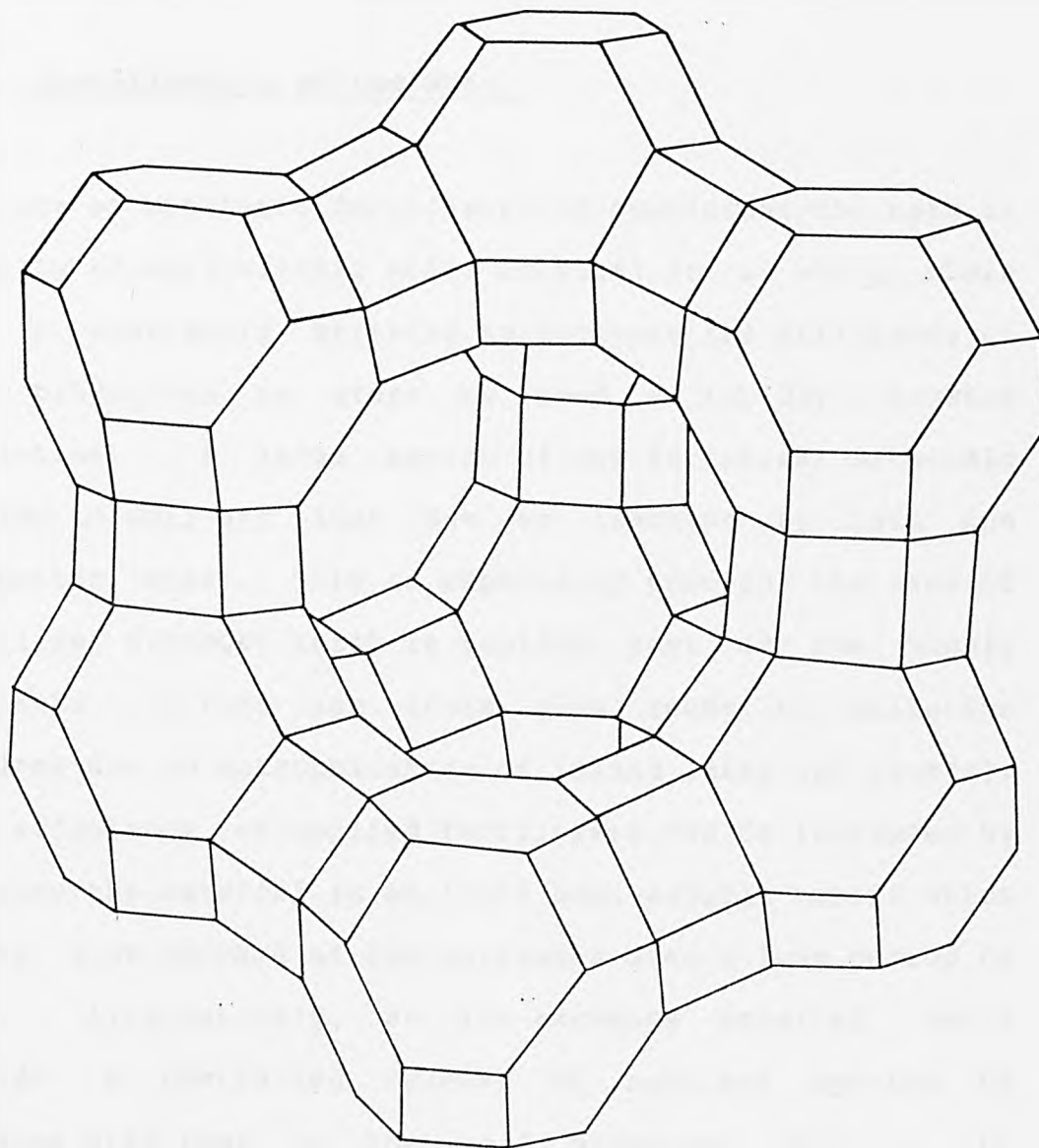


Figure 1.4: The Structure of Zeolites X and Y.

1.8. Justification of the Work.

The use of synthetic fertilizers to supplement the natural fertility of agricultural soils is vital in a world where man is constantly striving to increase the efficiency of crop production in order to feed a rapidly growing population. A large amount of the fertilizer materials applied to soil are lost due to leaching by rain and irrigation water. This is especially true for the case of fertilizer nitrogen which is rapidly lost as the highly leachable nitrate ion (this also leads to pollution problems due to eutrophication of inland lakes and rivers). The efficiency of applied fertilizers can be increased by encasing the material in an inert semi-soluble matrix which allows slow release of the nutrients over a long period of time. Alternatively, an ion-exchange material could provide a controlled release of nutrient species by exchange with ions in the soil solution; this is the principle behind slow release zeolite fertilizers.

Although field and greenhouse trials involving natural zeolite fertilizers and soil amendments have been undertaken, to the knowledge of the author no systematic chemical study has been carried out into the use of zeolites as slow-release fertilizers. This work attempts to correct that position. Firstly it is important to determine the stability of the zeolite fertilizer under conditions which may be found in the soil environment.

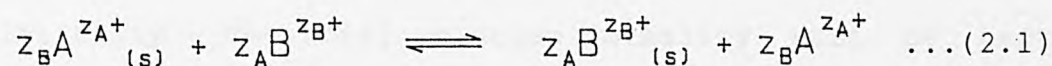
Zeolites have limited stability under acid conditions so it is necessary to determine whether faujasite zeolites will remain intact under the relatively mild acid conditions found in some soils, for long enough for them to perform their function as slow release fertilizers. Hydronium exchange and hydrolysis of zeolites X and Y under these conditions will therefore be investigated. It is also proposed to measure isotherms involving the exchange of the fertilizer elements nitrogen (as ammonium ions) and potassium. It must be stressed however, that this work does not aim to provide a complete evaluation of the suitability of synthetic faujasite zeolites as commercially viable slow release fertilizers, but rather to provide useful background chemical data and an impetus for future work on the development of synthetic zeolite fertilizers.

2. THEORY OF ION-EXCHANGE.

2.1. Ion-Exchange Equilibria.

2.1.1. The Ion-Exchange Isotherm.

The binary ion-exchange reaction between the ions A (initially in solution) and B (initially in the exchanger) may be written as:



where z_A , z_B are the charges on the ions A and B respectively and the subscript (s) refers to the solution phase.

The exchange equilibrium for these ions is conveniently characterised by an ion-exchange isotherm which is a plot of the equivalent fraction of ion A in the exchanger (E_A) against the equivalent fraction of A in the solution phase ($E_{A,s}$) at constant temperature, pressure and total normality T_N . The term "normality" refers to the number of equivalents of a component per unit volume of solution.

The equivalent fractions for a binary exchange are given by:

$$E_{i,s} = \frac{z_i m_i}{z_A m_A + z_B m_B} \dots (2.2)$$

$$E_i = \frac{z_i M_i}{z_A M_A + z_B M_B} \dots (2.3)$$

where m_A , m_B are the concentrations (mol dm^{-3}) of A and B in solution, and M_A , M_B are the concentrations (mol kg^{-1}) of A and B in the exchanger.

Experimentally the ion-exchange isotherm is determined by contacting solutions containing the ions A and B in different proportions but having constant total normality, with samples of either the homoionic A or B zeolite. After equilibration the solution and exchanger phases are separated and their compositions are determined analytically. The total solution normality must be kept constant because the selectivity of the zeolite for the ion A is not only a function of E_A but also of T_N .

For the exchanger phase, the number of equivalents per unit mass is fixed by the exchange capacity of the zeolite (although it is important to state whether this is in terms of the wet or the dry zeolite) which is determined by the number of moles of aluminium per unit mass. Thus for a zeolite which is neither under- nor over-exchanged:

$$Z_A M_A + Z_B M_B = M_{Al} \quad \dots(2.4)$$

where M_{Al} is the concentration (mol kg^{-1}) of lattice aluminium in the zeolite.

For binary exchanges $E_A = 1 - E_B$ and $E_{A,S} = 1 - E_{B,S}$. Thus an isotherm plot of E_A versus $E_{A,S}$ fully defines the equilibrium at the specified temperature, pressure and

total normality. This is not true for an exchange involving ions A,B...n since then:

$$E_{A,s} = \frac{Z_A m_A}{\sum_{i=A}^n Z_i m_i} \quad \dots(2.5)$$

In this case it is necessary to specify i-1 equivalent fractions in each phase in order to fully define the equilibrium.

The experimental selectivity of the exchanger for a given ion at any composition may be quantified by a selectivity quotient α , where:

$$\alpha = \frac{E_A \cdot E_{B,s}}{E_B \cdot E_{A,s}} \quad \dots(2.6)$$

α may be determined graphically for any value of E_A directly from the isotherm plot in terms of the ratio of Area I divided by Area II as shown in figure 2.1.

The conditions for selectivity are:

$\alpha > 1$: zeolite selective for ingoing ion A

$\alpha = 1$: zeolite shows no preference

$\alpha < 1$: zeolite selective for outgoing ion B.

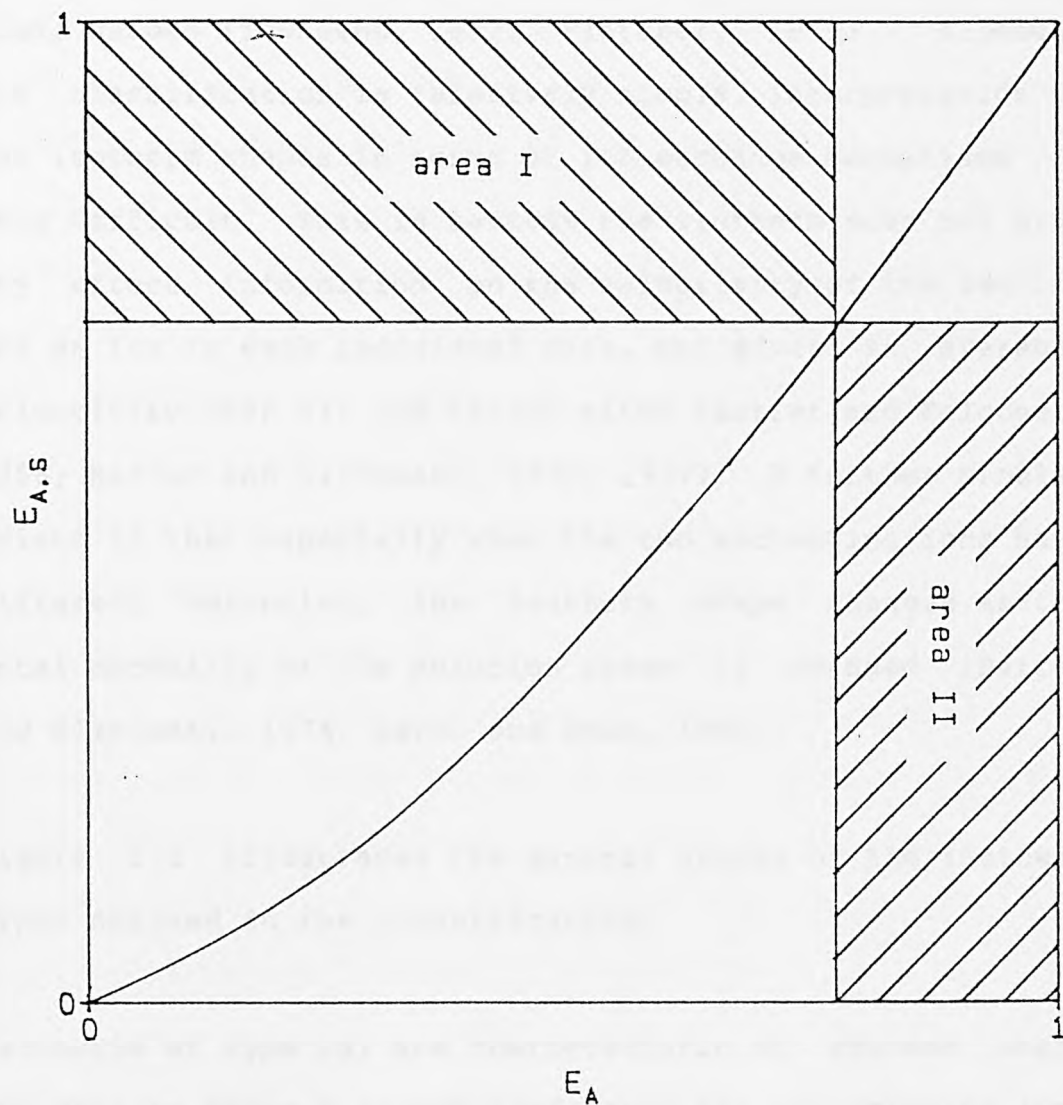


Figure 2.1:

Binary Ion-Exchange Isotherm, showing graphical determination of the selectivity coefficient α :

$$\alpha = \frac{\text{area I}}{\text{area II}}$$

2.1.2. Classification of Binary Isotherms.

Ion-exchange isotherms may be classified on the basis of their shapes (Townsend, 1977; Fletcher, 1979). Although the classification is relatively simple, interpretation of the isotherm shapes in terms of ion-exchange mechanisms is very difficult. This is because the isotherm does not give any direct information on the selectivity of the zeolite for an ion in each individual site, but gives an averaged selectivity over all the cation sites (Barrer and Falconer, 1956; Barrer and Klinowski, 1972; 1977). A further problem exists in that especially when the two exchanging ions have different valencies, the isotherm shape changes as the total normality of the solution phase is changed (Barrer and Klinowski, 1974; Barri and Rees, 1980).

Figure 2.2 illustrates the general shapes of the isotherm types defined in the classification.

Isotherms of type (a) are characteristic of systems where the zeolite shows a strong preference for the outgoing ion, B, at all or most compositions. Similarly in type (b) isotherms, the zeolite shows a strong preference for the ingoing ion, A. Examples of type (a) isotherms are the exchange of lithium into zeolites NaA (Sherry and Walton, 1967), NaX (Sherry, 1966) and KX (Parakrama, 1983). Examples of type (b) isotherms are the exchange of calcium and strontium into NaA (Sherry and Walton, 1967).

Type (c) and (d) isotherms are similar to types (a) and (b) but in these cases the complete replacement of ion B is not possible. Partial exchange may occur when the ingoing ion is too large, either in the bare or hydrated state, to enter part of the zeolite structure (Sherry, 1966). Incomplete exchange may also be due to the available space in the channels and cages of the zeolite being filled by a large ion before complete exchange has been achieved. This has been observed for the exchange of alkylammonium ions into clinoptilolite (Barrer and Sammon, 1955). Barrer and Sammon (1955) also suggested that highly charged cations may be excluded from some zeolites due to the formation of local excesses of negative charge on the framework when, for example, three sodium ions are replaced by one lanthanum ion. Not all occurrences of partial exchange can be explained in these terms, however. Barri and Rees (1980) observed that exchange of magnesium into zeolite CaA at 65°C, terminated at 40%, whilst much higher levels of magnesium exchange occurred in zeolite NaA.

Examples of type (c) isotherms include the exchange of cobalt and nickel into ammonium mordenite (Barrer and Townsend, 1976). Examples of type (d) isotherms are the exchange of ammoniated silver into NaY and Na mordenite (Fletcher and Townsend, 1980).

Types (e), (e'), (f) and (f') isotherms are characterised by a sigmoid curve; types (f) and (f') also exhibit partial

exchange. Type (e) and (f) isotherms are characteristic of systems where the zeolite shows little preference for either ion and where the selectivity changes little with composition. Systems exhibiting type (e') and (f') exchanges clearly show very different selectivities to those of type (e) and (f). In types (e') and (f') the sigmoidal shape is very pronounced and in some cases there is an almost vertical portion to the curve. The strong selectivity reversals may indicate the presence of at least two cation sites exhibiting very different selectivities but this may not always be the case. Examples of sigmoidal isotherms include: type (e) K-Na exchange in zeolite X (Franklin, 1984); type (e'), Rb-Na exchange in zeolite P (Barrer and Munday, 1971); type (f), Cu and Mn exchange into ammonium mordenite (Barrer and Townsend, 1976); and type (f'), Mg-Na exchange in zeolite A (Franklin, 1984).

Irreversible exchange may occur in zeolites when precipitation of one of the ions occurs within the zeolite framework (e.g., lead in zeolites NaX and NaY (O'Connor and Townsend, 1985)) or when impurities within the zeolite dissolve out during exchange (Loizidou, 1982). Irreversibility may also result from redistribution of ions in the zeolite as a result of drying (Townsend, 1977).

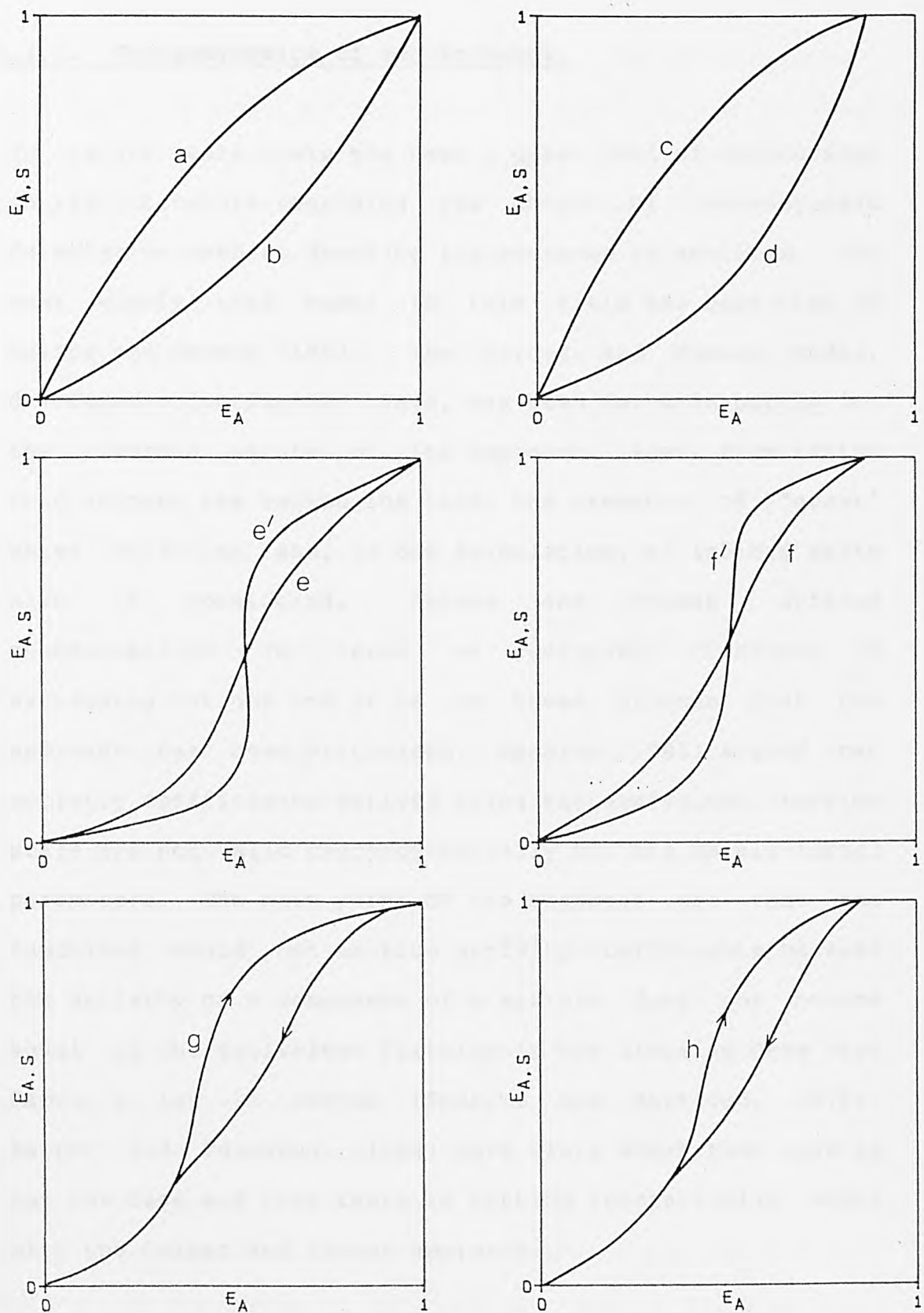


Figure 2.2:
Classification of Binary Ion-Exchange Isotherms.
See Text for Explanation.

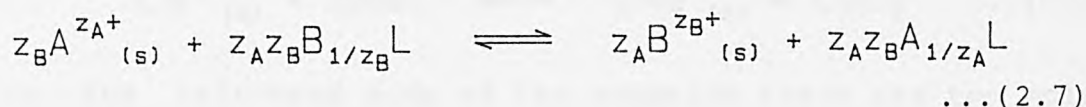
2.1.3. Thermodynamics of Ion-Exchange.

In recent years there has been a great deal of controversy in the literature regarding the choice of thermodynamic formulation used to describe ion-exchange in zeolites. The most widely used model in this field has been that of Gaines and Thomas (1953). The Gaines and Thomas model, developed primarily for clays, has been favoured partly for the rigorous nature of its approach. Apart from taking into account the exchanging ions, the presence of "guest" water molecules and, in one formulation, of imbibed salts also is considered. Gaines and Thomas defined concentrations in terms of equivalent fractions of exchanging cations and it is on these grounds that the approach has been criticised. Sposito (1981) argued that activity coefficients derived using the equivalent fraction scale are not valid thermodynamically but are merely formal parameters. The main point of the argument was that the functions could not be true activity coefficients because the activity of a component of a mixture does not become equal to the equivalent fraction in the limiting case when Raoult's law is obeyed (Sposito and Mattigod, 1979). Barrer and Townsend (1984) have since shown that this is not the case and that there is nothing intrinsically wrong with the Gaines and Thomas approach.

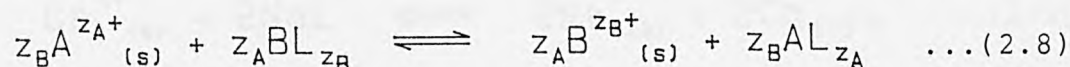
The problem arises because it is possible to write the exchange reaction in two different (though equally valid)

ways. These are either in terms of moles of exchanging ions (in which case the components in the zeolite lattice are AL_{z_A} and BL_{z_B}), or in terms of equivalents of exchanging ions (the components then being $A_{1/z_A}L$ and $B_{1/z_B}L$). Here L represents a part of the zeolite lattice containing one mole of negative charge. These two conventions give rise to three recognised formal treatments for determining zeolite phase activity coefficients and consequently the equilibrium constant for exchange.

Gapon (1933) formulated the reaction equation as follows:



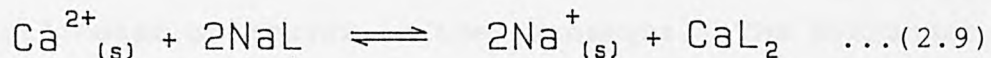
Alternatively, the equation may be expressed in an exactly equivalent manner by the more commonly used formulation due to Vanselow (1932):



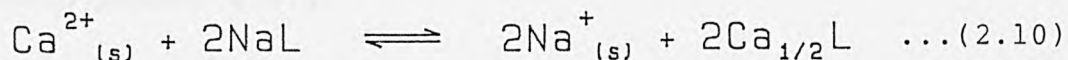
Using the Gapon (1933) equation it is then logical to define the concentrations of the exchanging species in terms of a mole fraction which differs from the Vanselow choice. However, Gaines and Thomas (1953) used the Vanselow reaction equation but expanded the exchanger phase activities in terms of cationic equivalent fractions (cf. equations 2.2 and 2.3). This approach, while correct mathematically, mixes the two concentration scales (X_i and

E_i) and leads to a more complicated formulation than is seen for either of the other two (Barrer and Townsend, 1984; Townsend, 1986). This point will be discussed further in the following sections.

For heterovalent exchange the form of the Vanselow reaction equation requires a change in the number of moles of zeolite on exchange. To illustrate the point, consider the exchange of sodium and calcium. Using the Vanselow formulation the equation is



On the left-hand side of the equation there are two moles of sodium zeolite but on the right-hand side there is only one mole of calcium zeolite. Writing the same equation according to the Gapon formulation gives



In this case the number of moles of zeolite remains constant. For this reason, concentrations defined in terms of Gapon mole fractions happen to equal numerically concentrations defined in terms of equivalent fractions. This matter is discussed further in ensuing sections. Throughout this thesis, a formulation based on Gapon's choice of mole has been followed.

2.1.3.1. The Gapon Mole Fraction Formulation.

Hogfeldt, Ekedahl and Sillen (1950) first developed a model for the thermodynamic treatment of ion-exchange based on the Gapon formulation of the reaction equation, and with concentrations expressed in terms of Gapon's definition of mole fraction, for resins. Using the same definition of standard states as adopted by Gaines and Thomas (1953) the Gapon mole fraction formulation is developed as follows.

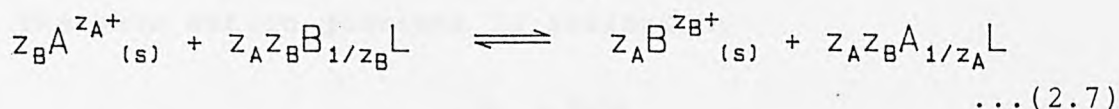
The Gaines and Thomas model takes into account the presence of "guest" water molecules in the exchanger. The exchanger imbibes water and the degree of imbibition can be different for different ion-exchanged forms; therefore the exchanger phase is considered to comprise the wet solid. The standard states then follow. For water the standard state is chosen such that the activity of the water is the same in each phase, i.e.,

$$a_w = a_{w,s} = a_{w,v} \quad \dots(2.11)$$

where a_w , $a_{w,s}$, and $a_{w,v}$ are the activities of the water in the exchanger phase, solution phase and vapour phase respectively. Using Raoult's law to define ideality (Barrow, 1973), the exchanger phase standard state is then the homoionic zeolite immersed in an infinitely dilute solution of the same ion.

Applying these principles to the Gapon mole fraction formulation, it is clear that when $E_A = 1$ then $a_A = 1$, $h_A = 1$ and $a_w = 1$, and when $E_B = 1$ then $a_B = 1$, $h_B = 1$ and $a_w = 1$. Here a_A , a_B , h_A and h_B are the activities and activity coefficients respectively, of ions A and B in the zeolite.

Referring again to the Gapon equation:



The equilibrium constant is then defined as

$$K_a = \frac{a_{B,s}^{z_A}}{a_{A,s}^{z_B}} \cdot \frac{a_A^{z_A z_B}}{a_B^{z_A z_B}} \quad \dots(2.12)$$

where $a_{A,s}$ and $a_{B,s}$ are the activities of ions A and B in solution.

The equilibrium constant can now be expanded in terms of concentrations and the appropriate activity coefficients to give:

$$K_a = \frac{(m_B \gamma_B)^{z_A}}{(m_A \gamma_A)^{z_B}} \cdot \left[\frac{E_A h_A}{E_B h_B} \right]^{z_A z_B} \quad \dots(2.13)$$

where h_A , h_B are activity coefficients of A and B in association with their equivalent amount of lattice.

γ_A , γ_B are "individual ion activity coefficients" of species A^{z_A+} and B^{z_B+} in solution.

The Gapon mole fraction, x_i , is defined by

$$x_i = \frac{n_{i1/z_i} L}{n_{A1/z_A} L + n_{B1/z_B} L} = E_i \quad \dots(2.14)$$

In equation 2.14 the numerical equivalence between the Gapon mole fraction x and the cationic equivalent fraction E is shown, as referred to in the previous section.

The mass action quotient is defined by

$$K_{M,E} = \frac{m_B^{z_A}}{m_A^{z_B}} \cdot \frac{E_A^{z_A z_B}}{E_B^{z_A z_B}} \quad \dots(2.15)$$

Combining equations 2.13 and 2.15 gives the relationship between K_a and $K_{M,E}$:

$$K_a = K_{M,E} \cdot \frac{\gamma_B^{z_A}}{\gamma_A^{z_B}} \cdot \left[\frac{h_A}{h_B} \right]^{z_A z_B} \quad \dots(2.16)$$

It is convenient at this point to introduce a third quotient which is used to describe the exchange reaction. This includes a solution phase activity correction and so is often called a corrected selectivity quotient though, for convenience here, we will refer to it as the Hogfeldt corrected selectivity quotient.

$$K_H = \Gamma \cdot K_{M,E} \quad \dots(2.17)$$

where Γ is the solution phase activity correction factor:

$$\Gamma = (\gamma_B^{z_A} / \gamma_A^{z_B}) \quad \dots(2.18)$$

Also, it is clear that

$$K_a = K_H \cdot \left[\frac{h_A}{h_B} \right]^{z_A z_B} \quad \dots(2.19)$$

The Gibbs-Duhem equation is now introduced:

$$\sum_i n_i d\mu_i = 0 \quad \dots(2.20)$$

n_i is the number of moles of the i^{th} component.

By definition the chemical potential μ is given by

$$\mu_i = \mu_i^\theta + RT \ln a_i \quad \dots(2.21)$$

or
$$d\mu_i = RT d \ln a_i \quad \dots(2.22)$$

since μ_i^θ is a constant.

For a three component system the Gibbs-Duhem equation is

$$n_{A_{1/z_A}L} d \ln a_A + n_{B_{1/z_B}L} d \ln a_B + n_w d \ln a_w = 0 \quad \dots(2.23)$$

since the RT terms cancel. a_w is the activity of the water in the zeolite.

In this case $n_{A_{1/z_A}L}$ and $n_{B_{1/z_B}L}$ refer to the number of moles of species $A_{1/z_A}L$ and $B_{1/z_B}L$ (which happens to be the number of equivalents of A^{z_A+} and B^{z_B+} in the zeolite).

Therefore, since

$$x_i = \frac{n_{i_{1/z_i}L}}{n_{A_{1/z_A}L} + n_{B_{1/z_B}L}} = E_i \quad \dots(2.14)$$

dividing equation 2.22 throughout by $(n_{A_{1/z_A}L} + n_{B_{1/z_B}L})$ gives:

$$E_A d\ln a_A + E_B d\ln a_B + \nu_{W,H} d\ln a_W = 0 \quad \dots(2.24)$$

where

$$\nu_{W,H} = \frac{n_W}{n_{A_{1/z_A}L} + n_{B_{1/z_B}L}} \quad \dots(2.25)$$

Expanding equation 2.24:

$$E_A d\ln(E_A h_A) + E_B d\ln(E_B h_B) + \nu_{W,H} d\ln a_W = 0 \quad \dots(2.26)$$

and since $x.d\ln x = dx$

$$dE_A + dE_B + E_A d\ln h_A + E_B d\ln h_B + \nu_{W,H} d\ln a_W = 0 \quad \dots(2.27)$$

Since $E_A = 1 - E_B$, $dE_A = -dE_B$, and therefore

$$E_A d\ln h_A + E_B d\ln h_B + \nu_{W,H} d\ln a_W = 0 \quad \dots(2.28)$$

The logarithmic form of equation 2.18 is:

$$\ln K_a = \ln K_H + z_A z_B \ln h_A - z_A z_B \ln h_B \quad \dots(2.29)$$

Differentiating:

$$0 = d\ln K_H + z_A z_B d\ln h_A - z_A z_B d\ln h_B \quad \dots(2.30)$$

since K_a is a constant.

Combining equations 2.28 and 2.30:

$$E_A d\ln h_A + E_B d\ln h_A + \frac{E_B}{z_A z_B} d\ln K_H + \nu_{W,H} d\ln a_W = 0 \quad \dots(2.31)$$

Rearranging:

$$d \ln h_A = - \frac{E_B}{Z_A Z_B} d \ln K_H - \nu_{W,H} d \ln a_w \quad \dots(2.32)$$

Also:

$$E_A d \ln h_B + E_B d \ln h_B - \frac{E_B}{Z_A Z_B} d \ln K_H + \nu_{W,H} d \ln a_w = 0 \quad \dots(2.33)$$

So that

$$d \ln h_B = \frac{E_B}{Z_A Z_B} d \ln K_H - \nu_{W,H} d \ln a_w \quad \dots(2.34)$$

Integrating first equation 2.32:

$$\int_{\ln h_A(E_B=0)}^{\ln h_A(E_B)} d \ln h_A = \frac{1}{Z_A Z_B} \int_{\ln K_H(E_B=0)}^{\ln K_H(E_B)} E_B d \ln K_H + W_1 \quad \dots(2.35)$$

where

$$W_1 = - \int_{\ln a_w(E_B=0), I}^{\ln a_w(E_B), I} \nu_{W,H}^{(AB)} d \ln a_w - \int_{\ln a_w=0(E_B=0), I=0}^{\ln a_w(E_B=0), I} \nu_{W,H}^{(A)} d \ln a_w \quad \dots(2.36)$$

I is the ionic strength. Thus, for example, in the second integral the integration is carried out from an infinitely dilute solution to the ionic strength of the experimental solution.

$\nu_{W,H}^{(AB)}$ and $\nu_{W,H}^{(A)}$ are the values of $\nu_{W,H}$ at $E_B=0$ and at a composition E_A, E_B respectively. ($\ln h_A = 0$ when $E_B = 0$ (i.e. when $E_A = 1$)).

Therefore:

$$\ln h_A = \frac{-1}{Z_A Z_B} \int_{\ln K_H(E_B=0), 0}^{\ln K_H(E_B), E_B} d(E_B \ln K_H) + \frac{1}{Z_A Z_B} \int_{E_B=0}^{E_B} \ln K_H dE_B + W_1 \quad \dots (2.37)$$

$$\ln h_A = \frac{-1}{Z_A Z_B} E_B \ln K_H + \frac{1}{Z_A Z_B} \int_0^{E_B} \ln K_H dE_B + W_1 \quad \dots (2.38)$$

or, in terms of E_A :

$$\ln h_A = \frac{E_A}{Z_A Z_B} \ln K_H - \frac{1}{Z_A Z_B} \ln K_H + \frac{1}{Z_A Z_B} \int_{E_A}^{E_A=1} \ln K_H dE_A + W_1 \quad \dots (2.39)$$

Following a similar procedure for h_B :

$$\int_{\ln h_B(E_A=0)}^{\ln h_B(E_A)} d \ln h_B = \frac{1}{Z_A Z_B} \int_{\ln K_H(E_A=0)}^{\ln K_H(E_A)} E_A d \ln K_H + W_2 \quad \dots (2.40)$$

where

$$W_2 = - \int_{\ln a_W(E_A=0)}^{\ln a_W(E_A)} \nu_{W,H}^{(AB)} d \ln a_W - \int_{\ln a_W=0(E_A=0)}^{\ln a_W(E_A=0)} \nu_{W,H}^{(B)} d \ln a_W \quad \dots (2.41)$$

and $\nu_{W,H}^{(B)}$ is the value of $\nu_{W,H}$ at $E_A = 0$

$$\ln h_B = \frac{1}{Z_A Z_B} E_A \ln K_H + \frac{1}{Z_A Z_B} \int_0^{E_A} \ln K_H dE_A + W_2 \quad \dots (2.42)$$

Substituting equations 2.39 and 2.42 into equation 2.29, and simplifying gives:

$$\ln K_a = \int_0^1 \ln K_H dE_A + W_3 \quad \dots(2.43)$$

$$W_3 = Z_A Z_B (W_1 - W_2), \text{ or}$$

$$W_3 = -Z_A Z_B \left[\int_{\ln a_W(E_B=0)}^{\ln a_W(E_A=0)} \nu_{W,H}^{(AB)} d \ln a_W - \int_{\ln a_W=0(E_B=0)}^{\ln a_W(E_B=0)} \nu_{W,H}^{(A)} d \ln a_W + \int_{\ln a_W=0(E_A=0)}^{\ln a_W(E_A=0)} \nu_{W,H}^{(B)} d \ln a_W \right] \quad \dots(2.44)$$

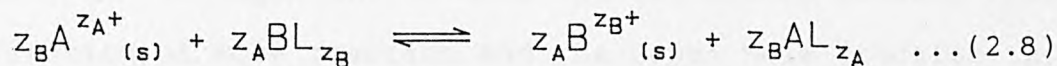
or more succinctly:

$$W_3 = Z_A Z_B \int_{\ln a_W=0(E_A=1, I=0)}^{\ln a_W=0(E_B=1, I=0)} \nu_{W,H} d \ln a_W \quad \dots(2.45)$$

Barrer and Klinowski (1974) have shown that for ion-exchange in zeolites, the first integral in equation 2.44 is usually small. Also, the last two integrals, although individually quite large, are generally nearly self cancelling. W_3 may often therefore be neglected in the calculation of K_a . Since the last two integrals in equation 2.44 may be of significant size in themselves it is dubious whether W_1 and W_2 should be neglected when calculating the zeolite phase activity coefficients. Despite this these terms are commonly ignored.

2.1.3.2. The Cationic Mole Fraction Approach.

If the exchange reaction is described according to the Vanselow reaction equation, i.e:



then the equilibrium constant is defined by:

$$K_a = \frac{a_{B,s}^{z_A}}{a_{A,s}^{z_B}} \cdot \frac{\alpha_A^{z_B}}{\alpha_B^{z_A}} \quad \dots(2.46)$$

The equilibrium constant must be the same whichever reaction equation is used, therefore it is clear that $a_A \neq \alpha_A$ and $a_B \neq \alpha_B$ unless $z_A = z_B = 1$.

Neglecting the water terms, expansion of the Gibbs-Duhem equation (eqn. 2.20) leads to:

$$n_{AL_{z_A}} d \ln \alpha_A + n_{BL_{z_B}} d \ln \alpha_B = 0 \quad \dots(2.47)$$

In this case $n_{AL_{z_A}}$, $n_{BL_{z_B}}$ refer to the number of moles of species AL_{z_A} and BL_{z_B} , i.e. the number of moles of ions A^{z_A+} and B^{z_B+} , with activities α_A and α_B , in the zeolite.

The cationic mole fraction approach derived by Argersinger, Davidson and Bonner (1950) is formulated in terms of the

Vanselow mole fraction X_i defined by:

$$X_i = \frac{n_{iLz_i}}{n_{ALz_A} + n_{BLz_B}} \quad \dots(2.48)$$

Again it is important to note the difference between this definition of mole fraction and the Gapon mole fraction x_i (equation 2.23). In this case the zeolite phase activities are expanded to give:

$$a_i = X_i f_i \quad \dots(2.49)$$

Dividing equation 2.47 throughout by $(n_{ALz_A} + n_{BLz_B})$ and simplifying leads to:

$$X_A d \ln f_A + X_B d \ln f_B = 0 \quad \dots(2.50)$$

In this approach the corrected selectivity quotient K_V is defined by:

$$K_V = \frac{a_{B,s}^{z_A}}{a_{A,s}^{z_B}} \cdot \frac{X_A^{z_B}}{X_B^{z_A}} \quad \dots(2.51)$$

so that

$$K_a = K_V \cdot \frac{f_A^{z_B}}{f_B^{z_A}} \quad \dots(2.52)$$

or

$$0 = d \ln K_V + z_B d \ln f_A - z_A d \ln f_B \quad \dots(2.53)$$

Combining equations 2.50 and 2.53 leads finally to:

$$z_B \ln f_A = -E_B \ln K_V + \int_0^{E_B} \ln K_V dE_B \quad \dots(2.54)$$

$$z_A \ln f_B = E_A \ln K_V - \int_0^{E_A} \ln K_V dE_A \quad \dots(2.55)$$

and, for K_a :

$$\ln K_a = \int_0^1 \ln K_V dE_A \quad \dots(2.56)$$

It is interesting to note that, although the formulation is in terms of cationic mole fractions, the dependent variables f_A , f_B and the function K_a are expressed in terms of equivalent fractions. This follows unavoidably once equations 2.50 and 2.53 are combined.

2.1.3.3. The Gaines and Thomas Approach.

The Gaines and Thomas (1953) approach involves equivalent fractions defined by:

$$E_i = \frac{z_i n_{iL} z_i}{z_A n_{AL} z_A + z_B n_{BL} z_B} \quad \dots(2.57)$$

The zeolite phase activities are expanded to give:

$$\alpha_i = E_i g_i \quad \dots(2.58)$$

Equation 2.47 is then multiplied by $z_A z_B / (z_A n_{AL} z_A + z_B n_{BL} z_B)$ to give, after simplifying:

$$(z_B - z_A) dE_A + z_B E_A d \ln g_A + z_A E_B d \ln g_B = 0 \quad \dots(2.59)$$

The corrected selectivity quotient is defined by:

$$K_G = \frac{a_{B,s}^{z_A}}{a_{A,s}^{z_B}} \cdot \frac{E_A^{z_B}}{E_B^{z_A}} \quad \dots(2.60)$$

so that

$$K_a = K_B \cdot \frac{g_A^{z_B}}{g_B^{z_A}} \quad \dots(2.61)$$

or

$$0 = d \ln K_B + z_B d \ln g_A - z_A d \ln g_B \quad \dots(2.62)$$

Combining equations 2.59 and 2.62 leads finally to:

$$z_B \ln g_A = (z_B - z_A) E_B - E_B \ln K_B + \int_0^{E_B} \ln K_B dE_B \quad \dots(2.63)$$

and

$$z_A \ln g_B = -(z_B - z_A) E_A + E_A \ln K_B - \int_0^{E_A} \ln K_B dE_A \quad \dots(2.64)$$

Combining equations 2.62, 2.63 and 2.64 gives an equation for K_a such that:

$$\ln K_a = (z_B - z_A) + \int_0^1 \ln K_B dE_A \quad \dots(2.65)$$

2.1.3.4. Comparison of the Thermodynamic Formulations.

Looking again at the formulation based on Gapon's definition of the mole, equation 2.28 states:

$$E_A d\ln h_A + E_B d\ln h_B + \nu_{W,H} d\ln a_w = 0 \quad \dots(2.28)$$

Now, for ideal behaviour, h_A and h_B must be unity for all E_A, E_B . Therefore:

$$\nu_{W,H} d\ln a_w = 0 \quad \dots(2.66)$$

so that $a_w = 1$ for all E_A, E_B for ideal behaviour.

Similarly, the cationic mole fraction approach (including the water term) leads to:

$$X_A d\ln f_A + X_B d\ln f_B + \nu_{W,V} d\ln \alpha_w = 0 \quad \dots(2.67)$$

where

$$\nu_{W,V} = n_w / (n_{ALz_A} + n_{BLz_B}) \quad \dots(2.68)$$

and following a similar argument $a_w = 1$ for all E_A, E_B for ideal behaviour.

However using the Gaines and Thomas approach, we obtain:

$$(z_B - z_A) dE_A + z_B E_A d\ln g_A + z_A E_B d\ln g_B + z_A z_B \nu_{W,G} d\ln \alpha_w = 0 \quad \dots(2.69)$$

where
$$\nu_{W,G} = n_W / (Z_A n_{ALZ_A} + Z_B n_{BLZ_B}) \quad \dots(2.70)$$

Again, for ideal behaviour, $g_A = g_B = 1$ for all E_A, E_B , and equation 2.69 becomes:

$$(Z_B - Z_A) dE_A + Z_A Z_B \nu_{W,G} d \ln \alpha_W = 0 \quad \dots(2.71)$$

Thus for ideal behaviour:

$$d \ln \alpha_W = \frac{-(Z_B - Z_A)}{Z_A Z_B \nu_{W,G}} \cdot dE_A \quad \dots(2.72)$$

Obviously, this is an overly complicated and clumsy definition of ideal behaviour.

The equation for K_a which follows from Gapon's choice of mole is:

$$\ln K_a = \int_0^1 \ln K_H dE_A + W_3 \quad \dots(2.43)$$

If the system is behaving ideally, by definition $K_H = K_a$ for all E_A, E_B since $h_A = h_B = 1$ for all compositions.

If this is the case, from equations 2.45 and 2.66, the right-hand side of equation 2.43 reduces to K_a and the equation is consistent. The same conclusion holds for the cationic mole fraction approach.

However, if we neglect the water terms, K_a derived by the Gaines and Thomas approach is given by:

$$\ln K_a = (Z_B - Z_A) + \int_0^1 \ln K_G dE_A \quad \dots (2.65)$$

One of the ambiguities of the Gaines and Thomas approach is now revealed. If, for the ideal case, K_G is replaced by K_a , equation 2.65 then becomes:

$$\ln K_a = (Z_B - Z_A) + \ln K_a \quad \dots (2.73)$$

This equation is inconsistent with the requirement that for the ideal case, for all E_A, E_B , then since $g_A = g_B = 1$, K_a should equal K_G . This inconsistency has now been resolved (Townsend, 1986), as follows.

If the water term is included in equation 2.65, it becomes:

$$\ln K_a = (Z_B - Z_A) + \int_0^1 \ln K_G dE_A - Z_A Z_B \int_{\ln a_w=0(E_A=1, I=0)}^{\ln a_w=0(E_B=1, I=0)} \nu_{w,G} d \ln a_w \quad \dots (2.74)$$

For ideal behaviour we can substitute K_a for K_G and $d \ln a_w$ can be replaced by equation 2.72 to give:

$$\ln K_a = (Z_B - Z_A) + \ln K_a - Z_A Z_B \int_1^0 \frac{-\nu_{W,G}(Z_B - Z_A)}{Z_A Z_B \nu_{W,G}} \cdot dE_A \quad \dots(2.75)$$

or

$$\ln K_a = (Z_B - Z_A) + \ln K_a - (Z_B - Z_A) \quad \dots(2.76)$$

and the equation is consistent (Townsend, 1986).

2.1.3.5. Thermodynamic Procedure for Partial Exchange.

As discussed in section 2.1.2, the extent of ion-exchange in some systems may be limited by partial exchange. In these cases the composition $E_A = 1$ is never attained and so the integral in equation 2.43 cannot be evaluated.

For cases of partial exchange, the thermodynamic quantities may be obtained by normalising the isotherm data (Barrer, Klinowski and Sherry, 1973). This operation consists of dividing all the values of E_A by the maximal value obtained experimentally, i.e. $E_A(\text{max})$. Thus:

$$E_A^{(N)} = E_A / E_A(\text{max}) \quad \dots(2.77)$$

Also:

$$E_B^{(N)} = 1 - E_A^{(N)} \quad \dots(2.78)$$

where $E_A^{(N)}$ and $E_B^{(N)}$ are the normalised equivalent fractions of A and B in the zeolite.

In effect, this operation implies that those ions and sites with which, and into which, the counter ion A^{Z_A+} does not exchange may be regarded as part of the zeolite lattice, and not involved in exchange. They may still however affect the exchange equilibrium but this is allowed for in the activity coefficients.

2.1.3.6. The Solution Phase Correction.

In section 2.1.3 it was shown that the solution phase correction factor Γ was given by:

$$\Gamma = (\gamma_B^{z_A} / \gamma_A^{z_B}) \quad \dots(2.17)$$

Although the absolute values of γ_A and γ_B (which are individual ion activity coefficients) cannot be found, the ratio Γ can still be calculated.

For the salt AX, a mean ionic activity coefficient is defined by:

$$\gamma_{\pm AX}^{(z_A+z_X)} = \gamma_A^{z_X} \cdot \gamma_X^{z_A} \quad \dots(2.79)$$

Expressed logarithmically this becomes:

$$\ln \gamma_{\pm AX} = \frac{1}{z_A+z_X} (z_X \ln \gamma_A + z_A \ln \gamma_X) \quad \dots(2.80)$$

and for salt BX:

$$\ln \gamma_{\pm BX} = \frac{1}{z_B+z_X} (z_X \ln \gamma_B + z_B \ln \gamma_X) \quad \dots(2.81)$$

Multiplying equation 2.80 by $z_B(z_A+z_X)/z_X$ and then rearranging gives:

$$\log (\gamma_B^{z_A} / \gamma_A^{z_B}) = \frac{1}{z_X} (z_A(z_B+z_X) \ln \gamma_{\pm BX} - z_B(z_A+z_X) \ln \gamma_{\pm AX}) \quad \dots(2.82)$$

However, this is not quite what is required since the result is in terms of the experimental mean molal activity coefficients of the pure salts. What is in fact required is a ratio expressed in terms of the individual ion activity coefficients for a mixed salt solution.

$$\log(\gamma_B^{z_A} / \gamma_A^{z_B}) = \frac{1}{z_X} (z_A(z_B + z_X) \ln \gamma_{\pm BX}^{(AX)} - z_B(z_A + z_X) \ln \gamma_{\pm AX}^{(BX)}) \quad \dots(2.83)$$

where $\gamma_{\pm AX}^{(BX)}$ is the mean molal activity coefficient of the salt AX in the presence of salt BX.

Glueckauf (1949) derived expressions for these quantities in terms of the pure salt activity coefficients.

$$\log \gamma_{\pm AX}^{(BX)} = \log \gamma_{\pm AX} - \frac{m_{B,S}}{4I} \left[k_1 \log \gamma_{\pm AX} - k_2 \log \gamma_{\pm BX} - \frac{K_3}{1+I^{1/2}} \right] \quad \dots(2.84)$$

and

$$\log \gamma_{\pm BX}^{(AX)} = \log \gamma_{\pm BX} - \frac{m_{A,S}}{4I} \left[k_4 \log \gamma_{\pm BX} - k_5 \log \gamma_{\pm AX} - \frac{K_6}{1+I^{1/2}} \right] \quad \dots(2.85)$$

where $K_1 = z_B(2z_B - z_A - z_X)$

$$K_2 = z_A(z_B + z_X)^2(z_A + z_X)^{-1}$$

$$K_3 = \frac{1}{2}z_A z_B z_X(z_A - z_B)^2(z_A + z_X)^{-1}$$

$$K_4 = z_A(2z_A - z_B + z_X)$$

$$K_5 = z_B(z_A + z_X)^2(z_B + z_X)^{-1}$$

$$K_6 = \frac{1}{2}z_A z_B z_X(z_B - z_A)^2(z_B + z_X)^{-1}$$

and I is the ionic strength ($I = \frac{1}{2} \sum_i m_i z_i^2$).

3. EXPERIMENTAL.

3.1. Chemical Reagents.

The zeolites used in this study were all obtained "ex-manufacturer" as powders in the sodium form. The materials were donated by Laporte Industries (Widnes), Unilever Research (Port Sunlight), BDH Chemicals Ltd. and Grace Chemical Division. One sample (designated hereafter as NaA (Charnell)) was synthesised in the laboratory using a procedure described by Charnell (1971). All the zeolites were exchanged into the homo-ionic form before use and were stored in the hydrated state over saturated ammonium chloride.

All other chemicals used in the work were purchased from either BDH or Fisons, and were analytical grade reagents.

3.2. Synthesis of Zeolite A

A sample of zeolite A was synthesised in the laboratory using a procedure described by Charnell (1971). Zeolite A crystals were grown by reacting sodium metasilicate with sodium aluminate, using triethanolamine as a stabilising and buffering, or complexing, agent. 100 g of sodium metasilicate nonahydrate ($\text{Na}_2\text{SiO}_3 \cdot 9\text{H}_2\text{O}$) and 100 cm³ of triethanolamine (2,2',-2'',-nitrilotriethanol) were dissolved in 700 cm³ of distilled water. The solution was filtered with the aid of vacuum. The aluminate solution was prepared by dissolving 80 g of sodium aluminate (NaAlO_2) and 100 cm³ of triethanolamine in 700 cm³ of distilled water. The solution was filtered under vacuum.

The aluminate solution was stirred into the silicate solution (forming a gel) in a 1 dm³ polypropylene beaker. The beaker was covered with a large clock glass and placed in a thermostatted water bath at 80°C.

Crystallisation was complete in three weeks. The zeolite crystals were separated from the synthesis solution, washed with distilled water, and dried in an oven at 60°C. The quality and size of the crystals was determined by scanning electron microscopy (SEM) and laser diffractometry.

3.3. Preparation of homoionic Zeolites.

3.3.1. Sodium Zeolites.

The zeolites used were exchanged into the homoionic sodium form by three 24 hour exchanges with 1 mol dm^{-3} sodium nitrate solution at 25°C . After the third exchange the zeolite phase was separated from the solution by centrifugation, washed twice with very dilute sodium hydroxide solution and once with distilled water. The zeolite was then dried overnight in an oven at 60°C and then the dry powder was stored over saturated sodium nitrate solution in a desiccator, allowing at least three weeks for an equilibrium water content to be taken up by the crystals.

3.3.2. Potassium Zeolites.

20 g of the appropriate sodium zeolite required twenty exchanges with 500 cm^3 of 1 mol dm^{-3} potassium nitrate solution to remove greater than 99% of the sodium initially present in the zeolite. The first few exchanges were of one or two hours duration, but subsequent exchanges were allowed to proceed for 24 hours. The zeolite was eventually separated and washed with very dilute potassium hydroxide solution and distilled water, and stored over saturated sodium nitrate solution as above.

3.4. Investigation of Hydronium Exchange.

The exchange reaction between hydronium ions and zeolites A, X and Y was investigated using pH and ion-selective electrodes. An aliquot of zeolite was introduced into a stirred solution of distilled water, dilute acid, or dilute salt, and the pH and cation concentrations were monitored.

Initially the voltage responses of the pH and ion-selective electrodes were monitored using a chart recorder. The pH and the cation concentration were then determined as a function of time from measurements of the positions of the pen traces, using calibration curves. However, this proved unsatisfactory for three reasons: (1) the procedure was very slow and time consuming; (2) the time base of the chart recorder was not very accurate, especially at slower chart speeds; and (3) electrical noise and interferences between the two channels of the chart recorder made it difficult to measure the position of the pen traces accurately. These problems were overcome by interfacing the electrodes with a micro-computer.

3.4.1. Design of Computer Interface.

The computer used to interface the pH and ion-selective electrodes was an Acorn, BBC model B, 32K RAM machine with a 6502 second processor. The second processor expanded the

RAM of the system to 64K and enabled BASIC programs to be run at a faster speed. The main advantage of the BBC computer is that it has a built-in, four channel analogue to digital (A/D) converter. Each of the four inputs can accept voltages in the range 0 - 1.8 V and will produce a corresponding number in the range 0 - 65520. Although the unit is fitted with a 12 bit converter, in practice only 10 bit accuracy can be assumed. The computer used for the interface was slightly modified by the City University Computer Unit. This involved the replacement of a diode in the A/D converter and had the effect of minimising drift and random noise.

Two millivoltmeters were used to measure the voltages generated by the electrodes. The pH electrode was connected to a Corning Eel model 109 pH meter. The ion-selective electrode was connected to an Orion model 701 A digital millivoltmeter. The outputs from these millivoltmeters were connected to a two-channel JJ Instruments CR 652 A chart recorder. The pens of the chart recorder are linked mechanically to two re-directing potentiometers. By applying a voltage across the potentiometer a continuously variable voltage was produced which was proportional to the pen position. This voltage then supplied the input to the A/D converter.

The circuit diagram of the interface is given in figure 3.1. A 1.5 V alkaline "Duracell" cell was used to provide a stable, no-fade voltage across the re-directing

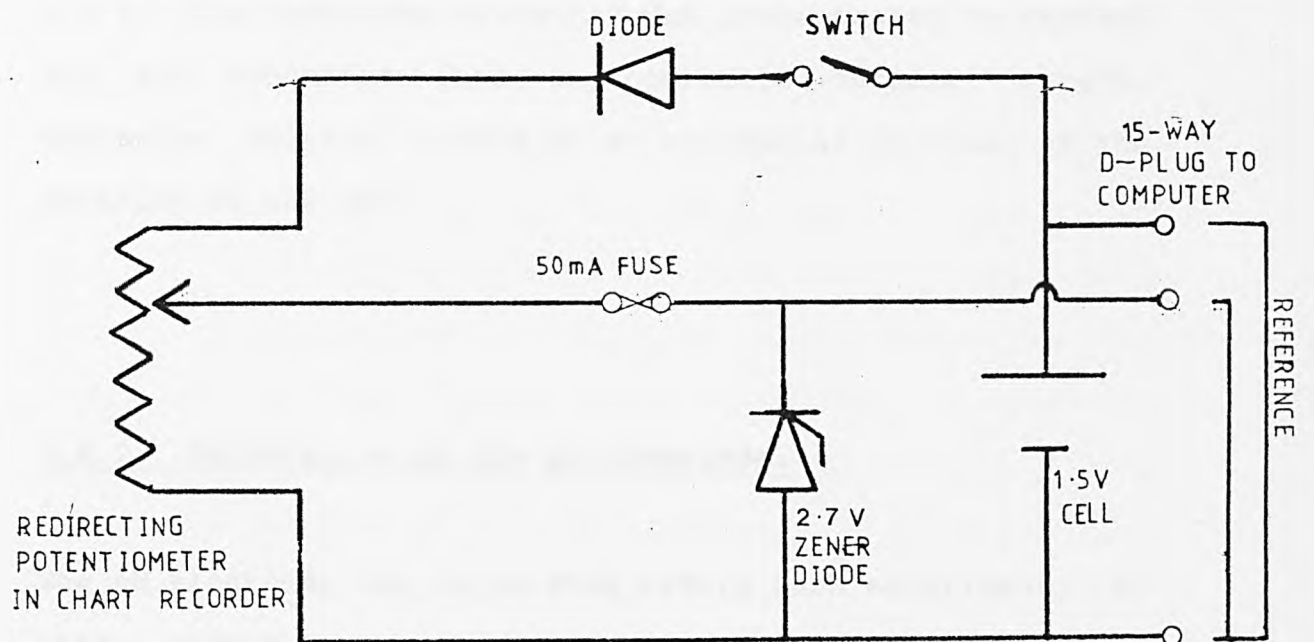


Figure 3.1:
Circuit Diagram of Computer Interface.

potentiometer. A full scale deflection of the pen produced a change in the input voltage to the computer from 0 to 1.5 V. The remaining circuitry was incorporated to protect the A/D converter from any possible current surges, excessive voltage inputs or an accidental reversal of the polarity of the cell.

3.4.2. Calibration of the pH Electrode.

The pH electrode was calibrated before each experiment, at three points in the pH range. Commercial buffer solutions with pH values, at 20°C, of 4.00, 7.01 and 9.24 were used. The combination pH electrode was lowered into a stirred solution of one of the buffers, and the pH value was entered into the computer. When the pH reading was steady, a key was pressed on the computer and the voltage response was recorded. The reading taken by the computer was an average of several hundred measurements taken over a period of two to three seconds. The data were fitted to a straight line ($\text{pH} = f(\text{voltage response})$) by linear regression, and the coefficients of the line were passed to a data file on disc to be read by the interface program.

3.4.3. Calibration of the Ion-Selective Electrode.

The recommendations of the manufacturers state that the ion-selective electrodes should be calibrated and used in solutions with a constant background ionic strength of between 0.1 and 1 mol dm⁻³. Obviously, in order to measure, in real time, the release of cations from a zeolite in contact with distilled water, this was not possible. However, it was found that if the electrode was calibrated under the same conditions as would occur in the subsequent experiment, accurate measurements could still be obtained. The ion-selective electrode was therefore calibrated by step-wise additions of standard solutions of the relevant cation, to a known volume of distilled water. The electrode was very sensitive to electrical noise when used under conditions of very low ionic strength, but by taking time-averaged readings with the computer, most of the noise could be smoothed out.

50 cm³ of very pure distilled water (section 3.4.6) were pipetted into a 100 cm³ polypropylene beaker. The ion-selective electrode, its calomel reference electrode and the combination pH electrode were then lowered into the solution, which was stirred by a magnetic stirrer. It was important for the pH electrode to be also in the solution during the calibration because the reading of the ion-selective electrode was affected, to a small extent, by its presence. The ion-selective electrode was calibrated

in the range 10^{-5} to 4×10^{-3} mol dm $^{-3}$. Standard solutions of 0.1 and 1 mol dm $^{-3}$ were injected into the solution using a 10 or 100 μ l* syringe. The additions are given in table 3.1.

Table 3.1. Addition of Standard solutions in the Calibration Procedure.

<u>μl of solution added</u>	<u>cation concentration / mol dm$^{-3}$</u>
5 (0.1 mol dm $^{-3}$)	1×10^{-5}
5 "	2×10^{-5}
10 "	4×10^{-5}
10 "	6×10^{-5}
10 "	8×10^{-5}
10 "	1×10^{-4}
50 "	2×10^{-4}
100 "	4×10^{-4}
100 "	6×10^{-4}
100 "	8×10^{-4}
100 "	1×10^{-3}
50 (1 mol dm $^{-3}$)	2×10^{-3}
100 "	4×10^{-3}

Using small volume additions meant that the total volume of the added solution was always less than 1% of the volume of the calibration solution, and so this increase could be neglected. If the electrode was calibrated to higher concentrations than 4×10^{-3} mol dm $^{-3}$, separate solutions were made up.

* 1 l = 1 dm 3 within experimental uncertainty.

After each addition, the new cation concentration was entered into the computer and when it had stabilised the reading was taken by pressing a key on the computer. An average of several hundred readings, taken over a period of two to three seconds, was recorded by the computer.

The calibration data were fitted by the computer to a polynomial equation of the form $y = a_0 + a_1x + a_2x^2 \dots$, where y is the negative logarithm of the cation concentration and x is the corresponding voltage reading. The data were fitted "by eye", using the lowest order polynomial which produced a smooth curve, passing through all the points. Usually a third order polynomial was selected. The plot of \log (cation concentration) versus electrode voltage is linear at higher concentrations but becomes non-linear in the low-level region. Once the polynomial fit had been accepted, the coefficients of the equation were passed to a data file on disc, to be read by the interface program.

The listings of the calibration programs are given in Appendix 2.

3.4.4. The Interface Program.

The computer program which was written to monitor the hydronium exchange experiments, measured and recorded the pH and the cation concentration of the solution against an accurate time base. The program first read the coefficients of the fitted equations of the pH and ion-selective electrode calibrations from disc. Data were then recorded by pressing a key on the computer at the same time as the zeolite was added to the solution. The A/D converter of the computer then read in turn the inputs from the pH electrode, the ion-selective electrode, and the external reference voltage. Readings were taken for each point, for periods of between about 0.2 to 3 seconds, according to how far the experiment had proceeded. An average value of the pH, cation concentration and the time of the reading was then calculated and stored in an array. For the first 30 seconds of the experiment, when the pH and the cation concentration was changing rapidly, averages of 50 readings were taken every second; for the next 90 seconds averages of 100 readings were taken every 5 seconds; between one and a half and five minutes, readings were taken every 10 seconds from averages of 200 readings; and after 5 minutes readings were taken every minute from averages of 500 readings. At the end of the run a description and the conditions of the experiment were entered into the computer and all the data were saved to disc for subsequent analysis. The interface program is listed in Appendix 2.

3.4.5. Original Experimental Apparatus.

The design of the original experimental apparatus is illustrated in figure 3.2. The reaction cell consisted of a 100 cm³ polypropylene beaker fitted with a plastic lid. Holes were drilled into the lid to accommodate the combination pH electrode, the ion-selective electrode and its calomel reference electrode, and a nitrogen purge inlet. The electrodes were connected to two millivoltmeters and, through a 2-channel chart recorder and interface, to a BBC model B micro-computer, as described in previous sections. The solution was stirred by a teflon coated magnetic stirrer bar, and was insulated from any heat produced from the stirrer motor by a polystyrene block.

The experiment could be conducted either with the experimental solution in contact with carbon dioxide in the atmosphere, or with a nitrogen purge. It was important to exclude all traces of carbon dioxide from the reaction cell when conducting the experiment under nitrogen; however it was found that there were residual amounts of carbon dioxide in the cylinders of BOC, oxygen-free "white spot" nitrogen which were used. The concentration of carbon dioxide was later measured using a calibrated gas chromatograph, and was found to be 0.0376% in one cylinder. Carbon dioxide was therefore removed from the nitrogen stream by passing the gas through a column containing soda

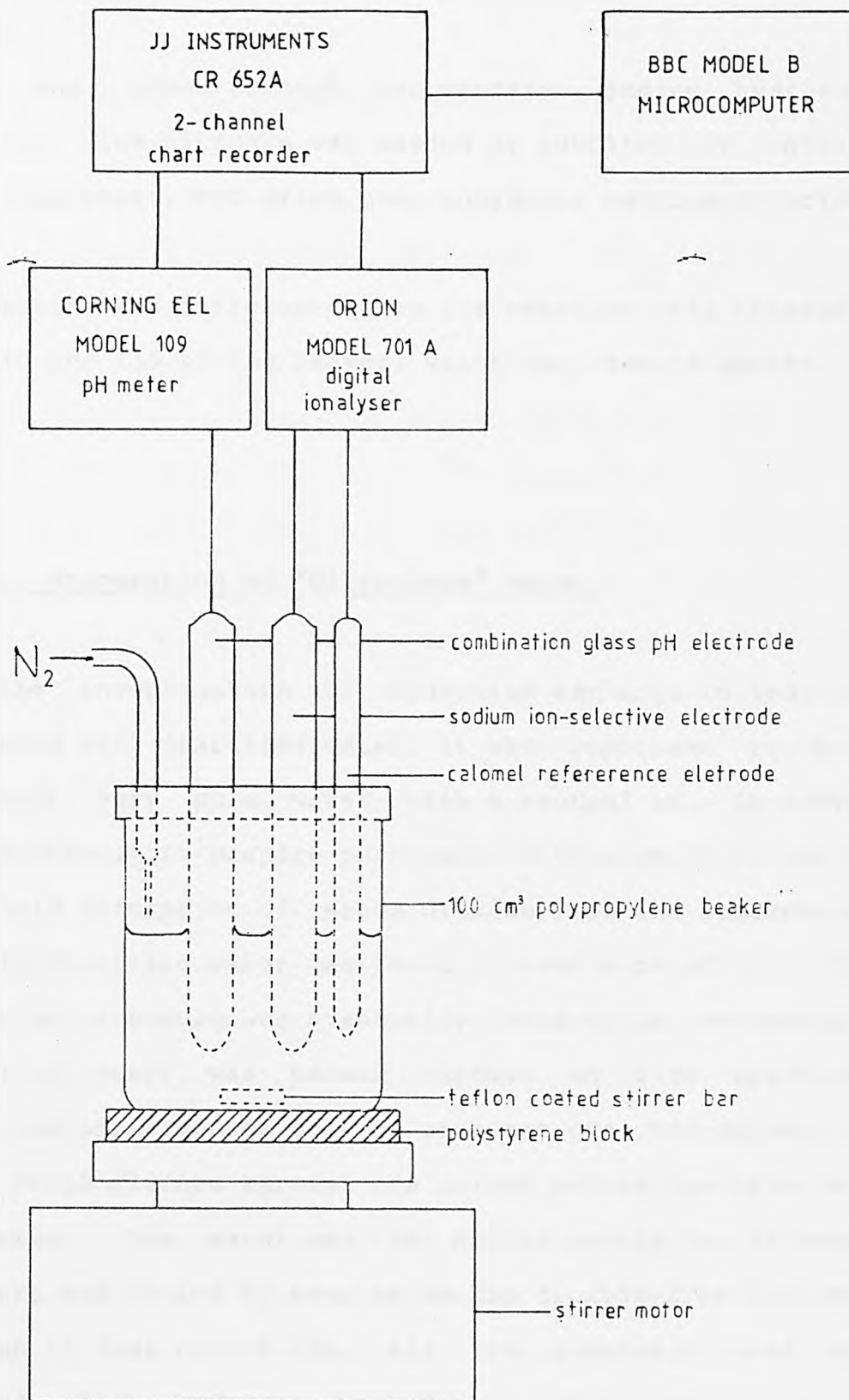


Figure 3.2:
Original Experimental Apparatus.

lime and then through concentrated sodium hydroxide solution. The nitrogen was washed by bubbling it through distilled water, and dried over anhydrous calcium chloride.

The zeolite was introduced into the reaction cell through a hole in the lid of the beaker, which was then re-sealed.

3.4.6. Preparation of "Ultra-Pure" Water.

For the investigation of hydronium exchange in zeolites contacted with distilled water, it was important to have available very pure water with a neutral pH. It proved very difficult to prepare pure water with a pH of 7, due to the rapid absorption of carbon dioxide from the atmosphere. Freshly distilled water was found to have a pH of 5.2. The following procedure was eventually found to be successful. Distilled water was passed through an Elga "Spectrum" mixed-bed ion-exchange column, at least one bed-volume of water being flushed through the column before the water was collected. The water was then boiled gently for at least 24 hours and cooled by passing carbon dioxide-free nitrogen through it just before use. All the glassware used was "Pyrex" which had been washed thoroughly with hot nitric acid, and rinsed copiously with distilled water to remove any sodium from the surface of the glass. The water produced had a pH of between 6.9 and 7.0.

3.4.7. Measurement of Dissolved Carbon Dioxide.

The concentration of dissolved carbon dioxide in solution was measured at the end of each hydronium exchange experiment using an Orion Research carbon dioxide gas-sensing electrode. The zeolite suspension was transferred to a glass centrifuge tube, which was sealed with a rubber bung. The zeolite was separated from the solution by centrifugation at $4,000 \text{ min}^{-1}$ for five minutes. 40 cm^3 of the solution phase were then pipetted into a 100 cm^3 glass beaker. The carbon dioxide electrode was placed in the solution, which was stirred by a magnetic stirrer. The carbonate and hydrogen carbonate ions in solution were converted into free carbon dioxide, which could be detected by the electrode, by adjusting the pH to 5.0. This was achieved by the addition of 10 cm^3 of a buffer solution prepared by mixing 50 cm^3 of potassium hydrogen phthalate (0.1 mol dm^{-3}) with 22.6 cm^3 of sodium hydroxide (0.1 mol dm^{-3}). The response of the electrode was monitored on a chart recorder. The concentration of carbon dioxide rose rapidly as the buffer was added to the solution, reached a maximum, and then gradually began to fall again as the gas diffused out of solution. The concentration was calculated from the maximum reading. The carbon dioxide electrode was calibrated about once a week, by the addition of buffer to standard solutions of sodium hydrogen carbonate, and a calibration curve was drawn. The calibration was checked daily at two points on the curve,

and corrected as necessary.

The result obtained by this method gave the total concentration of the species CO_3^{2-} , HCO_3^- and $\text{CO}_2(\text{aq})$ in solution. From this value, and from the pH, it was possible to calculate the distribution of the different species (section 3.4.10).

3.4.8. Elimination of Evaporation from the Reaction Cell.

Passing a stream of dry nitrogen over the experimental solution eliminated carbon dioxide from the reaction cell but also caused evaporation of water from the cell. This made it difficult to obtain accurate data on the pH and the cation concentration in solution, especially over longer periods of time. The evaporation was prevented by adjusting the partial pressure of water vapour in the nitrogen stream to equal the vapour pressure of water above the experimental solution. This was achieved by the use of a "diffusion cell".

3.4.8.1. Design of the Diffusion cell.

The mole fraction of water vapour in a nitrogen stream could be very carefully controlled by the use of a "diffusion cell". This consists of a flask containing distilled water, connected to a nitrogen stream through a capillary or small bore tube (figure 3.3). The water vapour pressure in the flask is controlled by thermostating the flask in a water bath, and the water vapour pressure in the nitrogen stream can then be calculated using diffusion theory.

3.4.8.2. Theory of the Diffusion Cell.

Considering a binary gas mixture, the unidirectional diffusion of species A in the x direction is described by Fick's first law, viz:

$$J_A = -D_{AB} \cdot \frac{dC_A}{dx} \quad \dots(3.1)$$

where J_{AB} is the flux of gas A in $\text{mol s}^{-1} \text{ cm}^{-2}$,

D_{AB} is the inter diffusion coefficient of gas A in the presence of B, in $\text{cm}^2 \text{ s}^{-1}$,

C_A is the concentration of gas A / mol cm^{-3} ,

and x is the distance in cm.

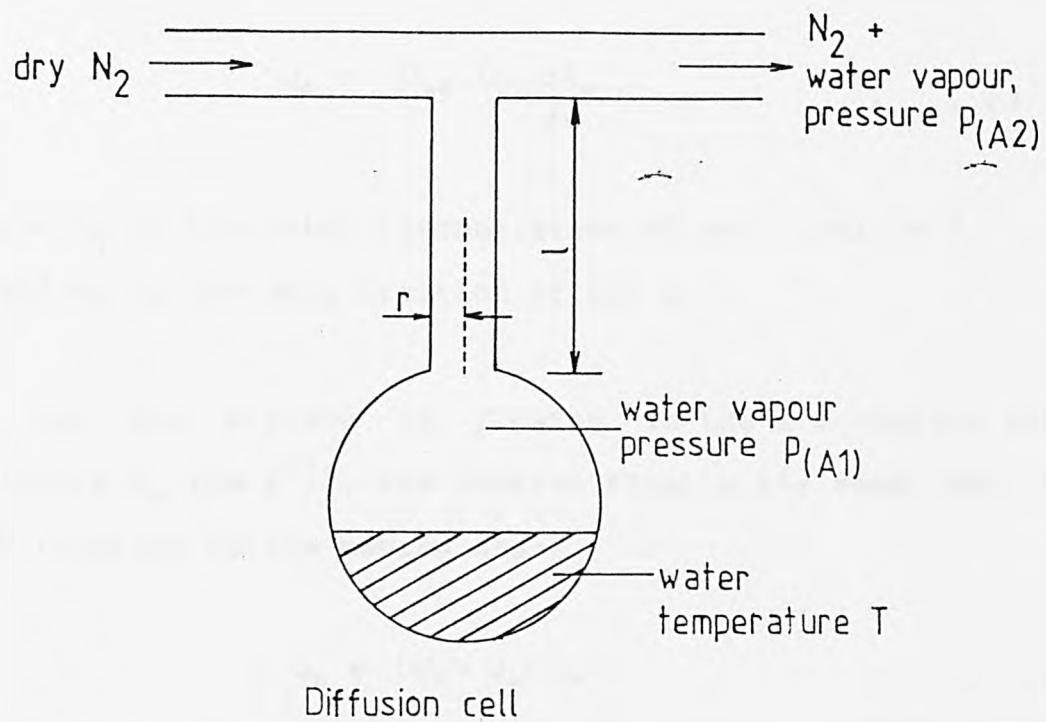


Figure 3.3:
Design of the Diffusion Cell.

In terms of mole fractions:

$$J_A = -D_{AB} \cdot C_T \cdot \frac{dX_A}{dx} \quad \dots(3.2)$$

where C_T is the total concentration of gas / mol cm⁻³,
and X_A is the mole fraction of gas A.

If the gas mixture is flowing in the x direction with velocity U_m (cm s⁻¹), the Fickian flow is the same but is now relative to the moving gas:

$$J_A = (U_A - U_m) C_A \quad \dots(3.3)$$

U_A is the velocity of gas A / cm s⁻¹.

Relative to a fixed coordinate system, the flux of A is found by adding $U_m C_A$ to the expression for J_A . i.e., from equation 3.3:

$$J_A = U_A C_A \quad \dots(3.4)$$

Or from equation 3.2:

$$J_A = U_m C_A - D_{AB} \cdot C_T \cdot \frac{dX_A}{dx} \quad \dots(3.5)$$

For a binary mixture of gases A and B:

$$U_m = C_T (J_A + J_B) \quad \dots(3.6)$$

and

$$U_m C_A = X_A (J_A + J_B) \quad \dots(3.7)$$

Substituting equation 3.7 into equation 3.5 gives:

$$J_A = X_A (J_A + J_B) - D_{AB} \cdot C_T \cdot \frac{dX_A}{dx} \quad \dots(3.8)$$

Considering the diffusion of gas A through a stagnant layer of B, $J_B = 0$. Therefore, equation 3.8 becomes:

$$J_A = J_A X_A - D_{AB} \cdot C_T \cdot \frac{dX_A}{dx} \quad \dots(3.9)$$

Rearranging:

$$J_A dx = \frac{-D_{AB} C_T}{(1-X_A)} dX_A \quad \dots(3.10)$$

If the mole fraction of A is $X_{A(1)}$ at the point x_1 , and $X_{A(2)}$ at x_2 (where $x_2 - x_1 = l$, the length of the capillary), equation 3.10 can be integrated between these limits to give:

$$J_A = \frac{D_{AB} C_T}{l} \ln \left[\frac{1-X_{A(2)}}{1-X_{A(1)}} \right] \quad \dots(3.11)$$

The mole fraction X_A can be replaced by the partial pressure p_A using the relationship:

$$X_A = p_A / p \quad \dots(3.12)$$

where p is the total pressure.

Also, if the gases are assumed to behave ideally, C_T can be replaced by p/RT . Equation 3.11 then becomes:

$$J_A = \frac{D_{AB}P}{RTl} \ln \left[\frac{p-p_{A(2)}}{p-p_{A(1)}} \right] \quad \dots(3.13)$$

The flow of gas A through the capillary, Q_A is given by:

$$Q_A = \pi r^2 J_A \quad \dots(3.14)$$

Substituting equation 3.13 into 3.14:

$$Q_A = \frac{\pi r^2 D_{AB} P}{RTl} \ln \left[\frac{p-p_{A(2)}}{p-p_{A(1)}} \right] \quad \dots(3.15)$$

where r is the radius of the capillary.

The flow of gas A away from the diffusion cell must be equal to the flow through the capillary. Under steady state conditions the partial pressure of A in the carrier gas stream is constant and equal to $p_{A(2)}$:

$$Q_A = QC_A = \frac{Q p_{A(2)}}{RT} \quad \dots(3.16)$$

where Q is the volumetric flow rate of the carrier gas.

Equating equations 3.15 and 3.16 gives:

$$\frac{Q p_{A(2)}}{RT} = \frac{\pi r^2 D_{AB} P}{RTl} \ln \left[\frac{p-p_{A(2)}}{p-p_{A(1)}} \right] \quad \dots(3.17)$$

Simplifying and solving for $p_{A(1)}$ leads to:

$$p_{A(1)} = p + \left[(p_{A(2)} - p) \cdot \exp \left[\frac{-10 p_{A(2)}}{p \pi r^2 D_{AB}} \right] \right] \quad \dots (3.18)$$

Values of the inter diffusion coefficient D_{AB} are available for many pairs of gases but it is possible to calculate D_{AB} as a function of temperature using a theoretical equation. The equation is based on kinetic theory, with allowances made for intermolecular interactions, and includes terms derived from the Lennard-Jones expression for intermolecular forces (Hirschfelder, Curtiss and Bird, 1954). It is given by:

$$D_A = \frac{0.001858 T^{3/2} [(M_A + M_B) / M_A M_B]^{1/2}}{p \sigma_{AB}^2 \Omega_{AB}} \quad \dots (3.19)$$

where T is the absolute temperature / K,

M_A, M_B are the molecular weights of gases A and B
/ g mol⁻¹,

Ω_{AB} is the collision integral, and is a function of
 kT/ϵ_{AB} ,

$\sigma_{AB}, \epsilon_{AB}$ are force constants in the Lennard-Jones
potential function,

k is the Boltzmann constant.

σ and ϵ are available for many pure gases, from tables. If data are not available they may be calculated using the relationships:

$$\sigma = 1.18 V_0^{1/3} \quad \dots(3.20)$$

where V_0 is the molar volume in $\text{cm}^3 \text{mol}^{-1}$, and σ is in Angstroms, and

$$KT/\epsilon = 1.30 T/T_c \quad \dots(3.21)$$

where T_c is the critical temperature of the gas.

σ_{AB} and ϵ_{AB} are evaluated from the sum and product averages respectively:

$$\sigma_{AB} = (\sigma_A + \sigma_B)/2 \quad \dots(3.22)$$

$$\epsilon_{AB} = (\epsilon_A \cdot \epsilon_B)^{1/2} \quad \dots(3.23)$$

Ω_{AB} is determined by calculating kT/ϵ_{AB} for the particular system and finding the corresponding value of Ω_{AB} from tables.

It has been shown that values of D_{AB} calculated using this procedure rarely differ by more than 10% from experimental values (Reid and Sherwood, 1958).

3.4.8.3. Calculation of the Diffusion Cell Parameters.

The temperature required in the diffusion cell to prevent the flow of water vapour in or out of the reaction cell was determined by an iterative procedure using a computer.

Starting with an arbitrary temperature for the diffusion cell T_1 , a value of D_{AB} was calculated using the procedure outlined above. This was then used to calculate $p_{A(1)}$, the water vapour pressure required in the diffusion cell. Using a polynomial function of the form $y = a_0 + a_1x + a_2x^2 \dots$, the temperature required to develop this water vapour pressure could be calculated. This gave a new value of T_1 which was then used to recalculate D_{AB} ... The iteration was continued until T_1 changed by less than 0.0001%.

3.4.9. Re-design of Experimental Apparatus.

Apart from the inclusion of the diffusion cell in the experimental apparatus, several other refinements were also made. The polypropylene beaker was replaced by a 100 cm³ glass polarography cell. The lid to this vessel was closely fitting which meant that the reaction cell was gas-tight even with the electrodes in place. Carbon dioxide-free nitrogen passed into the reaction cell and was vented through a tube containing soda lime. Carbon dioxide was thus totally excluded from the reaction cell. The conventional pH electrode was replaced by Russell low conductivity glass combination pH electrode. This allowed very accurate measurements of pH to be made even in solutions of very low ionic strength. The calomel reference electrode was replaced by a Russell double junction reference electrode, with the outer compartment filled with distilled water. This eliminated any possible contamination of the solution by electrolyte outflowing from the reference electrode. The simple magnetic follower was replaced by a Gallenkamp "non-vortexing stirrer". This is a flat disc of teflon containing a small magnet, with two holes drilled from the sides of the disc through to the opposite faces. The effect was to produce very efficient agitation of the solution without forming a vortex or breaking the surface of the liquid. The major benefit of these changes in the apparatus was to greatly cut down on the noise in the electrodes, and to improve the accuracy of the measurements.

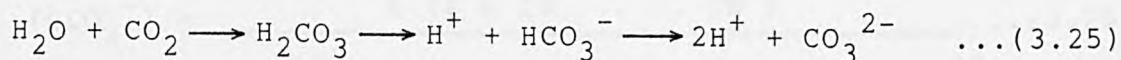
3.4.10. Calculation of Hydronium Exchange.

If the reaction between sodium zeolite and distilled water is just a simple ion-exchange reaction, then the number of equivalents of sodium released must equal the number of equivalents of hydronium ion exchanged. The number of equivalents of hydronium ion exchanged can be calculated from the decrease in concentration of H^+ and the concomitant increase in concentration of OH^- . This is because for each H^+ ion exchanged there is one OH^- ion "in excess"; the solubility product must, however, remain constant at $10^{-14} \text{ mol dm}^{-3}$. The total number of moles of hydronium ion exchanged is therefore given by:

$$[H^+]_i - [H^+]_f + [OH^-]_f - [OH^-]_i \quad \dots(3.24)$$

where $[H^+]_i$, $[OH^-]_i$ are the initial concentrations of H^+ , OH^- , and $[H^+]_f$, $[OH^-]_f$ are the final concentrations of H^+ , OH^- .

When carbon dioxide dissolves in solution the situation is slightly different, because the reaction of CO_2 with water produces "hydrogen carbonate", carbonate and hydronium ions.



Each HCO_3^- ion is associated with one H^+ ion, and each CO_3^{2-} ion with two H^+ ions.

The total CO_2 concentration is determined using a gas-sensing electrode at pH 5; under these conditions more than 98% of the carbon dioxide is present as H_2CO_3 . This measured CO_2 concentration, C , is therefore approximately equal to the total concentration of all the carbon species at the pH of the experimental solution, i.e.

$$C = [\text{H}_2\text{CO}_3] + [\text{HCO}_3^-] + [\text{CO}_3^{2-}] \quad \dots(3.26)$$

The proportion of each individual species can be calculated from the ionisation constants of H_2CO_3 and HCO_3^- (Harned and Scholes, 1941; Harned and Davis, 1943).

$$\frac{[\text{H}^+] [\text{HCO}_3^-]}{[\text{H}_2\text{CO}_3]} = 4.16 \times 10^{-7} \quad \dots(3.27)$$

$$\frac{[\text{H}^+] [\text{CO}_3^{2-}]}{[\text{HCO}_3^-]} = 4.84 \times 10^{-11} \quad \dots(3.28)$$

Solving equations 3.26, 3.27 and 3.28 simultaneously gives the concentrations of the species HCO_3^- and CO_3^{2-} :

$$[\text{HCO}_3^-] = \frac{4.16 \times 10^{-7} \cdot C \cdot [\text{H}^+]}{[\text{H}^+]^2 + 4.16 \times 10^{-7} [\text{H}^+] + 2.01 \times 10^{-17}} \quad \dots(3.29)$$

$$[\text{CO}_3^{2-}] = \frac{C \times 2.07 \times 10^{-17}}{[\text{H}^+]^2 + 4.16 \times 10^{-7} [\text{H}^+] + 2.01 \times 10^{-17}} \quad \dots(3.30)$$

The number of moles of hydronium ions produced by the reaction of CO_2 with water can then be calculated.

3.5. Measurement of Ion-Exchange Isotherms.

The ion-exchange isotherms were constructed by contacting a small amount of zeolite with the appropriate exchange solutions, and allowing equilibrium to be attained. The zeolite and solution phases were then separated and analysed for the exchanging cations.

0.2 g of zeolite were accurately weighed into a 60 cm³ polypropylene bottle. 50 cm³ of the exchange solution, containing the ions A and B in differing proportions but with a constant total normality, were then pipetted into the bottle. The bottles were sealed with "Teflon" tape and the caps replaced. They were then placed on a "rotary equilibrator", a device which rotated the bottles on a wheel which dipped into a thermostatted water bath. The solutions were thus constantly agitated and, although the bottles were only in the water bath for part of each revolution, they were maintained at the constant temperature of the water bath. After a period of 24 hours, the zeolite and solution phases were separated. The solution was passed through a 0.45 μ m cellulose nitrate membrane filter under vacuum, the filter cake being allowed to drain thoroughly. The filtrate was retained for analysis. The filter cake, membrane and any zeolite particles adhering to the filter unit, or to the inside of the plastic bottle, were washed into a 250 cm³ beaker with distilled water. The zeolite phase was then analysed after

dissolution in nitric acid (see section 3.6.4). To determine points at the extrema of the isotherms either a larger volume of exchange solution was used, or the zeolite was subjected to multiple exchanges. In this case the zeolite was contacted with a fresh volume of the exchange solution, one or more times as above, for one hour. In the last exchange the zeolite was contacted with the exchange solution for 24 hours as before. The zeolite was separated from the solution after each exchange, by filtration. Great care was taken to ensure that no zeolite was lost in this process. The filter cake and membrane were returned to the empty bottle and any zeolite adhering to the filter unit was washed back into the bottle with the fresh exchange solution.

3.6. Analysis of Zeolites.

All bulk zeolite samples were analysed for water, silicon, aluminium and cation content. The experimental procedures for these analyses are given in the following sections.

3.6.1. Water Analysis.

The water content of the zeolite was determined thermogravimetrically. 0.2 g of the zeolite sample were weighed into a platinum crucible and heated at a temperature of $1,200^{\circ}\text{C}$ for one hour. After cooling in a desiccator, the crucible was re-weighed and the water content of the zeolite determined from the weight loss. Ammonium ion-exchanged zeolites also lose ammonia on heating. The water content of these zeolites was therefore determined after allowing for the contribution of ammonium to the weight loss.

3.6.2. Silicon Analysis.

Silicon in the zeolite samples was determined gravimetrically as SiO_2 . 0.2 g of zeolite were accurately weighed into a platinum crucible and mixed with about five times the weight of fusion mixture (an equimolar mixture of anhydrous sodium and potassium carbonate). The crucible was heated to $1,200^{\circ}\text{C}$ over three "Meker" burners, for two hours. After allowing to cool to just below red-heat, the

crucible was placed in a platinum dish containing about 20 cm³ of distilled water. 30 cm³ of concentrated hydrochloric acid were introduced slowly and the platinum dish covered with a clock glass. After the evolution of carbon dioxide had ceased, the platinum dish and its contents were heated on a steam bath for one hour. The clock glass and the crucible were then removed and thoroughly rinsed with distilled water, any solid particles adhering to the crucible being washed back into the platinum dish. 1 cm³ of concentrated sulphuric acid was added, and the contents of the dish evaporated to complete dryness on the steam bath. After crushing any lumps with a glass rod, 30 cm³ of 1:1 hydrochloric acid and a few drops of concentrated sulphuric acid were added to the residue. The solution was then evaporated to dryness for a second time. 30 cm³ of 5% hydrochloric acid were added to this residue, and the mixture was warmed on the steam bath for fifteen minutes. The precipitate was filtered through "Whatman's number 42" ashless filter paper, washed thoroughly with hot, very dilute hydrochloric acid, and then with distilled water. The filtrate was made up to 250 cm³ in a volumetric flask and retained for subsequent aluminium analysis. The filter paper containing the silica precipitate was placed in a weighed platinum crucible and heated over a small, yellow Bunsen flame to dry the paper. The temperature of the flame was then gradually increased to char the filter paper; great care was taken to ensure that it did not catch fire. Finally, the crucible was

heated to 1200°C for one hour to remove any traces of carbon, and in order to dehydrate the silica. After cooling in a desiccator, the crucible was re-weighed to give the weight of the precipitate. To determine the exact SiO_2 content of the precipitate, the following procedure was carried out. The precipitate in the platinum crucible was moistened with a little distilled water and 2 to 3 drops of concentrated sulphuric acid, followed by about 5 cm^3 of 40% hydrofluoric acid were added. The crucible was placed on a hot plate inside a fume-cupboard, and the solution was evaporated to dryness. The crucible was then heated to $1,200^{\circ}\text{C}$ for fifteen minutes and, after cooling in a desiccator, reweighed. The hydrofluoric acid volatilises the silica in the precipitate but not any sodium and potassium chloride remaining in the residue after washing. The loss in weight during this stage then represented the weight of pure SiO_2 in the zeolite sample.

3.6.3. Aluminium Analysis.

Aluminium was determined gravimetrically as the 8-hydroxyquinolate, $\text{Al}(\text{C}_9\text{H}_6\text{ON})_3$. 50 or 100 cm^3 of the filtrate from the silica analysis, or of a filtrate obtained after dissolution of the zeolite in nitric acid (section 3.6.4.), were pipetted into a 600 cm^3 beaker. The solution was just neutralised with concentrated ammonium hydroxide, and then made slightly acidic by the addition of 4 cm^3 of 1:1 hydrochloric acid. The solution in the beaker

was made up to 200 cm³ with distilled water and warmed on a steam bath to about 70°C. 10 cm³ of a 20% aqueous ammonium acetate solution were added dropwise until a permanent precipitate just formed. After heating to 100°C, 20 cm³ of 20% ammonium acetate were added and the precipitate digested on the steam bath for 30 minutes. The colour of the supernatant liquid was next checked: if yellow, enough oxine had been added, otherwise a little more oxine solution was required. After cooling to about 50°C, the precipitated aluminium "oxinate" was collected on a preweighed "P4" sintered glass crucible and washed with 100 cm³ of warm "wash solution", followed by a small amount of distilled water. The precipitate was dried to constant weight at 120 - 130°C and weighed as Al(C₉H₆ON)₃.

The oxine solution was prepared by dissolving 25 g of 8-hydroxyquinoline in 60 cm³ of glacial acetic acid. This solution was then diluted to 350 cm³ with distilled water and filtered. The filtrate was then made up to 500 cm³ to give a 5% solution.

The "wash solution" was prepared by diluting 4 cm³ of oxine solution to 500 cm³ with distilled water. The solution was then neutralised with dilute ammonia solution using bromo-cresol purple indicator and made up to 1 dm³.

3.6.4. Cation Analysis.

In order to analyse for cation content, the zeolite was dissolved in nitric acid in order to release the cations into solution. 0.2 g of zeolite were weighed into a 250 cm³ beaker and slurried with a little distilled water. 70 - 80 cm³ of concentrated nitric acid were added, and the solution was heated on a hot-plate at 90°C for two days. The filtrate was made up to 250 cm³ in a volumetric flask.

3.6.4.1. Analysis for Sodium and Potassium.

Sodium and potassium were analysed after suitable dilution in the range 0 - 25 ppm, using a Corning model 400 flame photometer. The instrument was calibrated using seven standard solutions, and a calibration curve calculated using a polynomial least squares, curve fitting routine on a computer. The absorbance of each sample was measured along with the nearest standard solutions above and below the sample, to allow for any drift in the calibration curve. If the calibration drifted by more than a few percent, the instrument was re-calibrated. No interferences were encountered.

3.6.4.2. Analysis for Calcium.

Calcium was determined in the range 0 - 7 ppm using a Perkin-Elmer model 370 atomic absorption spectrophotometer

at a wavelength of 310.3 nm. 1,000 ppm of sodium was added both to standard solutions and to the diluted samples as an ionisation suppressant. Aluminium was known to interfere (Parakrama, 1983) so 50 ppm of aluminium were added to the standard solutions. The aluminium content of the diluted samples was also adjusted to 50 ppm.

3.6.4.3. Analysis for Ammonium.

Ammonium was analysed using a standard Kjeldahl method (Vogel, 1978). 50 or 100 cm³ of filtrate obtained from dissolution of the zeolite in nitric acid, or a weighed aliquot of solid zeolite was introduced into a Kjeldahl flask, with a few anti-bumping stones. The Kjeldahl flask was connected via a spray trap to a condenser, the lower end of which dipped into 10 cm³ of standard 0.1 mol dm⁻³ hydrochloric acid in a conical flask. 50 cm³ of 20% sodium hydroxide solution were added to the Kjeldahl flask through a tap funnel. The flask was heated so that the contents boiled gently and the distillation was continued for 20 to 30 minutes. The condenser was then removed from the conical flask after rinsing its tip with a little distilled water, and the excess acid titrated with standardised 0.1 mol dm⁻³ borax solution using methyl red as indicator. The amount of acid consumed during the distillation corresponded to the amount of ammonia in the sample.

3.7. Thermodynamic Treatment of Equilibrium Ion-Exchange Data.

3.7.1. Thermodynamic Reversibility.

For the thermodynamic ion-exchange theory to be applied, the isotherm must be shown to be reversible. Thermodynamic reversibility was checked for each isotherm using a "wet" method (Barrer and Townsend, 1976; Townsend, 1977). The zeolite was exchanged two or three times with a solution containing only the entering ion, A.

The zeolite was separated from the solution by filtration through a 0.45 μm membrane and then re-contacted with a solution containing a mixture of the ions A and B. After equilibration the zeolite and solution phases were separated and analysed in the normal way. This method avoids drying the zeolite at any time. It has been suggested (Barrer and Townsend, 1976) that redistribution of the ions may occur on drying and this redistribution may cause irreversible exchange.

3.7.2. The Solution Phase Correction.

The value of the solution phase correction factor, Γ , may be calculated from the mean molal activity coefficients for pure salt solutions, using the procedure described by

Glueckauf (1949), which is outlined in section 2.1.3.5. The Glueckauf procedure requires knowledge of the mean molal activity coefficients of each salt at the ionic strength of the experimental solution. When these data are unavailable, and for the case of heterovalent exchange, when the ionic strength of the solution changes with its composition, the activity coefficients may be calculated using a modified Debye-Huckel equation (Robinson and Stokes, 1970).

$$\log \gamma_{\pm AX} = \frac{-A z_A z_X I^{1/2}}{1 + B a I^{1/2}} + b I \quad \dots(3.31)$$

where A and B are constants for a given solvent at a given temperature, and a and b are constants for a given salt in that solvent. For water at 25°C the values of A and B are:

$$A = 0.5115 \text{ dm}^{3/2} \text{ mol}^{-1/2} \quad \text{and} \\ B = 3.291 \times 10^7 \text{ cm}^{-1} \text{ mol}^{-1/2} \text{ dm}^{3/2}.$$

If the activity coefficients of a particular salt are known at at least two different ionic strengths, the values of the constants a and b can be determined, allowing $\gamma_{\pm AX}$ to be calculated for any ionic strength (Barrer and Townsend, 1976; Townsend, 1977).

Rearranging and simplifying equation 3.31 gives:

$$a = \frac{-A z_A z_X I^{1/2} - \log \gamma_{\pm AX} + b I}{B I^{1/2} (\log \gamma_{\pm AX} - b I)} \quad \dots(3.32)$$

For example, the activity coefficients of sodium nitrate at 25°C are:

$$\gamma_{\pm\text{NaNO}_3} = 0.762 \text{ at } I = 0.1 \text{ mol dm}^{-3} \text{ and}$$

$$\gamma_{\pm\text{NaNO}_3} = 0.703 \text{ at } I = 0.2 \text{ mol dm}^{-3}.$$

Substituting these values into equation 3.32 gives two equations in a and b:

$$a = \frac{-0.5115 (0.1)^{1/2} - \log(0.762) + 0.1b}{3.291 \times 10^7 \times (0.1)^{1/2} (\log(0.762) - 0.1b)} \dots(3.33a)$$

$$a = \frac{-0.5115 (0.2)^{1/2} - \log(0.703) + 0.2b}{3.291 \times 10^7 \times (0.2)^{1/2} (\log(0.703) - 0.2b)} \dots(3.33b)$$

Since a is a constant, equations 3.33a and 3.33b can be equated giving rise to a quadratic equation in b. After simplification this reduces to:

$$2.620b^2 - 2.137b + 0.1654 = 0 \dots(3.34)$$

The solutions to this equation are:

$$b = 0.8868 \text{ and } b = -0.0712.$$

Substituting these values back into equation 3.33a gives values for a of:

$$a = -2.0903 \times 10^{-8} \quad \text{and} \quad a = 4.4025 \times 10^{-8}.$$

Since a is an "ion size parameter" (Robinson and Stokes, 1970) and therefore must be positive, the appropriate values of a and b are:

$$a = 4.4025 \times 10^{-8} \quad \text{and} \quad b = -0.07118.$$

Values of the constants a and b, calculated from literature values of $\gamma_{\pm AX}$ (Robinson and Stokes, 1970) and subsequently used to calculate the solution phase correction factor, Γ , are listed below.

Table 3.2. Values of the Constants a and b in the Extended Debye-Huckel Equation (25°C).

salt	a	b
sodium nitrate	4.4025×10^{-8}	-0.07118
potassium nitrate	4.0600×10^{-8}	-0.17649
ammonium nitrate	1.6179×10^{-8}	0.07673
calcium nitrate	4.1719×10^{-8}	0.02745

The units of a are cm, and the units of b are $\text{dm}^3 \text{mol}^{-1}$.

3.7.3. Calculation of the Equilibrium Constant for Exchange.

The zeolite phase equivalent fractions are given by equation 2.3:

$$E_i = \frac{Z_i M_i}{Z_A M_A + Z_B M_B} \quad \dots (2.3)$$

The exchange capacity is determined by the total number of equivalents of ions A and B in the zeolite rather than from the aluminium content. Any hydronium exchange which may have occurred is therefore ignored. Also, the requirement that the exchange capacity of the zeolite remains constant may not always be fulfilled. These omissions are necessary for the thermodynamic theory to be applied. As long as the hydronium exchange is relatively low the error is likely to be small. However, the general neglect of hydronium exchange in the literature in the past may explain variations in the values of ΔG^\ominus reported for identical systems, especially if one equivalent fraction is inferred from the other using the relationship $E_B = 1 - E_A$.

The calculation of thermodynamic data for binary ion-exchange equilibria can be broken down into several stages:

1. Firstly, the mass action quotient, $K_{M,E'}$, is calculated.
2. The solution phase correction factor, Γ , is then determined, and from this the corrected selectivity quotient, K_H , is determined.
3. $\ln K_H$ is plotted as a function of E_A and a polynomial of the form $\ln K_H = a_0 + a_1 E_A + a_2 E_A^2 \dots$ is fitted to the data.
4. The "best-fit" polynomial is integrated analytically between the limits $E_A = 0$ and $E_A = 1$ to give a value of the equilibrium constant K_a .
5. The zeolite phase activity coefficients are calculated by analytically integrating the best-fit polynomial between the appropriate limits (equations 3.39 and 3.42). By repeating the calculation many times, over the range $E_A = 0$ to $E_A = 1$, plots of h_A and h_B as a function of E_A can be drawn.

The order of the best-fit polynomial can be determined "by-eye" or analytically using a function such as the sum of the residuals, R (Barri and Rees, 1980).

$$R = \left[\frac{\sum_{i=1}^n (x_i - \bar{x}_i)^2}{n - m - 1} \right]^{1/2} \quad \dots (3.35)$$

where x_i and \bar{x}_i are the values of $\ln K_H$ determined experimentally and from the polynomial equation, respectively; n is the number of experimental points and m is the order of the polynomial.

A low value of R indicates a good fit. Generally the higher the order the lower the value of R . However, at high orders of polynomial there may be an excessive amount of "flap" at the extrema of the isotherm. Also, the polynomial curve may pass through all the experimental points, giving rise to a low value of R , but there may be a number of sharp turning points within the range of the data which would give a very unlikely correlation between $\ln K_H$ and E_A . The use of R as a factor describing the "goodness of fit" must therefore be made very judiciously and the shape of the polynomial curve should be checked "by eye".

3.7.4. Calculation of the Standard Free Energy of Exchange

For an equilibrium reaction, the standard free energy change, ΔG^\ominus , is calculated from the relationship:

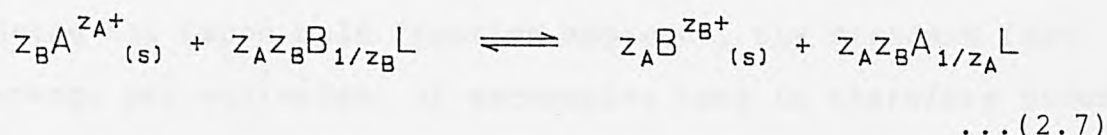
$$\Delta G^\ominus = -RT \ln K \quad \dots(3.36)$$

where K is the equilibrium constant,

R is the gas constant ($=8.314 \text{ JK}^{-1} \text{ mol}^{-1}$) and

T is the absolute temperature.

The thermodynamic parameters in this thesis are calculated using the Gapon mole fraction approach (section 2.1.3.1). Using this formulation the exchange reaction equation is written:

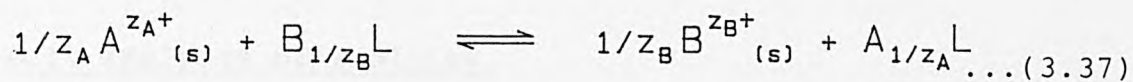


and the equilibrium constant is defined by:

$$K_a = \frac{a_{B,s}^{z_A}}{a_{A,s}^{z_B}} \cdot \frac{a_A^{z_A z_B}}{a_B^{z_A z_B}} \quad \dots(2.12)$$

However, substituting this value of the equilibrium constant into equation 3.37 would not give the value of ΔG^\ominus per equivalent of exchange, which is required.

Dividing equation 2.7 throughout by $z_A z_B$ gives:



The equilibrium constant, K'_a , is therefore:

$$K'_a = \frac{a_{B,s}^{1/z_B} \cdot a_A}{a_{A,s}^{1/z_A} \cdot a_B} \dots (3.38)$$

The relationship between the equilibrium constants K_a and K'_a is obviously:

$$K'_a = K_a^{1/z_A z_B} \dots (3.39)$$

or

$$\ln K'_a = \frac{\ln K_a}{z_A z_B} \dots (3.40)$$

Using the Gapon mole fraction approach, the standard free energy per equivalent of exchanging ions is therefore given by:

$$\Delta G^\ominus = \frac{-RT \ln K_a}{z_A z_B} \dots (3.41)$$

4. RESULTS AND DISCUSSION.

4.1. Analysis of Zeolites.

The weight percent, oxide and unit cell compositions of the zeolites used are given in tables 4.1 to 4.5. The results presented are all averages of a number of analyses. Typically, the water and cation percentage weights are averages of 4 analyses, the aluminium content an average of 6 analyses and the silicon content an average of 8 to 12 analyses. The errors obtained in a typical analysis are illustrated by the results obtained for zeolite NaY (Grace):

H ₂ O	26.083 ± 0.080%
Na ₂ O	9.390 ± 0.043%
Al ₂ O ₃	15.898 ± 0.099%
SiO ₂	48.289 ± 0.217%
Total	99.660 ± 0.255%

Table 4.1 shows the composition of the zeolite NaA (Charnell) sample which was synthesised in the laboratory. The Si/Al ratio was a few percent higher than the theoretical value of 1; the difference is probably due to the presence of small amounts of silicate impurities. The sample was found to give the standard X-ray diffraction

pattern. Using a JEM / JOEL 100B electron microscope, the zeolite was examined at a magnification of 1000 x. This showed that the zeolite consisted of cubic crystals having edge dimensions of 8 to 10 μm . Particle size analysis, using a Malvern Instruments laser diffractometer, indicated that the crystals formed aggregates, 95% of which were in the range 6 to 24 μm .

The Si/Al ratios of the NaA (Laporte) and CaA (Laporte) samples equal 1 within experimental uncertainty (table 4.1). The unit cell water content of the calcium zeolite is about 10% higher than the sodium zeolite from which it was prepared, reflecting the higher void fraction of the calcium zeolite which arises because two sodium ions are replaced by one calcium ion.

It should be noted that in table 4.2 zeolite NaX (Laporte) was not the starting material for the preparation of CaX (Laporte). The zeolites were from different batches and had different Si/Al ratios.

The cation / Al ratio for each zeolite gives the cation deficiency (hydronium exchange) value. The hydronium exchange probably occurs when the zeolite is washed after being exchanged into the homoionic form. The hydronium exchange level in zeolites NaA (Charnell), NaA (Laporte) and NaX (Laporte) was about 7% in each case. The amount of hydronium exchange in the calcium A and X zeolites was

lower (1-2%). Drummond, De Jong and Rees (1983) and Allen et al (1983) have suggested that hydronium exchange in CaA is inhibited due to the strong competition of Ca^{2+} ions for exchange sites, and to the thermodynamic stability of the calcium zeolite.

Hydronium exchange in the NaY samples (table 4.3) was also lower (1.5-3%) and this is in agreement with other observations, which suggest that the degree of hydronium exchange decreases as the Si/Al ratio increases. The relatively low total analysis in the Unilever samples is probably due to impurities which were not analysed.

	<u>NaA (Charnell)</u>	<u>NaA (Laporte)</u>	<u>CaA (Laporte)</u>
H ₂ O	23.77	22.418	22.431
Na ₂ O	15.23	15.587	0.1113
CaO	-	-	15.460
Al ₂ O ₃	26.82	27.609	28.588
SiO ₂	32.46	32.416	33.332
Total	98.28	98.030	99.922
Cat./Al	0.9342	0.9288	0.9896
Si/Al	1.0269	0.9962	0.9893

Table 4.1: Compositions (wt.%) of zeolite A samples.

	<u>NaX (Laporte)</u>	<u>NaX (BDH)</u>	<u>CaX (Laporte)</u>
H ₂ O	26.250	24.632	22.632
Na ₂ O	13.205	14.900	0.1137
CaO	-	-	13.899
Al ₂ O ₃	23.240	24.271	25.917
SiO ₂	37.595	35.875	37.472
Total	100.290	99.678	100.034
Cat./Al	0.9347	1.0099	0.9823
Si/Al	1.3726	1.2542	1.2268

Table 4.2: Compositions (wt.%) of zeolite X samples.

	<u>NaY Grace</u>	<u>KY Grace</u>	<u>NaY Laporte</u>	<u>NaY Unilever (2.75)</u>	<u>NaY Unilever (2.70)</u>
H ₂ O	26.083	22.350	30.201	24.47	26.02
Na ₂ O	9.390	0.140	9.680	9.08	8.98
K ₂ O	-	13.820	-	-	-
Al ₂ O ₃	15.898	15.543	14.533	15.13	15.02
SiO ₂	48.289	47.419	43.370	48.95	47.84
Total	99.660	99.272	97.784	97.63	97.86
Cat/Al	0.9717	0.9772	1.0957	0.9873	0.9853
Si/Al	2.5772	2.5886	2.5321	2.7451	2.7025

Table 4.3: Composition (wt.%) of Zeolite Y Samples.

NaA (Charnell)	0.93	Na ₂ O	Al ₂ O ₃	2.05	SiO ₂	5.02	H ₂ O
NaA (Laporte)	0.93	Na ₂ O	Al ₂ O ₃	1.99	SiO ₂	4.60	H ₂ O
CaA (Laporte)	0.02	Na ₂ O	0.99 CaO	Al ₂ O ₃	2.00	SiO ₂	5.14 H ₂ O
NaX (Laporte)	0.93	Na ₂ O	Al ₂ O ₃	2.75	SiO ₂	6.39	H ₂ O
NaX (BDH)	1.01	Na ₂ O	Al ₂ O ₃	2.51	SiO ₂	5.74	H ₂ O
CaX (Laporte)	0.01	Na ₂ O	0.98 CaO	Al ₂ O ₃	2.45	SiO ₂	4.94 H ₂ O
NaY (Grace)	0.97	Na ₂ O	Al ₂ O ₃	5.15	SiO ₂	9.29	H ₂ O
KY (Grace)	0.015	Na ₂ O	0.96 K ₂ O	Al ₂ O ₃	5.18	SiO ₂	8.14 H ₂ O
NaY (Laporte)	1.10	Na ₂ O	Al ₂ O ₃	5.06	SiO ₂	11.76	H ₂ O
NaY (Unilever-2.75)	0.99	Na ₂ O	Al ₂ O ₃	5.49	SiO ₂	9.15	H ₂ O
NaY (Unilever-2.70)	0.98	Na ₂ O	Al ₂ O ₃	5.41	SiO ₂	9.80	H ₂ O

Table 4.4: Oxide compositions of zeolite samples.

NaA (Charnell)	Na _{11.21} H _{0.79} (AlO ₂) ₁₂ (SiO ₂) _{12.32} · 30.10 H ₂ O
NaA (Laporte)	Na _{11.15} H _{0.85} (AlO ₂) ₁₂ (SiO ₂) _{11.95} · 27.57 H ₂ O
CaA (Laporte)	Na _{0.24} Ca _{5.96} (AlO ₂) ₁₂ (SiO ₂) _{12.00} · 30.80 H ₂ O
NaX (Laporte)	Na _{75.64} H _{5.28} (AlO ₂) _{80.92} (SiO ₂) _{111.08} · 259 H ₂ O
NaX (BDH)	Na _{86.02} (AlO ₂) _{85.18} (SiO ₂) _{106.82} · 245 H ₂ O
CaX (Laporte)	Na _{0.62} Ca _{42.04} H _{1.52} (AlO ₂) _{86.22} (SiO ₂) _{105.78} · 213 H ₂ O
NaY (Grace)	Na _{52.15} H _{1.52} (AlO ₂) _{53.67} (SiO ₂) _{138.33} · 249 H ₂ O
KY (Grace)	Na _{0.79} K _{51.49} H _{1.22} (AlO ₂) _{53.50} (SiO ₂) _{138.50} · 218 H ₂ O
NaY (Laporte)	Na _{59.56} (AlO ₂) _{54.36} (SiO ₂) _{137.64} · 320 H ₂ O
NaY (Unilever-2.75)	Na _{50.61} H _{0.66} (AlO ₂) _{51.27} (SiO ₂) _{140.73} · 235 H ₂ O
NaY (Unilever-2.70)	Na _{51.00} H _{0.86} (AlO ₂) _{51.86} (SiO ₂) _{140.14} · 254 H ₂ O

Table 4.5: Unit cell compositions of zeolite samples.

4.2. Hydronium Exchange in Zeolites.

The pH of freshly prepared suspensions of zeolites in water is usually between 9 and 10.5. This observation is well known and has been explained by limited hydrolysis of the zeolite (Breck, 1974; Cook et al, 1982). Drummond, De Jong and Rees (1983) observed that when zeolite NaA is slurried with water the pH increase is accompanied by a simultaneous release of sodium into solution. Drummond, De Jong and Rees (1983) also found that the pH began to drop after about one hour and pointed out that the initial concentration of hydronium ions in solution is insufficient to account for the observed levels of sodium removed. They therefore suggested that, as a result of some initial hydronium exchange, zeolite break-down occurred resulting in a release of hydronium ions into solution, and thus allowing further exchange to occur. They suggested that the rate of hydrolysis eventually decreases due to the stability of HA, and the diffusion of hydronium ions to the outer solution gave rise to the observed pH drop.

The observation of hydronium exchange and possible hydrolysis of zeolites, even in water with a relatively high pH, has very important implications for studies of ion-exchange. Despite this, to the knowledge of the author, no detailed systematic study of hydronium exchange in zeolites under these conditions, has been published in the literature. A systematic study using zeolites A, X and Y was therefore carried out.

Figures 4.1 to 4.12 illustrate experimental results in which zeolite NaA (Charnell) was contacted with distilled water for a period of three hours. These experiments were carried out using the "original" experimental apparatus as illustrated in figure 3.2. The zeolite to water ratio was varied from 8 to 0.2 g dm^{-3} (in reality 0.4 to 0.01 g of zeolite in 50 cm^3 of distilled water). Each experiment was conducted first with the solution blanketed by a flowing stream of nitrogen, and then an identical experiment was undertaken with a normal laboratory atmosphere (section 3.4).

The figures show the changes in both sodium concentration and pH with time. The two independent variables are plotted as pNa (the negative log of the sodium concentration) and pOH, on an inverted y-axis. This means that moving in the positive direction of the y-axis represents an increase in both the sodium concentration and the pH.

The data from these experiments are summarised in tables 4.6 and 4.7. The number of moles of sodium released from the zeolite and the number of moles of hydronium removed from solution (inferred from the pH and the carbon dioxide concentration in solution, section 3.4.10) are also tabulated. The ratio a/b is equal to the number of equivalents of sodium released per equivalent of hydronium ion removed from solution. For a simple, stoichiometric

ion-exchange reaction to be occurring this ratio should of course equal 1. The larger the value of a/b , the greater the deviation from this simple situation. The percentage hydronium exchange is calculated from the cation deficiency within the zeolite with respect to its theoretical exchange capacity, as determined from the aluminium content. This cation deficiency is in turn inferred by subtracting the sodium observed in solution from the sodium content that was known to be present initially in the zeolite. Note that any hydronium content present in the original zeolite sample is added to this inferred cation deficiency (table 4.5).

As can be seen from figures 4.1 to 4.8, when the zeolite was contacted with distilled water there was a very rapid increase in the pH from about 7 to between 9.5 and 10.5. For experiments carried out under nitrogen, the pH remained constant at the maximum value attained but when the solution was open to the atmosphere the pH began to decrease after about five minutes. This is due to dissolution of carbon dioxide in the solution, which reacts with water to give "hydrogen carbonate", carbonate and hydronium ions. The sodium concentration in solution continued to rise under both sets of conditions. However, this increase was only marked in the presence of air, being very slight when the solution was blanketed with nitrogen.

Consider first the experiments conducted under nitrogen. There is an approximately linear relationship between the amount of sodium released and the zeolite / water ratio (tables 4.6 and 4.7); the same is true for the amount of hydronium ion exchanged. However, the proportion of sodium removed from the zeolite increases markedly as the zeolite / water ratio decreases. This is reflected in the hydronium exchange levels. The NaA (Charnell) zeolite had an initial cation deficiency of 6.6% (table 4.1) and this rose to 8.6, 9.0, 13.2 and 28.8% when the zeolite / water ratio was 8, 4, 1 and 0.2 g dm^{-3} respectively. The hydronium exchange level was inferred from the solution sodium concentration; the accuracy of this measurement decreases at lower sodium concentrations. The estimated error in the percentage hydronium exchange values was $\pm 0.02\%$ at a zeolite / water ratio of 8 g dm^{-3} , and $\pm 0.8\%$ at 0.2 g dm^{-3} . The trend is, however, clear and very high levels of hydronium ion-exchange occurred when the zeolite / water ratio was small. The ratio a/b lies between 3 and 4 at higher zeolite / water ratios indicating that 3 to 4 times the amount of sodium was released as was hydronium ion absorbed. At a zeolite / water ratio of 0.2 g dm^{-3} the discrepancy was much larger, the value of a/b being greater than 9, and appears to be linked to the high hydronium exchange levels.

Table 4.6 shows that CO_2 was detected in solution in some cases even when the experiments were conducted under

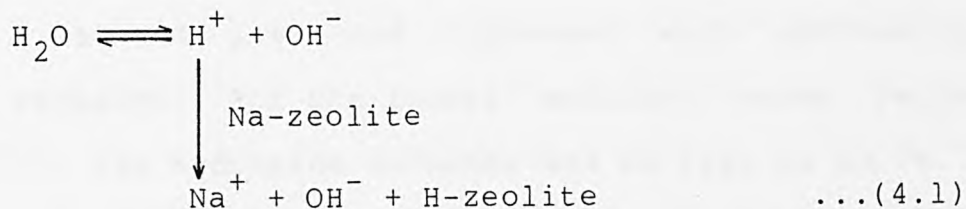
nitrogen. This shows that the reaction vessel was not 100% gas-tight. The levels of carbon dioxide detected were however very low, and did not appear to affect the pH significantly.

The results of experiments conducted in air are summarised in table 4.7, and in figures 4.11 and 4.12. It can be seen from these results that the zeolite has a "buffering" effect on the pH; the pH fell much more slowly at higher zeolite / water ratios. When the zeolite / water ratio was 0.2 g dm^{-3} the pH fell rapidly, attaining an equilibrium value of 7.7 in only two hours.

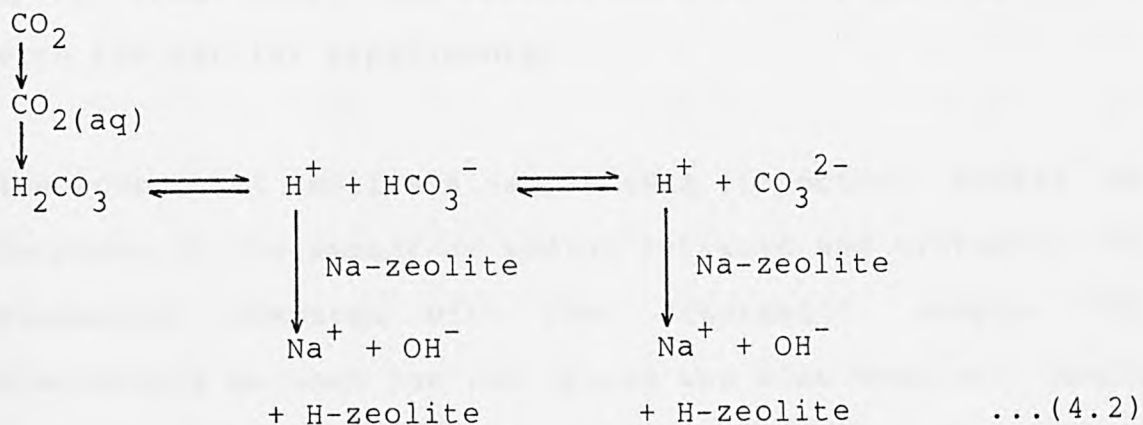
The concentration of carbon dioxide dissolved in solution after three hours was also related to the amount of zeolite present. The decrease in the concentration between zeolite / water ratios of 4 and 8 g dm^{-3} can be explained in terms of a limiting concentration of carbon dioxide in solution being reached, and reflects small variations in the partial pressure of the gas in the laboratory air at different times.

The observations can be explained by considering the following reaction sequences:

1. The initial sharp rise in pH and sodium ion concentration is due to $\text{Na}^+ - \text{H}^+$ exchange in the zeolite:



2. When the solution is in contact with air the pH then falls due to dissolution of CO_2 . This reacts with water to give "hydrogen carbonate", carbonate and hydronium ions. Some of the hydronium ions are exchanged into the zeolite releasing more sodium, buffering the solution against a decrease in pH and allowing more carbon dioxide to be dissolved.



The discrepancy between the sodium released and the hydronium ion exchanged in these experiments was less than in the case of experiments conducted under nitrogen. The ratio a/b for the experiments carried out in air was between 1.26 and 1.89 and increased with increasing hydronium exchange. For the lowest zeolite / water ratio (0.2 g dm^{-3}), the hydronium exchange was as high as 43.7%.

Tables 4.8 and 4.9 and figures 4.13 to 4.16 compare the results of contacting two different zeolite A and zeolite X samples. The zeolite NaA (Charnell) sample was suspended in distilled water which had not been further treated and which had an initial pH of about 5.2. The pH of the solution was 0.2 to 0.3 pH units lower than the corresponding experiments using "ultra-pure water" with an initial pH of 7 (see section 3.4.6 and tables 4.6 and 4.7). Apart from this, the results were in very good agreement with the earlier experiments.

The commercial zeolite A sample (NaA (Laporte)) showed an increase in the amount of sodium released and hydronium ion exchanged, compared with the "Charnell" sample. The discrepancy between the two values was also smaller. Apart from the method of preparation, the only apparent difference between the two samples was the particle size. The Charnell zeolite had an average particle size of about $10 \mu\text{m}$, whereas the commercial sample had a much smaller particle size of about $1 \mu\text{m}$.

The results from the two zeolite X samples are similar and lie within the range of values seen for the two zeolite A samples. The zeolite NaX (BDH) showed evidence of a slight initial over-exchange of about 1% which explains the much lower hydronium exchange level after contact compared with the NaX (Laporte) sample (6.5% initial hydronium exchange). All the zeolites showed an increase of between 2.5 and 3.5% in hydronium exchange for experiments conducted under nitrogen, and double this (5 to 5.5%) when the solution was in contact with air.

Figures 4.17 to 4.20 and tables 4.10 and 4.11 show the results of experiments involving the suspension of calcium zeolites A and X in distilled water. The increase in pH of solutions contacted with these zeolites was much lower than when sodium zeolites were used. Thus the final pH of the solutions contacted with CaA was about 1 pH unit lower than when NaA was used, whereas the difference between CaX and NaX was much larger. For the experiments carried out under nitrogen the pH after contact was only 7.4 for CaX compared to over 10 for the sodium X zeolites. Also, the amount of calcium released from the zeolite (in terms of the number of equivalents) was greater than the amount of sodium released from NaX. The discrepancy between the calcium released and hydronium ion exchanged was therefore very large (a/b being between 500 and 900). For the experiments in air, the calcium released was only slightly higher but the increase in the hydronium ion exchanged brought the

ratio a/b down to about 24.

The hydronium exchange in CaA rose from an initial 1.04% to about 3% under nitrogen and to about 4.3% in air. For CaX the initial hydronium exchange was 1.8% and this rose to about 6.1 and 7.4% for the experiments carried out under nitrogen and in air respectively.

An interesting effect is illustrated in figure 4.22. This experiment (CaA in distilled water) was carried out in air and run for 24 hours. After the initial sharp rise in pH from 7 to 9.6 (this is difficult to see on the figure due to the necessary compression of the ordinate scale), this value decreased steadily due to dissolution of carbon dioxide. The solution pH reached an equilibrium value of 7.6 after 6 hours, and maintained this value for the next 12 hours. The sudden dip in the pH after 18 hours by about 0.4 pH units was a result of three "Meker" burners being ignited. The extra CO_2 in the atmosphere, due to the combustion of natural gas, caused the pH of the solution to fall, and illustrates the sensitivity of the system to local variations in the concentration of CO_2 in the atmosphere.

By contrast, figure 4.21 shows the result of contacting zeolite CaA with distilled water under nitrogen for a period of 24 hours. The pH quickly reached and maintained a constant value, but the calcium concentration continued

to increase steadily. The reason for this increase was unclear for some time. It was then thought that rather than being a real effect this must be due to evaporation of water from the reaction cell as a result of passing dry nitrogen over the solution. This was confirmed by weighing the reaction cell and its contents before and after the experiment. Subsequently, in order to prevent evaporation taking place when using a nitrogen purge, the diffusion cell apparatus was designed and constructed (section 3.4.8).

The remaining experiments were all carried out using the diffusion cell apparatus and all the solutions were blanketed under nitrogen. In figures 4.23 to 4.26 it can be seen that the sodium concentration in solutions contacted with zeolites A and X under these conditions remained constant on reaching the maximum value after a few minutes. Table 4.12 shows that the results obtained using zeolites NaA (Charnell), NaA (Laporte), NaX (Laporte) and NaX (BDH): all agree closely with those obtained previously. The value of a/b , the discrepancy between the amount of sodium released and hydronium ion exchanged, is more reproducible under these carefully controlled conditions, yielding a value of about 3.4 for both the A samples but about 2 for the X materials.

Table 4.12 also lists the results obtained when three different zeolite Y samples were added to distilled water.

The equilibrium pH's of the suspensions after contact with these zeolites were between 1 and 1.5 pH units lower than when zeolites A and X were used. The unit cell compositions of the Y zeolites (table 4.5) show only small differences between them. However, the amount of sodium removed from the different samples varies considerably. Zeolite NaY (Unilever - 2.70) gave the lowest concentration of sodium in solution after contact. About twice the amount of sodium was removed from zeolite NaY (Unilever - 2.75) but the amount of hydronium ion exchanged was also higher by a similar factor, and the ratio a/b was similar for both zeolites. For the zeolite NaY (Grace) the amount of sodium removed was about 10 times that for NaY (Unilever - 2.70) and was approximately the same as for zeolites A and X. The amount of hydronium ion exchanged by the zeolite was, however, much lower and this meant that the ratio a/b was very large. About 50 moles of sodium were released for every mole of hydronium ion exchanged. The hydronium exchange which occurred in the Unilever Y zeolites during contact with distilled water was relatively low (1-1.5%) but was higher in the Grace sample (over 4.5%).

The behaviour of the NaY (Grace) sample was investigated further. Different amounts of the zeolite were added to distilled water at zeolite / water ratios of between 8 and 0.5 g dm^{-3} . When the amount of zeolite was greater than 3 g dm^{-3} the zeolite / water ratio had no effect on the

magnitude of the solution pH after contact. At lower zeolite / water ratios the amount of hydronium ion exchanged was proportional to the amount of zeolite used. However, the amount of sodium removed from the zeolite was proportional to the zeolite / water ratio over the whole range. The discrepancy between the sodium removed and the hydronium ion exchanged was very large (a/b between 50 and 120) for all zeolite / water ratios, and there was no pattern in the results. These observations may be explained by the presence of imbibed sodium salts in the channels of the zeolite. However, analysis of the zeolite showed a small cation deficiency rather than any over-exchange. Also, analysis of the solution for chloride ion (the co-ion used in the preparation of the homoionic zeolite) by a colorimetric method (Vogel, 1974) after contact with the zeolite, was negative. The level of hydronium exchange in the zeolite increased from about 3% before contact to between 7 and 9% after. The hydronium exchange did not increase with decreasing zeolite / water ratio as was seen for zeolite A.

When zeolite NaY (Grace) was added to dilute sodium nitrate solutions having concentrations between 5×10^{-5} and $5 \times 10^{-4} \text{ mol dm}^{-3}$, the concentration of sodium had no effect on the amount of hydronium ion exchanged by the zeolite (table 4.14). The presence of sodium in solution before contact with the zeolite did, however, inhibit the removal of sodium from the zeolite. The hydronium exchange

in the zeolite increased from 3 to 7.6% when distilled water was used compared with an increase to 5.4% when the solution contained $5 \times 10^{-4} \text{ mol dm}^{-3}$ of sodium nitrate.

Tables 4.15 to 4.16 and figures 4.30 to 4.33 show the results obtained when zeolite NaY (Grace) was slurried with distilled water several times. The zeolite was contacted with distilled water for 15 minutes and then separated from the solution by filtration through a $0.45 \mu\text{m}$ cellulose nitrate membrane filter. The zeolite was re-contacted with a fresh sample of distilled water, and the procedure repeated.

In each of the experiments reported, the amount of sodium removed from the zeolite in the first contact was an order of magnitude higher than that removed in subsequent contacts. The pH fell gradually with each contact. The amount of sodium removed in the second and subsequent contacts was approximately constant.

Table 4.17 lists data for zeolite Y contacted 11 times with distilled water or dilute nitric acid solutions. The first 7 contacts were made with distilled water and the results were very similar to experiments where the number of contacts was 4 and 5, with the exception of the fifth. For this contact the sodium concentration was much higher and the pH much lower than for other contacts. The reason for this difference is unclear but is probably due to

contamination by acid or a leakage of CO_2 into the reaction cell. In contacts 8 to 11 the zeolite was added to dilute nitric acid solutions with an initial pH of between 4.2 and 3.4. The hydronium exchange in the zeolite jumped from nearly 16% to about 30% during these four contacts. Also, the balance between the amount of sodium removed and the hydronium ion exchanged was much closer. This result has been observed throughout this work. The amount of sodium removed from the zeolite was not very variable but when more hydronium ion was available for exchange, either from acid solutions or from the dissolution of carbon dioxide, the discrepancy between the sodium and hydronium ions was much smaller. However, there is always a considerable discrepancy between the two, so the amount of sodium removed cannot be explained in terms of a straightforward exchange of hydronium ions.

Drummond, De Jong and Rees (1983) tentatively suggested a mechanism to describe the hydrolysis of zeolite A. Their break-down mechanism involves the release of aluminium and silicon species into solution. However, in this study and in earlier work (Franklin, 1984; Townsend, Franklin and O'Connor, 1984) no such release was confirmed by straightforward analysis of the solution phase. Furthermore, the X-ray diffraction pattern of a sample of zeolite A, which was over 30% hydronium exchanged, remained substantially unchanged. However, it is emphasised that this does not necessarily mean that the zeolite itself was

unchanged; X-ray diffraction studies are not a good indication of whether damage to the zeolite has occurred or not.

McDaniel and Maher (1976) distinguished three categories of behaviour concerning the resistance of zeolites to acid attack, viz:

1. Those zeolites which cannot be exchanged into the hydrogen form without collapse of the aluminosilicate framework.
2. Those zeolites for which the hydrogen form may be prepared by a conventional ion-exchange process using dilute acid. Some aluminium removal from the framework may occur, the amount being dependent on the acid used and its concentration, but the observed crystallinity (as seen using X-ray diffraction) remains intact.
3. Those which can only be conveniently put into the hydrogen form by an indirect method such as ammonium ion-exchange followed by de-ammoniation (Kerr, 1973).

Zeolites A and X belong in the first category, whereas zeolite Y belongs in the third. Some of the more highly siliceous zeolites, such as heulandite, clinoptilolite and mordenite can be classified in the second group (Barrer and Klinowski, 1975).

Zeolite A is used as a detergent builder in a number of countries including Germany and the United States (Kuhl and Sherry, 1980; Schwuger and Smolka, 1977). As a result, the concentration of zeolite A in raw wastewater may be as high as 10 mg dm^{-3} (Allen et al, 1983). A number of studies have therefore been carried out to investigate the ion-exchange and hydrolysis of zeolite A in natural waters.

Allen et al (1983) investigated the hydrolysis of CaA in a test water of pH 8.2 at a zeolite / water ratio of 1 mg dm^{-3} . After two months about half the particulate aluminium and silicon remained while, after 30 weeks this had fallen to just 5%. The silicon / aluminium ratio of the zeolite was found to remain constant and so it was concluded that the hydrolysis occurred in a congruent fashion.

Muller (1979) looked at the hydrolysis of zeolite A when the concentration in solution was varied between 1 mg dm^{-3} and 10 g dm^{-3} . Muller found that at higher concentrations (for example 8 g dm^{-3}) the build-up of aluminium and silicon hydrolysis products inhibited further hydrolysis of the zeolite.

Cook et al (1982) made a study of the dissolution of zeolites NaA and CaA in acid solutions of various pH's. They measured the acid consumption of the zeolites by titrating with HCl at constant pH. At pH's of 5, 6 or 7,

the acid consumption fell below the value of 1 mole H^+ per mole of lattice aluminium, indicating simple ion-exchange. At pH 4 the acid consumption was greater than 1 mol H^+ / mol Al because of hydrolysis of the zeolite lattice. At pH 3 the zeolite dissolved completely. When the acid consumption and the amount of sodium released from a sample of NaA was plotted against the solution pH (after 6 days contact) Cook et al (1982) found breaks in the acid consumption curve at 0.33 and 1 mol H^+ / mol Al. The break at the lower acid consumption corresponds to the proportion of sodium ions in the oxygen 8-rings (Breck, 1974). This suggests that the sodium ions in the octagonal window exchange sites (one third of the total) are more readily exchanged by protons. At pH values of less than 7, and before zeolite break-down occurred, the acid consumption and sodium release curves were coincident indicating stoichiometric $Na^+ - H^+$ exchange. However, when the acid consumption was 0.33 mol H^+ / mol Al the amount of sodium released exceeded the acid consumed by 20 to 30%. This discrepancy was not commented upon.

zeolite/H ₂ O g dm ⁻³	pH before contact	pH after contact	[Na ⁺] mol dm ⁻³ x 10 ⁴	[CO ₂] measured mol dm ⁻³ x 10 ⁴	Figure number
8	6.96	10.34	8.32	0.34	4.1
4	7.05	10.10	5.01	<0.1	4.3
1	7.04	9.91	3.47	0.25	4.5
0.2	7.00	9.40	2.34	<0.1	4.7

zeolite/H ₂ O g dm ⁻³	a		b		ratio a/b	% hydronium exchange
	moles Na ⁺ released from zeolite x 10 ⁵	moles H ⁺ exchanged into zeolite inferred from [OH]. x 10 ⁵	moles H ⁺ exchanged into zeolite corrected for CO ₂ . x 10 ⁵			
8	4.16	1.09	1.35		3.08	8.56
4	2.51	0.630	0.630		3.98	8.97
1	1.74	0.406	0.566		3.07	13.20
0.2	1.17	0.126	0.126		9.29	28.82

Table 4.6: NaA (Charnell) contacted with distilled water for three hours. Under nitrogen.

zeolite/H ₂ O g dm ⁻³	pH before contact	pH after contact	[Na ⁺] mol dm ⁻³ x 10 ⁴	[CO ₂] measured mol dm ⁻³ x 10 ⁴	Figure number
8	7.02	9.21	9.77	7.08	4.2
4	7.00	8.72	11.70	8.13	4.4
1	6.80	8.10	8.91	5.50	4.6
0.2	7.00	7.73	3.89	2.14	4.8

zeolite/H ₂ O g dm ⁻³	a		b		ratio a/b	% hydronium exchange
	moles Na ⁺ from zeolite x 10 ⁵	moles H ⁺ into zeolite from [OH]. x 10 ⁵	moles H ⁺ into zeolite inferred for CO ₂ . x 10 ⁵	moles H ⁺ into zeolite corrected		
8	4.89	0.081	3.87	3.87	1.26	8.91
4	5.85	0.026	4.44	4.44	1.32	12.14
1	4.46	0.007	2.72	2.72	1.64	23.54
0.2	1.95	0.003	1.03	1.03	1.89	43.65

Table 4.7: NaA (Charnell) contacted with distilled water for three hours. In air.

zeolite	pH before contact	pH after contact	$[\text{Na}^+]$ $\text{mol dm}^{-3} \times 10^4$	$[\text{CO}_2]$ measured $\text{mol dm}^{-3} \times 10^4$	Figure number
NaA (Charnell)	5.25	10.15	4.90	<0.1	-
NaA (Laporte)	7.05	10.64	8.32	0.12	4.13
NaX (Laporte)	5.48	10.36	6.97	<0.1	-
NaX (BDH)	6.92	10.66	6.31	0.696	4.15

zeolite	a		b		ratio a/b	% hydronium exchange
	moles Na^+ from zeolite $\times 10^5$	moles H^+ into zeolite from $[\text{OH}^-] \times 10^5$	moles H^+ into zeolite inferred $\times 10^5$	moles H^+ into zeolite corrected for $\text{CO}_2 \times 10^5$		

NaA (Charnell)	2.45	0.734	0.734	0.734	3.34	8.91
NaA (Laporte)	4.16	2.183	2.90	2.90	1.43	10.97
NaX (Laporte)	3.49	1.162	1.162	1.162	3.00	10.35
NaX (BDH)	3.16	2.285	2.870	2.870	1.10	2.33

Table 4.8: Zeolites NaA and NaX (4 g dm^{-3}) contacted with distilled water for three hours.
Under nitrogen.

zeolite	pH before contact	pH after contact	$[\text{Na}^+]$ $\text{mol dm}^{-3} \times 10^4$	$[\text{CO}_2]$ measured $\text{mol dm}^{-3} \times 10^4$	Figure number
NaA (Charnell)	5.20	8.41	10.23	7.50	-
NaA (Laporte)	6.60	9.55	12.02	8.13	4.14
NaX (Laporte)	5.32	9.52	10.03	4.17	-
NaX (BDH)	6.49	9.39	9.77	6.26	4.16

zeolite	a moles Na^+ released from zeolite $\times 10^5$	moles H^+ exchanged into zeolite inferred from $[\text{OH}^-] \times 10^5$	b moles H^+ exchanged into zeolite corrected for $\text{CO}_2 \times 10^5$	ratio a/b	% hydronium exchange
NaA (Charnell)	5.12	0.013	3.80	1.35	11.45
NaA (Laporte)	6.01	0.177	2.71	2.22	12.67
NaX (Laporte)	5.02	0.166	3.65	1.38	12.03
NaX (BDH)	4.89	0.123	3.58	1.37	4.14

Table 4.9: Zeolites NaA and NaX (4 g dm^{-3}) contacted with distilled water for three hours. In air.

zeolite	pH before contact	pH after contact	$[Ca^{2+}]$ $mol\ dm^{-3} \times 10^4$	$[CO_2]$ measured $mol\ dm^{-3} \times 10^4$	Figure number
CaA (Laporte)	5.63	9.56	1.86	<0.1	-
CaA (Laporte)	6.18	9.60	2.24	<0.1	4.17
CaX (Laporte)	5.84	7.47	4.37	<0.1	4.19
CaX (Laporte)	6.08	7.42	4.79	<0.1	-

zeolite	a		b		ratio a/b	% hydronium exchange
	eq. Ca^{2+} released from zeolite $\times 10^5$	moles H^+ exchanged into zeolite inferred from $[OH] \cdot \times 10^5$	moles H^+ exchanged into zeolite corrected for $CO_2 \cdot \times 10^5$			
CaA (Laporte)	1.86	0.193	0.193	9.64	2.69	
CaA (Laporte)	2.24	0.202	0.202	11.09	3.03	
CaX (Laporte)	4.37	0.008	0.008	546	6.07	
CaX (Laporte)	4.37	0.005	0.005	874	6.07	

Table 4.10: Zeolites CaA and CaX ($4\ g\ dm^{-3}$) contacted with distilled water for three hours.
Under nitrogen.

zeolite	pH before contact	pH after contact	$[\text{Ca}^{2+}]$ $\text{mol dm}^{-3} \times 10^4$	$[\text{CO}_2]$ measured $\text{mol dm}^{-3} \times 10^4$	Figure number
CaA (Laporte)	5.72	8.33	3.63	0.992	-
CaA (Laporte)	5.97	8.47	3.55	0.912	4.18
CaX (Laporte)	5.96	6.87	4.93	0.525	4.20
CaX (Laporte)	6.10	6.90	5.12	0.537	-

zeolite	a		b		ratio a/b	% hydronium exchange
	eq. Ca^{2+} released from zeolite $\times 10^5$	moles H^+ exchanged into zeolite inferred from $[\text{OH}]\cdot \times 10^5$	moles H^+ exchanged into zeolite corrected for $\text{CO}_2\cdot \times 10^5$			
CaA (Laporte)	3.63	0.020	0.518	7.09	4.27	
CaA (Laporte)	3.55	0.020	0.479	7.41	4.21	
CaX (Laporte)	4.93	0.005	0.203	24.3	7.23	
CaX (Laporte)	5.12	0.004	0.210	24.4	7.42	

Table 4.11: Zeolites CaA and CaX (4 g dm^{-3}) contacted with distilled water for three hours. In air.

zeolite	pH before contact	pH after contact	$[Na^+]$ mol dm^{-3} $\times 10^4$	a moles Na^+ released $\times 10^5$	b moles H^+ exchanged $\times 10^5$	ratio a/b	% hydronium exchange	Figure No.
NaA (Charnell)	7.02	10.17	5.13	2.57	0.740	3.47	9.02	4.23
NaA (Laporte)	7.11	10.34	7.29	3.65	1.09	3.35	10.49	4.24
NaX (Laporte)	7.03	10.53	6.80	3.40	1.69	2.01	10.26	4.25
NaX (BDH)	7.12	10.47	5.57	2.79	1.48	1.89	1.94	4.26
NaY (Grace)	7.01	9.10	6.03	3.02	0.063	47.9	7.68	-
NaY (Unilever - 2.70)	7.00	9.03	0.627	0.314	0.054	5.82	2.18	4.27
NaY (Unilever - 2.75)	7.00	9.32	1.43	0.715	0.104	6.88	2.48	4.28

Table 4.12: Zeolites NaA, NaX and NaY ($4g\ dm^{-3}$) contacted with distilled water. Under nitrogen.

g zeolite dm ⁻³	pH before contact	pH after contact	[Na ⁺] mol dm ⁻³ x 10 ⁴	a moles Na ⁺ released x 10 ⁵	b moles H ⁺ exchanged x 10 ⁵	ratio a/b	% hydronium exchange
8	7.01	9.06	13.01	6.53	0.057	114	8.07
6	7.14	9.08	8.48	4.24	0.060	70.7	7.37
4	7.01	9.10	6.03	3.02	0.063	47.9	7.68
3	7.06	8.72	5.58	2.79	0.026	107	8.80
2	7.11	8.55	3.09	1.55	0.017	91.2	7.80
1	7.02	8.19	1.47	0.745	0.008	93.1	7.61
0.5	6.99	7.98	0.659	0.330	0.005	66.0	7.07

Table 4.13: Zeolite NaY (Grace) contacted with distilled water for 15 minutes.
Under nitrogen.

pH before contact	pH after contact	$[\text{Na}^+]$ before contact mol dm^{-3} $\times 10^4$	$[\text{Na}^+]$ after contact mol dm^{-3} $\times 10^4$	a moles Na^+ released $\times 10^5$	b moles H^+ exchanged $\times 10^5$	ratio a/b	% hydronium exchange
7.06	9.03	0	5.98	2.99	0.053	56.4	7.63
6.98	8.90	0.50	5.63	2.57	0.040	64.3	6.96
9.02	9.37	0.50	5.09	2.30	0.065	35.4	6.52
7.00	8.90	1.00	5.52	2.21	0.040	55.3	6.38
7.04	9.00	2.00	5.37	1.69	0.050	33.8	5.54
7.04	8.95	5.00	8.17	1.59	0.044	36.1	5.38

Table 4.14: Zeolite NaY (Grace) - 4 g dm^{-3} , contacted with sodium nitrate solutions for 15 minutes. Under nitrogen.

	contact	pH before contact	pH after contact	$[\text{Na}^+]$ mol dm^{-3} $\times 10^4$	a		b		ratio a/b	% hydronium exchange
					moles Na^+ released $\times 10^5$	moles H^+ exchanged $\times 10^5$				
1		7.01	8.95	5.51	2.76	0.045			61.3	7.26
2		6.94	8.61	0.610	0.305	0.020			15.3	7.75
3		7.11	8.60	0.623	0.312	0.020			15.6	8.25
4		7.00	8.47	0.732	0.366	0.015			24.4	8.84

Table 4.15: Zeolite NaY (Grace) - 4 g dm^{-3} , 4 contacts with distilled water for 15 minutes. Under nitrogen.

	contact	pH before contact	pH after contact	$[\text{Na}^+]$ mol dm^{-3} $\times 10^4$	a		b		ratio a/b	% hydronium exchange
					moles Na^+ released $\times 10^5$	moles H^+ exchanged $\times 10^5$				
1		7.15	9.03	5.20	2.60	0.053			49.1	7.00
2		7.15	8.77	0.643	0.322	0.029			11.1	7.52
3		7.00	8.36	0.929	0.465	0.011			42.3	8.26
4		7.04	8.36	0.945	0.473	0.011			43.0	9.02
5		7.12	8.32	0.755	0.378	0.010			37.8	9.63

Table 4.16: Zeolite NaY (Grace) - 4 g dm^{-3} , 5 contacts with distilled water for 15 minutes. Under nitrogen.

	contact	pH before contact	pH after contact	$[\text{Na}^+]$ mol dm^{-3} $\times 10^4$	a		b		ratio a/b	% hydronium exchange
					moles Na^+ released $\times 10^5$	moles H^+ exchanged $\times 10^5$				
1		7.05	9.00	6.20	3.10	0.050			62.0	7.80
2		7.06	8.69	1.17	1.59	0.024			66.3	10.35
3		7.07	8.63	0.839	0.420	0.021			20.0	11.03
4		6.98	8.58	0.773	0.387	0.019			20.4	11.65
5		7.10	7.81	4.21	2.11	0.003			703	15.03
6		7.01	8.49	0.748	0.374	0.015			24.9	15.63
7		6.90	8.32	0.729	0.365	0.011			33.2	16.22
8		4.13	7.98	1.37	0.685	0.375			1.83	17.31
9		3.45	6.64	4.83	2.42	1.773			1.36	21.19
10		3.65	6.72	3.40	1.70	1.119			1.52	23.92
11		3.44	6.06	6.85	3.43	1.811			1.89	29.42

Table 4.17: Zeolite NaY (Grace) - 4 g dm^{-3} , 11 contacts with distilled water for 15 minutes. Under nitrogen.

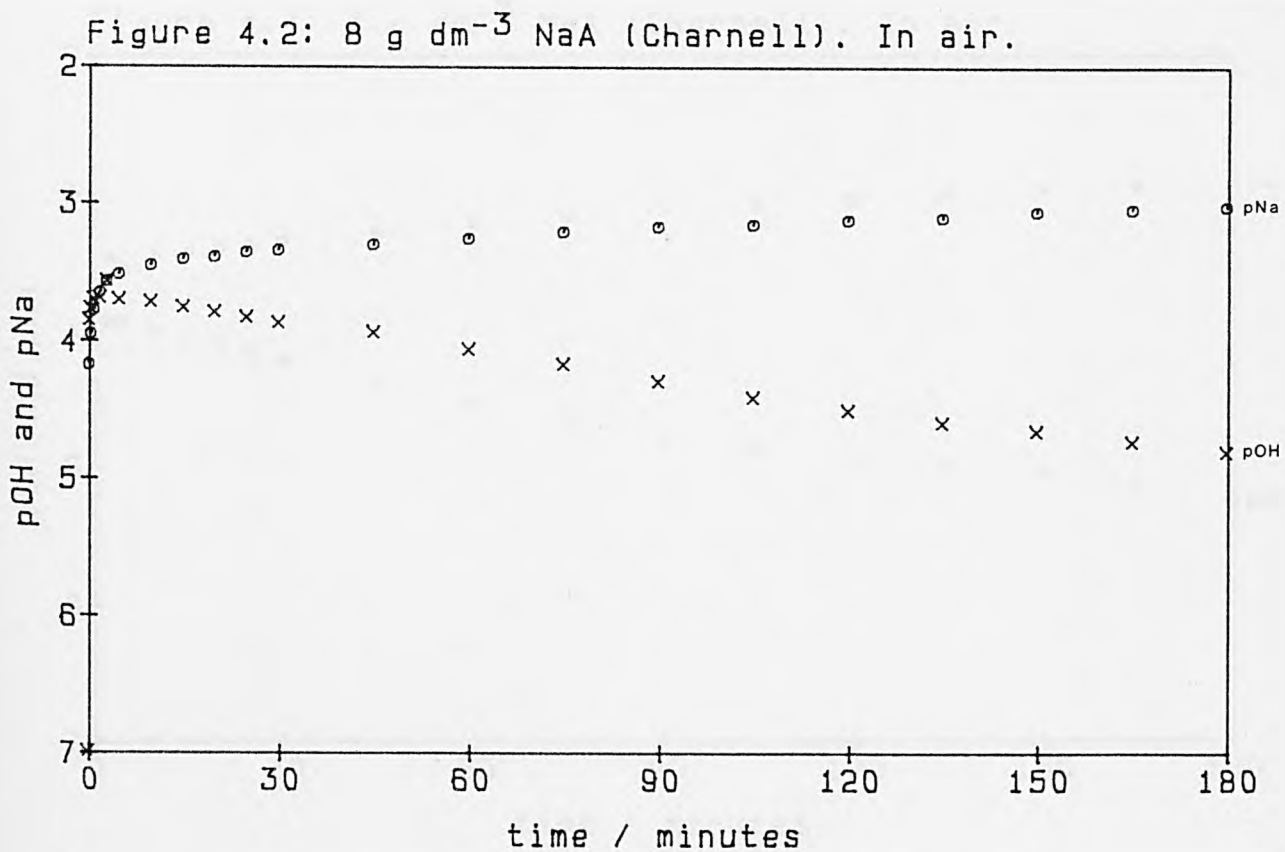
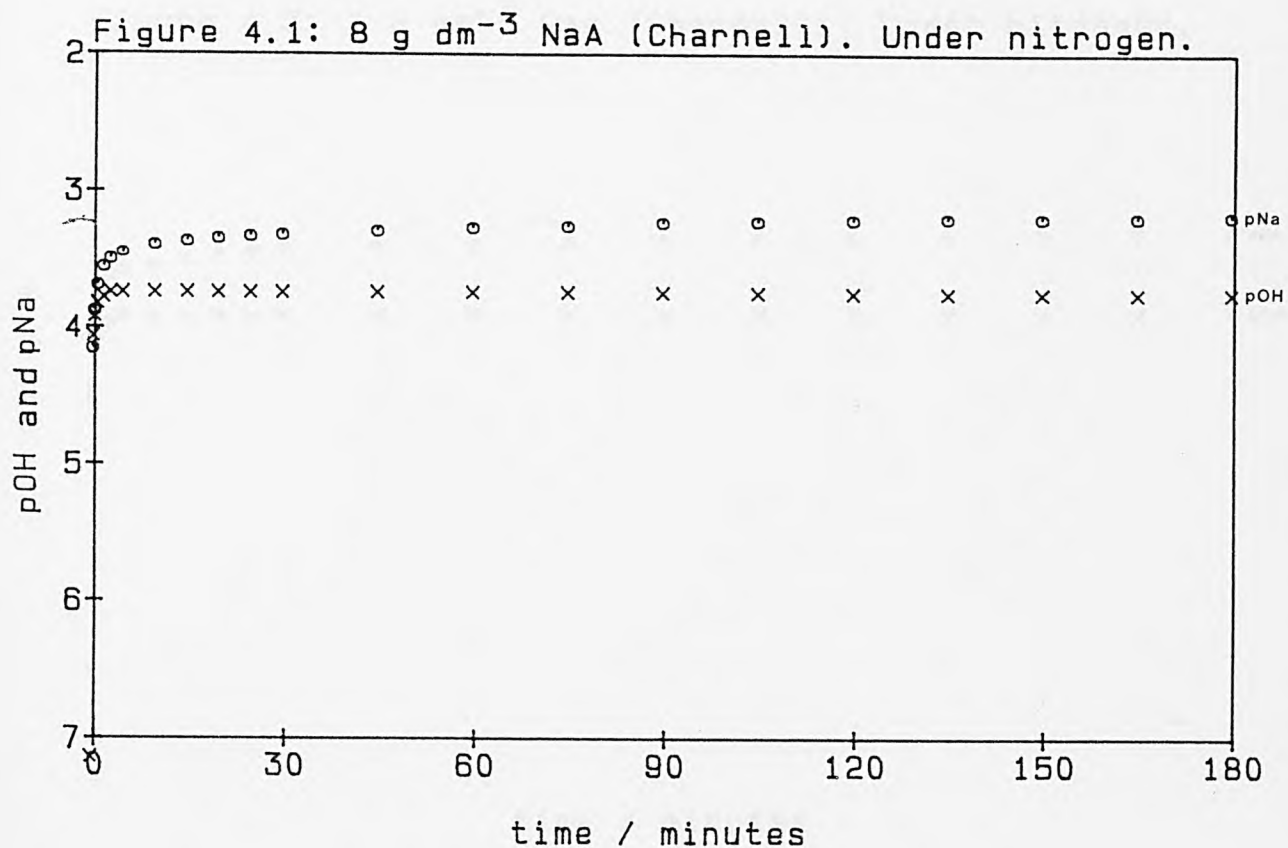


Figure 4.3: 4 g dm^{-3} NaA (Charnell). Under nitrogen.

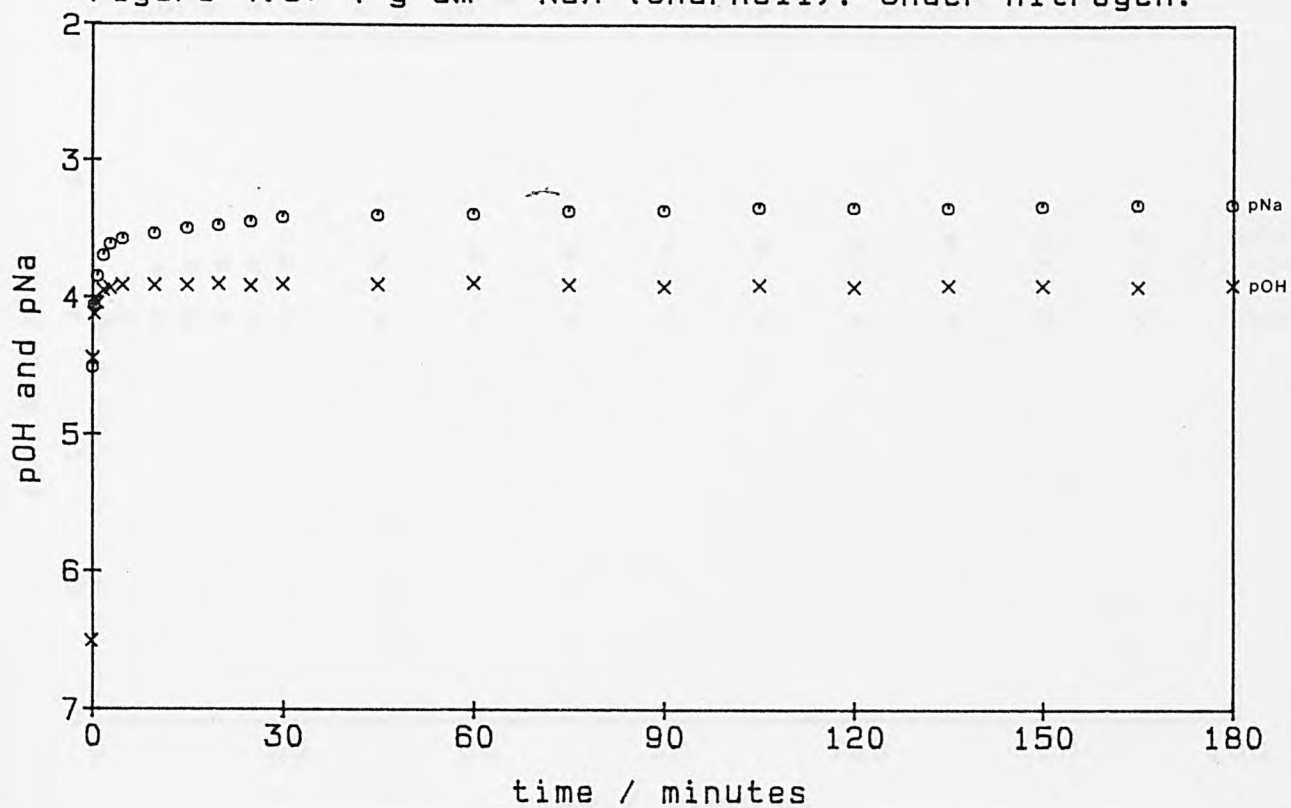


Figure 4.4: 4 g dm^{-3} NaA (Charnell). In air.

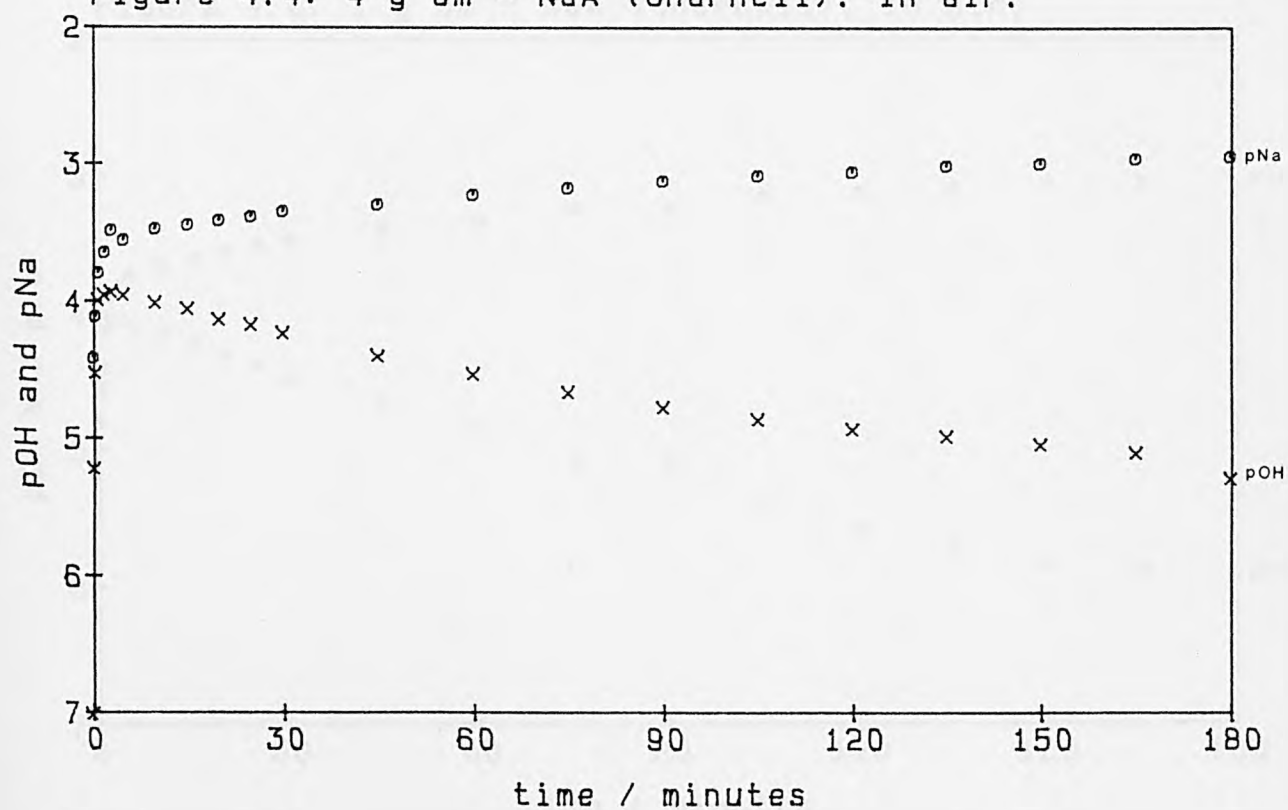


Figure 4.5: 1 g dm^{-3} NaA (Charnell). Under nitrogen.

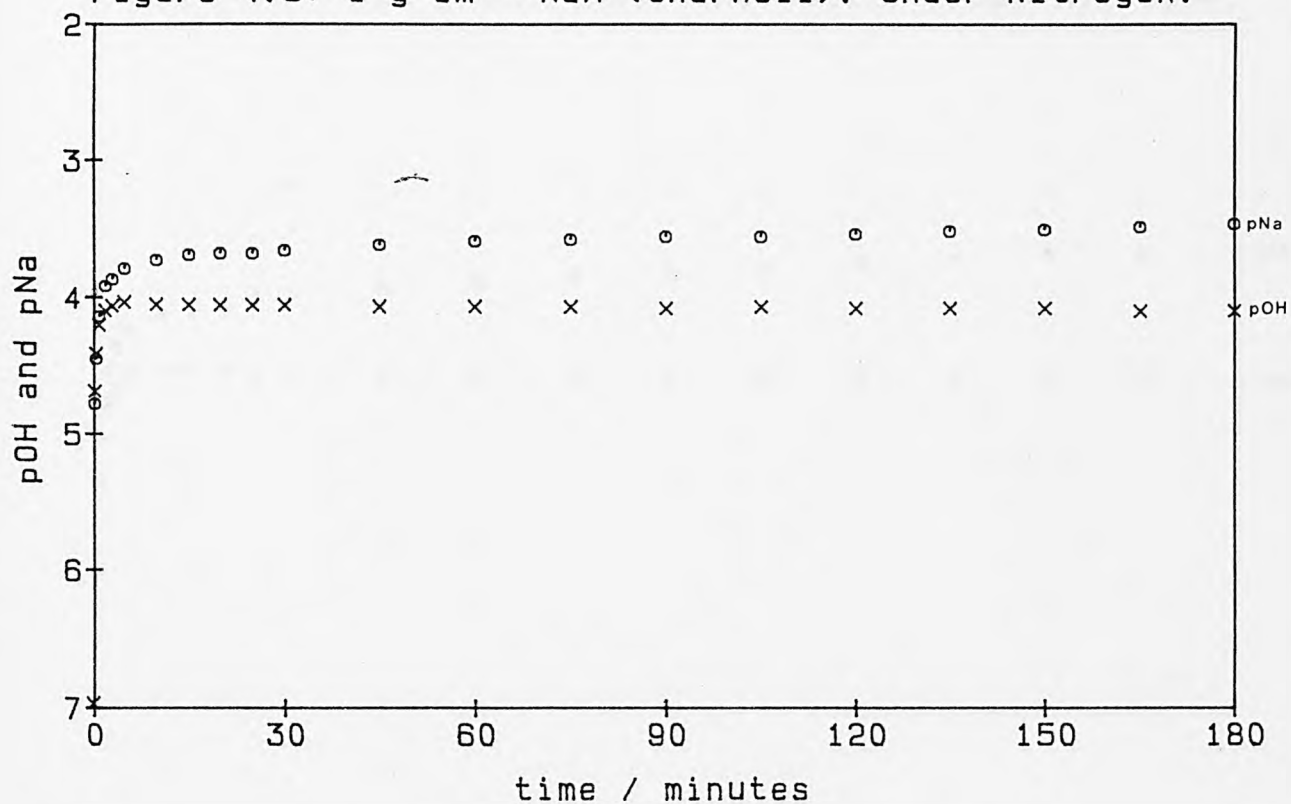


Figure 4.6: 1 g dm^{-3} NaA (Charnell). In air.

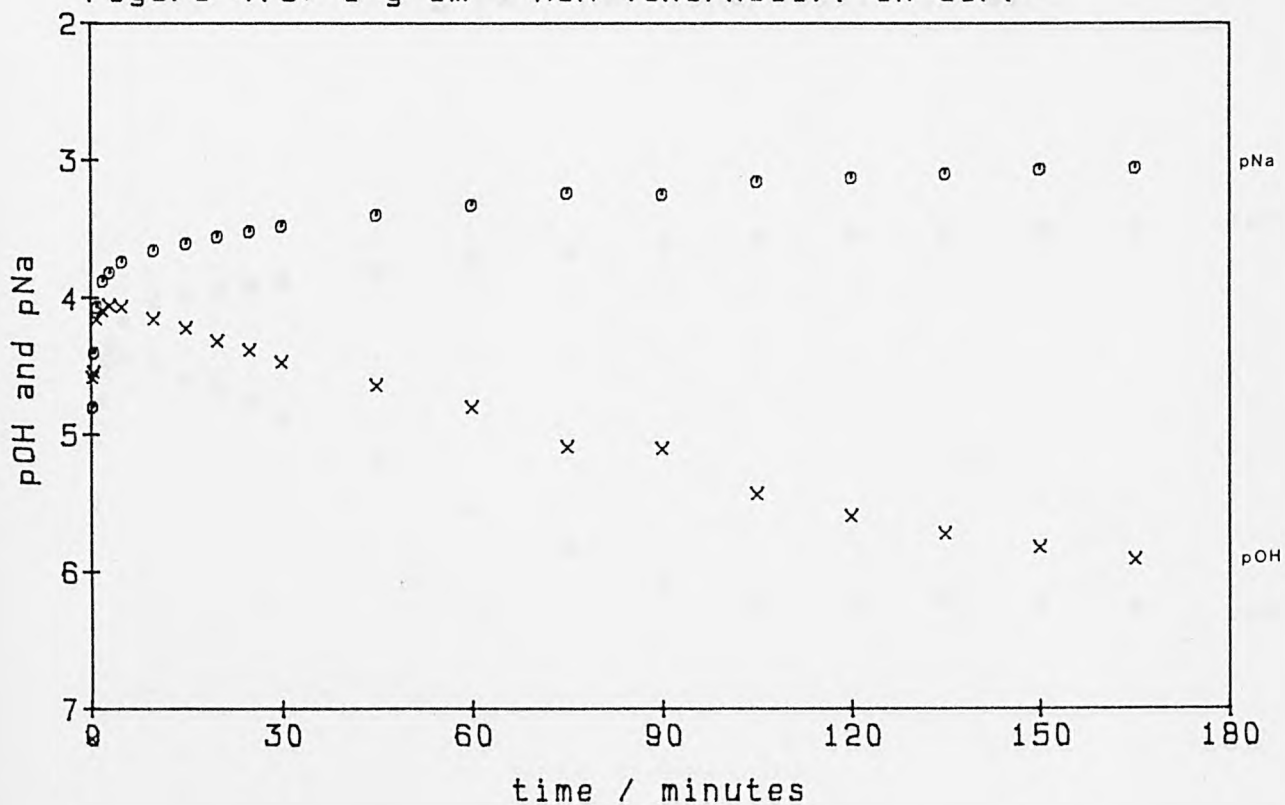


Figure 4.7: 0.2 g dm^{-3} NaA (Charnell). Under nitrogen.

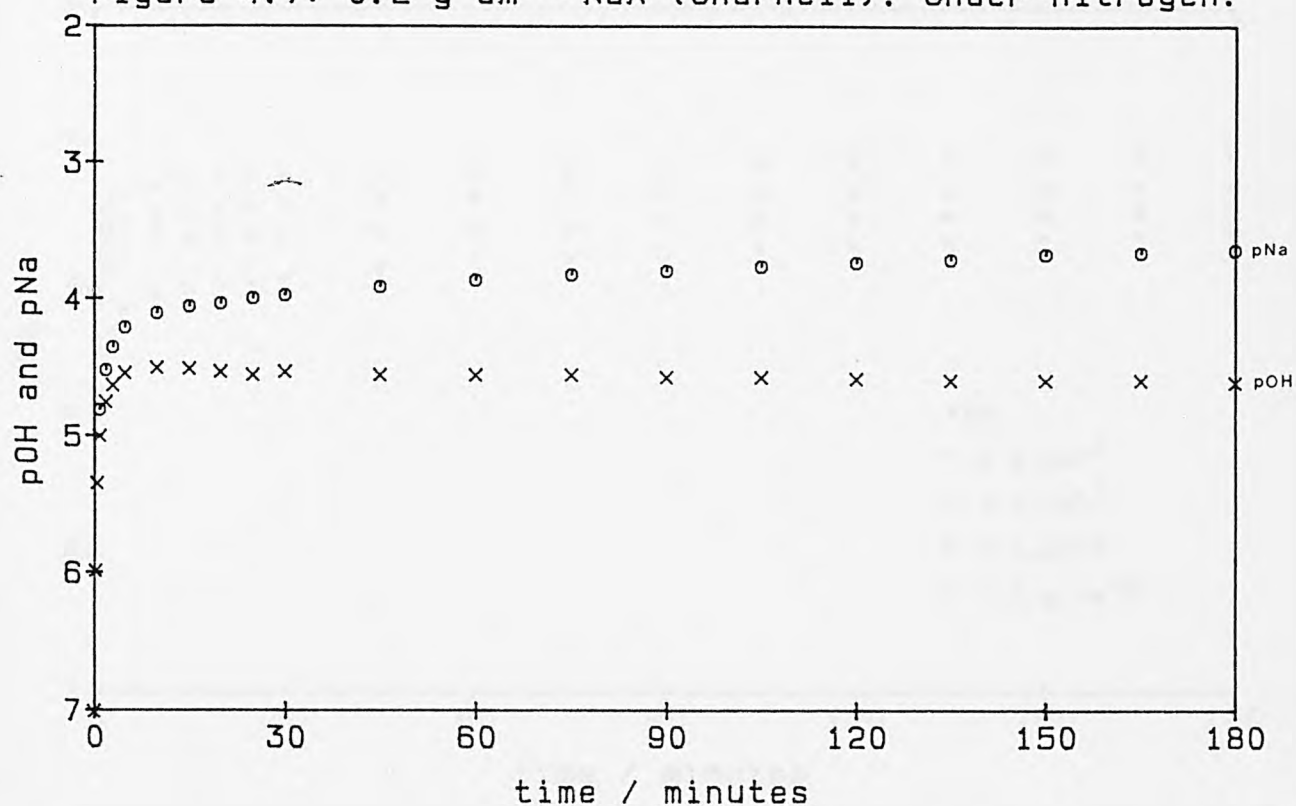


Figure 4.8: 0.2 g dm^{-3} NaA (Charnell). In air.

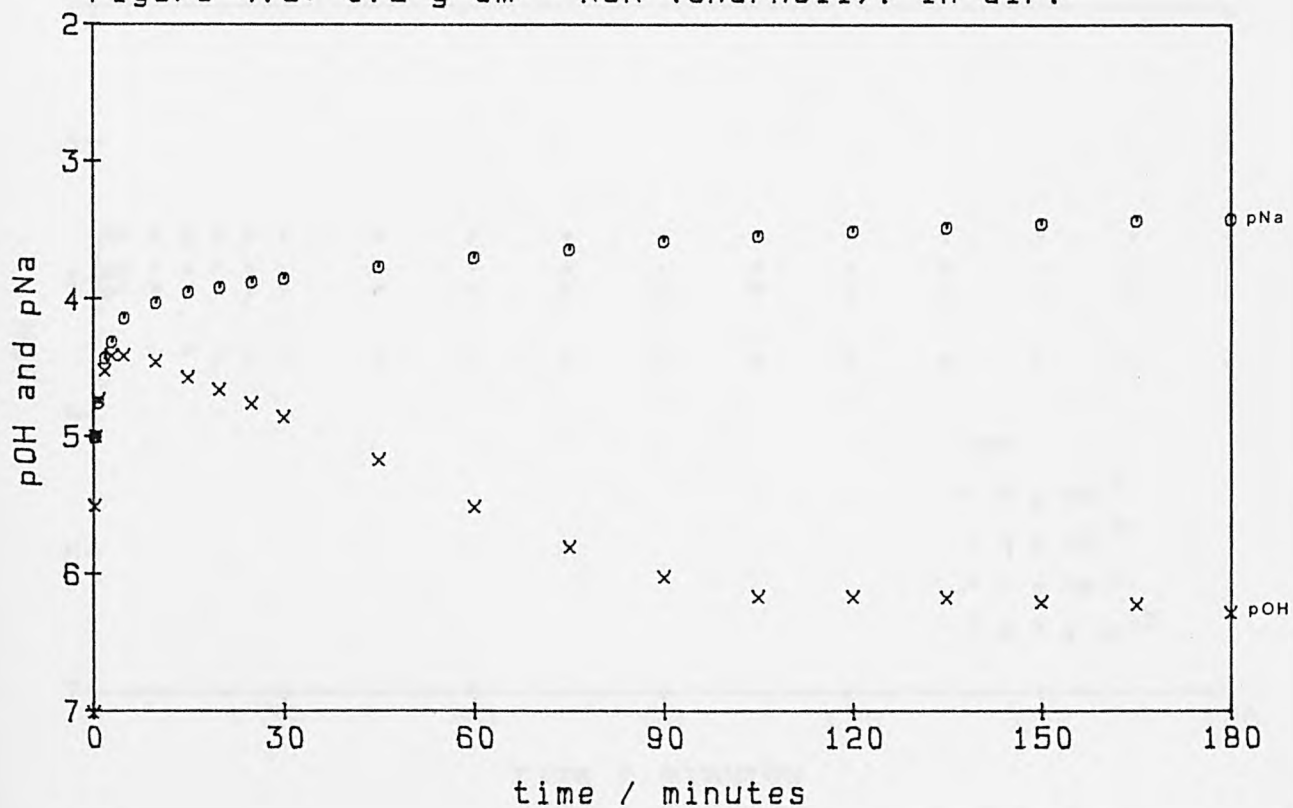


Figure 4.9: NaA (Charnell). Under nitrogen.

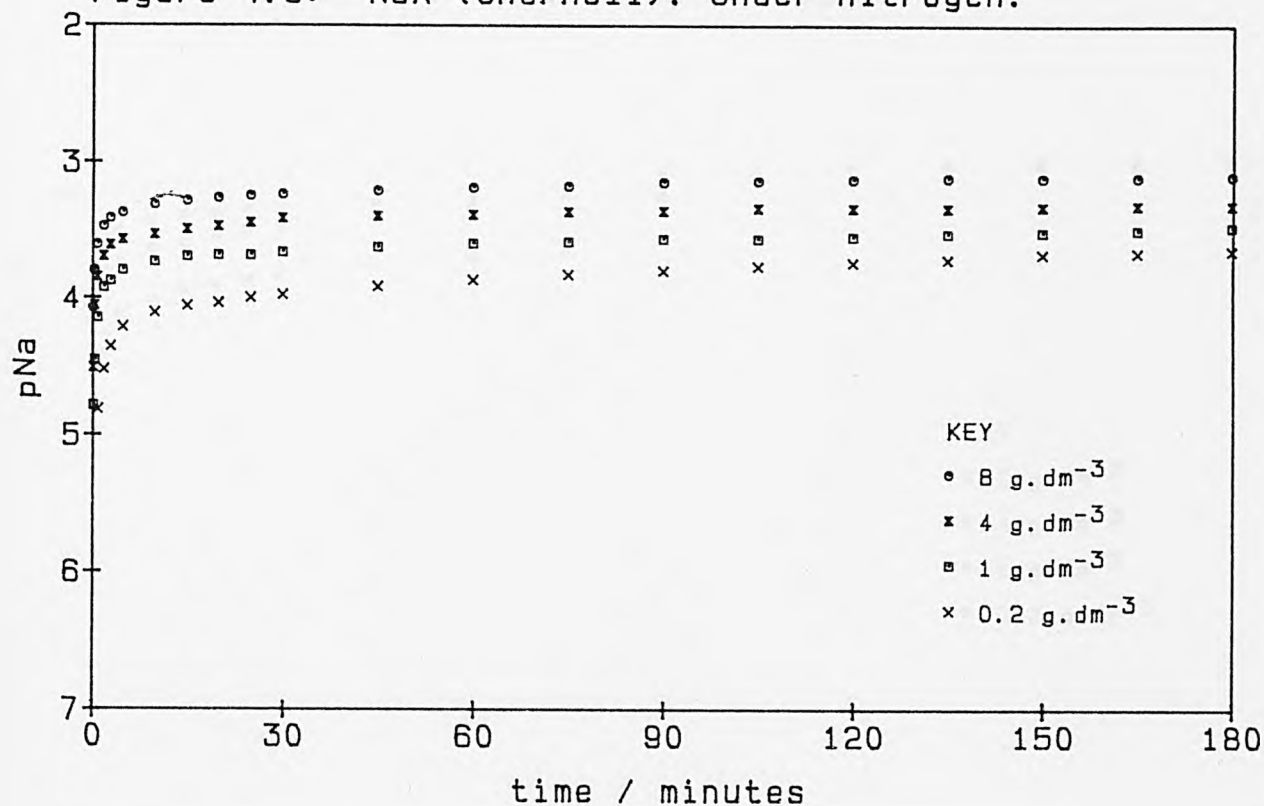


Figure 4.10: NaA (Charnell). Under nitrogen.

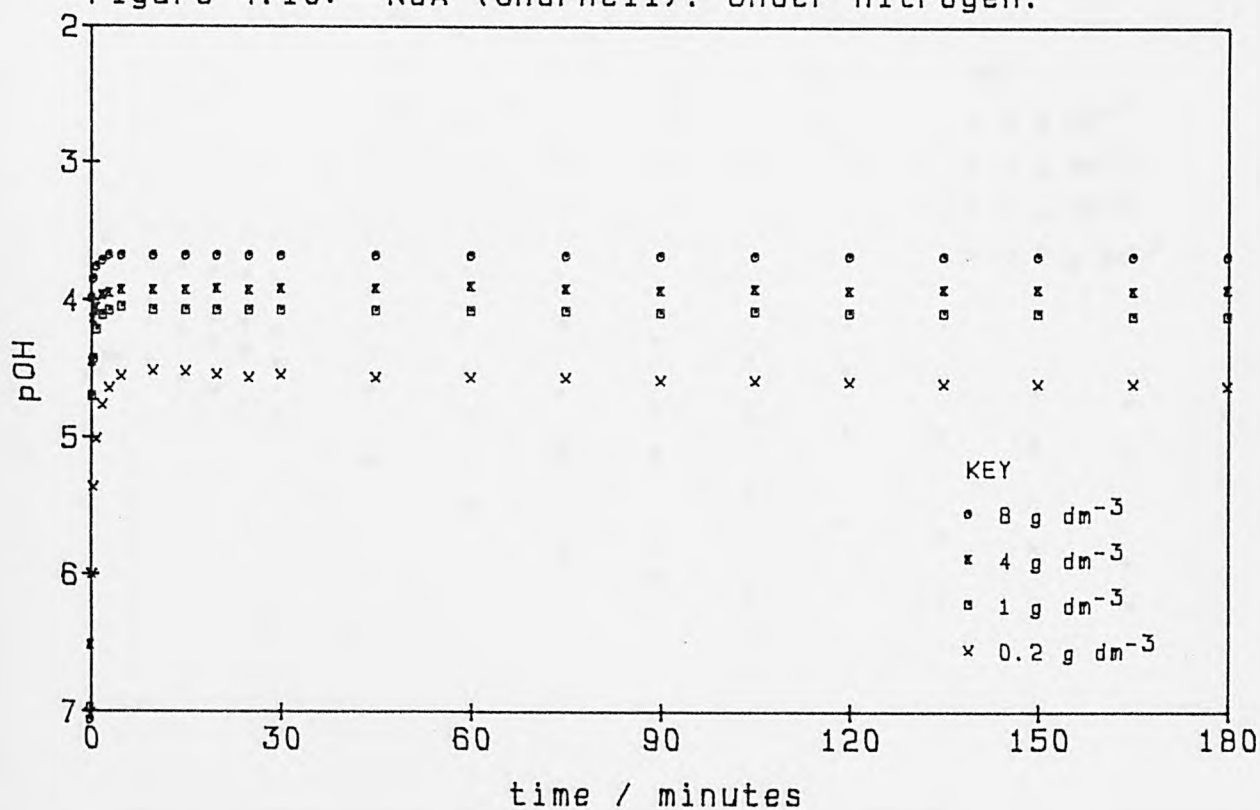


Figure 4.11: NaA (Charnell). In air.

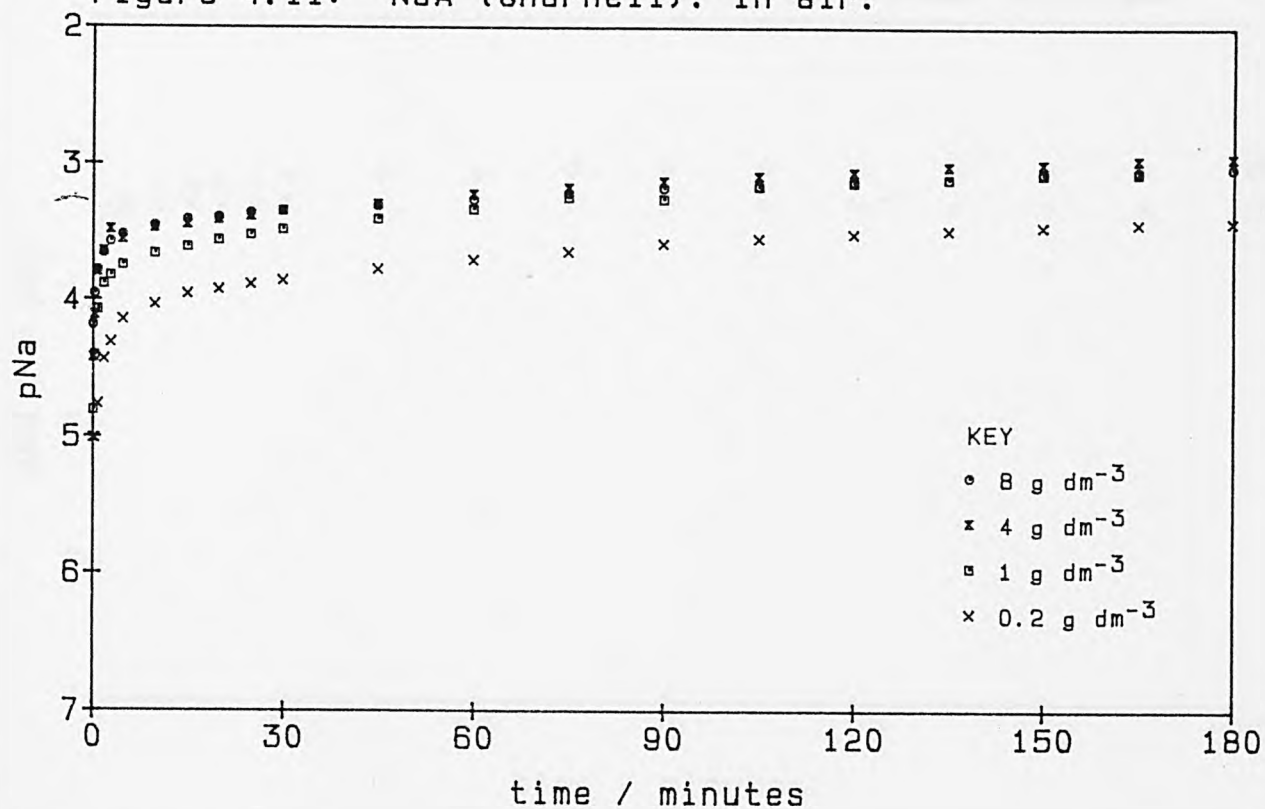


Figure 4.12: NaA (Charnell). In air.

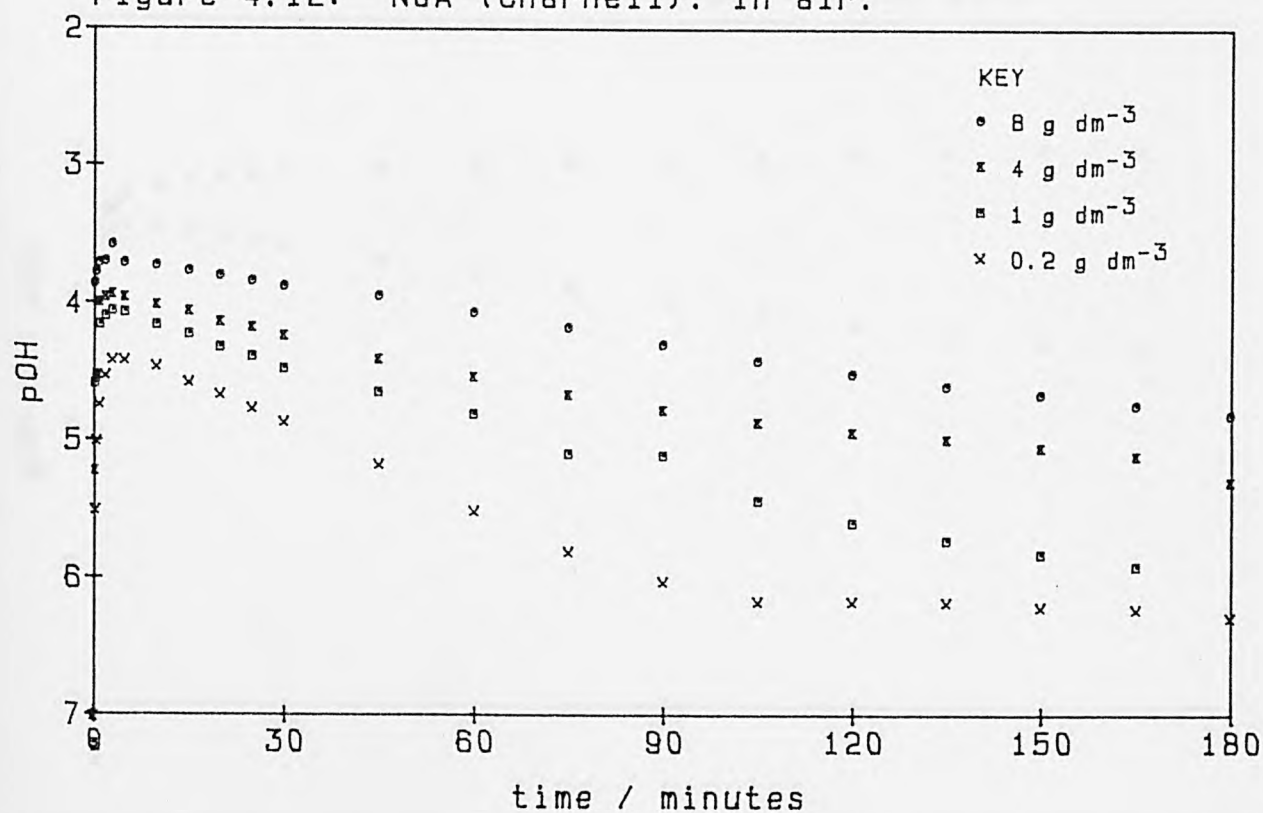


Figure 4.13: 4 g dm⁻³ NaA (Laporte). Under nitrogen.

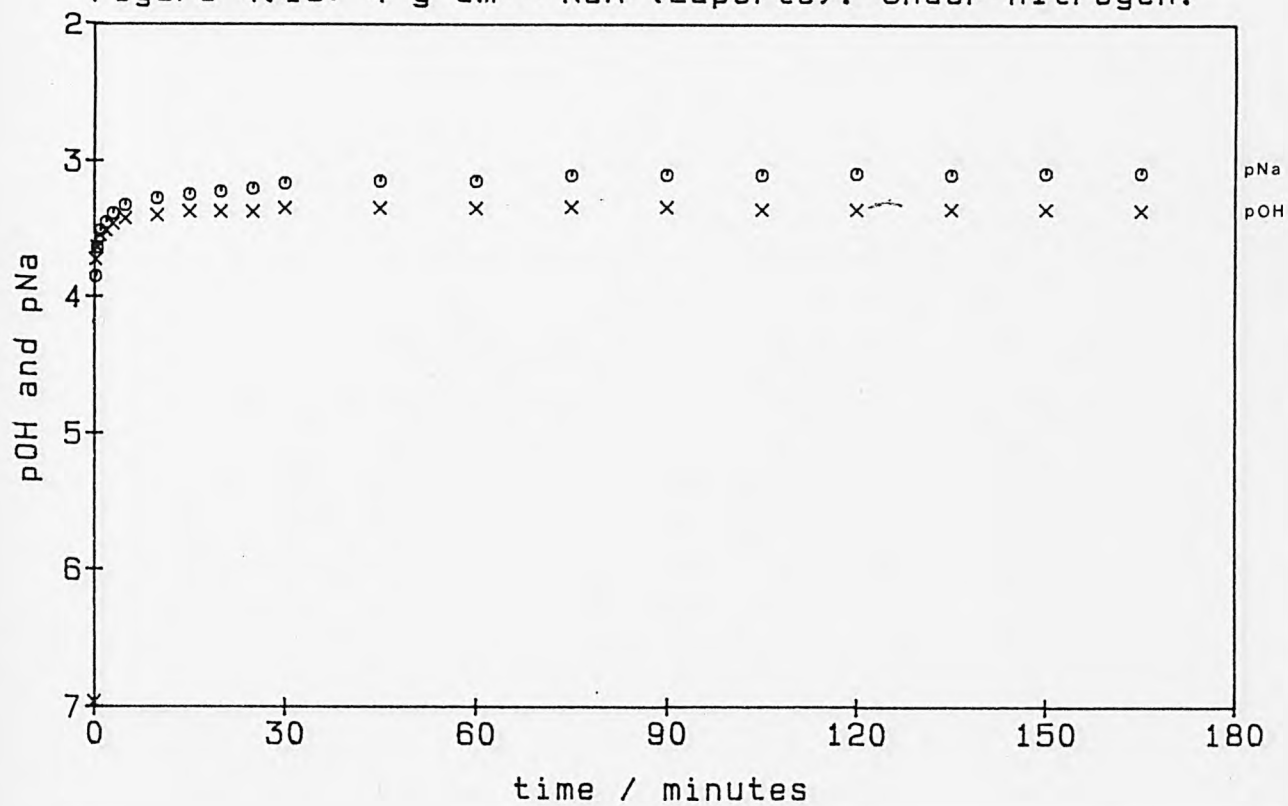


Figure 4.14: 4 g dm⁻³ NaA (Laporte). In air.

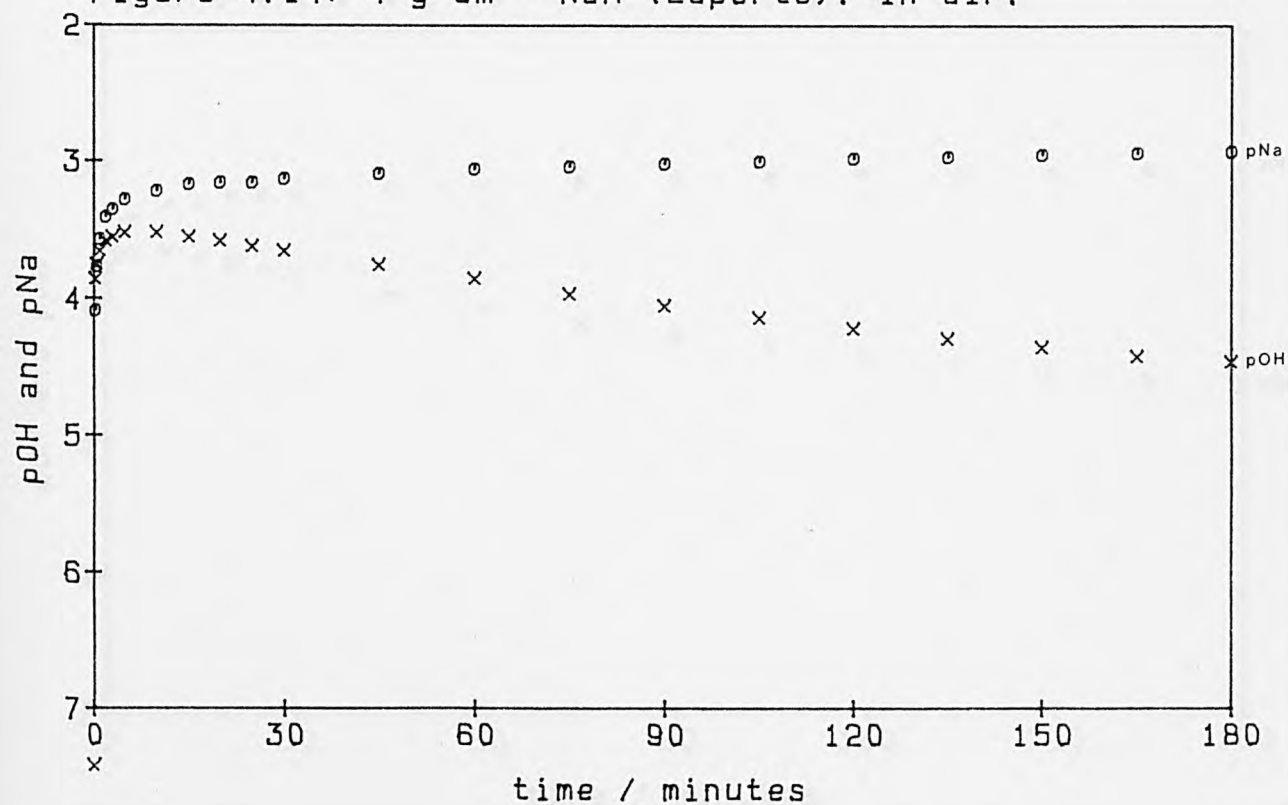


Figure 4.15: 4 g dm⁻³ NaX (BDH). Under nitrogen.

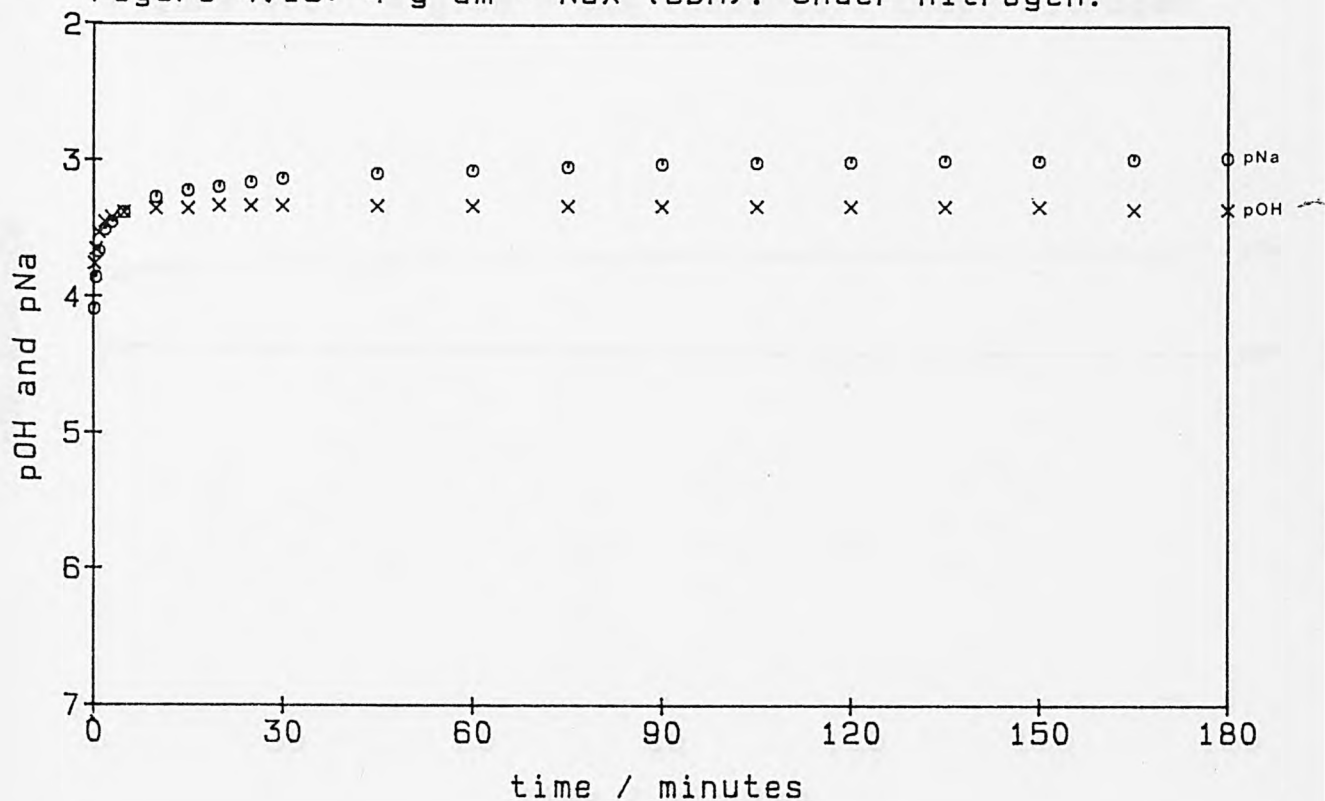
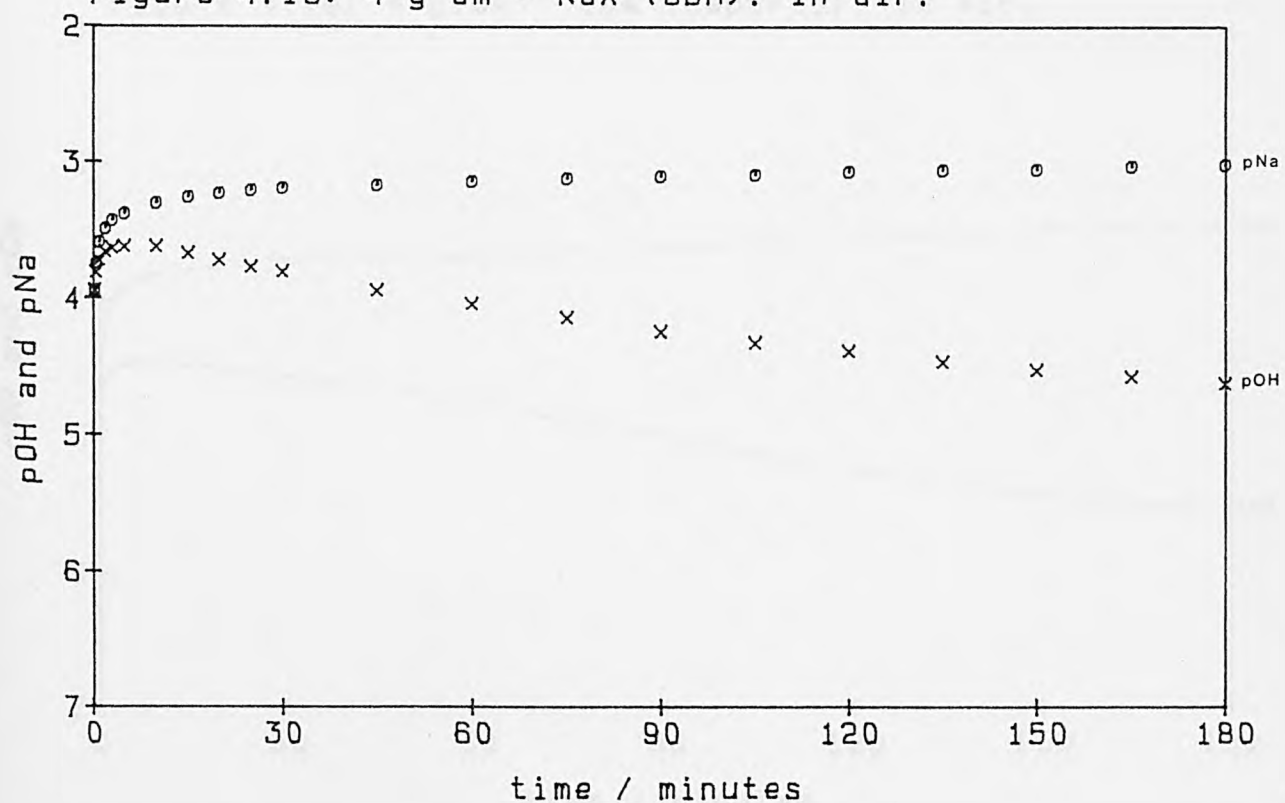
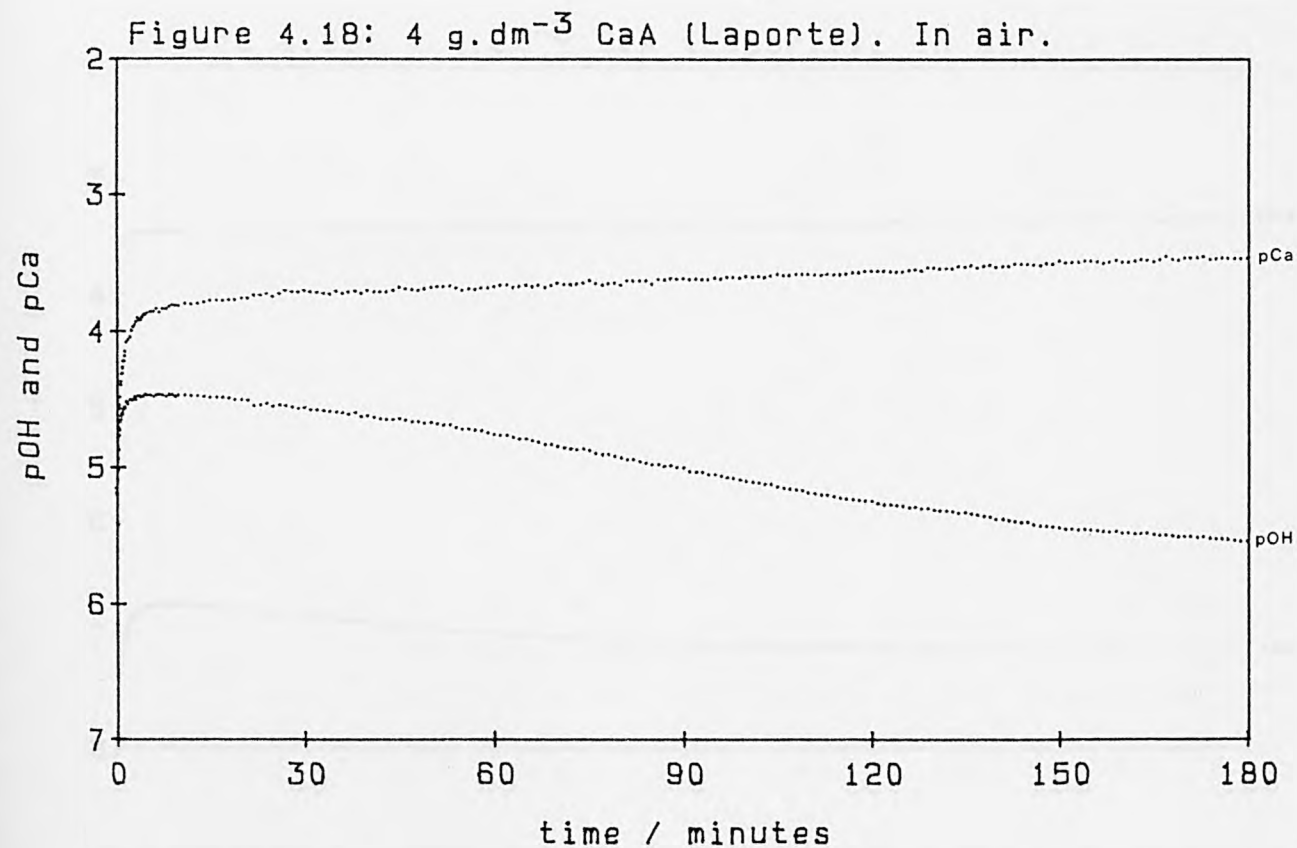
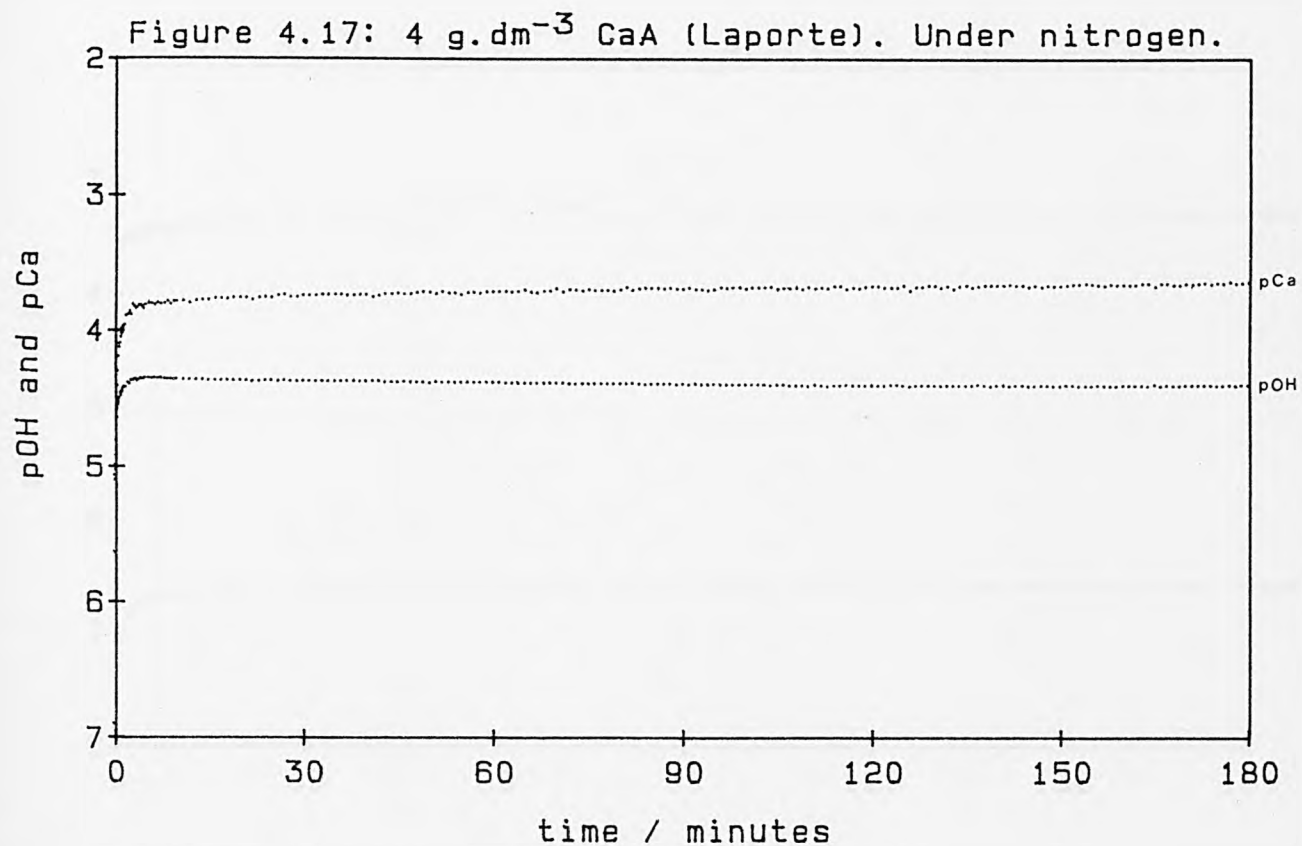
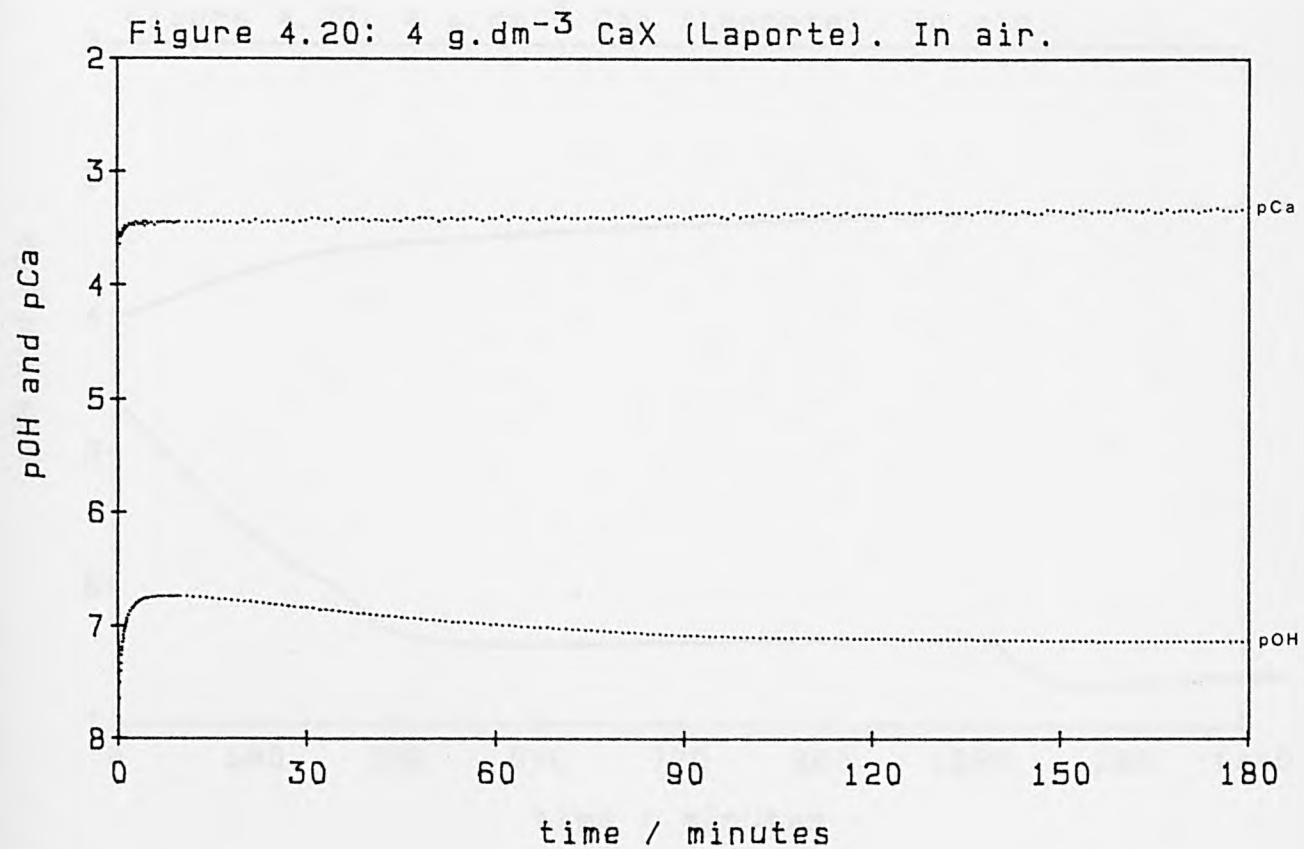
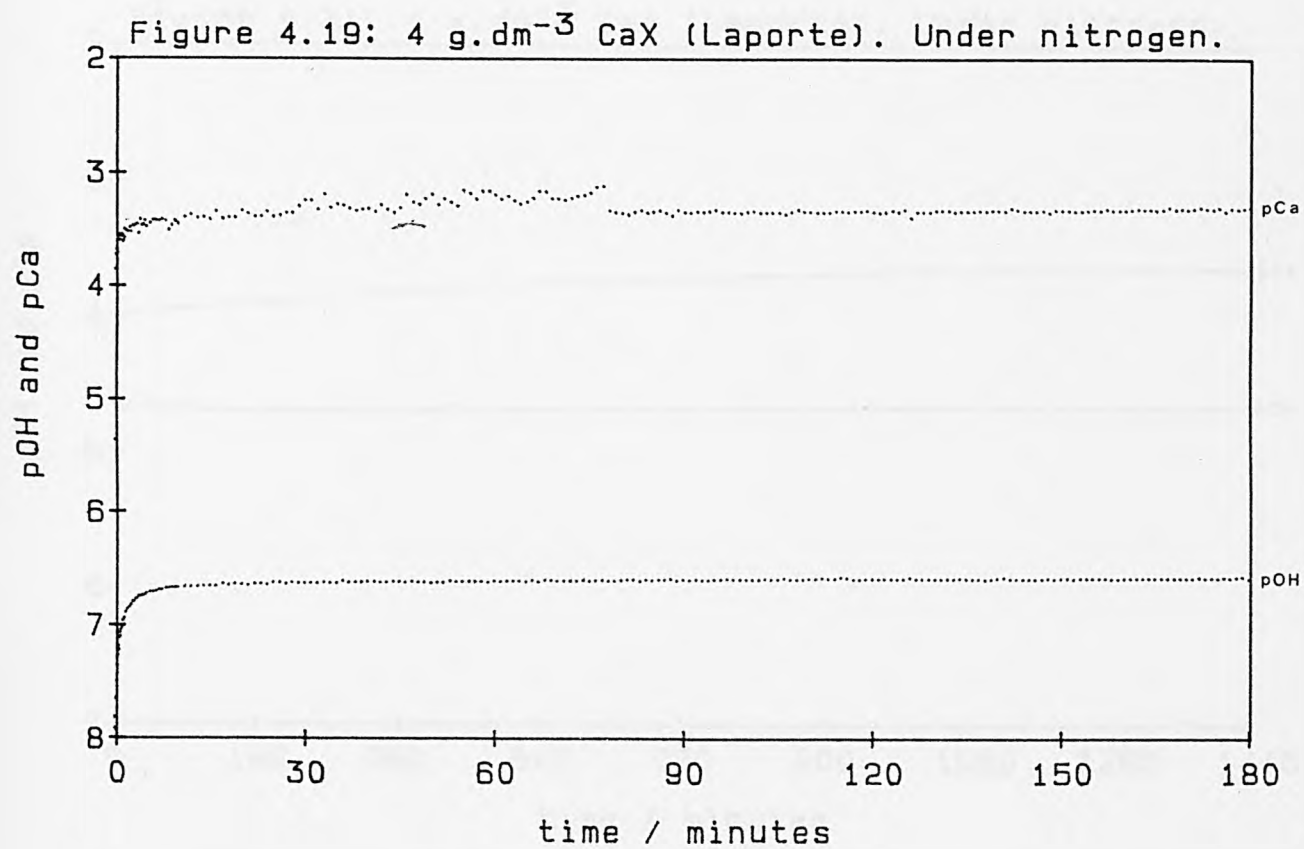
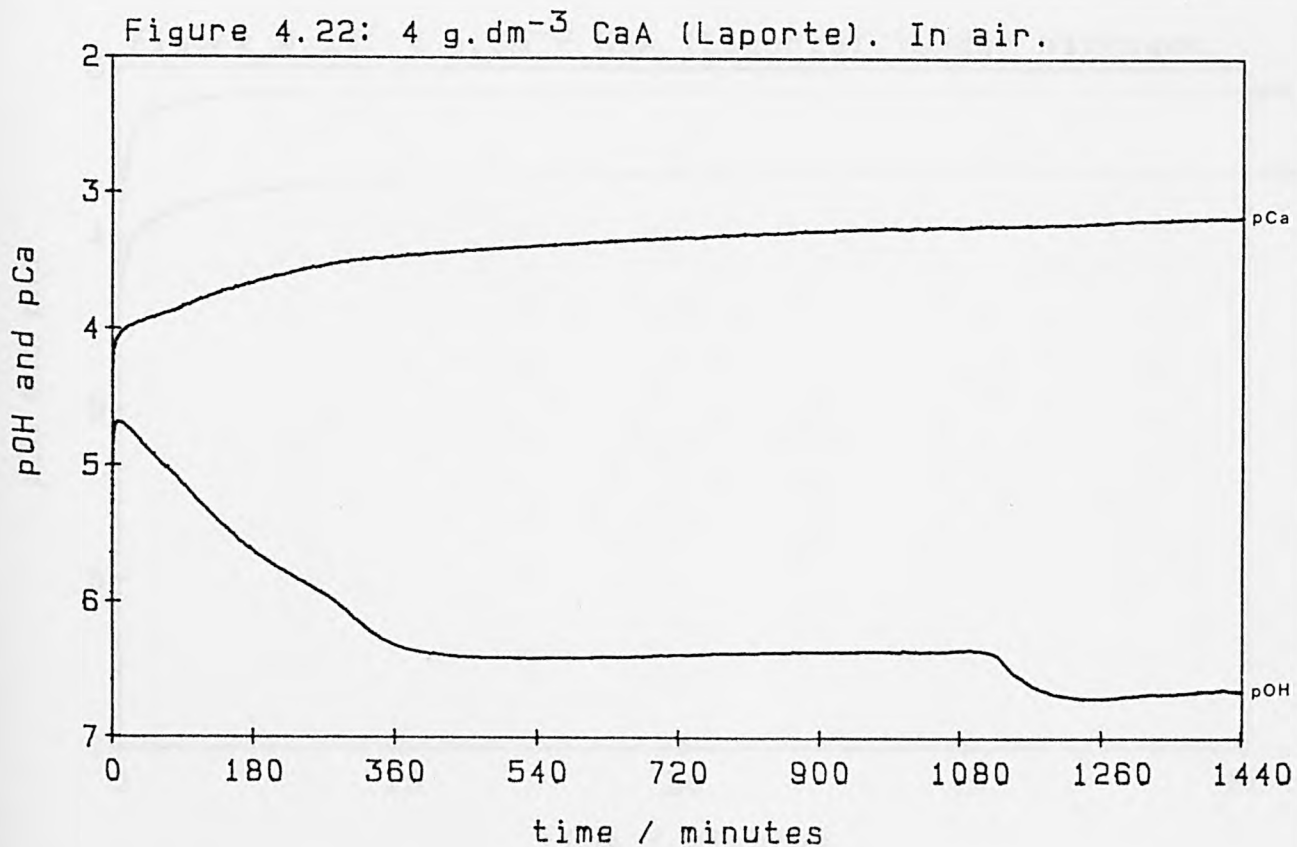
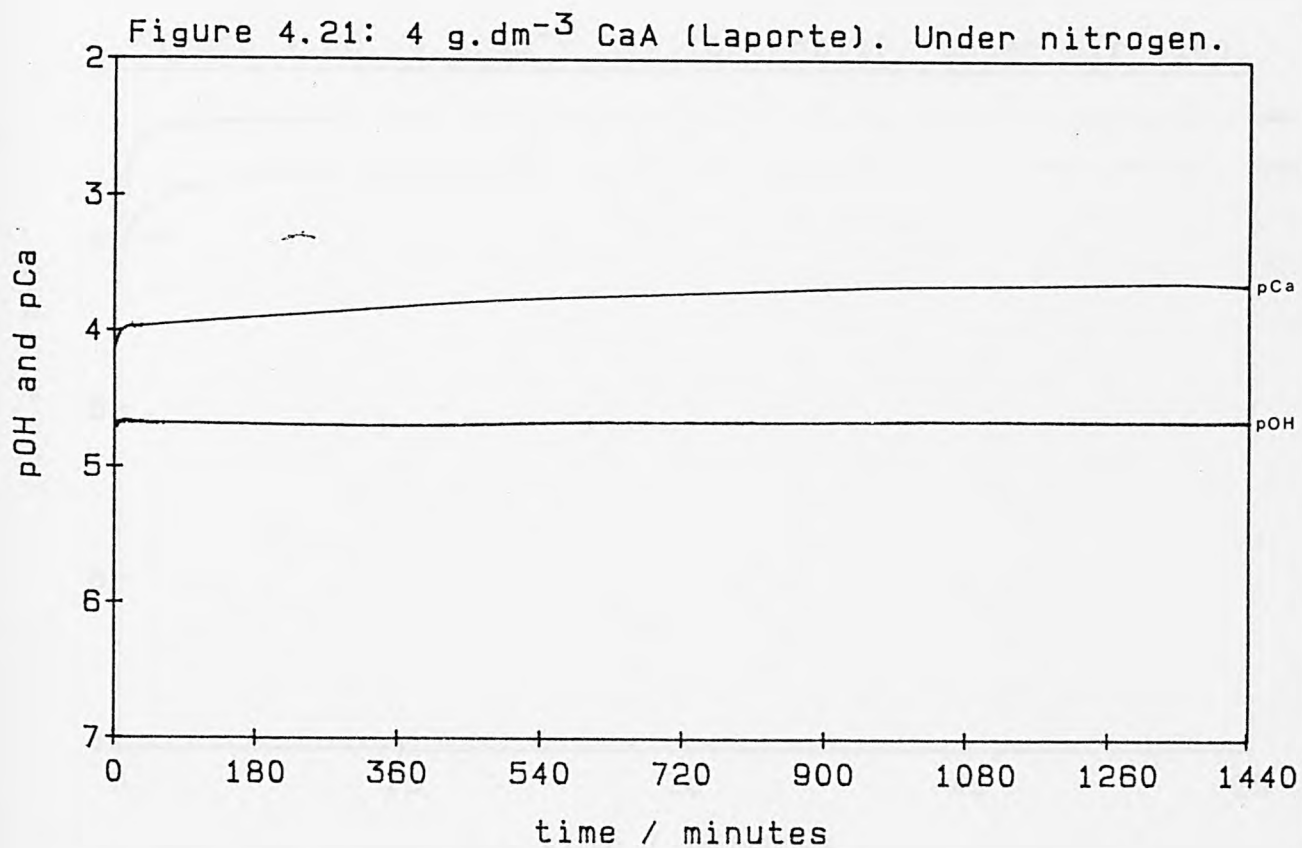


Figure 4.16: 4 g dm⁻³ NaX (BDH). In air.









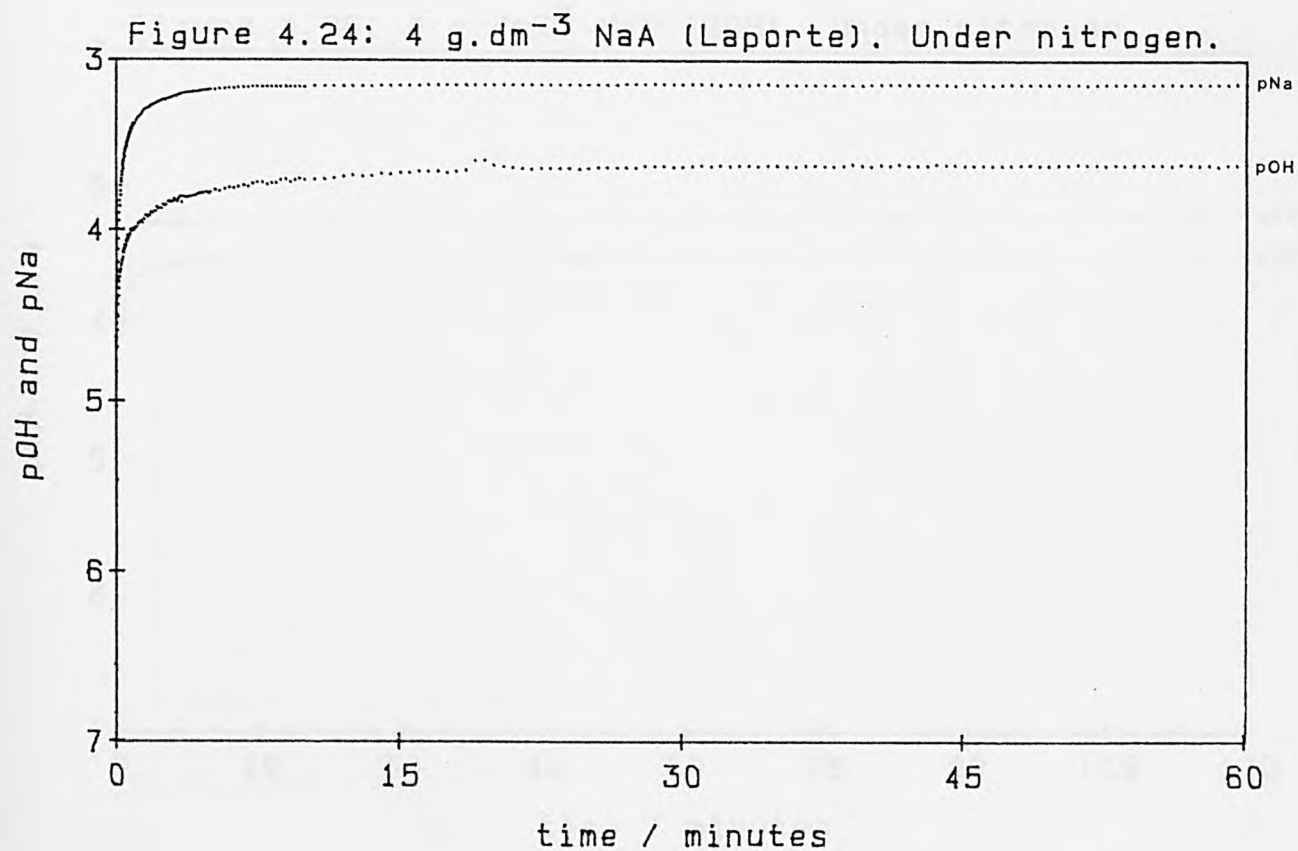
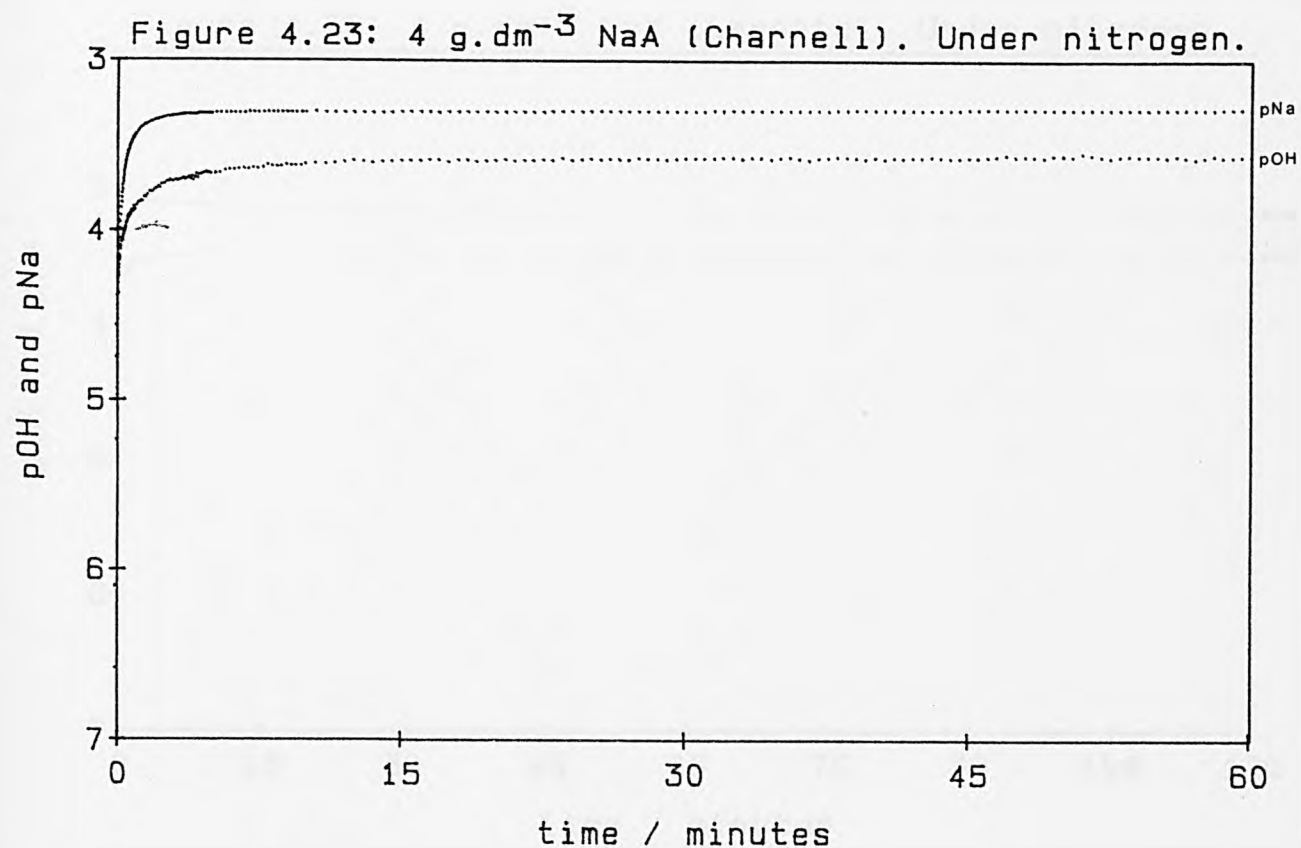


Figure 4.25: 4 g.dm⁻³ NaX (Laporte). Under nitrogen.

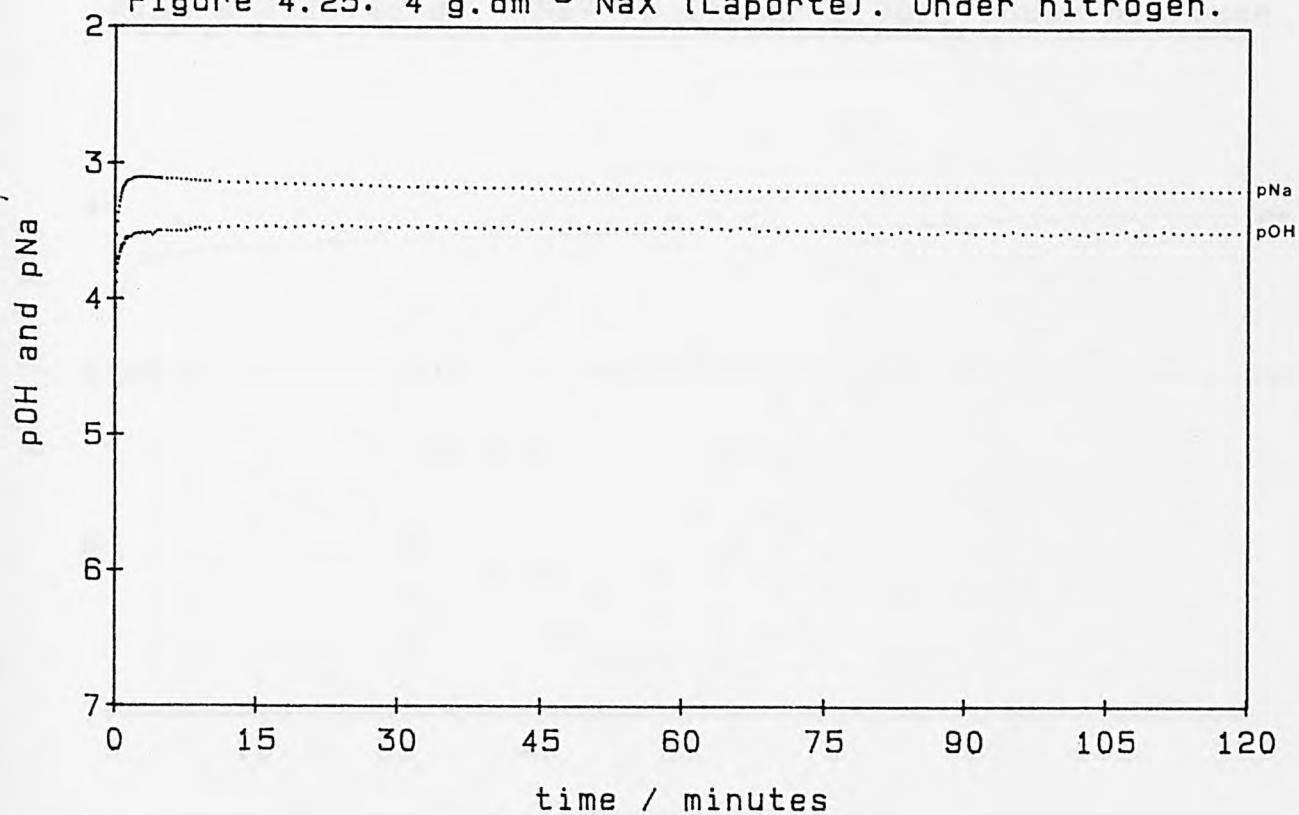
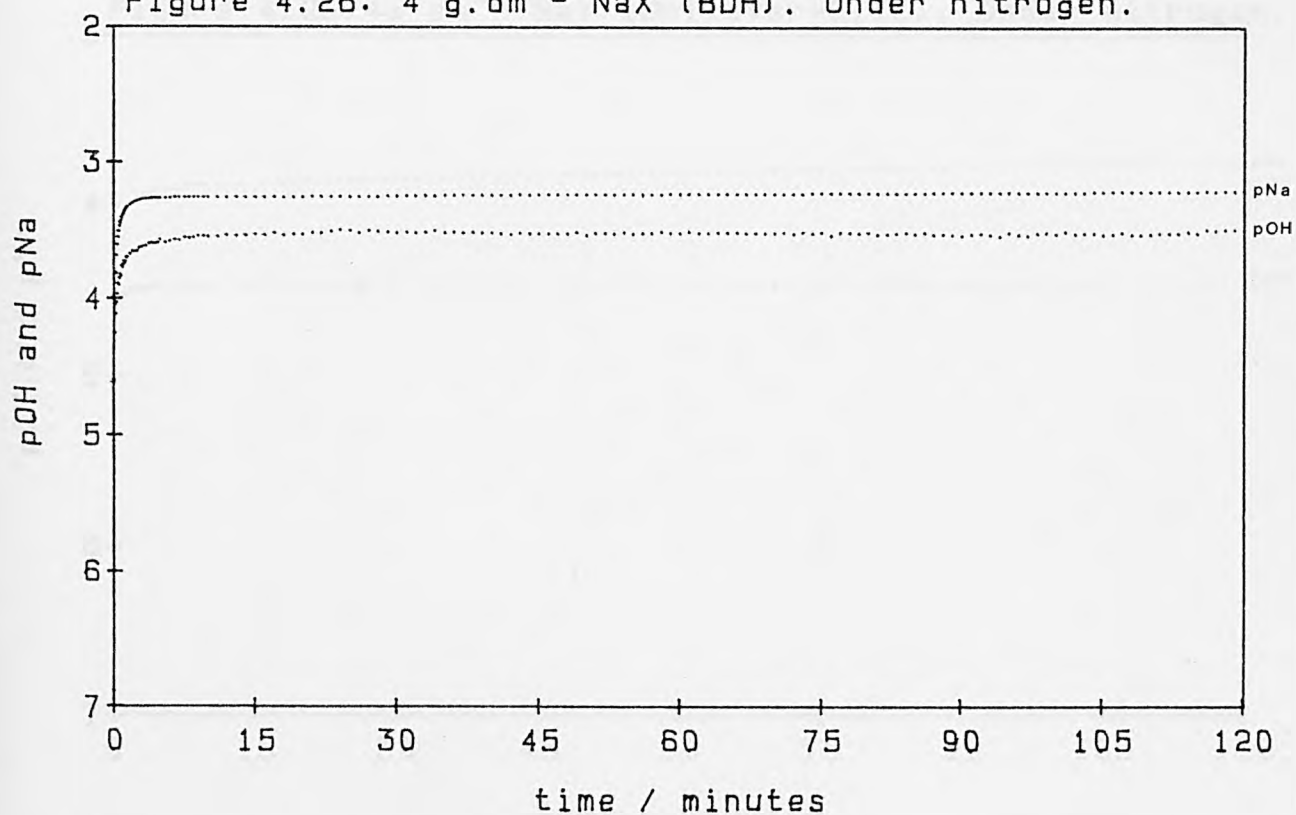
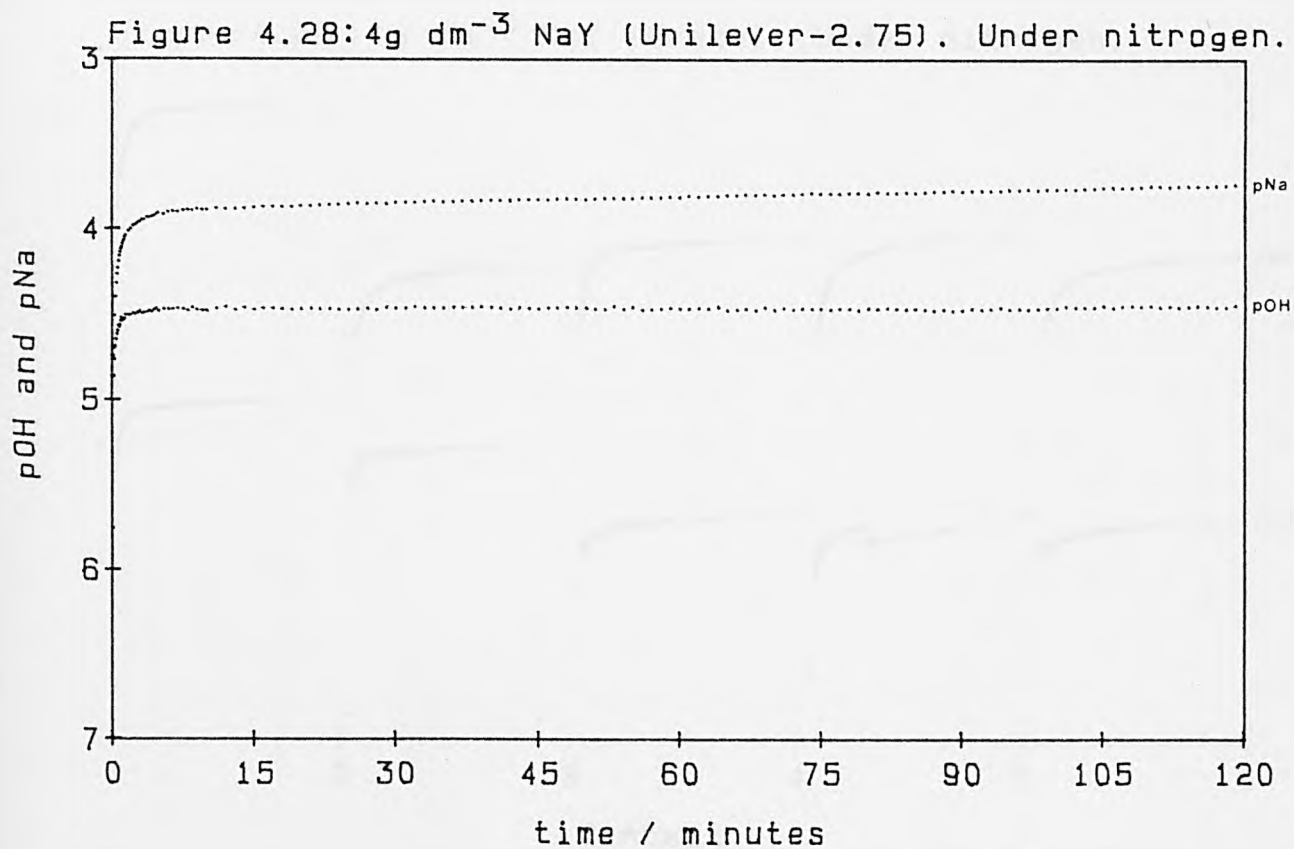
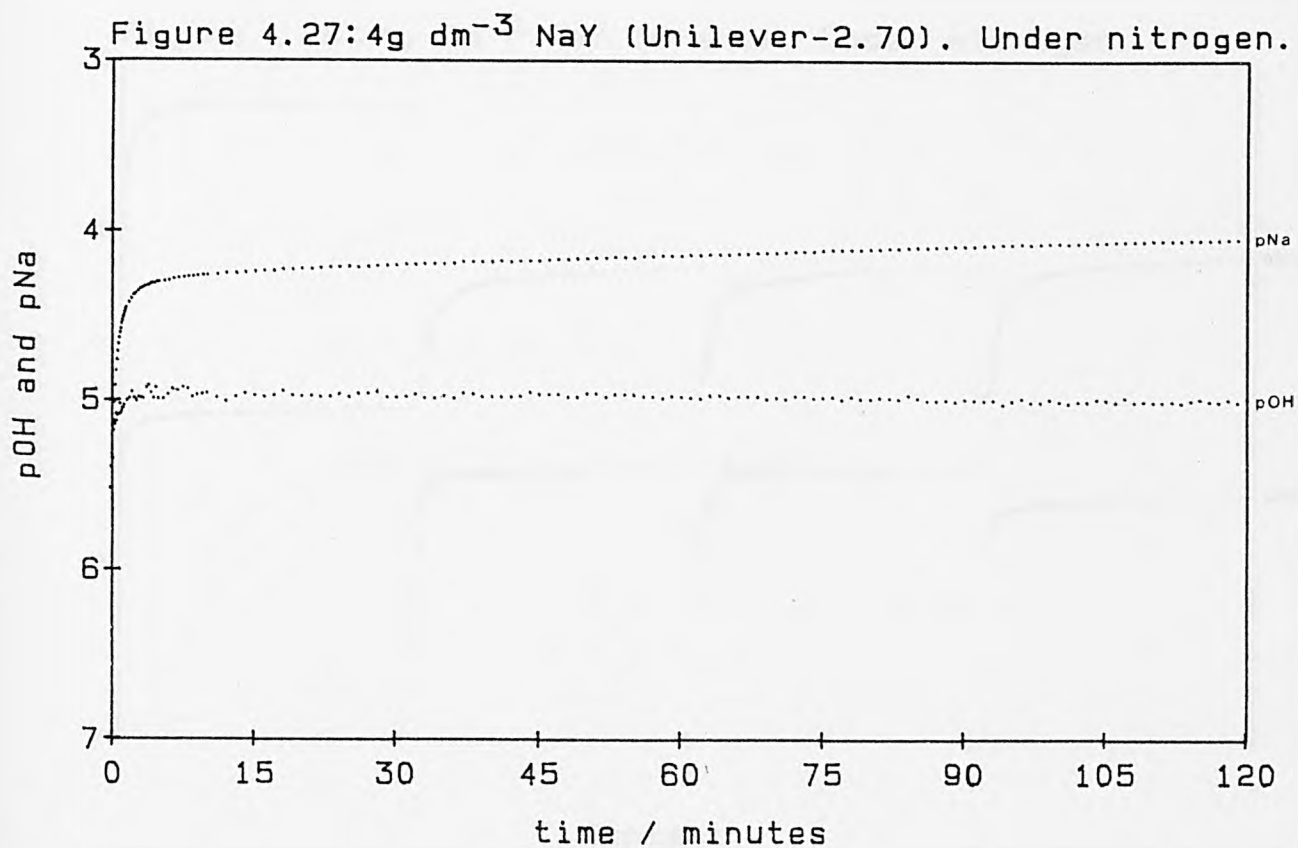
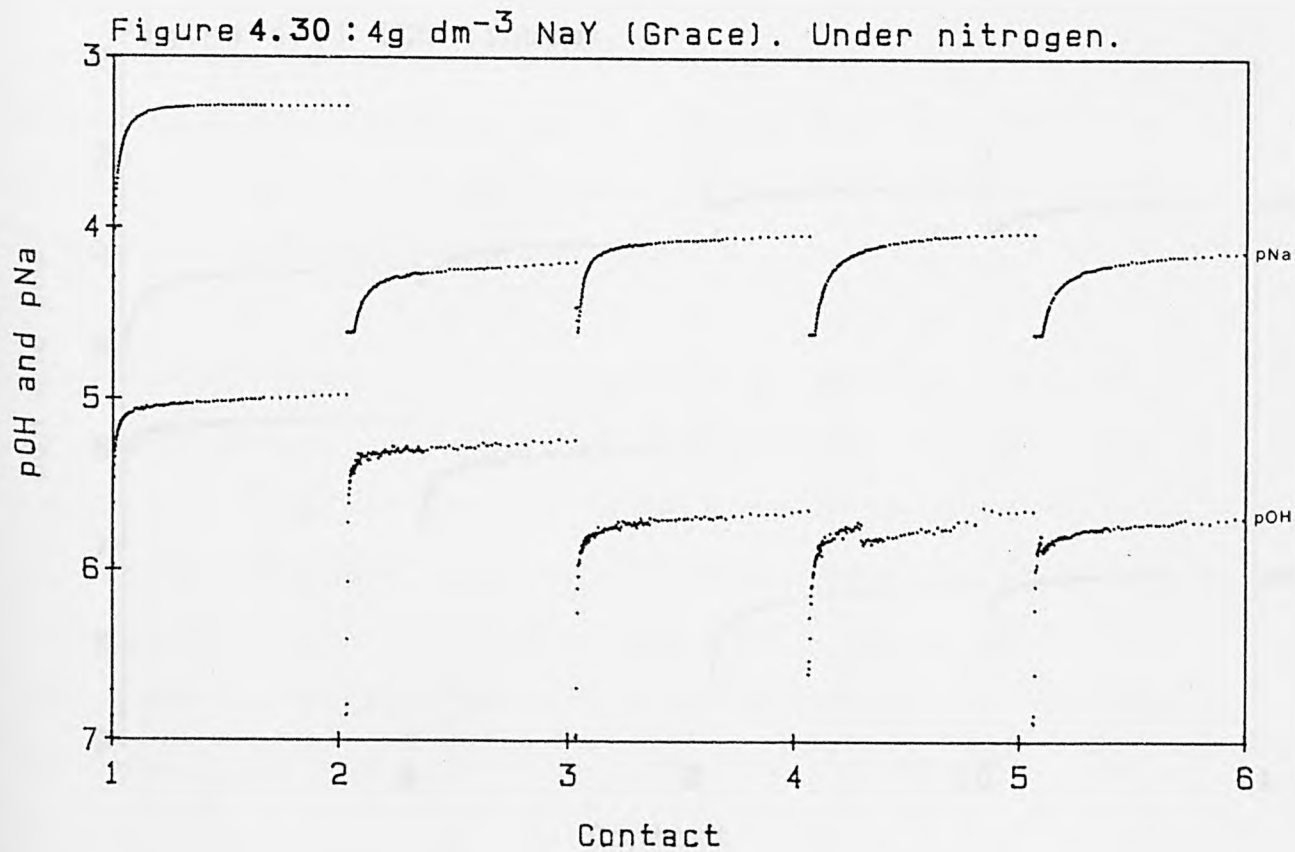
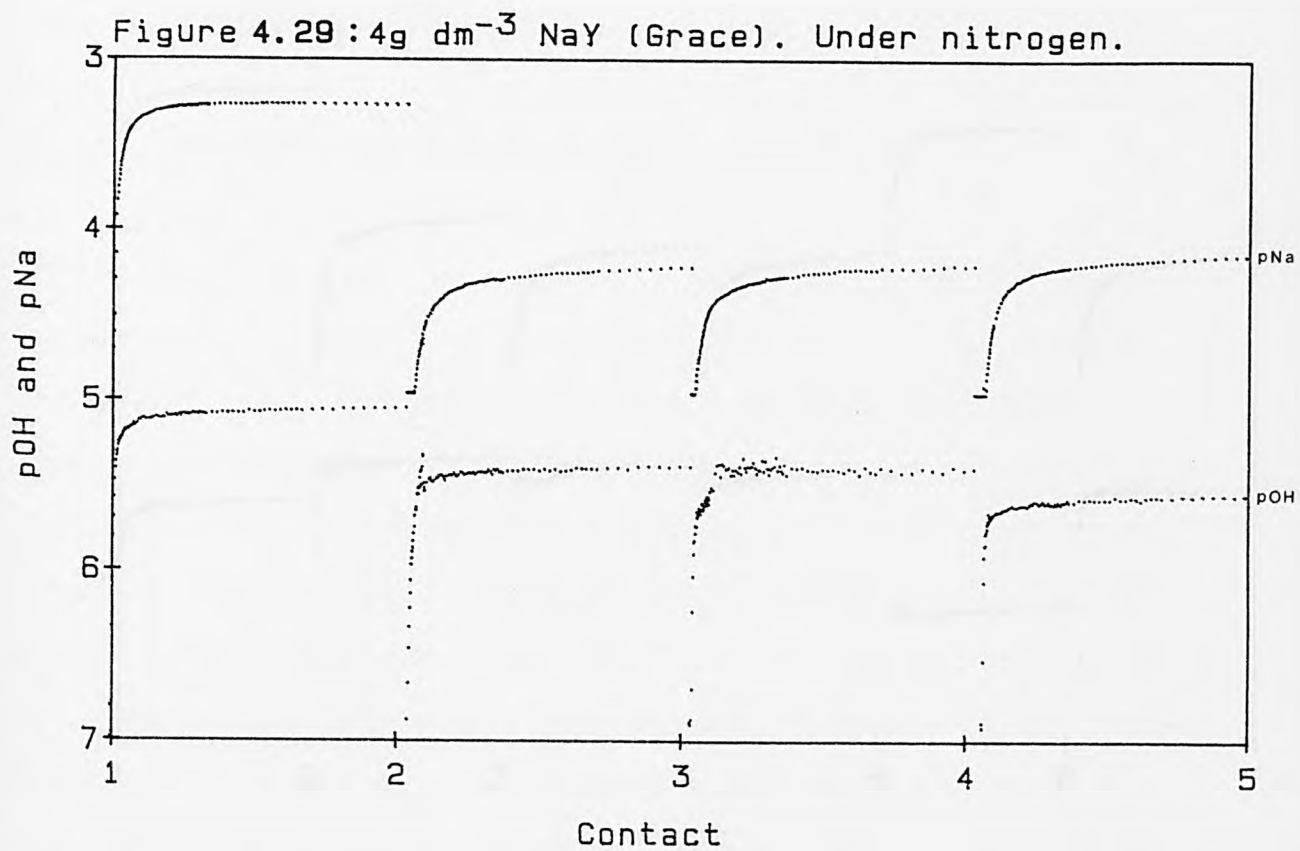
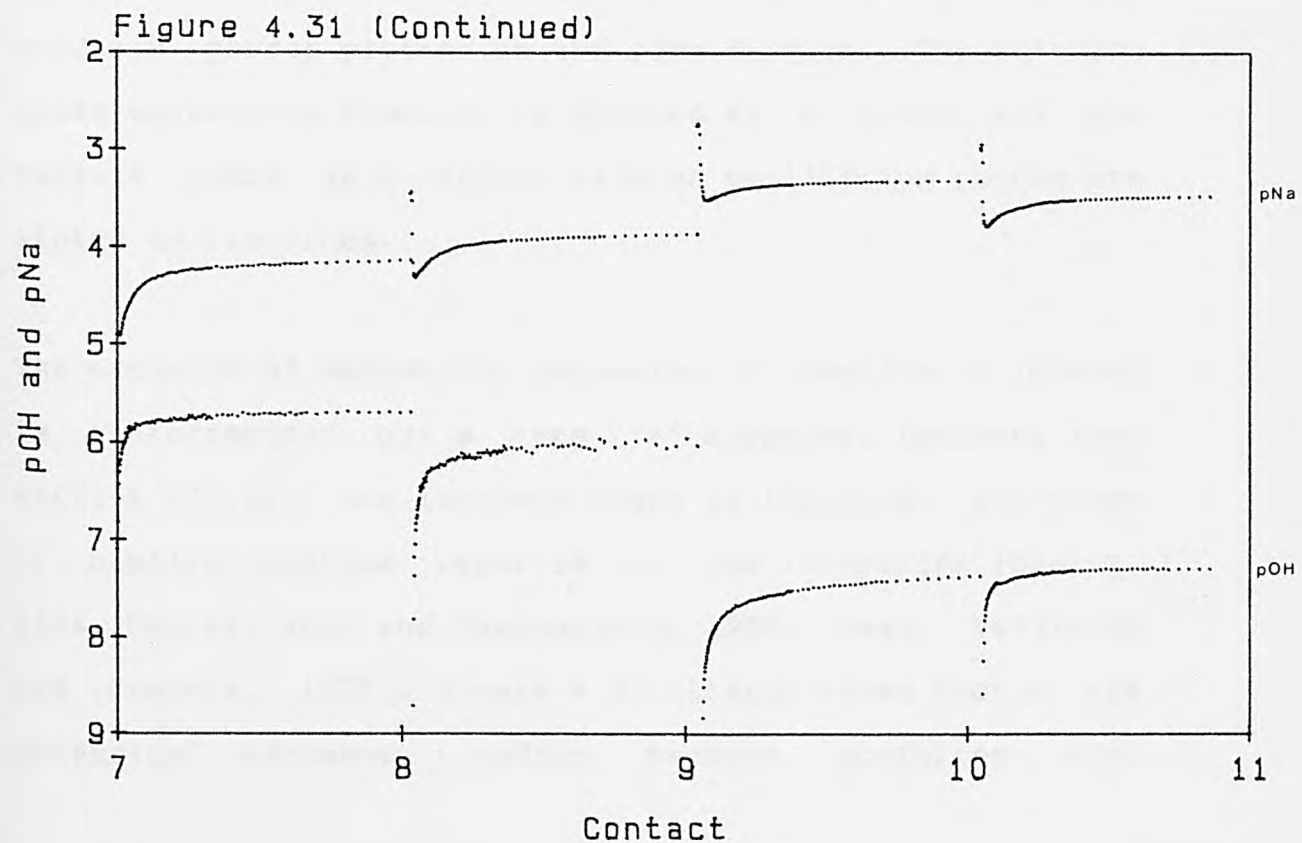
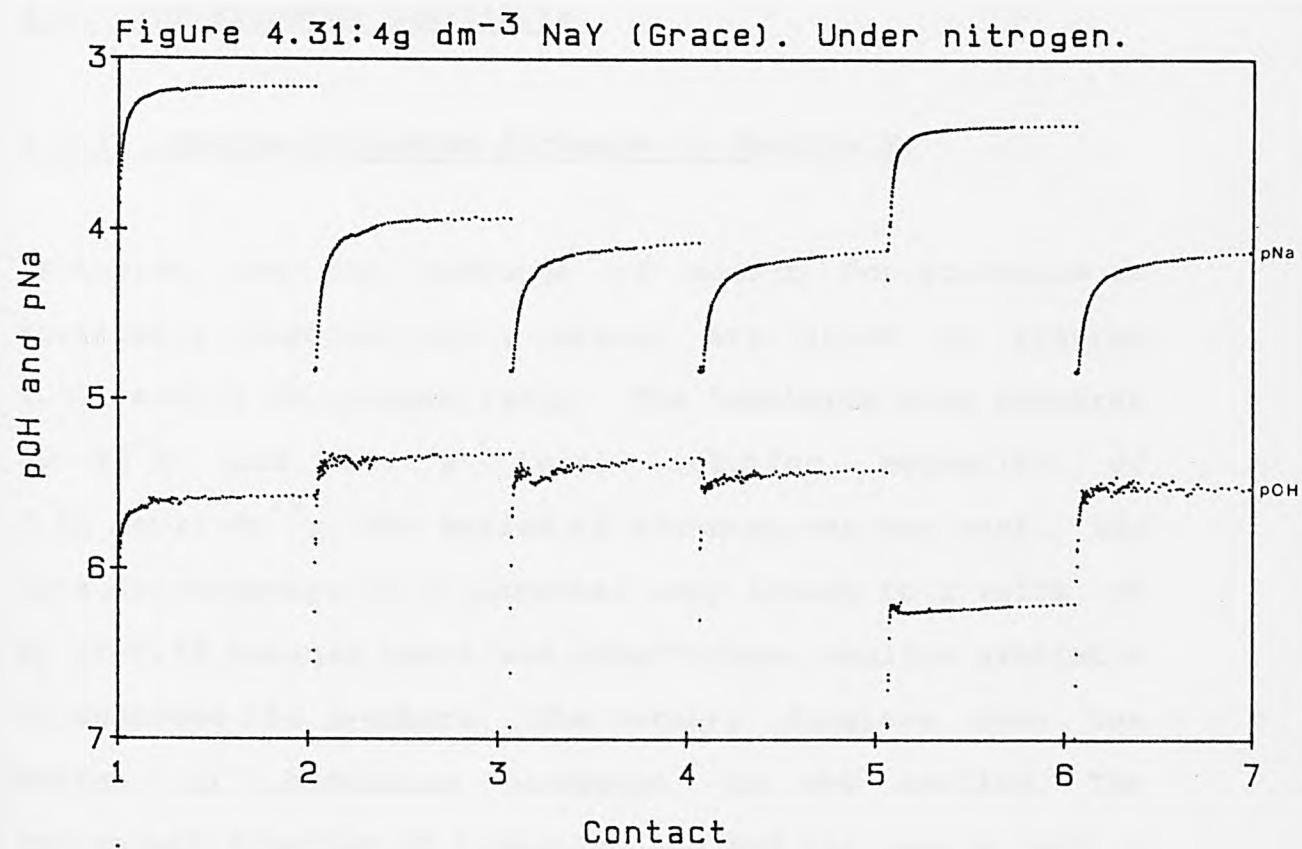


Figure 4.26: 4 g.dm⁻³ NaX (BDH). Under nitrogen.









4.3. Ion-Exchange Equilibria.

4.3.1. Sodium-Potassium Exchange in Zeolite Y.

Isotherms for the exchange of sodium for potassium in zeolites Y (Laporte) and Y (Grace) are shown in figures 4.32 and 4.36, respectively. The isotherms were measured at 25°C and at a total solution normality of 0.05 equiv dm⁻³; the period of exchange was one week. The data for exchange in Y (Laporte) only extend to a value of E_K of 0.75 because there was insufficient zeolite available to complete the isotherm. The ternary diagrams show the degree of hydronium exchange in the zeolite. The equivalent fraction of hydronium ion and the ions A and B are represented by the three coordinates of the ternary composition plot, with data for both the zeolite and solution phases plotted on the same diagram. The solution phase equivalent fraction is plotted as a cross and the zeolite phase as a circle; related equilibrium points are linked by tie-lines.

The exchange of sodium for potassium in zeolite Y (Grace) is characterised by a type "e" sigmoidal isotherm (see section 2.1.2). The isotherm shape is identical to those of similar systems reported in the literature (Sherry, 1966; Barrer, Rees and Shamsuzzoha, 1966; Maes, Verlinden and Cremers, 1978). Figure 4.37 clearly shows that at 68% potassium exchange, sodium becomes preferred over

potassium. This is likely to be due to the presence of at least two distinct crystallographic sites exhibiting differing selectivities for sodium and potassium ions.

Below 68%, exchange of sodium for potassium occurs in the supercages. Ions in the supercages exist in the hydrated state, in unlocalised positions surrounded by zeolitic water, or in site II* positions close to the six-oxygen windows leading to the sodalite cages (Broussard and Shoemaker, 1960; Baur, 1964; Mortier and Bosman, 1971). Potassium is preferred to sodium in these sites because of the greater coulombic attraction between the ionic framework and the smaller hydrated potassium ion (Nightingale, 1959). When the potassium content of zeolite Y (Grace) had risen to 36.5 ions per unit cell (p.u.c.) the zeolite began to show a preference for sodium. Hydronium exchange in this region of the isotherm was between 3.5 and 4.5%, which is equivalent to $1.5-2 \text{ H}^+$ p.u.c. This leaves between 15.2 and 15.7 sodium ions p.u.c., which is consistent with the number of ions found in the small pore system (sodalite cages and hexagonal prisms) of zeolite Y (Broussard and Shoemaker, 1969; Olson, 1970; Mortier and Bosman, 1971; Beagley, Dwyer and Ibrahim, 1978; Barrer, 1978). At these cation positions consideration of the framework-oxygen / cation internuclear distances leads to the conclusion that there are no water molecules interposed between the fixed anionic sites and the counterions (Broussard and Shoemaker, 1960; Sherry, 1966). The net

result of the effect of the free energy of partial cation dehydration, and of the free energy due to coulombic interactions between the partially dehydrated counter-ion and the anionic framework is a greater selectivity for sodium over potassium in the small cage sites (Sherry, 1966). It should be remembered that removal of sodium ions from exchange sites, and hydration of these cations will also contribute to the free energy change.

The Na-K isotherm for zeolite Y (Laporte) is non-sigmoidal over the range measured (figure 4.32), indicating no site heterogeneity in the large cages. The data was obtained without "forcing" the isotherm, i.e. no contacts with larger volumes of solution, or multiple exchanges were employed. The highest potassium exchange attained corresponds to the point where the zeolite changes from being selective for potassium ions and instead shows a preference for sodium. ^{The isotherm terminates at the point where} A selectivity reversal should occur. This illustrates further the relative ease of potassium exchange in the supercages.

The levels of hydronium exchange in the zeolite decreased with increasing potassium exchange. Consistent with this observation was the decrease in solution pH with increasing E_K . Townsend, Franklin and O'Connor (1984) found a similar relationship between the cation deficiency and the degree of ammonium exchange for NH_4 -Na exchange in zeolites X and Y. These observations can be explained in terms of the

relative selectivities of H^+ , Na^+ , K^+ and NH_4^+ in the large pore sites of faujasite-type zeolites. This will be discussed further in later sections.

Kinetic studies showed that the exchange of potassium for sodium in zeolite Y was very rapid. Therefore, in order to reduce the amount of hydronium exchange in the zeolite, the exchange period was reduced from seven days to 24 hours for subsequent isotherms. The Na-K isotherm for zeolite Y (Grace) was repeated, and, in order to vary the degree of hydronium exchange in a controlled way, separate isotherms were measured after adjusting the initial pH of the exchange solutions to 4, 3, 2.3 and 2 by the addition of dilute nitric acid. The "normal" pH of sodium / potassium exchange solutions was between 5.2 and 5.4 when no acid was added.

Figure 4.40 shows a sodium - potassium isotherm for zeolite Y (Grace) measured at the "normal" initial pH, using an exchange time of 24 hours. The isotherm shape is exactly the same as that for the zeolite exchanged for one week, but the level of hydronium exchange was substantially lower (cf. figure 4.36 with 4.40). For most of this isotherm, within experimental error, no hydronium exchange occurred. The solution pH's after exchange were only slightly higher than those found for the seven day exchange because the effect of dissolution of CO_2 is compensated for by additional hydronium exchange in the zeolite. In other

words the much higher hydronium exchange level for the seven day exchange is due to the diffusion of atmospheric carbon dioxide into the solution (section 4.2).

The pH after exchange was about 0.5 units lower for the pH isotherm measured at an initial pH of 4 compared to the isotherm obtained at "normal" pH, but the hydronium exchange in both cases was approximately zero (figure 4.44). In contrast, at an initial pH of 3 the hydronium exchange in the zeolite was about 5 to 6% for points where the potassium exchange was less than 80% (figure 4.48). Above the 80% potassium exchange level, the hydronium exchange increased significantly because these points were measured by contacting the same mass of zeolite with larger volumes of solution. The pH after exchange was between 3.8 and 4.9 for points measured after contacting 0.2 g of zeolite with 50 cm³ of solution. Using atomic absorption spectroscopy, no aluminium was detected in solution for any of the exchanges carried out at this initial pH of 3.

As can be seen from the ternary diagrams in figures 4.52 and 4.54, the hydronium exchange levels in the isotherms measured using initial pH's of 2.3 and 2 were very high. Also, aluminium was found in the solution phase after these exchanges. The pH's, total exchange levels and dealumination data for these isotherms are summarised in table 4.18. The hydronium exchange was calculated, as

before, from the difference between the total cation content and the aluminium content of the zeolite. Clearly, when aluminium has been extracted from the lattice this value does not represent the amount of hydronium ions in exchange sites because the exchange capacity of the zeolite has been changed by dealumination. In table 4.18, the degree of dealumination is represented by the number of aluminium ions per unit cell of the zeolite, removed into solution.

Table 4.18. Hydrolysis Data for Na-K Exchange in Zeolite Y (Grace) at pH 2 and pH 2.3.

pH 2.3			pH 2		
pH	total cation p.u.c.*	Al released p.u.c.	pH	total cation p.u.c.*	Al released p.u.c.
3.94	34.5	0.00	3.28	21.1	1.45
3.75	33.0	0.08	3.30	20.4	1.72
3.74	34.4	0.08	3.25	24.4	1.92
3.75	34.0	0.10	3.23	22.2	2.07
3.62	33.0	0.21	3.27	24.0	2.20
3.65	35.0	0.43	3.29	23.9	2.44
3.43	24.2	1.70	3.27	23.7	2.51
3.32	18.2	3.17	3.27	24.2	2.72
			3.27	24.9	2.74
			3.32	25.1	2.98
			3.33	24.9	3.17

*The exchange capacity of zeolite NaY (Grace) was 53.8 charges p.u.c.

The standard free energy of the ion-exchange reactions was calculated using the procedure outlined in section 3.7.4. Values obtained by integration of the best-fit polynomials were in very good agreement with those obtained by graphical integration.

For Na-K exchange in zeolite Y (Laporte) ΔG_{298}^{\ominus} was $-1.50 \text{ kJ equiv}^{-1}$. However, this value must be treated with caution as the isotherm only extended to 77% potassium exchange, the corrected selectivity plot being extrapolated to 100% exchange. Values of ΔG_{298}^{\ominus} (in kJ equiv^{-1}) for Na-K exchanges reported in the literature are listed below:

<u>Si/Al</u>	<u>ΔG_{298}^{\ominus}</u>	<u>Reference</u>
1.82	-0.82	Lai and Rees (1976)
2.38	-1.55	Barrer, Davies and Rees (1968)
2.56	-1.55	Maes, Verlinden and Cremers (1978)
2.67	-0.80	Sherry (1966)

ΔG_{298}^{\ominus} for the Na-K exchange in zeolite Y (Grace) under "normal" initial pH conditions was calculated to be $-0.90 \text{ kJ equiv}^{-1}$ when the period of exchange was 1 week, but only $-0.67 \text{ kJ equiv}^{-1}$ for the 24 hour exchange. Examination of the selectivity plots for these isotherms (figures 4.37 and 4.41) shows a slight decrease in the selectivity of the zeolite for potassium in the case of the longer exchange. This is due to competition by hydronium ions for the exchange sites in the zeolite. When the Na-K exchange data, measured under different pH conditions, were plotted on the same binary axes the pseudo-binary isotherms were near-coincident despite large differences in the levels of hydronium exchange. Visible differences were only seen when exchange took place under more severe acid conditions (pH 2.3 and pH 2) when dealumination of the framework started to occur. The zeolite phase equivalent

fractions are calculated from the total cation content of the zeolite. When hydronium exchange occurs the very high selectivity of the zeolite effectively means that cation exchange is limited to those sites which are not hydronium exchanged. Thus, the shape of the isotherm remains substantially unchanged but small changes in the selectivity of the zeolite can, under certain circumstances, have a relatively large effect on the value of ΔG^\ominus . These observations may account in part for discrepancies in the values of ΔG^\ominus reported in the literature for similar ion-exchange systems. The choice of exchange time, which must be long enough to allow the system to reach true equilibrium but as short as possible in order to reduce hydronium exchange, is then very important in the measurement of ion-exchange equilibria. Thermodynamic analysis of the systems measured at lower initial pH's was unreliable. These isotherms were not reversible and the complete range of E_K was not covered. Values of ΔG^\ominus calculated for these isotherms showed a broad scatter. This serves to emphasise the role of hydronium exchange as a cause for errors in the thermodynamic interpretation of data in the past.

The exchange of sodium for potassium in zeolite Y (Grace) was also measured at 2°C. There was very little difference in this isotherm compared to those measured at 25°C but the selectivity of the zeolite for potassium in the small cages was slightly lower at 2°C. The free energy of exchange, ΔG_{275}^\ominus , was -0.25 kJ equiv⁻¹.

4.3.2. Sodium - Potassium Exchange in Zeolite X.

The sodium - potassium ion-exchange isotherm in zeolite X (Laporte) is shown in figure 4.59. The isotherm is again sigmoidal and the preference of the zeolite changes from potassium to sodium at about 40% potassium exchange. This value agrees very well with that found by Sherry (1966). Sherry also explained this change in selectivity in terms of sodium exchange occurring at three different kinds of crystallographic site. Below 40% exchange, the zeolite shows a preference for potassium ions. Up to this point exchange occurs with the 33 cations p.u.c. in the large cages, which are probably present as hydrated ions (Baur, 1964). The next stage is the exchange of the 32 cations p.u.c. located near the rings of 6 tetrahedra which interconnect the supercages and sodalite cages (Broussard and Shoemaker, 1960). Finally, exchange of the 16 cations p.u.c. located in the small cage network of sodalite cages and hexagonal prisms takes place.

The hydronium exchange in zeolite X was higher than that found for zeolite Y under the same conditions. At a "normal" initial pH, after a 24 hour exchange, the hydronium exchange was between 2 and 6%. Again, the hydronium exchange was higher at the sodium end of the isotherm. When the background pH was reduced to 2.3 (figure 4.64), the hydronium exchange in zeolite X increased to between 25 and 46%. Isotherm points up to the

80% potassium exchange level were measured by contacting 0.2 g of zeolite with 50 cm³ of solution. When the volume of solution was increased to 100 cm³ in order to force more potassium into the zeolite, the "hydronium exchange" increased to over 83%. This was accompanied by release of aluminium into solution. For the other isotherm points however, the level of aluminium in solution remained below the atomic absorption spectroscopy detection limit of about 0.2 ppm. The data are summarised in table 4.19.

Table 4.19. Hydrolysis Data for Na-K Exchange in Zeolite X (Laporte) at pH 2.3.

pH	total cation p.u.c.*	Al released p.u.c.
6.18	59.6	0.00
6.03	59.5	0.00
5.58	58.8	0.00
6.22	60.8	0.00
6.07	60.3	0.00
5.19	58.6	0.00
5.79	43.4	0.00
4.23	13.2	3.34

*The exchange capacity of zeolite X (Laporte) was 80.9 charges p.u.c.

The value of ΔG_{298}^{\ominus} for Na-K exchange in zeolite X (Laporte) was $+0.188 \text{ kJ equiv}^{-1}$. This can be compared to values of ΔG_{298}^{\ominus} quoted in the literature of $-0.795 \text{ kJ equiv}^{-1}$ (Barrer, Rees and Shamsuzzoha, 1966) and $+0.585 \text{ kJ equiv}^{-1}$ (Sherry, 1966) for zeolite X with similar Si/Al ratios.

4.3.3. Sodium-Ammonium and Potassium-Ammonium Exchange in Zeolite Y.

The exchange of ammonium for sodium in zeolite Y has been studied extensively because of its importance in the preparation of cracking catalysts (Sherry, 1966; Sherry, 1969; Theng, Vansant and Uytterhoeven, 1968; Lai and Rees, 1976; Fletcher and Townsend, 1982; Franklin, 1984; Townsend, Franklin and O'Connor, 1984). The Na-NH₄ exchange isotherm in zeolite Y (Grace) is shown in figure 4.66. The isotherm is type "d" (section 2.1.2), terminating at 77% ammonium exchange. At the maximum exchange level the zeolite contained 40.0 ammonium ions and 1.9 hydronium ions per unit cell. The residual sodium amounted to 11.8 ions p.u.c.

Figure 4.74 shows the isotherm for the potassium - ammonium exchange in zeolite Y (Grace). The isotherm is type "c", the zeolite being markedly less selective for ammonium compared to potassium, and terminates at 83% ammonium exchange. The maximum exchange corresponded to 42.3

ammonium ions, 2.5 hydronium ions and 8.9 potassium ions per unit cell.

The structure of zeolites X and Y, in terms of a system of large and small pores, has already been discussed (sections 1.7.2 and 4.3.2). Access to the small pore system is achieved from the supercages via 6-oxygen windows with a free diameter of about 2.5 Å (Pekarek and Veseley, 1972). Studies have shown that exchange of ions such as potassium and silver proceeds to completion in both X and Y (Sherry, 1966; Barrer, Rees and Shamsuzzoha, 1966; Barrer, Davies and Rees, 1968; Lai and Rees, 1975) whereas 100% exchange of cesium, rubidium, strontium and rare-earth ions cannot be achieved under normal conditions (Barrer, Rees and Shamsuzzoha, 1966; Barrer, Davies and Rees, 1968; Sherry, 1968a; Lai and Rees, 1976; Rees and Zuyi, 1986). Incomplete exchange occurs because some ions are too large to pass through the 6-oxygen windows into the small pore system. It is thought that passage of ions through the oxygen 6-ring must be preceded by complete or partial dehydration of the cation (Sherry, 1966). Examination of data of dehydrated ion diameters (Pauling, 1960) leads to the conclusion that ions such as rubidium ($d=2.96$ Å) and cesium ($d=3.38$ Å) are just too large to pass through the oxygen 6-rings even when dehydrated. The rare earth cations have restricted access to the small pores because of their hydrated diameters (Nightingale, 1959), and complete dehydration does not occur because of the high energy required.

It has been found that exchange of ammonium and thallium ions proceeds to completion in zeolite X but not in Y (Sherry, 1966; Sherry, 1969; Franklin, 1984; Townsend, Franklin and O'Connor, 1984; Franklin et al, 1986). The result is of interest since the framework structure of zeolites X and Y is essentially the same. Tl^{+} is a large but polarisable cation; the greater framework charge density of zeolite X may be sufficient to deform the cation and allow it to pass through the six-ring.

Considerable disagreement exists in the literature concerning the maximum exchange levels of ammonium in faujasite-type zeolites of differing Si/Al ratios (Theng, Vansant and Uytterhoeven, 1968; Lai and Rees, 1976; Fletcher and Townsend, 1982; Franklin, 1984; Townsend, Franklin and O'Connor, 1984; Franklin et al, 1986). However, Franklin (1984) reported a clear trend of decreasing maximum ammonium exchange with increasing Si/Al ratio. A similar effect was found by Kuhl (1985) for rare-earth exchange in faujasites. Kuhl attributed his observations to small changes in the size of the six-oxygen windows with an increase in the Si/Al ratio.

When Dempsey, Kuhl and Olson (1969) plotted the aluminium content against the lattice parameter for faujasite zeolites, they observed discontinuities at 80 and 64 aluminium atoms per unit cell. Dempsey et al (1969) concluded that three different faujasite phases occur in

the Si/Al range. As the Si/Al ratio is increased the distribution of aluminium atoms in the six-rings changes from meta to para positions. Electrostatic interactions lead to sudden transitions in structure types at 80 and 64 Al p.u.c. Above 80 Al p.u.c. the meta form occurs and the six-rings have the greatest effective diameter due to the almost circular shape of the aperture and to the longer Al-O bond length. Below 64 Al p.u.c. the six-rings exist in the para form, or they include only one aluminium atom, and the free diameter is reduced due to a deformation of the windows. Between 64 and 80 Al p.u.c., the meta and para forms co-exist. The size of the ammonium ion ($d=2.86 \text{ \AA}$) is close to a critical maximum value above which total exclusion from the sodalite cages occurs. Thus, small changes in the diameter of the six-oxygen windows may determine whether or not ammonium ions can exchange into the small pore sites. Observations made by Kanavirez and Borisova (1982) on the adsorption of ammonia into the sodalite cages of faujasite zeolites agree with this hypothesis.

For the exchange of some ions in zeolites X and Y, the extent of exchange is seen to increase with increasing Si/Al ratio (Li and Rees, 1986). For ions such as cesium, the large ionic size ($d=3.34 \text{ \AA}$) effectively excludes it from the small cage system of zeolites X and Y, whatever the Si/Al ratio. At higher framework charge densities cesium cannot neutralise all the negative charges in the

supercages due to crowding, and complete exchange is not possible, even in the large cages.

It is interesting to note that even after allowing for hydronium exchange, the number of sodium ions remaining in the small cages after exchange with ammonium does not amount to the "magical" 16 which has been found in many previous studies (Sherry, 1966; Lai and Rees, 1976; Fletcher and Townsend, 1982). The same observation was made by Townsend, Franklin and O'Connor (1984). Also, exchange of ammonium into potassium Y resulted in about 2 more NH_4 ions entering the zeolite compared to when NaY was used.

ΔG_{298}^{\ominus} for Na- NH_4 exchange in zeolite Y (Grace) was calculated (after normalisation of the data) to be $-0.818 \text{ kJ equiv}^{-1}$. This is within the range of values of ΔG_{298}^{\ominus} for similar systems reported in the literature (which show large variations in the free energy of exchange) (Sherry, 1966; Theng, Vansant and Uytterhoeven, 1968; Lai and Rees, 1976; Fletcher and Townsend, 1982; Franklin, 1984). For the exchange of potassium for ammonium in zeolite Y (Grace) the normalised ΔG_{298}^{\ominus} value was calculated to be $+1.77 \text{ kJ equiv}^{-1}$.

4.3.4. Potassium - Calcium Exchange in Zeolite Y.

The K-Ca isotherm for zeolite Y (Grace) is shown in figure 4.74. The zeolite is on the whole, less selective for calcium than for potassium but at low values of E_{Ca} (below 0.1) the zeolite is more selective for calcium. The isotherm was not forced to the absolute maximum calcium exchange but extrapolation suggested that about 2 potassium ions p.u.c. could not easily be replaced. This cannot be due to non-exchangeable potassium since the zeolite was prepared by exchange from the sodium form. There may be a small number of sites in the sodalite cages which are not amenable to neutralisation by divalent ions. A similar observation was made by Townsend, Fletcher and Loizidou (1983) for Na-Ca exchange in zeolite X.

The free energy of exchange was calculated to be $+4.78 \text{ kJ equiv}^{-1}$.

4.3.5. Sodium - Hydronium and Potassium - Hydronium Exchange in Zeolite Y.

Sodium - hydronium and potassium - hydronium ion-exchange isotherms in zeolite Y (Grace) were measured at 25°C and at a total solution normality of 0.01 equiv dm⁻³. The exchanges were carried out in the diffusion cell apparatus described in section 3.4.9 in order to accurately monitor the solution pH. Tests showed that the exchange reaction was very rapid (the pH of the solution reached a constant value within two minutes of the zeolite being added) so an exchange time of just 15 minutes was used in order to minimise further hydrolysis of the zeolite.

The Na-H isotherm is shown in figure 4.78. The shape is near-identical with that of an isotherm published by Chu and Dwyer (1983). Chu and Dwyer measured sodium - hydronium exchange isotherms for several zeolites, including zeolite Y, by using an acid ion-exchange resin. This method permitted hydronium exchange via a very dilute acid solution and, the authors claimed, prevented hydrolysis of the zeolite by attack from excess acid.

The rectangular isotherm in figure 4.78 illustrates the very high selectivity of zeolite Y for hydronium over sodium ions. At about 20% hydronium exchange the selectivity coefficient, α , was over 400, and at 60% hydronium exchange was still greater than 100. These

observations explain the pH reaction which occurs when zeolite Y is contacted with distilled water at pH 7, and the relatively high levels of hydronium exchange which occur even under very mild acid conditions.

K-H exchange in zeolite Y again produced a near-rectangular isotherm (figure 4.80) but the selectivity for hydronium ion was considerably lower in this case (figure 4.81). These differences in the selectivity of zeolites X and Y for hydronium ions over other cations can be used to account for trends in the cation recovery with exchange levels for certain systems. Thus, the cation recovery for Na-NH₄ and Na-K exchanges in zeolites X and Y is lower at the sodium end of the isotherm (Townsend, Franklin and O'Connor, 1984) but no trend is seen for K-NH₄ exchange because the relative selectivity of zeolite Y for hydronium over K⁺ and NH₄⁺ is approximately the same.

Hydronium ion-exchange and dealumination of zeolite Y in the solution phase could provide a valuable direct method of preparing HY zeolite for cracking catalysts if large scale destruction of the framework can be avoided. Recently Lee and Rees (1986a) have published some initial results of a study which could lead to a quick method for the preparation of zeolite Y with varying degrees of dealumination. Although samples prepared in this way were not thermally stable, Lee and Rees (1986b) are currently investigating the possibility of annealing the damaged

crystal structure by the insertion of silicon using a separate preparative stage.

The solution pH's, cation contents and dealumination data for zeolite Y in the Na-H and K-H isotherms are summarised in table 4.20.

Table 4.20. Hydrolysis Data for Na-H and K-H Exchange in Zeolite Y (Grace).

Na-H Y			K-H Y		
pH	total cation p.u.c.*	Al released p.u.c.	pH	total cation p.u.c.+	Al released p.u.c.
5.27	43.6	0.00	3.95	42.0	0.00
4.68	34.0	0.00	3.71	35.3	0.00
4.35	27.5	0.00	3.37	27.7	0.35
3.86	19.2	0.00	3.21	22.5	0.97
3.29	14.2	0.47	3.08	17.6	2.2
2.65	12.8	2.6	2.96	15.3	3.2
2.54	10.8	3.5	2.81	12.5	4.0
2.40	9.0	4.1	2.61	9.6	4.3

*Exchange capacity 53.8 charges p.u.c.

+Exchange capacity 52.5 charges p.u.c.

4.3.6. Sodium - Aluminium Exchange in Zeolite Y.

The isotherm of sodium - aluminium exchange in zeolite Y (Grace) is shown in figure 4.82. The isotherm is highly rectangular and similar to those for trivalent rare-earth exchanges in zeolite Y reported by Sherry (1966) and Rees and Zuyi (1986). At low levels of exchange the zeolite is highly selective for aluminium, but a very sharp selectivity reversal occurs at about 60% aluminium exchange. The maximum exchange level corresponds to 24.3 aluminium ions, 12.7 sodium and 16.7 hydronium ions per unit cell. Interpretation of the isotherm is difficult for several reasons: (1) aluminium exists in solution as several different species as a function of pH (Marion et al, 1976); (2) hydronium exchange in the zeolite was very high due to the low pH of the aluminium exchange solutions, and (3) hydrolysis of the zeolite was impossible to detect by aluminium release from the framework because of the high background aluminium concentration.

Figure 4.8 shows the distribution of aluminium as a series of $\text{Al}(\text{OH})_6^{3-z}$ ($z=0-5$) monomers which are stable in solution at different pH's (Marion et al, 1976). At pH 3, over 98% of the aluminium is present as the trivalent ion Al^{3+} ($\text{Al}(\text{H}_2\text{O})_6^{3+}$), but at pH 5 the predominant species is $\text{Al}(\text{OH})_2^+$. Non-stoichiometric exchange of divalent cations in soils and clay minerals has been explained by the presence of metal-chloride ion pairs (Sposito et al, 1981; Sposito

et al, 1983). However, Fletcher and Townsend (1985) concluded that the intracrystalline environment of synthetic faujasite was sufficiently negatively charged to preclude substantial penetration of loosely bound associated species even when ion association in the electrolyte was extensive. Furthermore, Lee and Rees (1986b) have shown that the apparent charge of lanthanum ions in the small cages of zeolite Y is +3 before heat-treatment. The fact that Fletcher and Townsend (1985) ruled out significant levels of complexation within the zeolite crystals for the ions Ca^{2+} , Mg^{2+} and Cd^{2+} does not preclude complexation in the case of Al^{3+} . It is well known (Marion et al, 1976) that the form and degree of aluminium complexes is a strong function of pH and that both tetrahedral and octahedral species may be found in polymeric cations. It would be surprising indeed (bearing in mind the evidence produced in this thesis from chemical and masnmr data) if aluminium in numerous complex species did not exist within the channels of the zeolites.

From the observed high selectivity of zeolite Y for aluminium it is concluded that aluminium extracted from the zeolite framework by acid hydrolysis will at first be bound to anionic exchange sites in the zeolite. The subsequent release of aluminium into solution will then be controlled by the degree of hydronium exchange in the zeolite (in effect a zeolite phase "pH") as well as by the external solution pH.

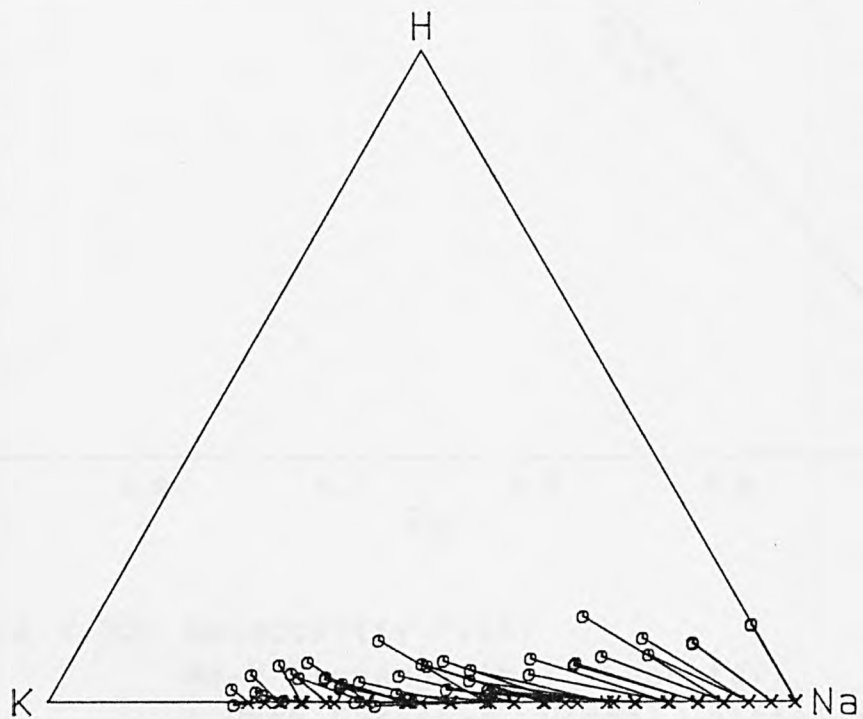
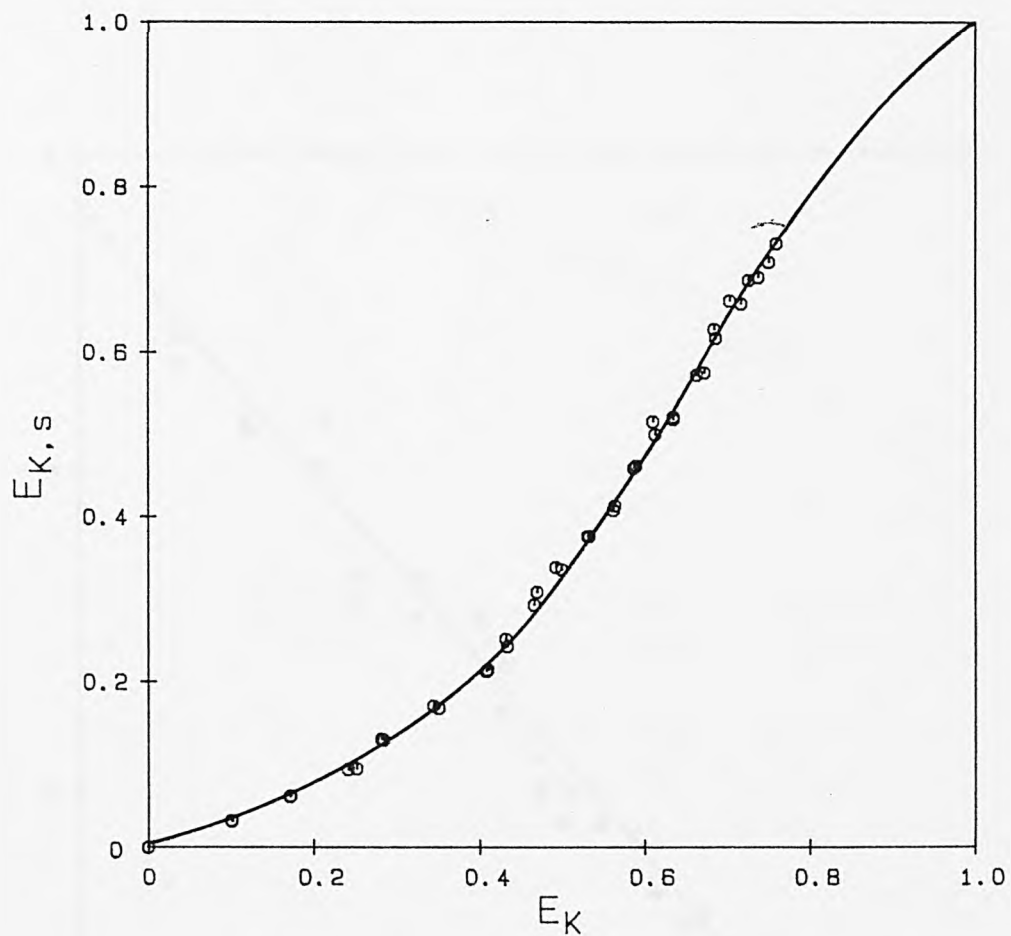


Figure 4.32: Na-K Exchange in Y (Laporte).
1 Week Exchange, Normal Initial pH.

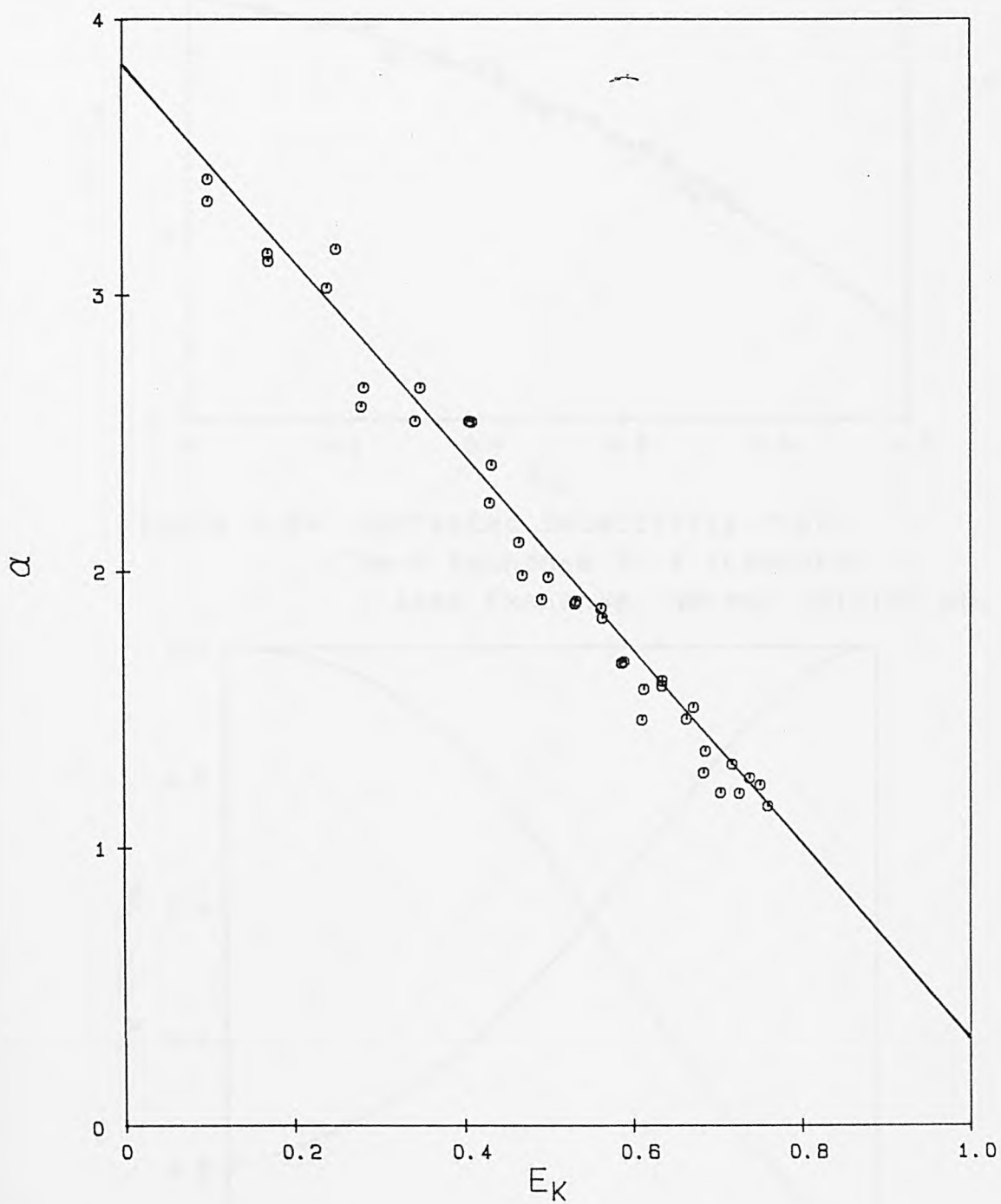


Figure 4.33: Selectivity Plot:
Na-K Exchange in Y (Laporte).
1 Week Exchange, Normal Initial pH.

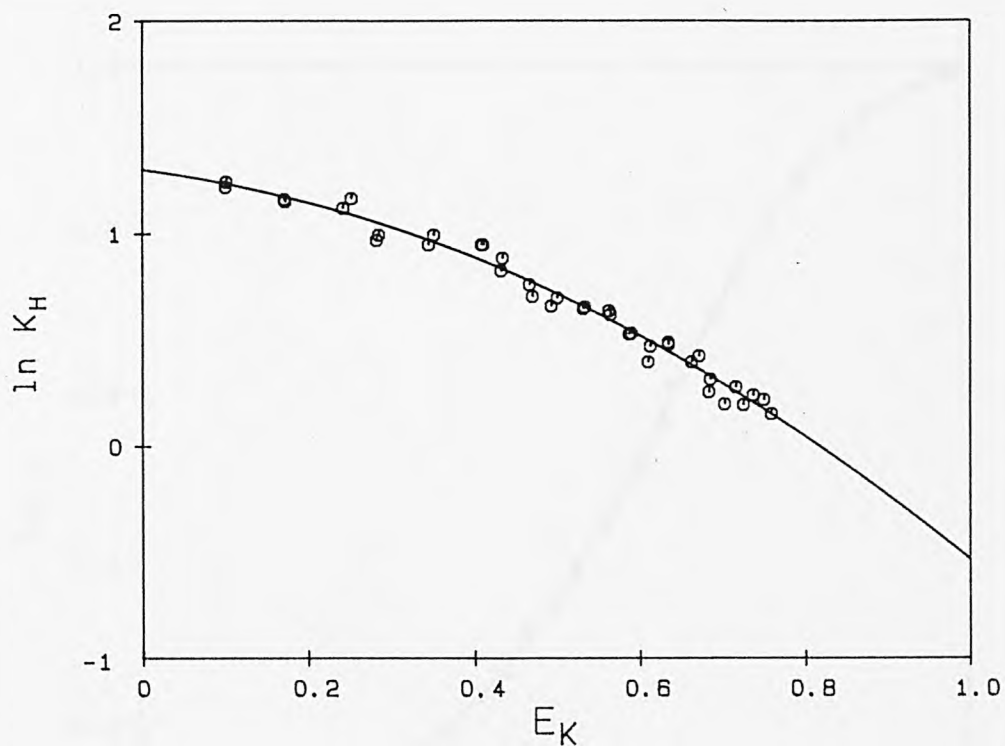


Figure 4.34: Corrected Selectivity Plot:
Na-K Exchange in Y (Laporte).
1 Week Exchange, Normal Initial pH.

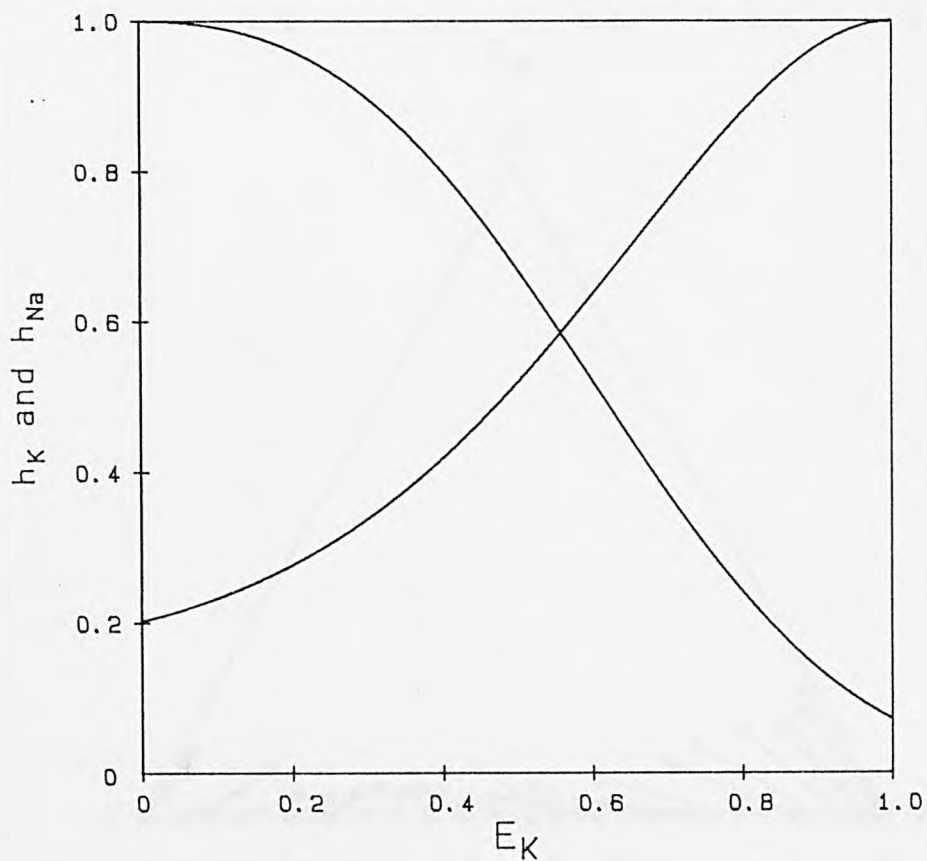


Figure 4.35: Zeolite Phase Activity Coefficients:
Na-K Exchange in Y (Laporte).
1 Week Exchange, Normal Initial pH.

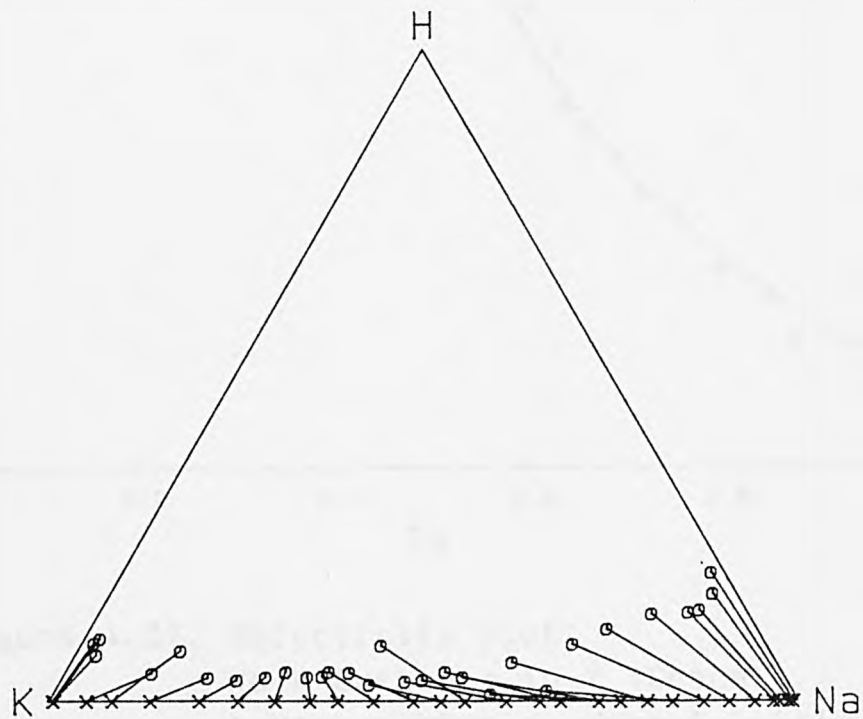
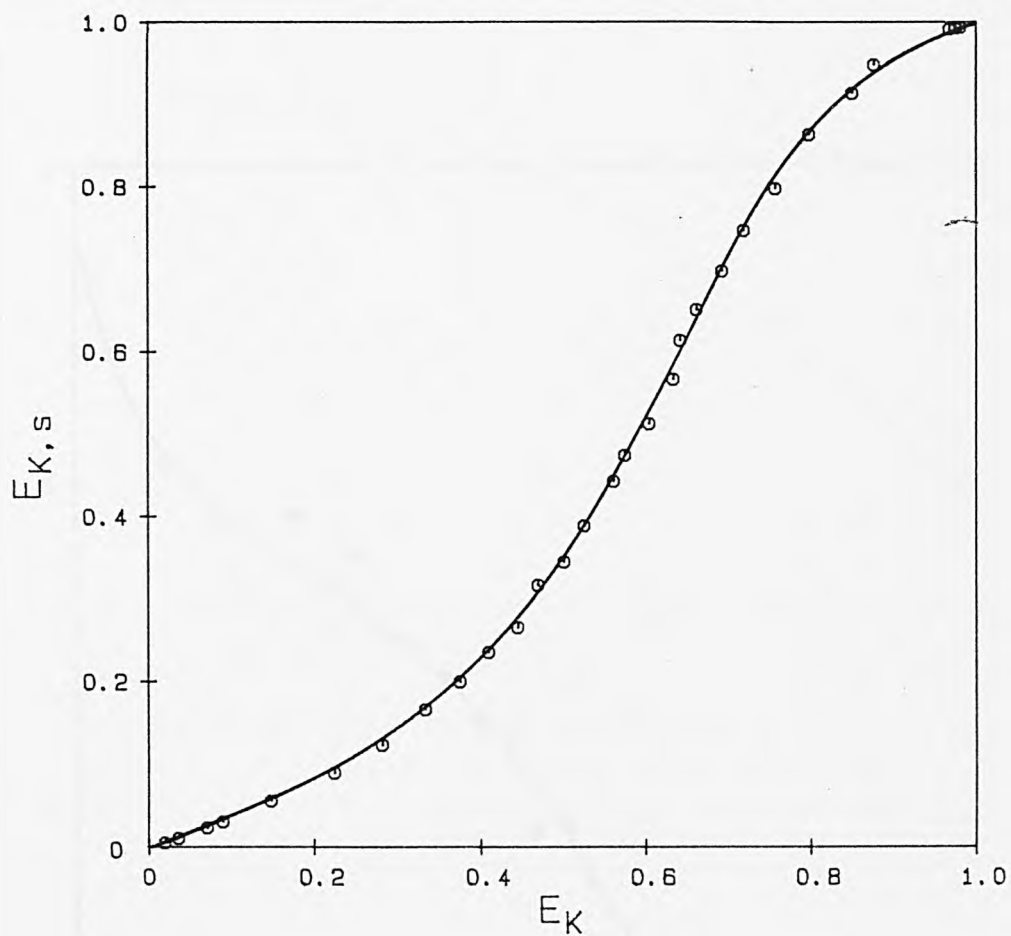


Figure 4.36: Na-K Exchange in Y (Grace).
1 Week Exchange, Normal Initial pH.

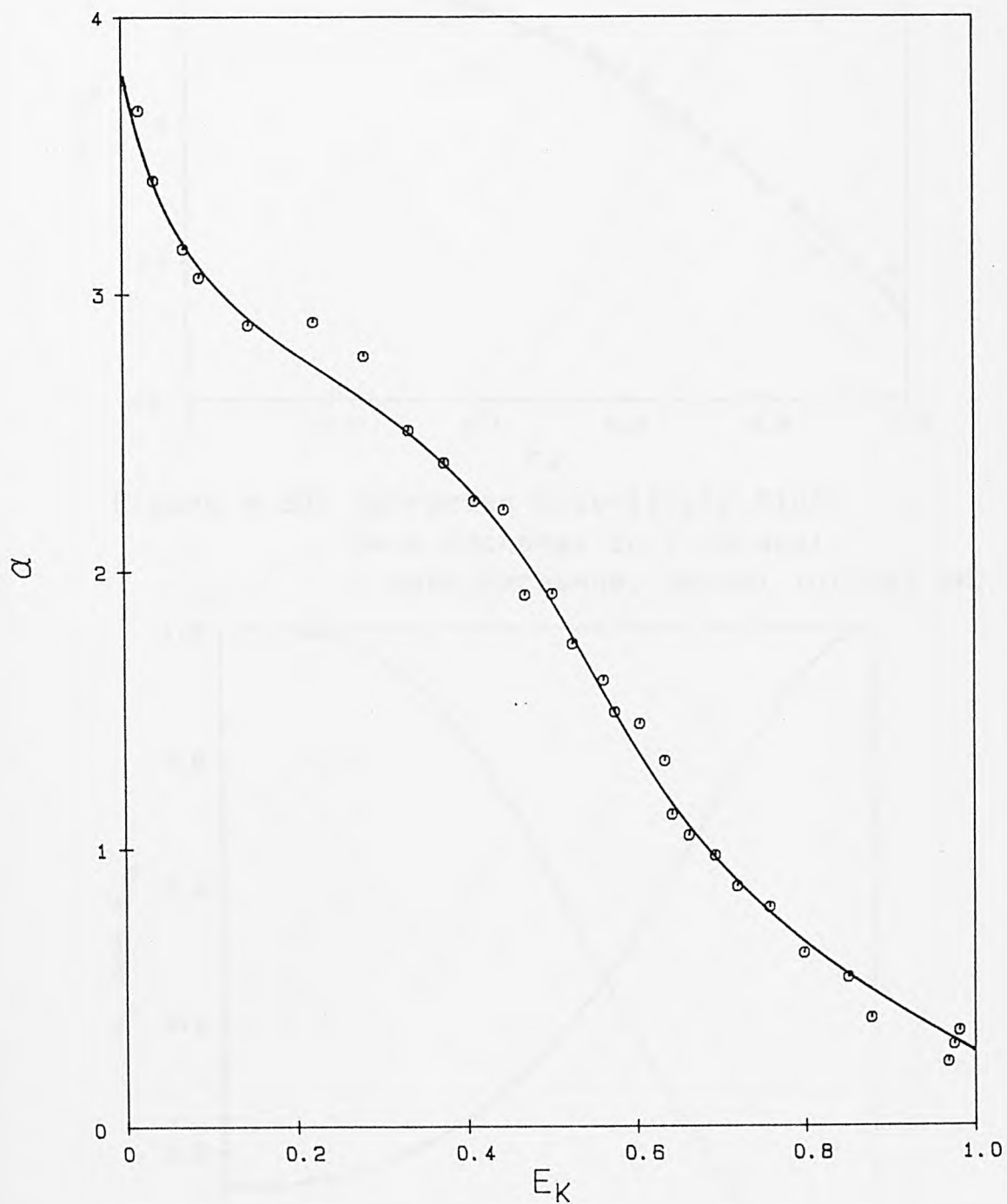


Figure 4.37: Selectivity Plot:
Na-K Exchange in Y (Grace).
1 Week Exchange, Normal Initial pH.

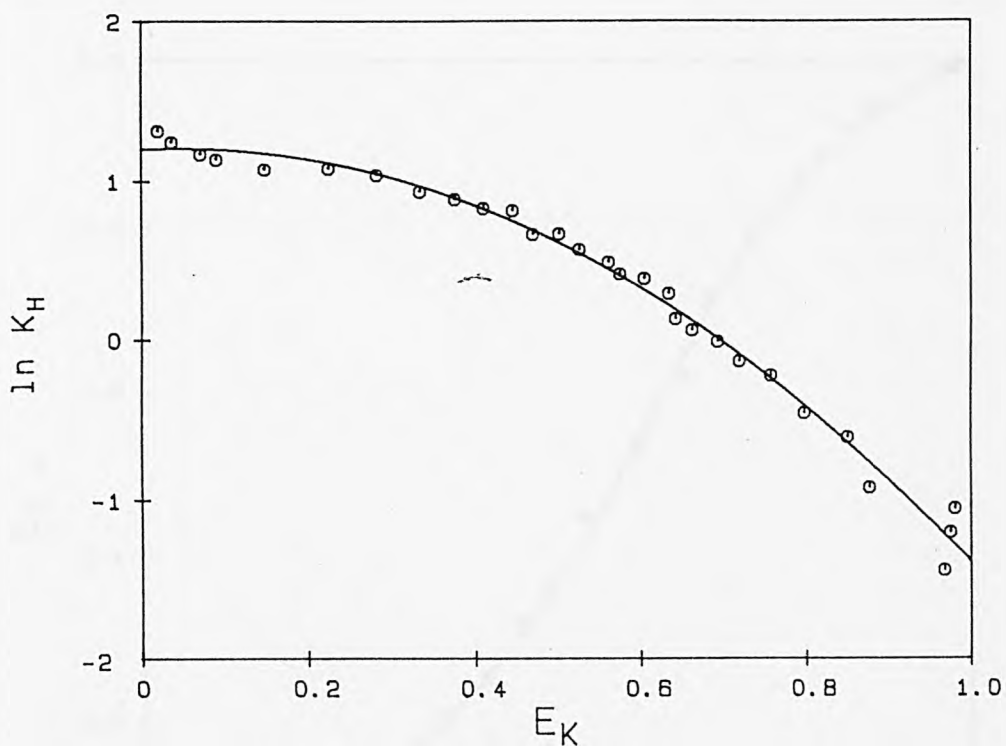


Figure 4.38: Corrected Selectivity Plot:
Na-K Exchange in Y (Grace).
1 Week Exchange, Normal Initial pH.

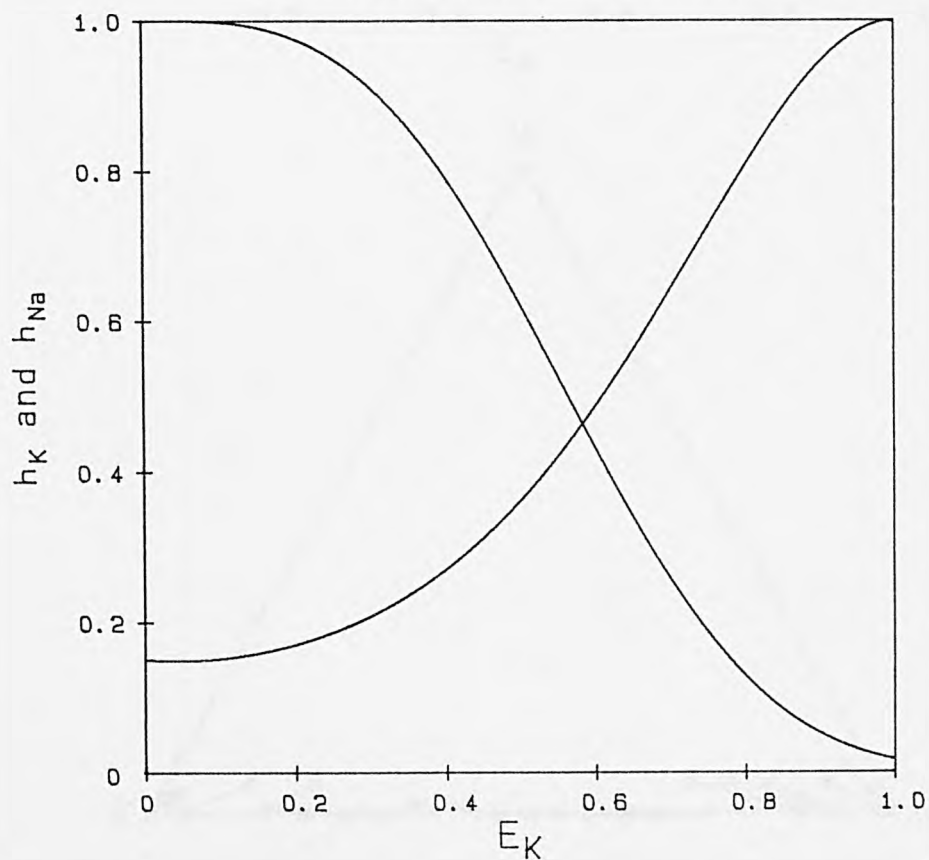


Figure 4.39: Zeolite Phase Activity Coefficients:
Na-K Exchange in Y (Grace).
1 Week Exchange, Normal Initial pH.

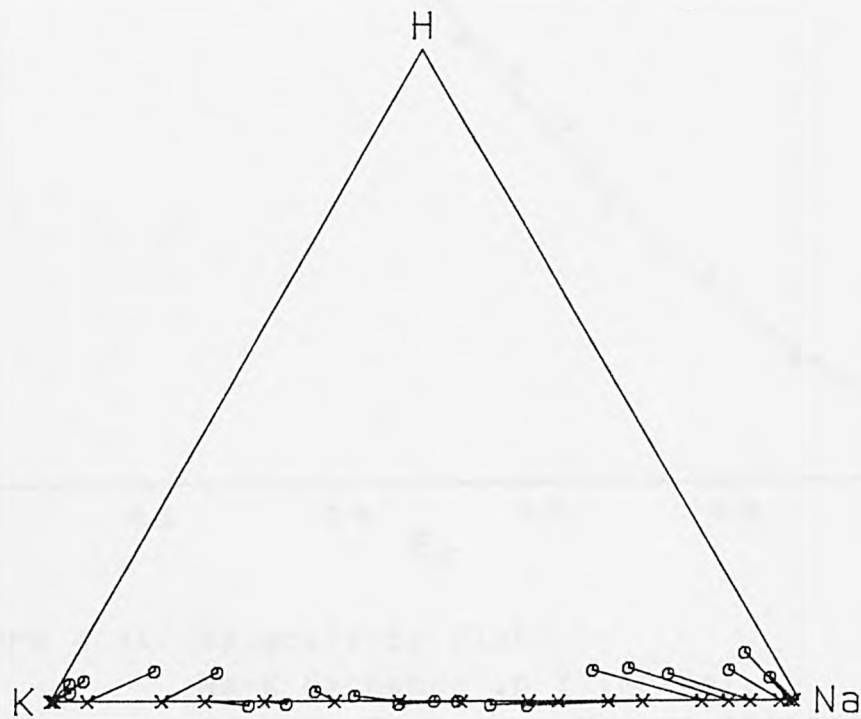
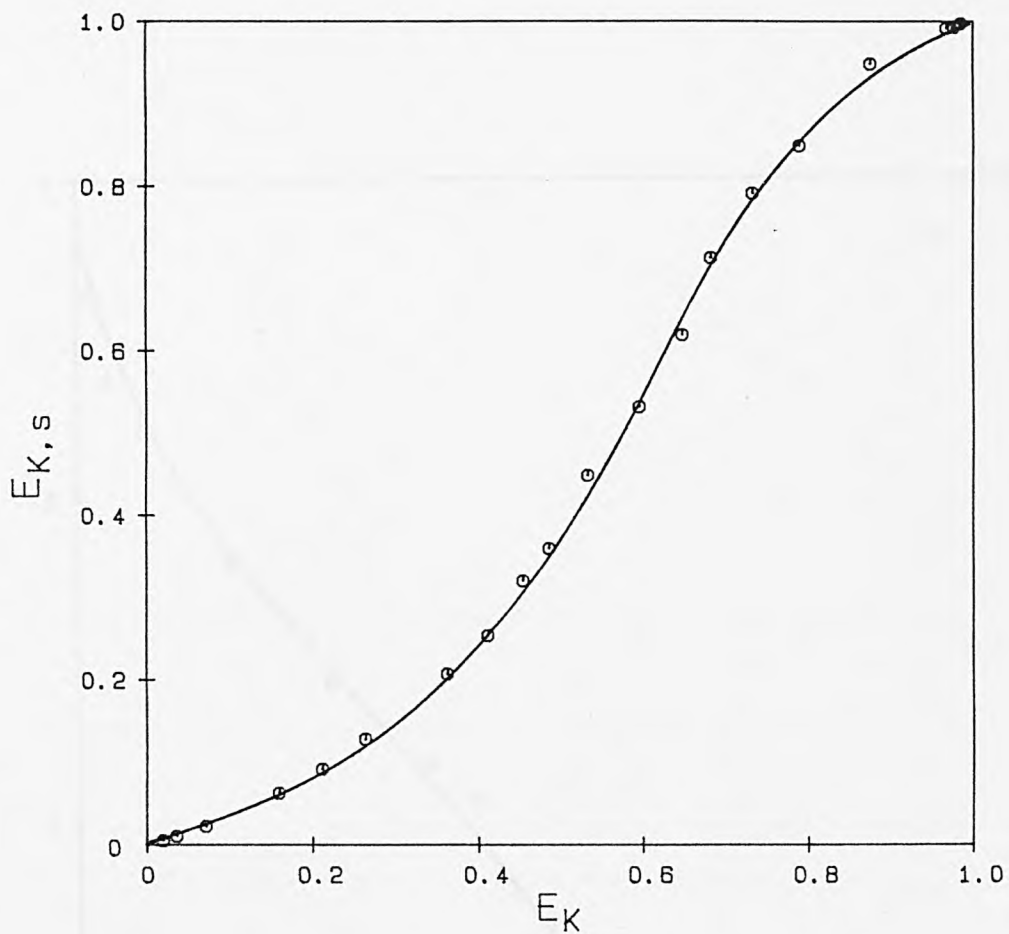


Figure 4.40: Na-K Exchange in Y (Grace).
24 Hour Exchange, Normal Initial pH.

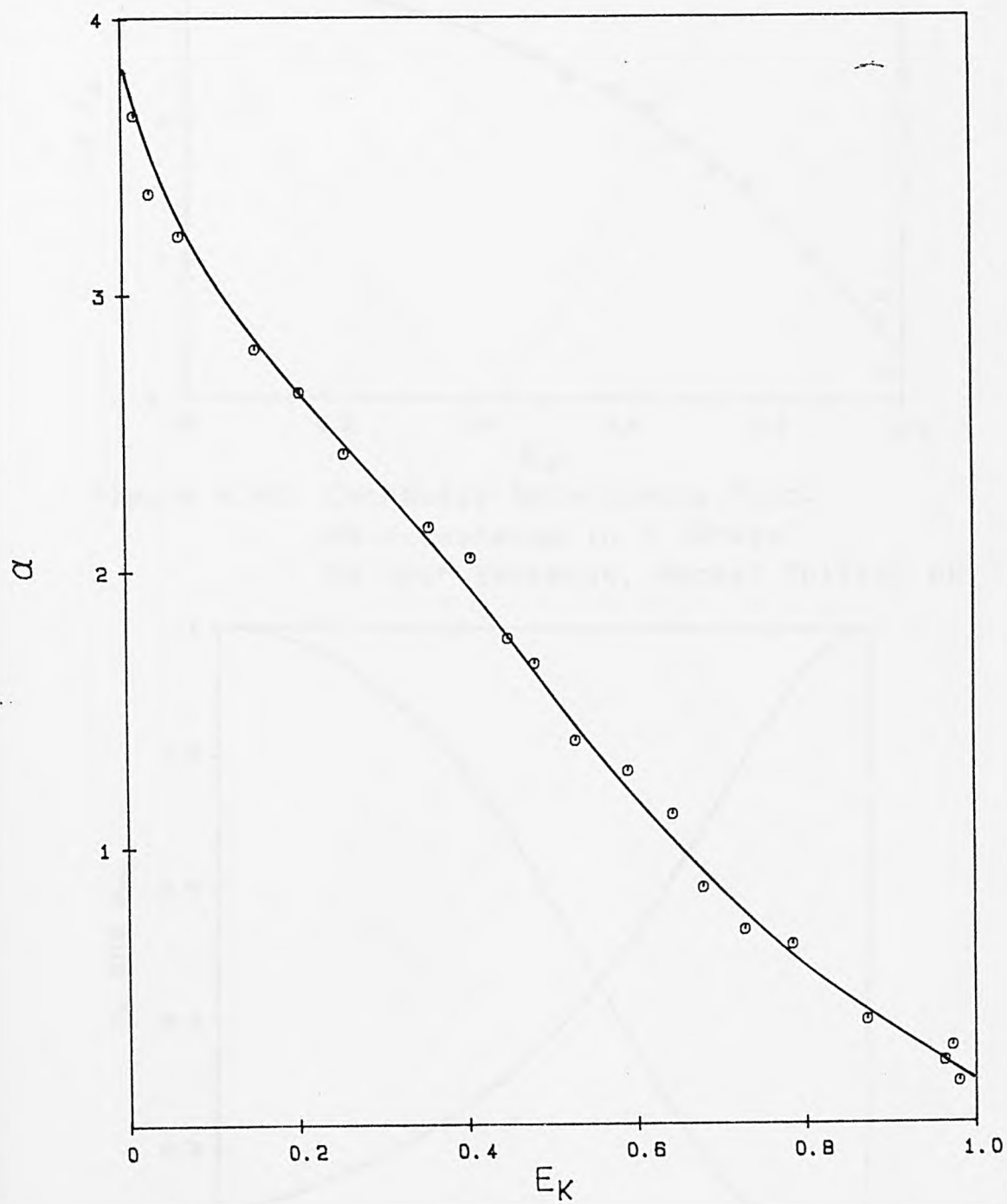


Figure 4.41: Selectivity Plot:
Na-K Exchange in Y (Grace).
24 Hour Exchange, Normal Initial pH.

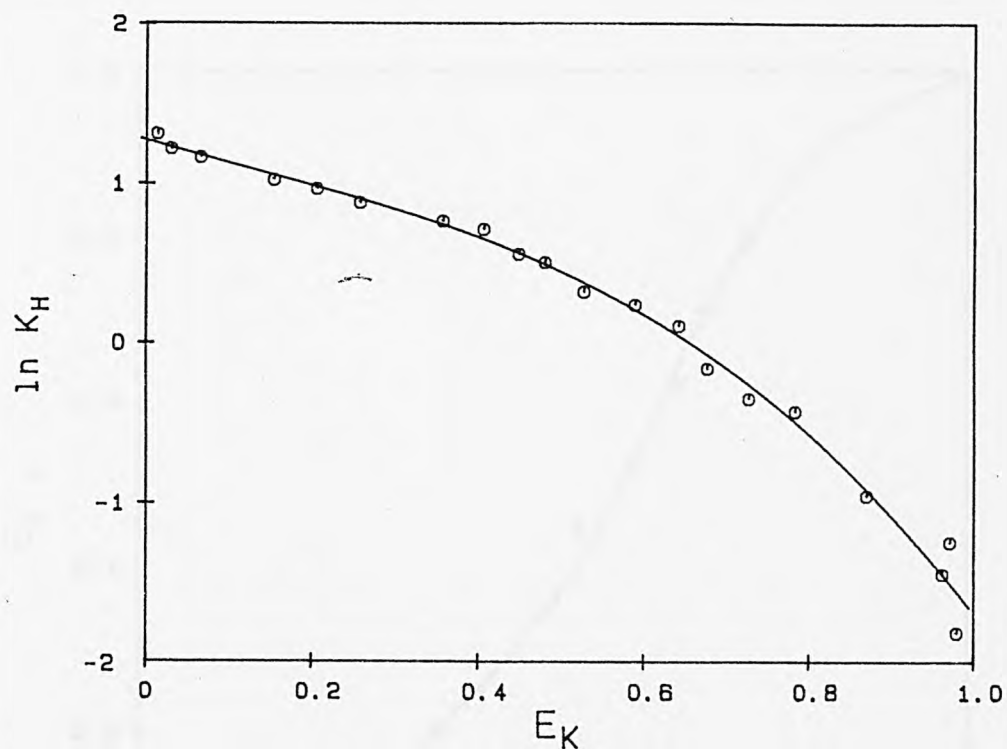


Figure 4.42: Corrected Selectivity Plot:
Na-K Exchange in Y (Grace).
24 Hour Exchange, Normal Initial pH.

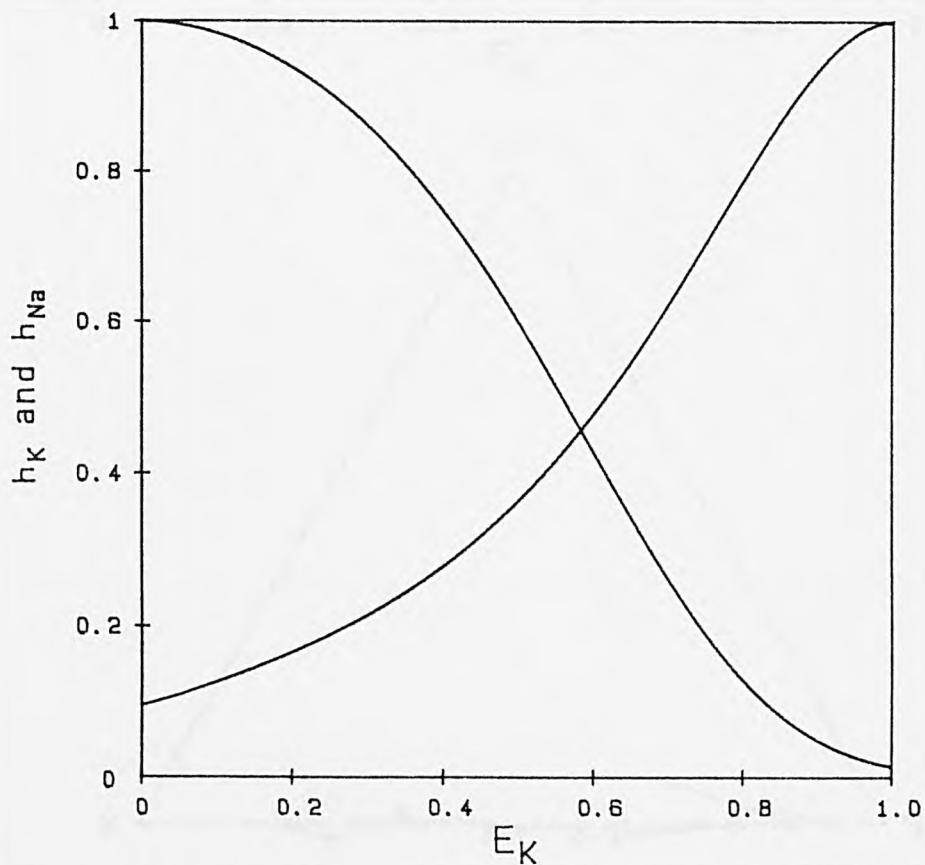


Figure 4.43: Zeolite Phase Activity Coefficients:
Na-K Exchange in Y (Grace).
24 Hour Exchange, Initial pH 4.

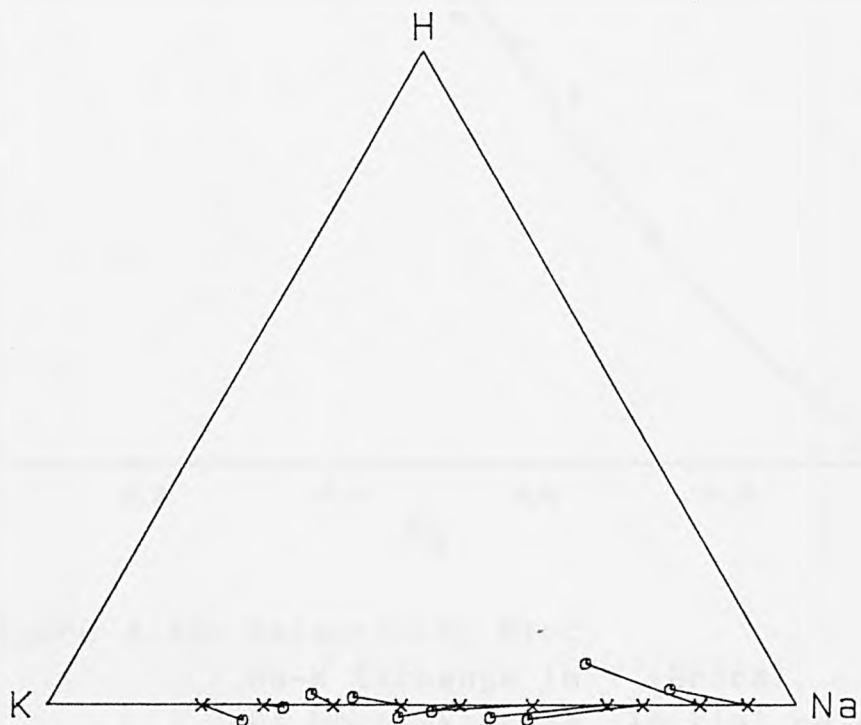
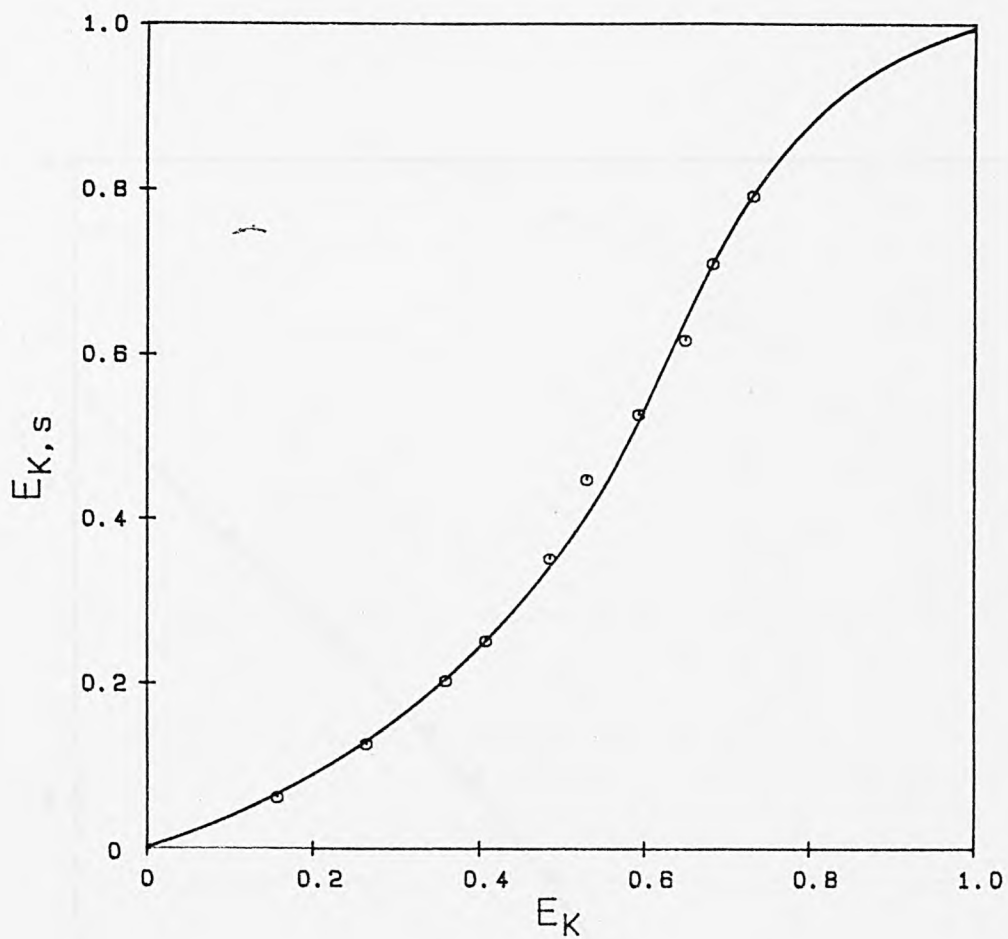


Figure 4.44: Na-K Exchange in Y (Grace).
24 Hour Exchange, Initial pH 4.

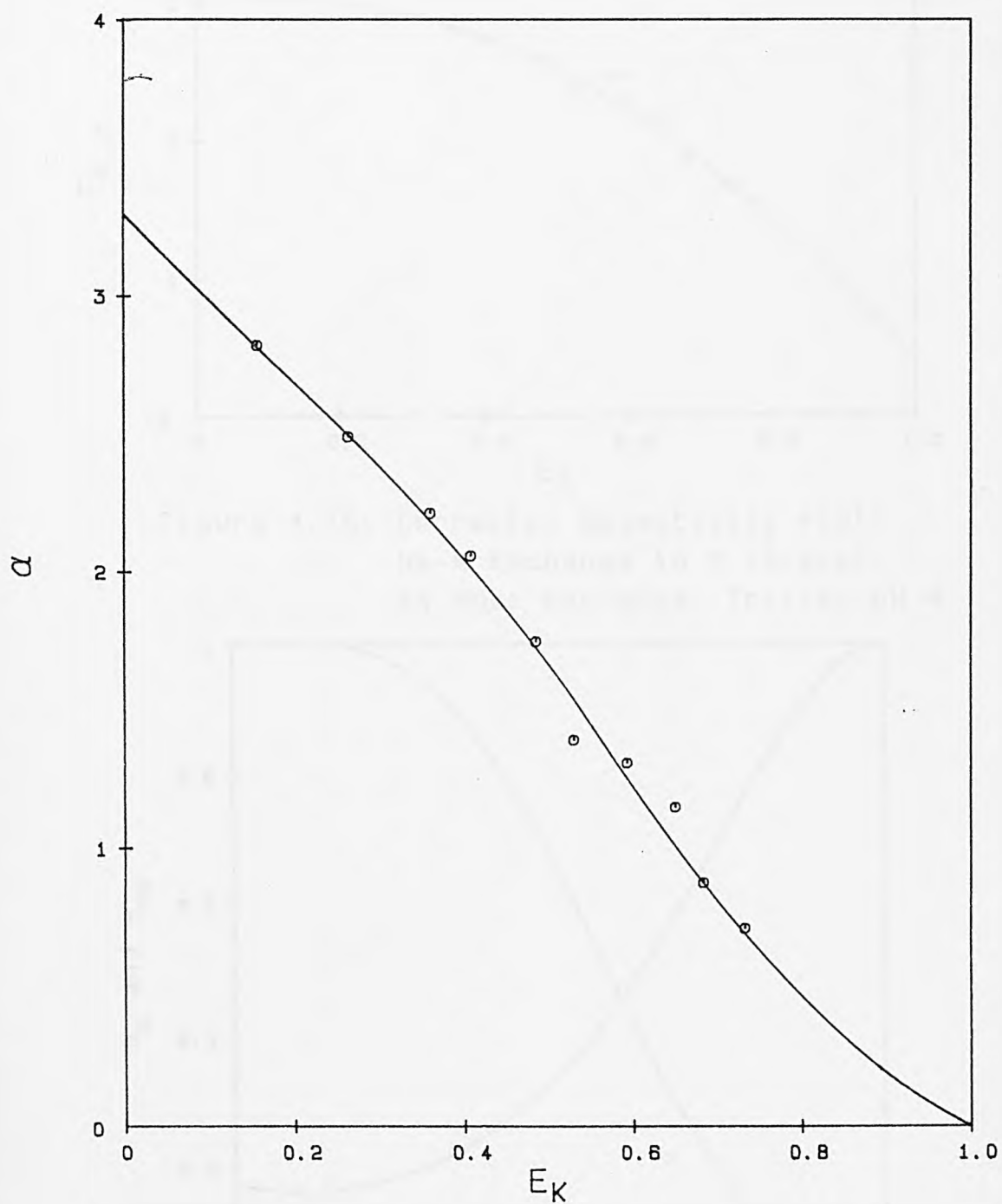


Figure 4.45: Selectivity Plot:
Na-K Exchange in Y (Grace).
24 Hour Exchange, Initial pH 4.

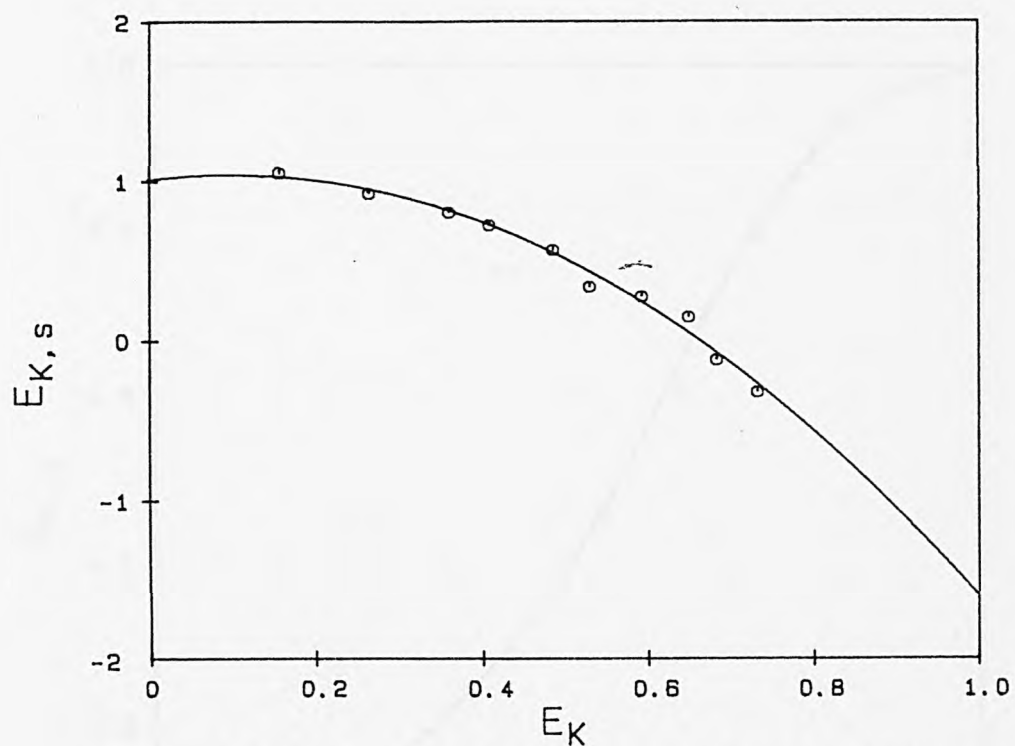


Figure 4.46: Corrected Selectivity Plot:
Na-K Exchange in Y (Grace).
24 Hour Exchange, Initial pH 4.

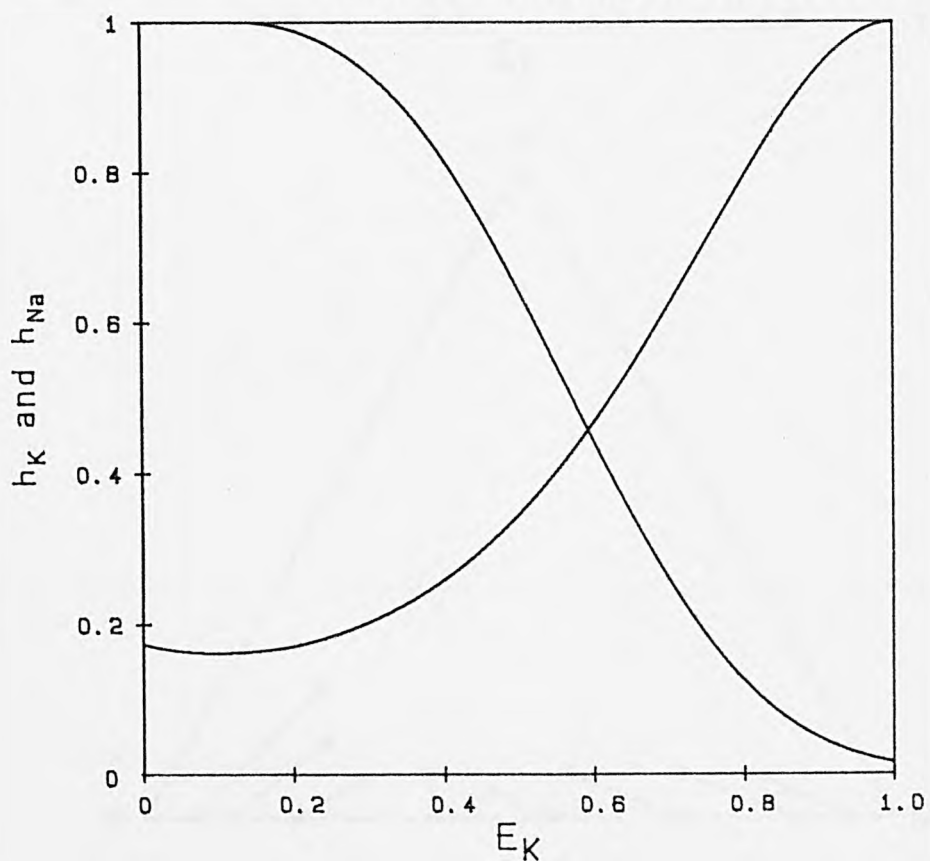


Figure 4.47: Zeolite Phase Activity Coefficients:
Na-K Exchange in Y (Laporte).
24 Hour Exchange, Initial pH 4.

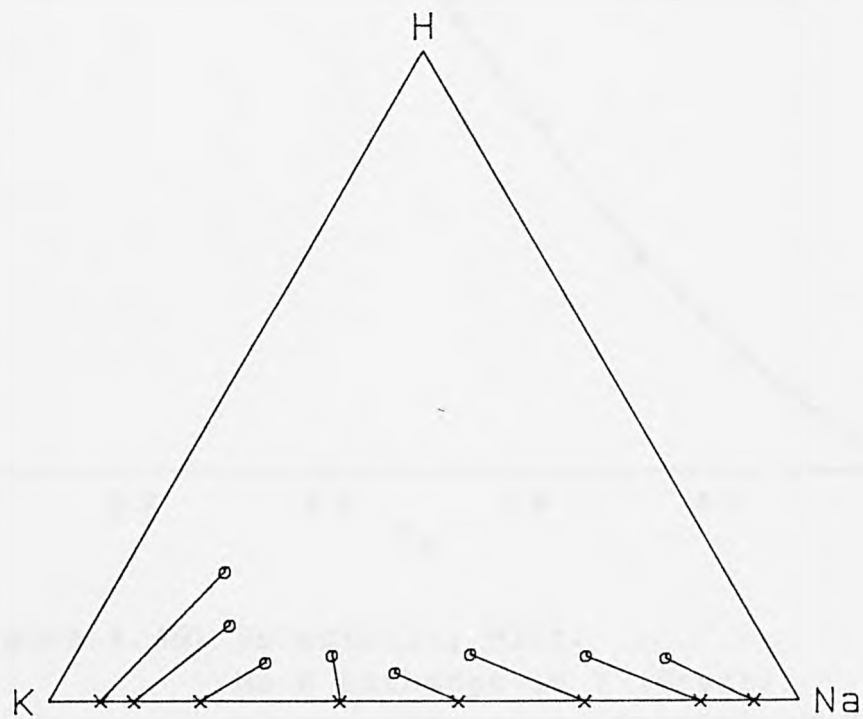
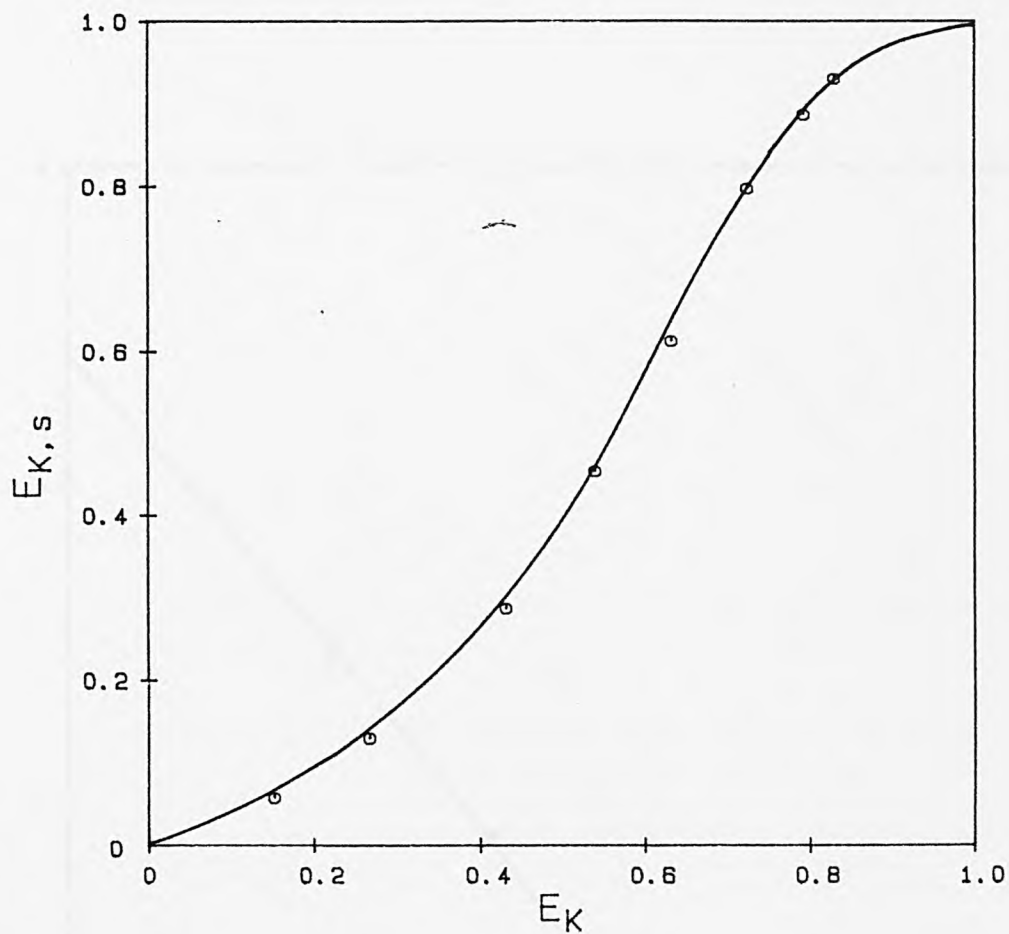


Figure 4.48: Na-K Exchange in Y (Grace).
24 Hour Exchange, Initial pH 3

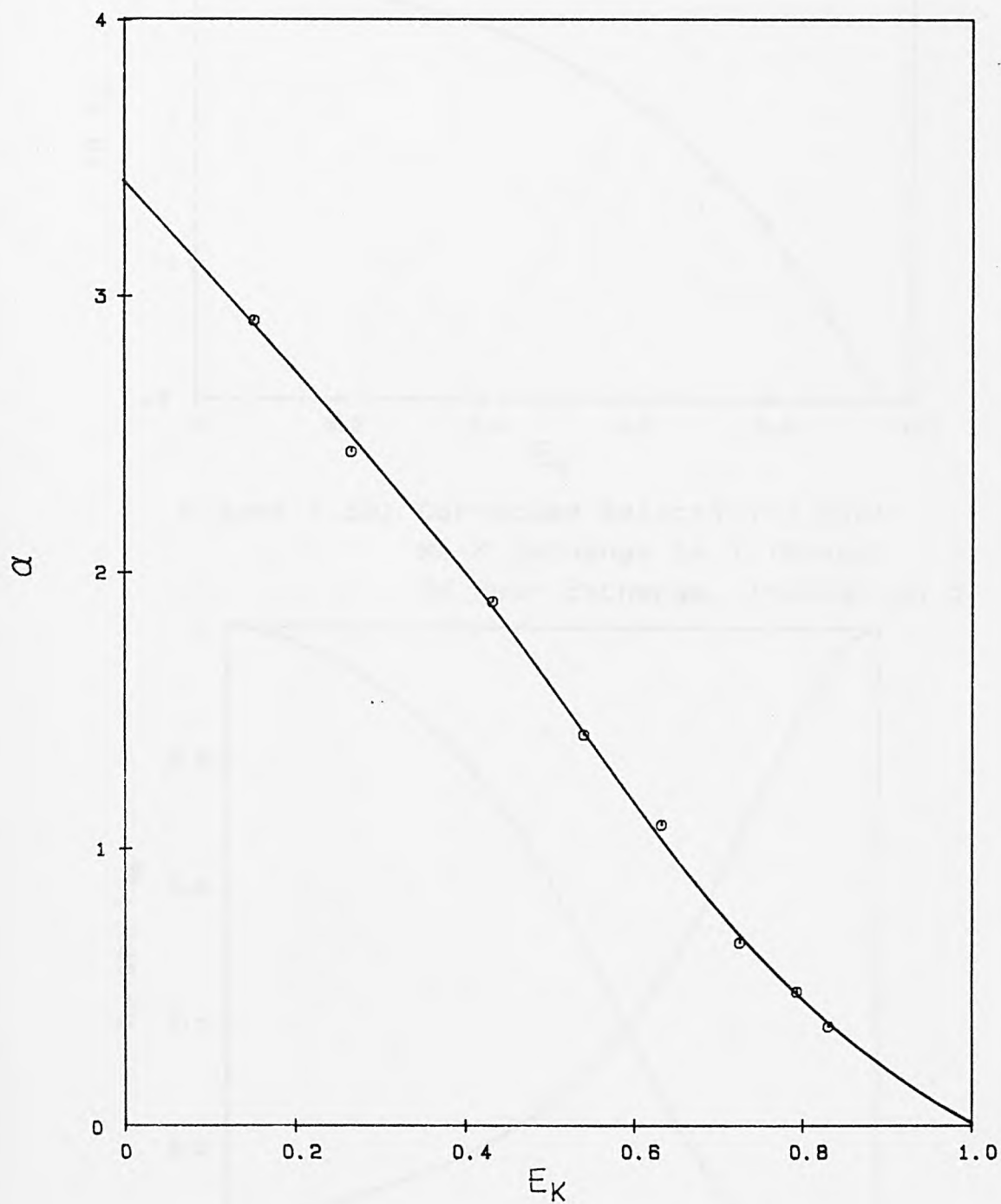


Figure 4.49: Selectivity Plot:
Na-K Exchange in Y (Grace).
24 Hour Exchange, Initial pH 3.

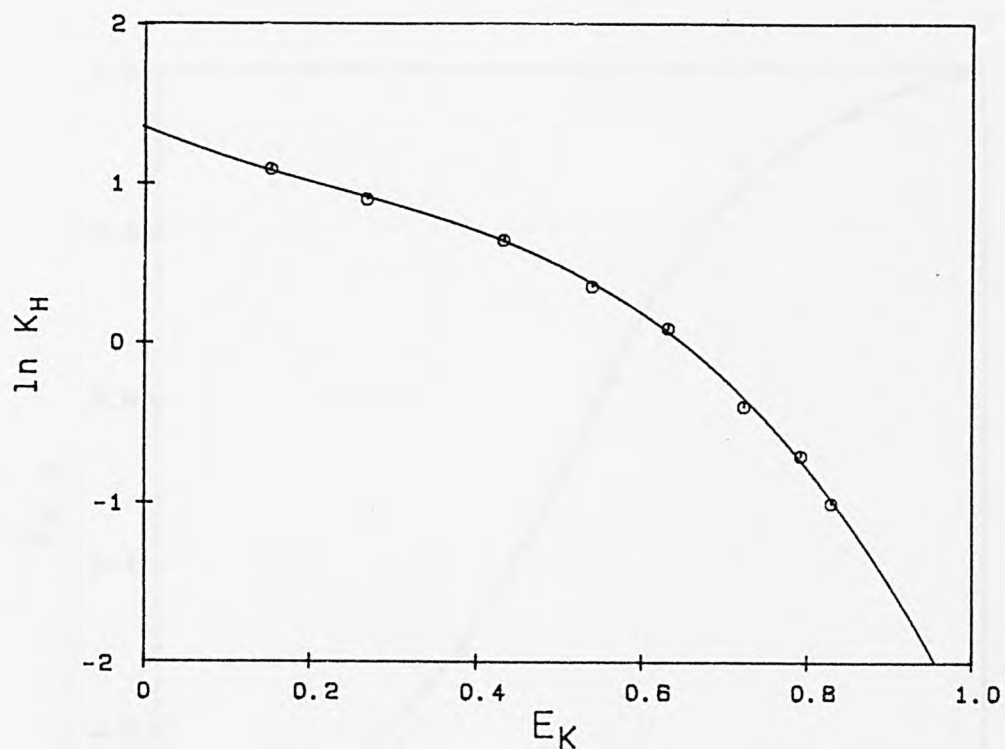


Figure 4.50: Corrected Selectivity Plot:
Na-K Exchange in Y (Grace).
24 Hour Exchange, Initial pH 3.

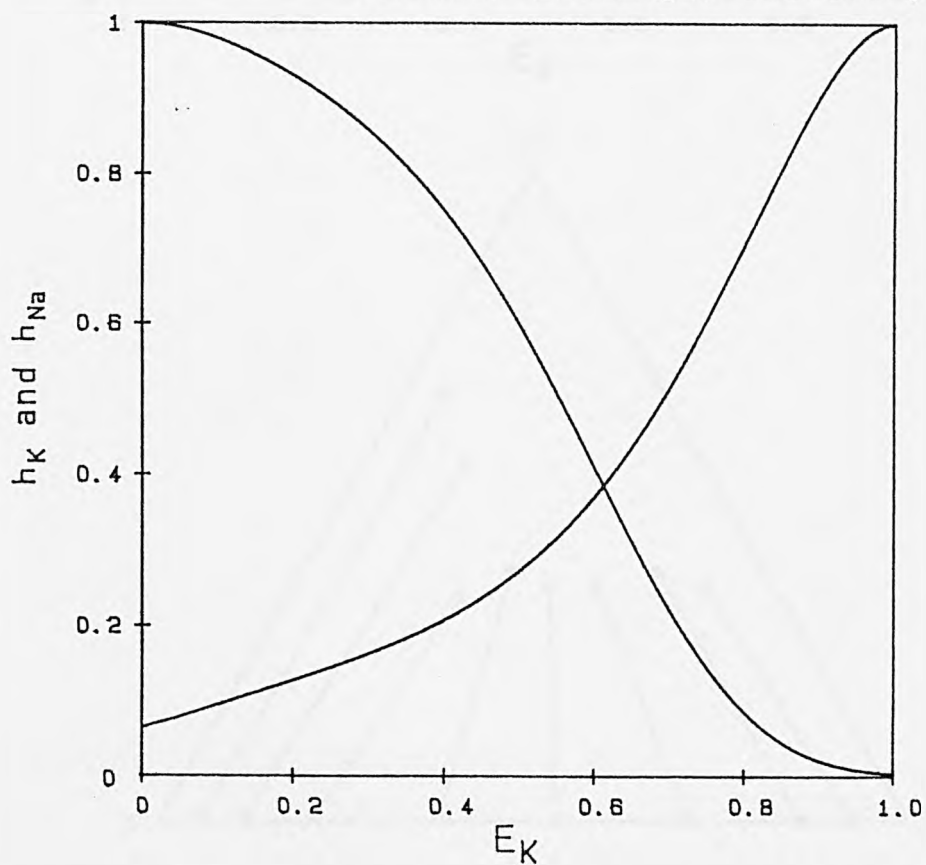


Figure 4.51: Zeolite Phase Activity Coefficients:
Na-K Exchange in Y (Grace).
24 Hour Exchange, Initial pH 3.

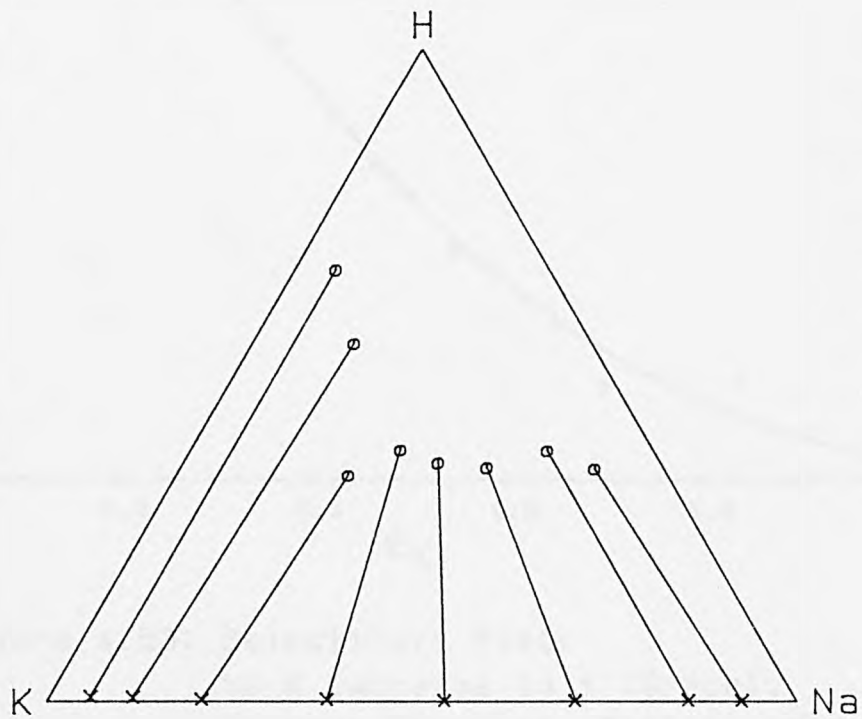
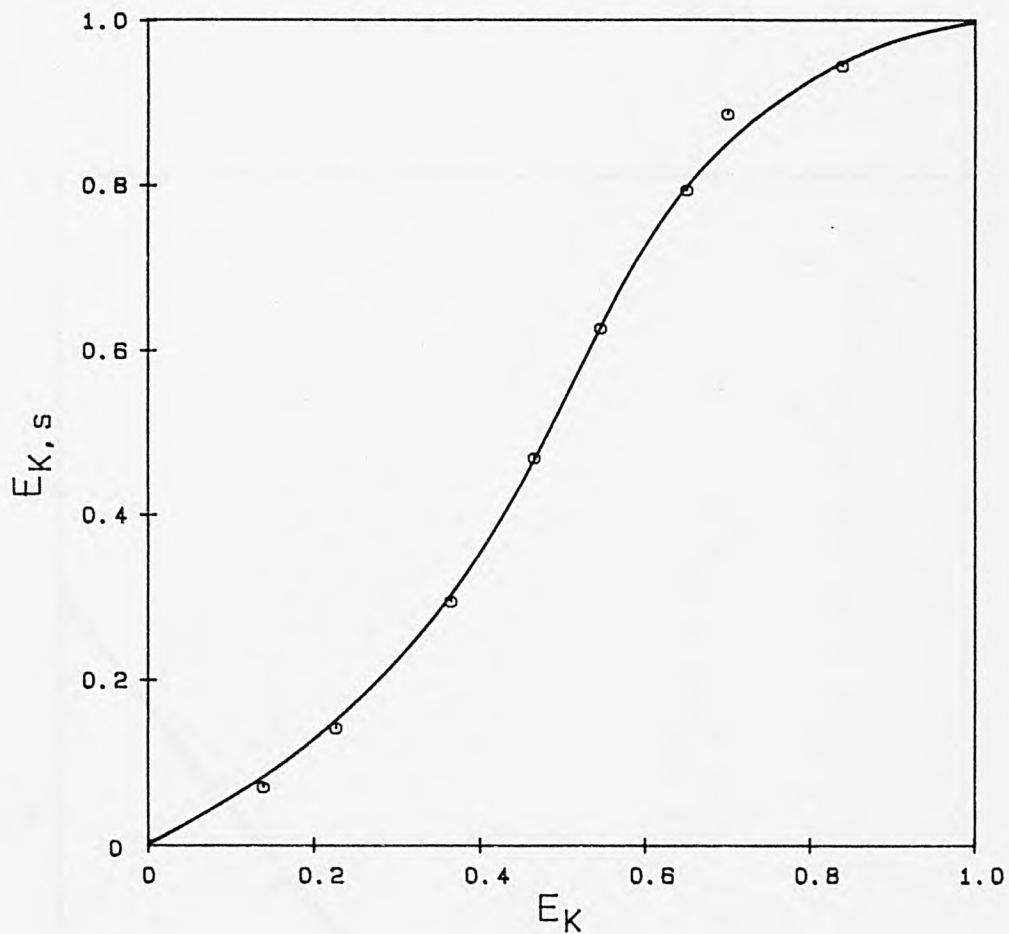


Figure 4.52: Na-K Exchange in Y (Grace).
24 Hour Exchange, Initial pH 2.3.

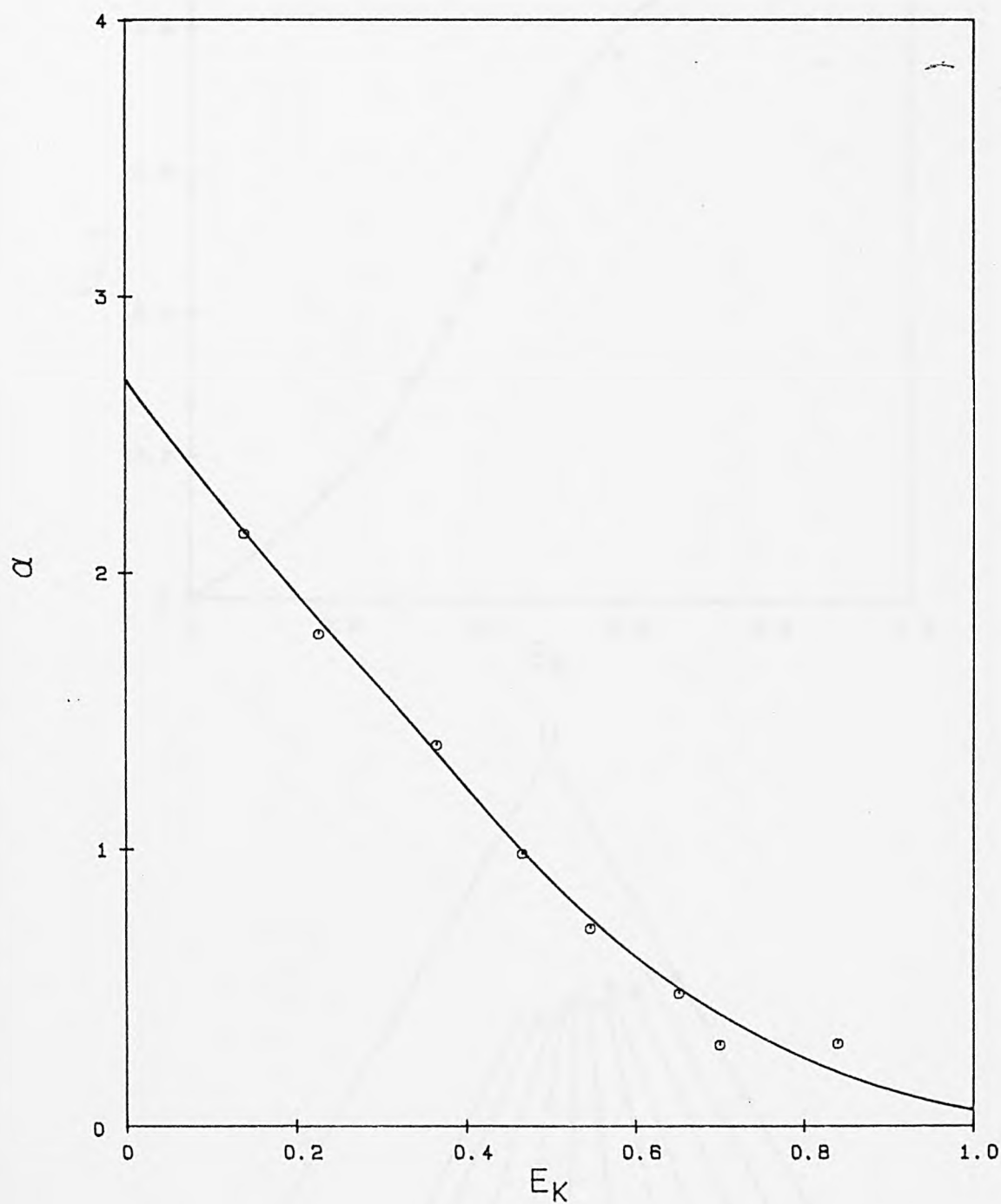


Figure 4.53: Selectivity Plot:
Na-K Exchange in Y (Grace).
24 Hour Exchange, Initial pH 2.3.

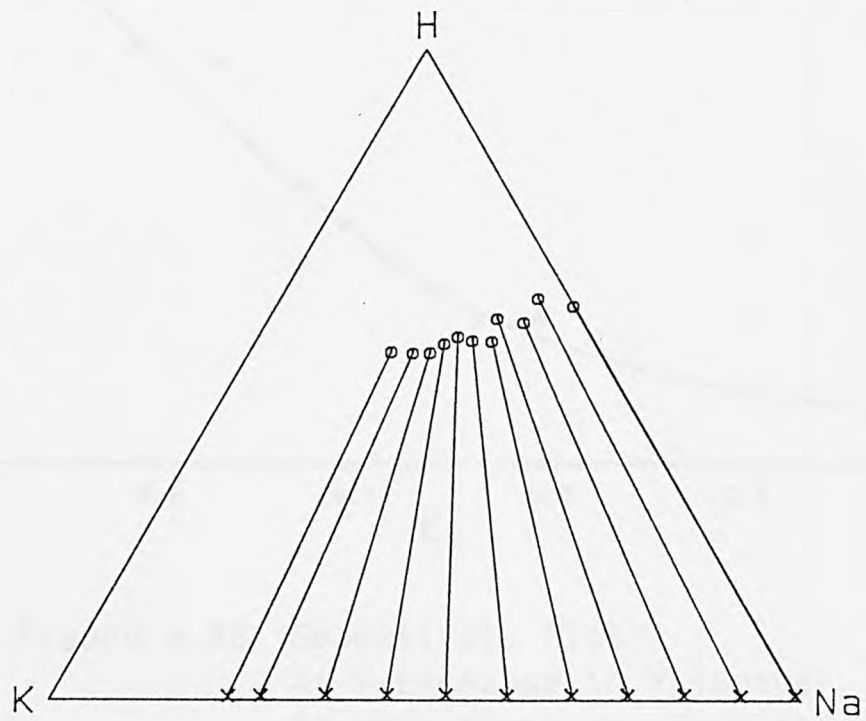
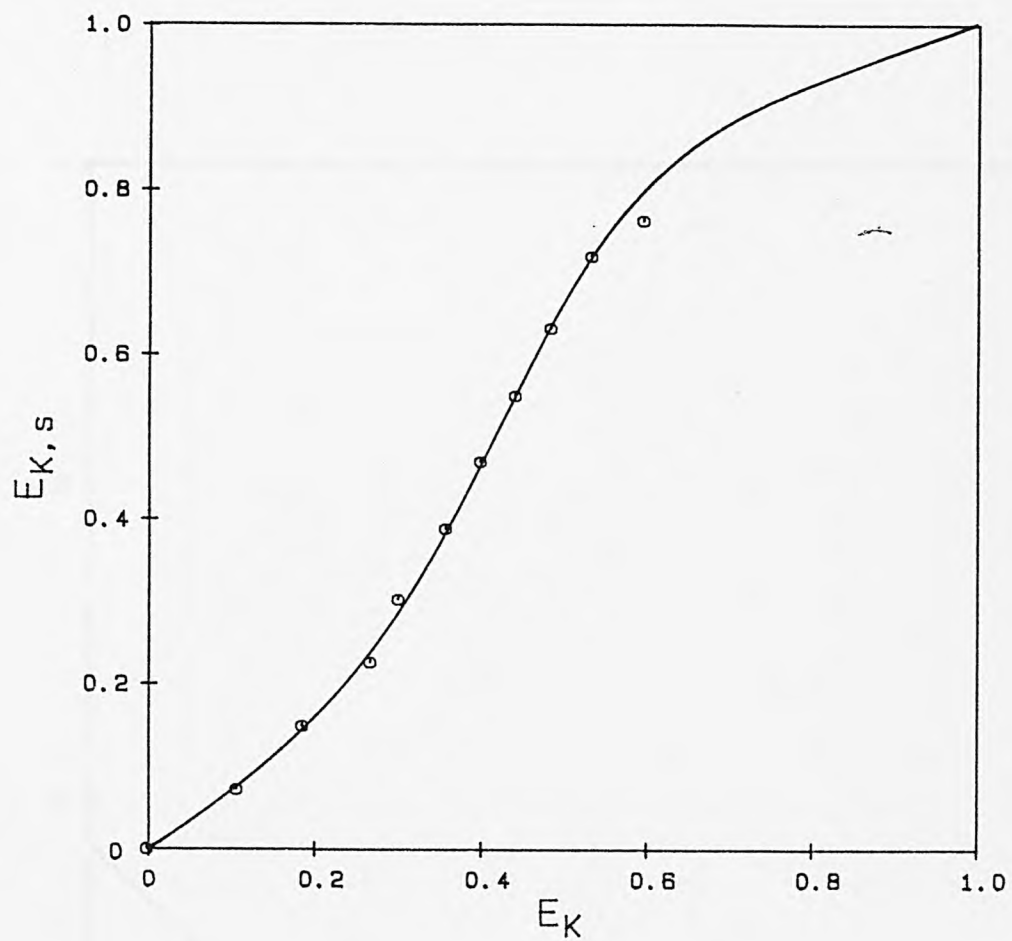


Figure 4.54: Na-K Exchange in Y (Grace).
24 Hour Exchange, Initial pH 2.

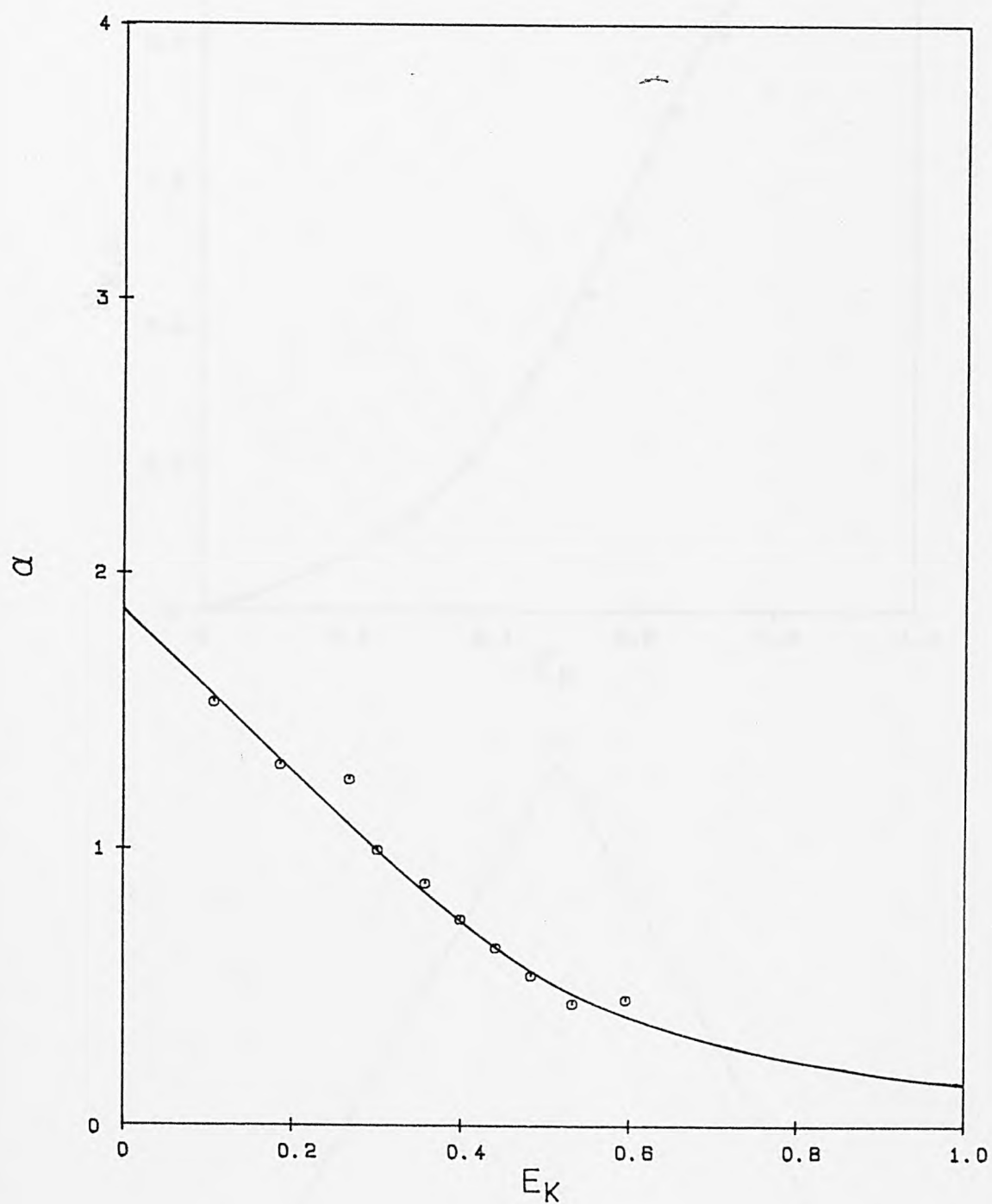


Figure 4.55: Selectivity Plot:
Na-K Exchange in Y (Grace).
24 Hour Exchange, Initial pH 2.

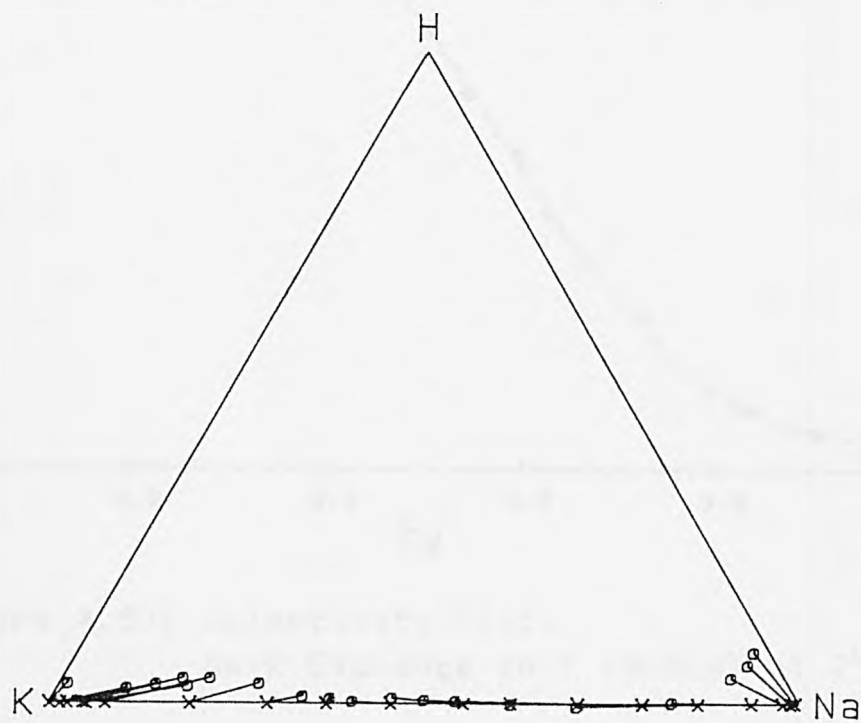
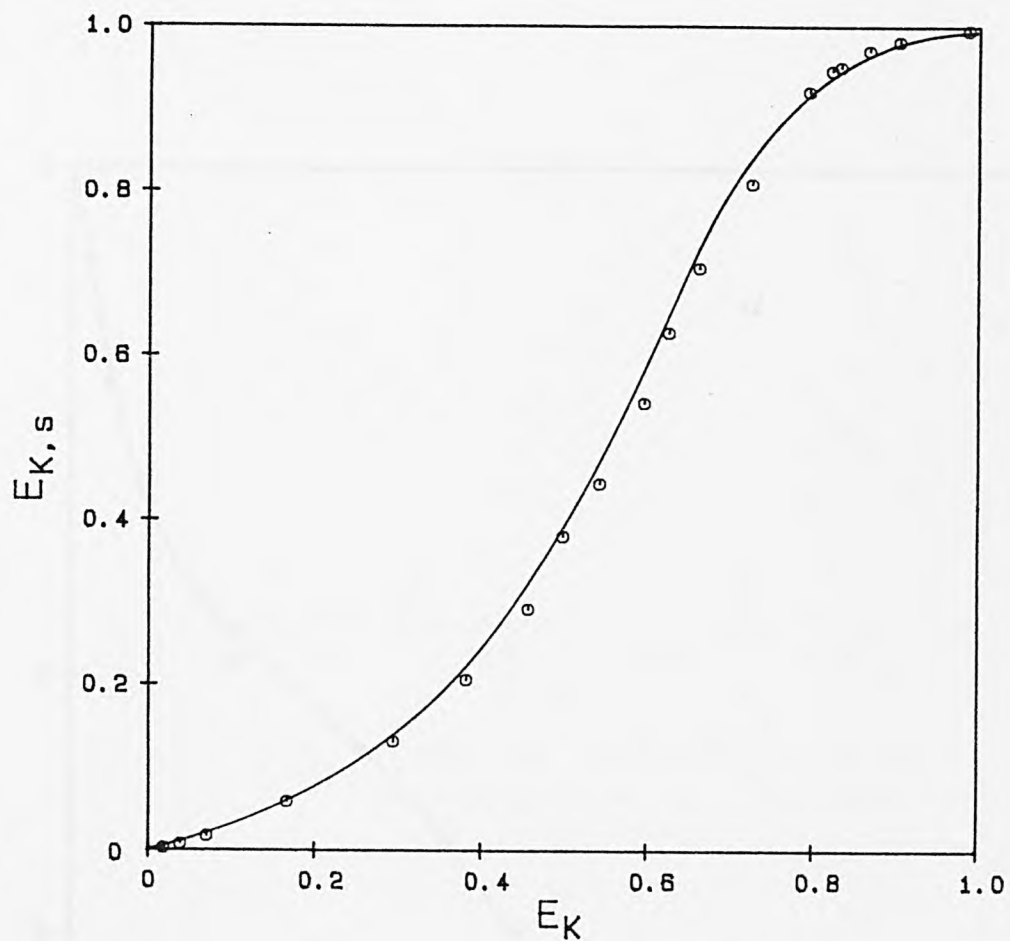


Figure 4.56: Na-K Exchange in Y (Grace) at 2°C.

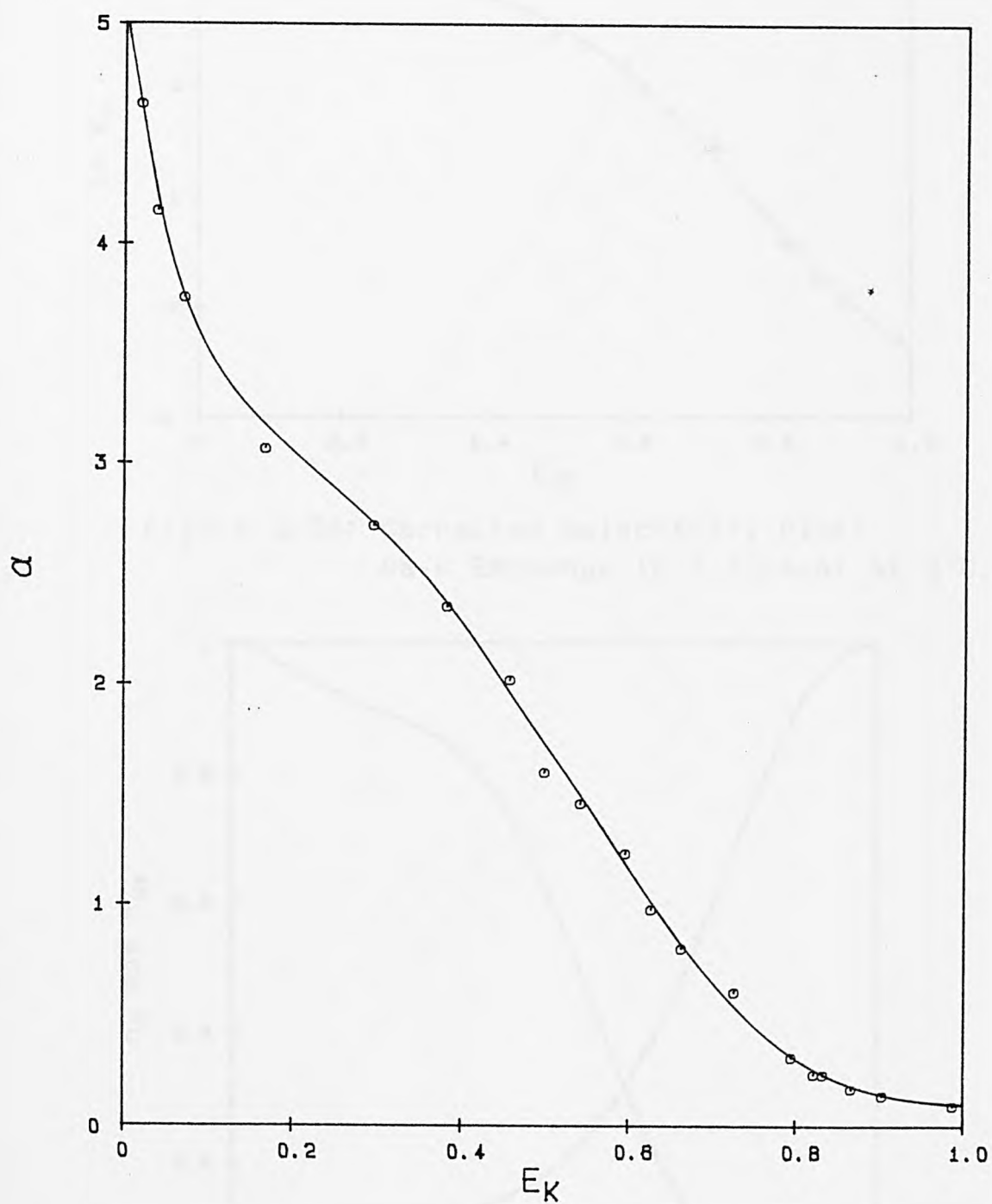


Figure 4.57: Selectivity Plot:
Na-K Exchange in Y (Grace) at 2°C.

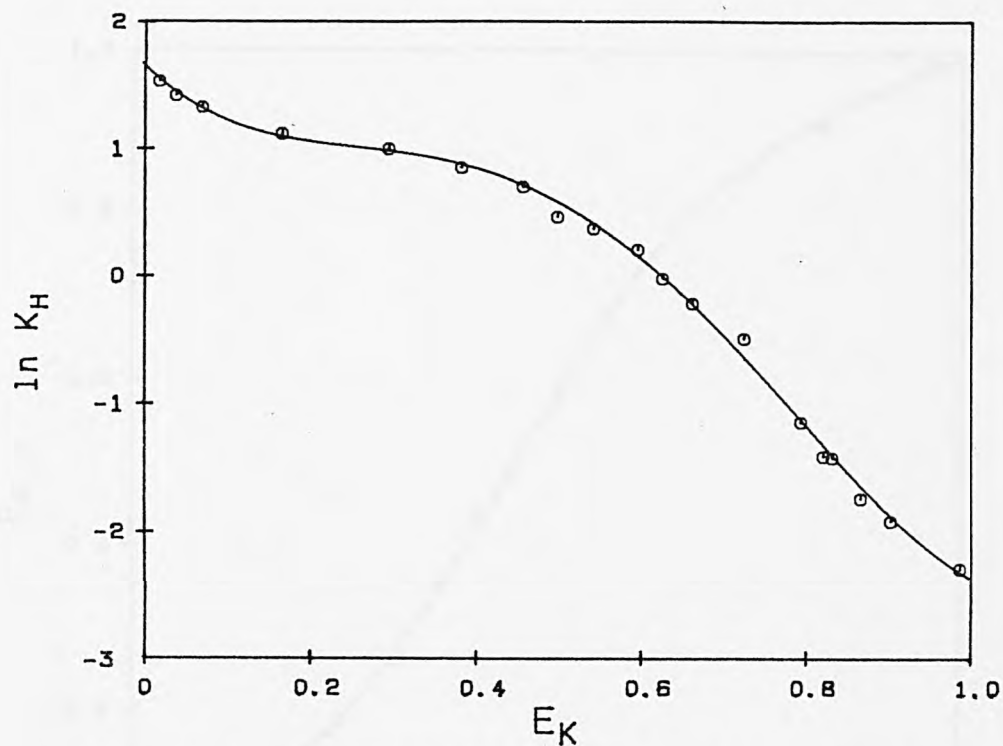


Figure 4.58: Corrected Selectivity Plot:
Na-K Exchange in Y (Grace) at 2°C.

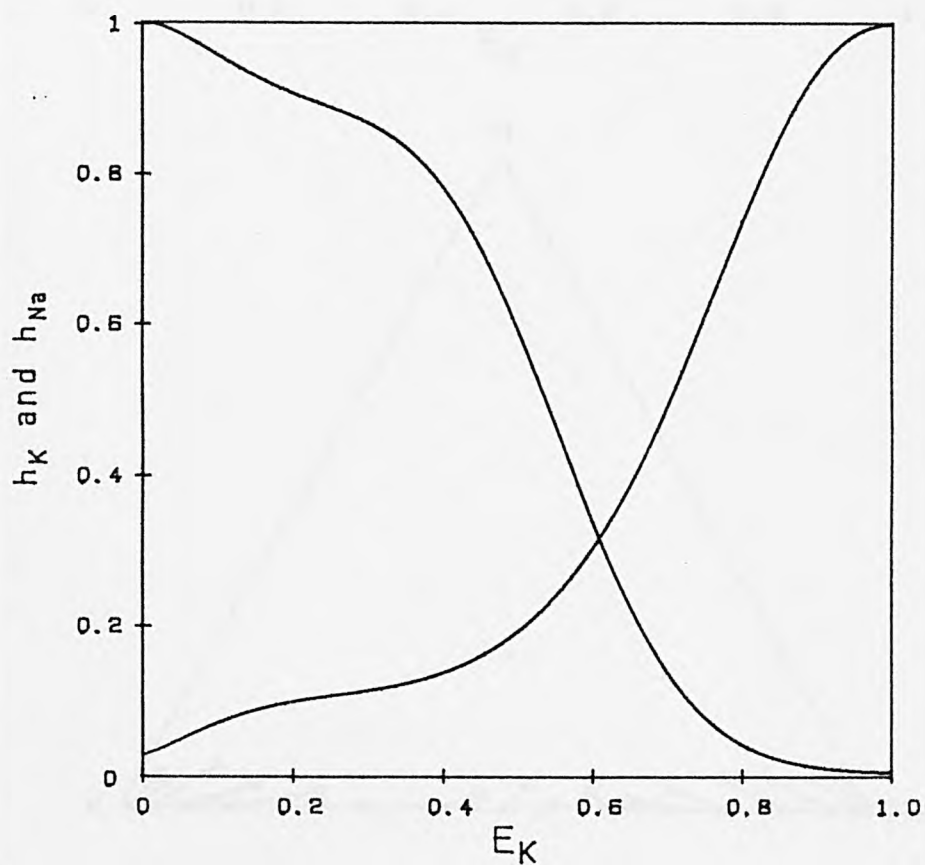


Figure 4.59: Zeolite Phase Activity Coefficients:
Na-K Exchange in Y (Grace) at 2°C.

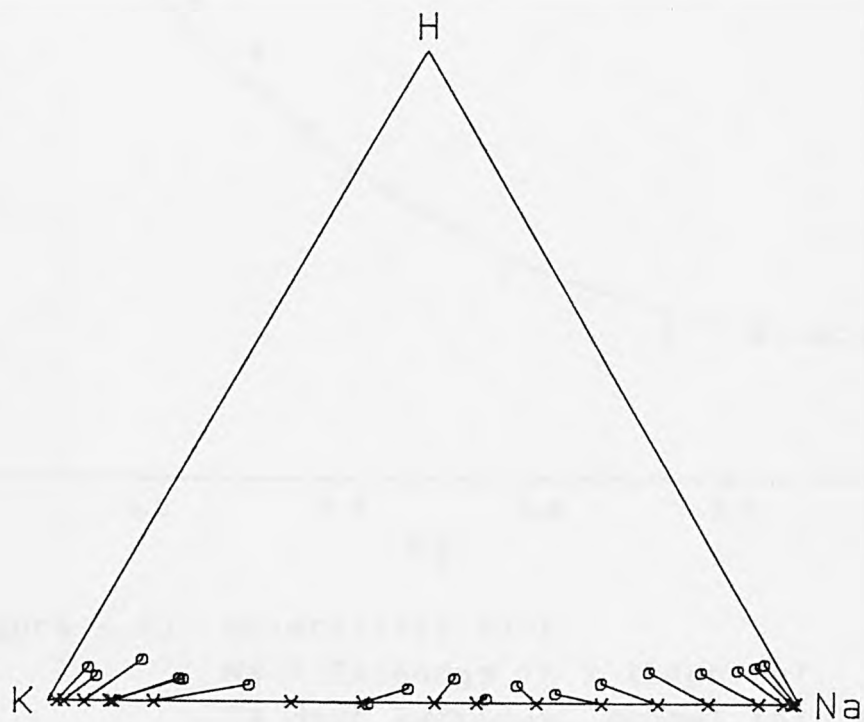
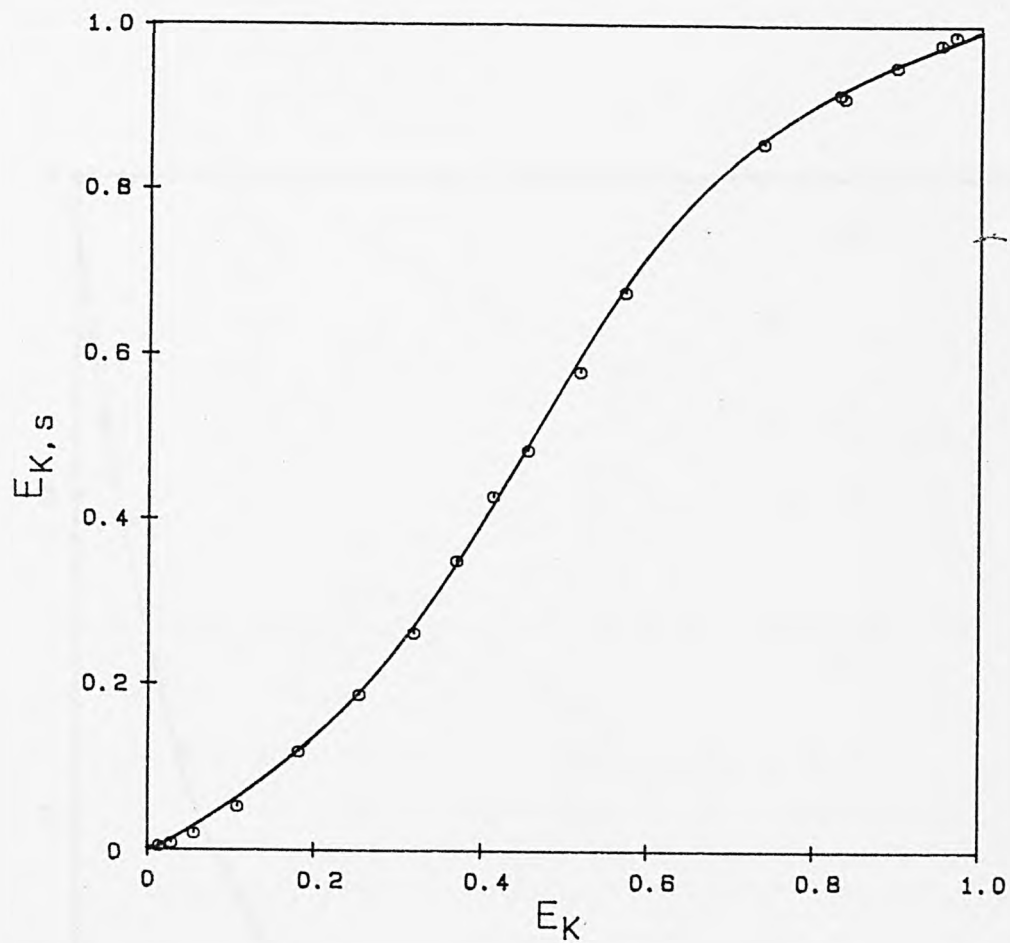


Figure 4.60: Na-K Exchange in X (Laporte).
24 Hour Exchange, Normal Initial pH.

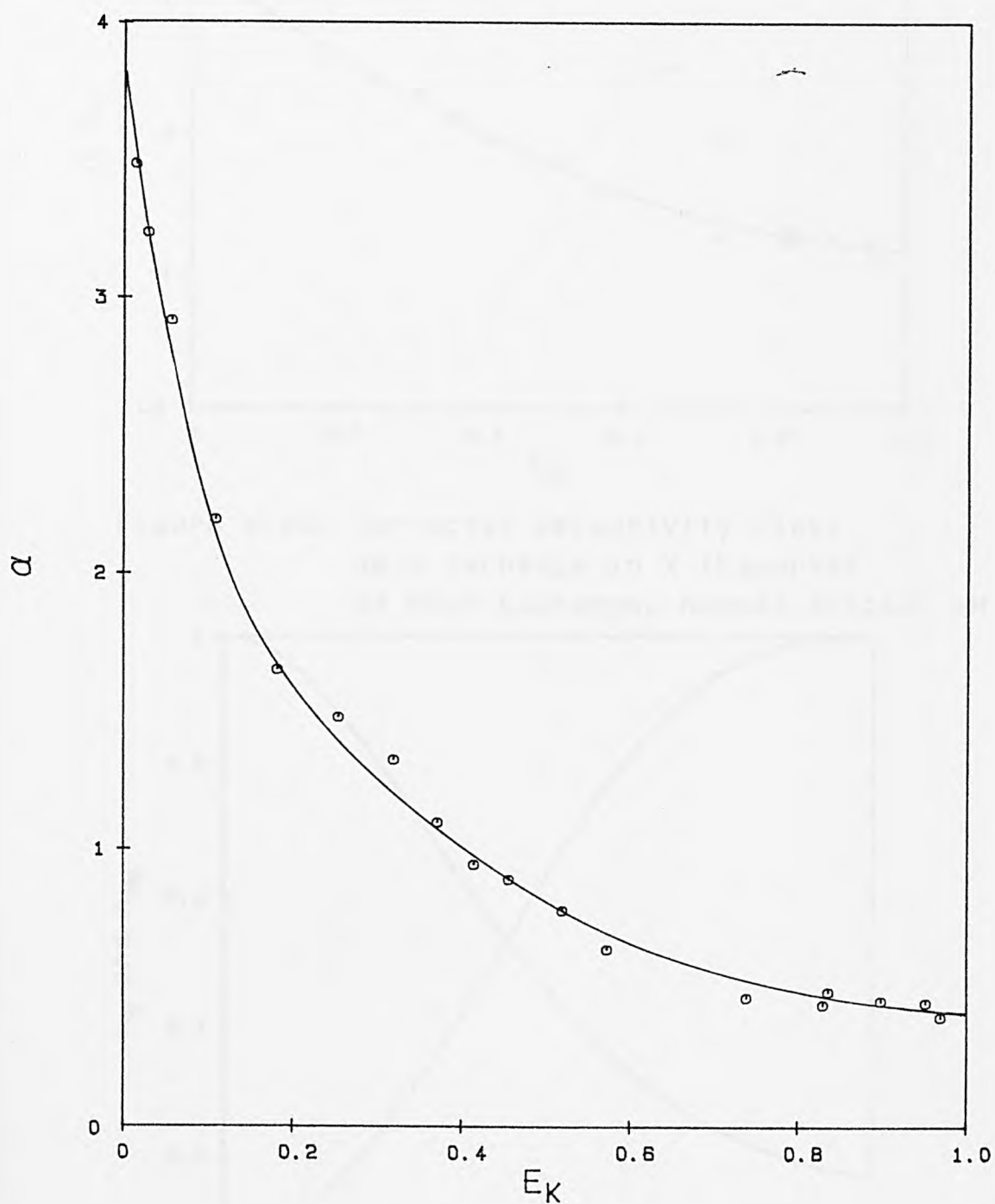


Figure 4.61: Selectivity Plot:
Na-K Exchange in X (Laporte).
24 Hour Exchange, Normal Initial pH.

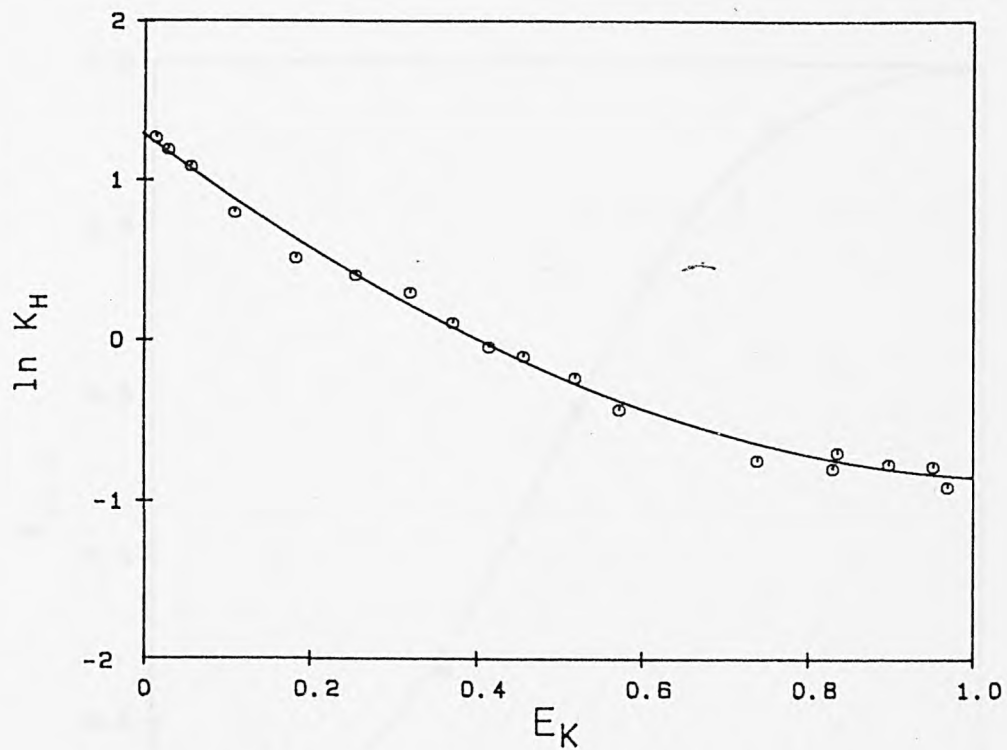


Figure 4.62: Corrected Selectivity Plot:
Na-K Exchange in X (Laporte).
24 Hour Exchange, Normal Initial pH.

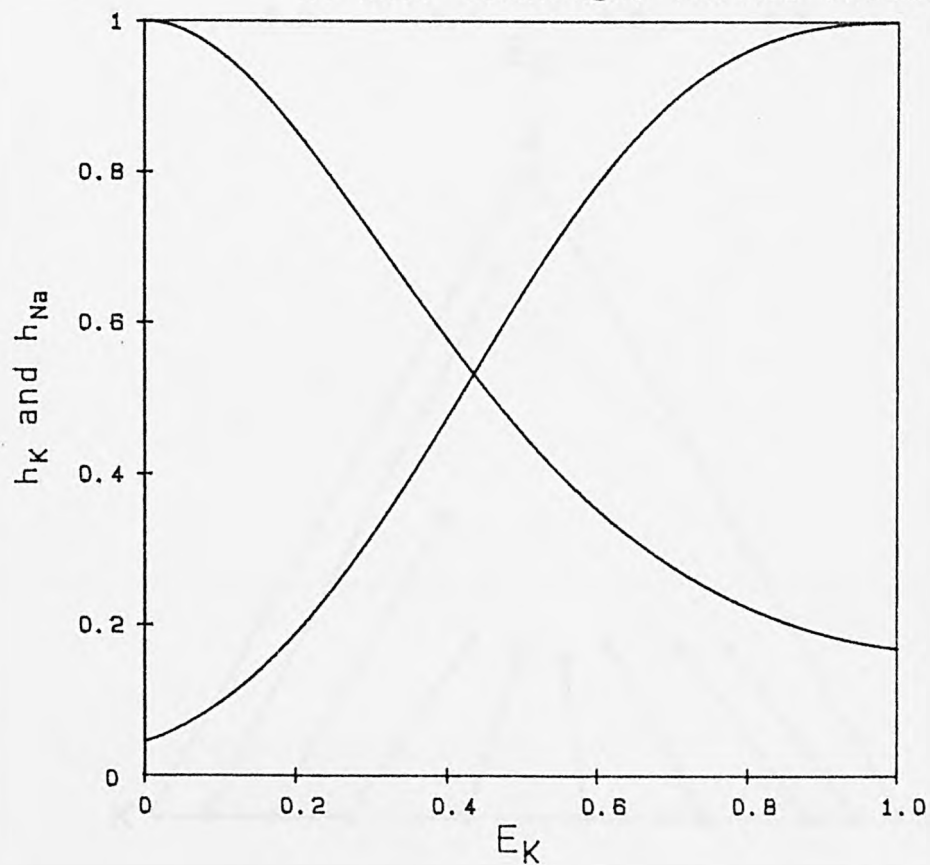


Figure 4.63: Zeolite Phase Activity Coefficients:
Na-K Exchange in X (Laporte).
24 Hour Exchange, Normal Initial pH.

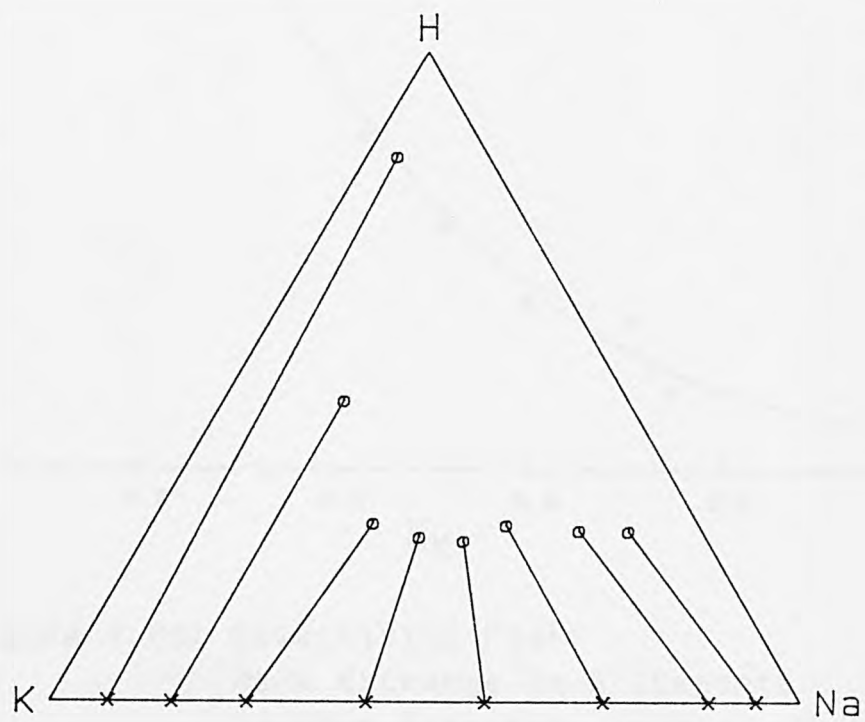
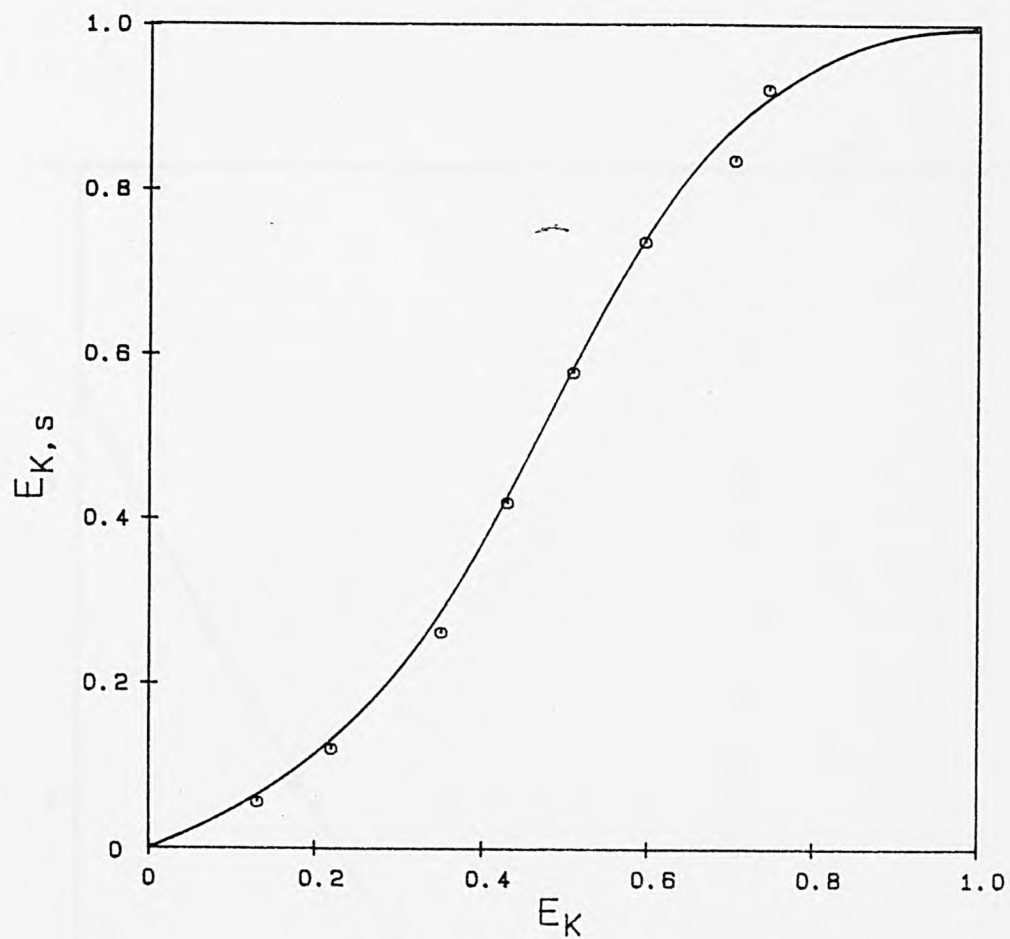


Figure 4.64: Na-K Exchange in X (Laporte).
24 Hour Exchange, Initial pH 2.3.

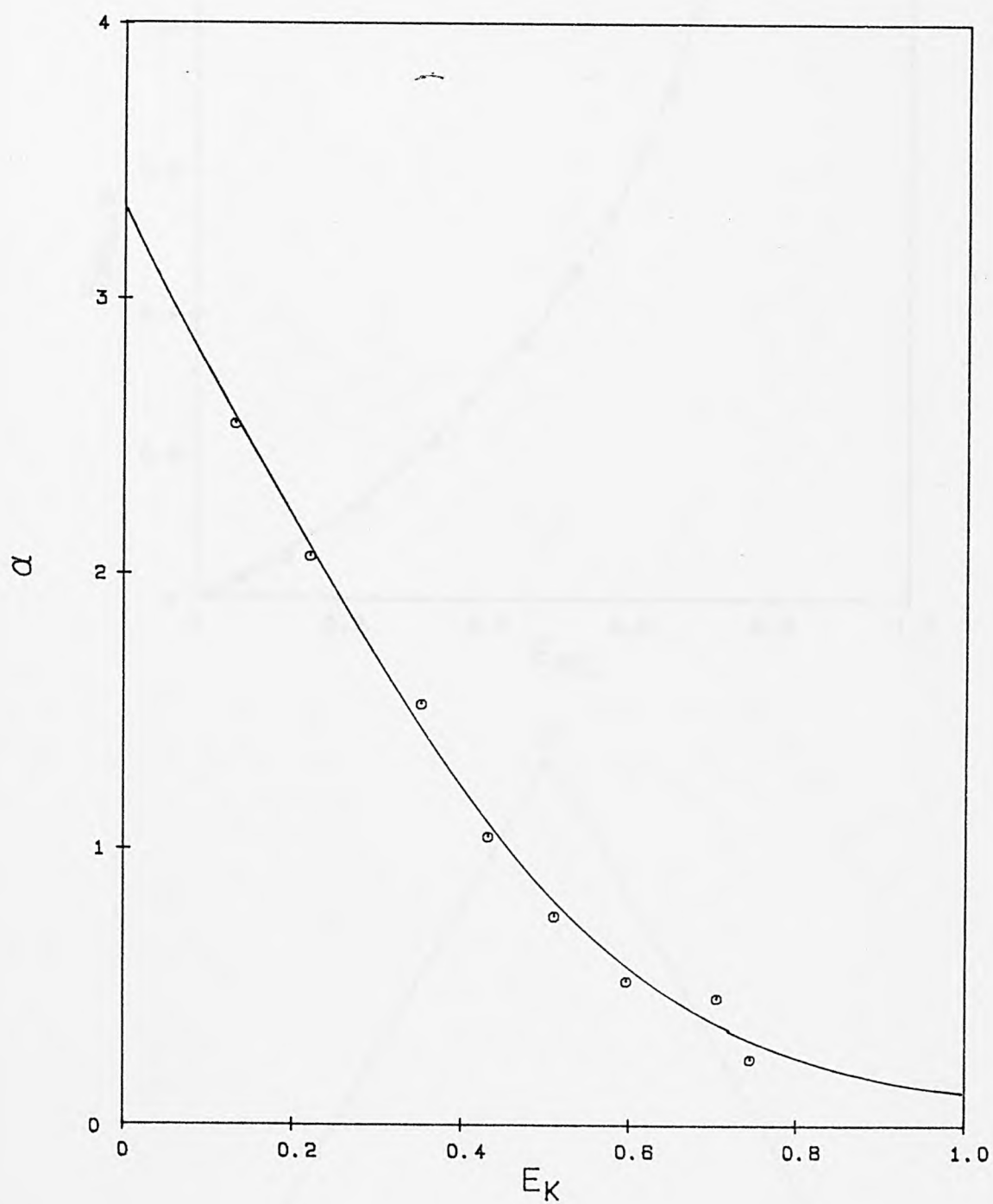


Figure 4.65: Selectivity Plot:
Na-K Exchange in X (Laporte).
24 Hour Exchange, Initial pH 2.3.

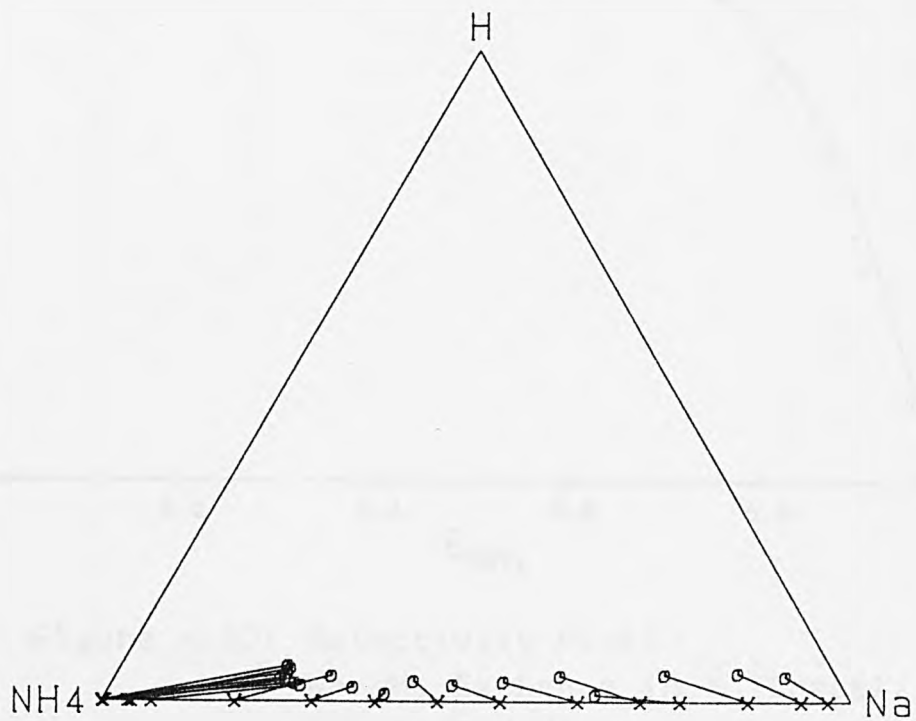
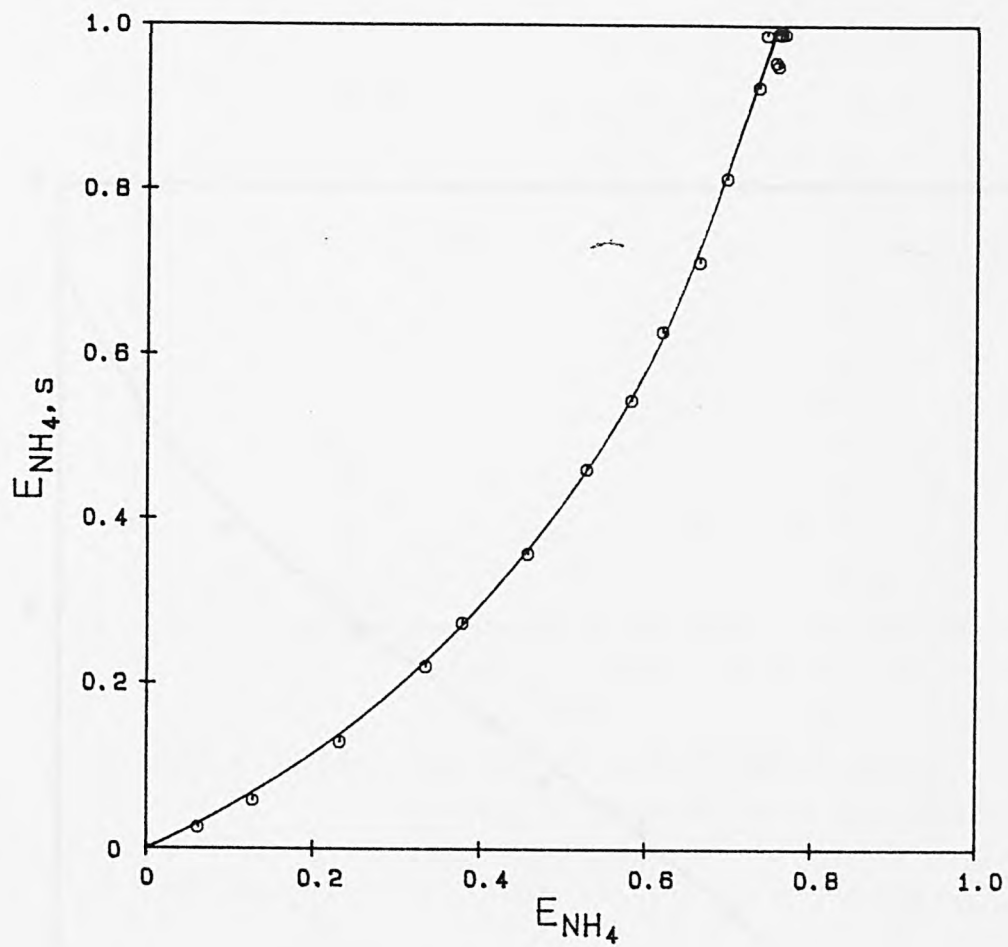


Figure 4.66: Na-NH₄ Exchange in Y (Grace).

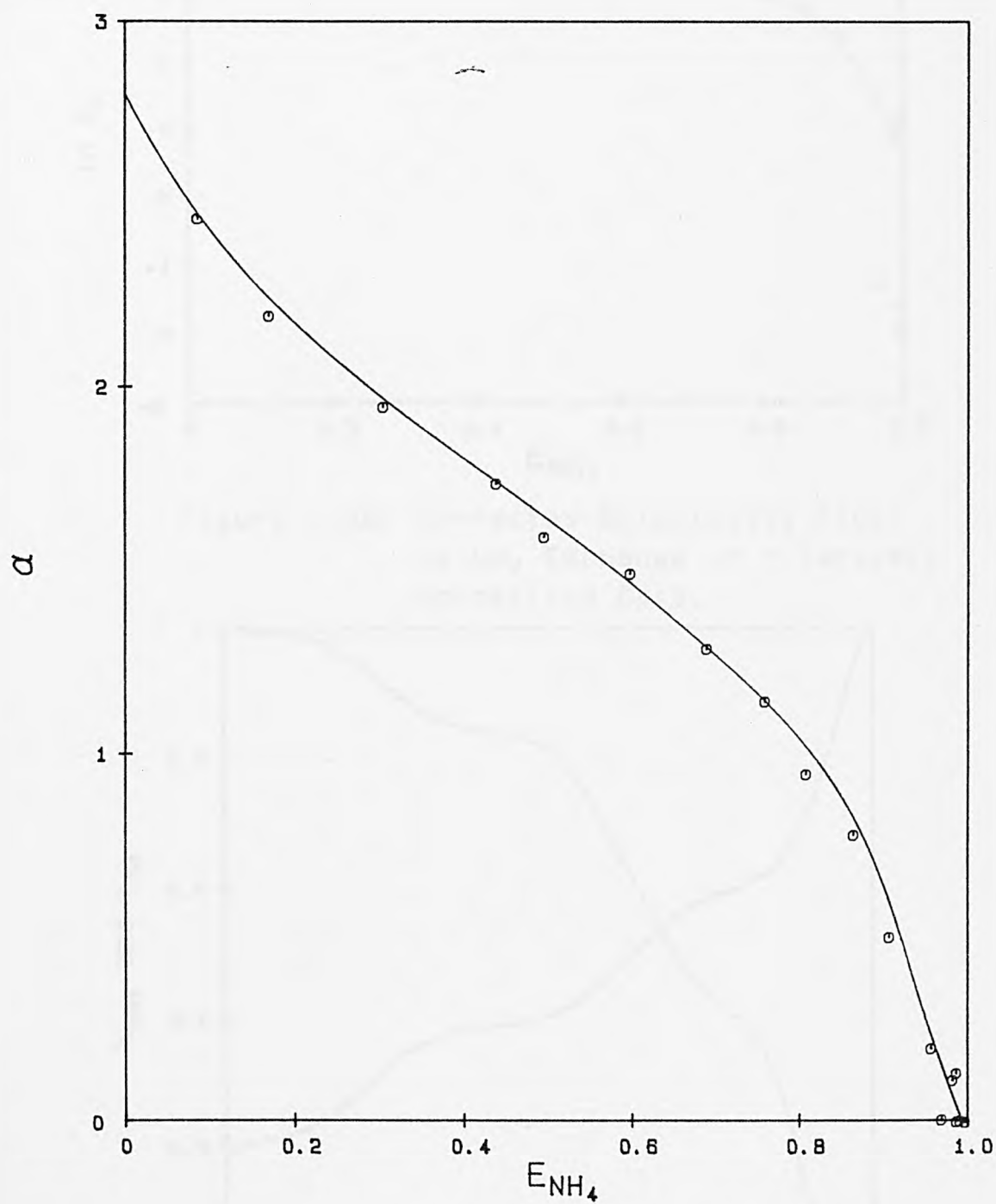


Figure 4.67: Selectivity Plot:
Na- NH_4 Exchange in Y (Grace).
Normalised Data.

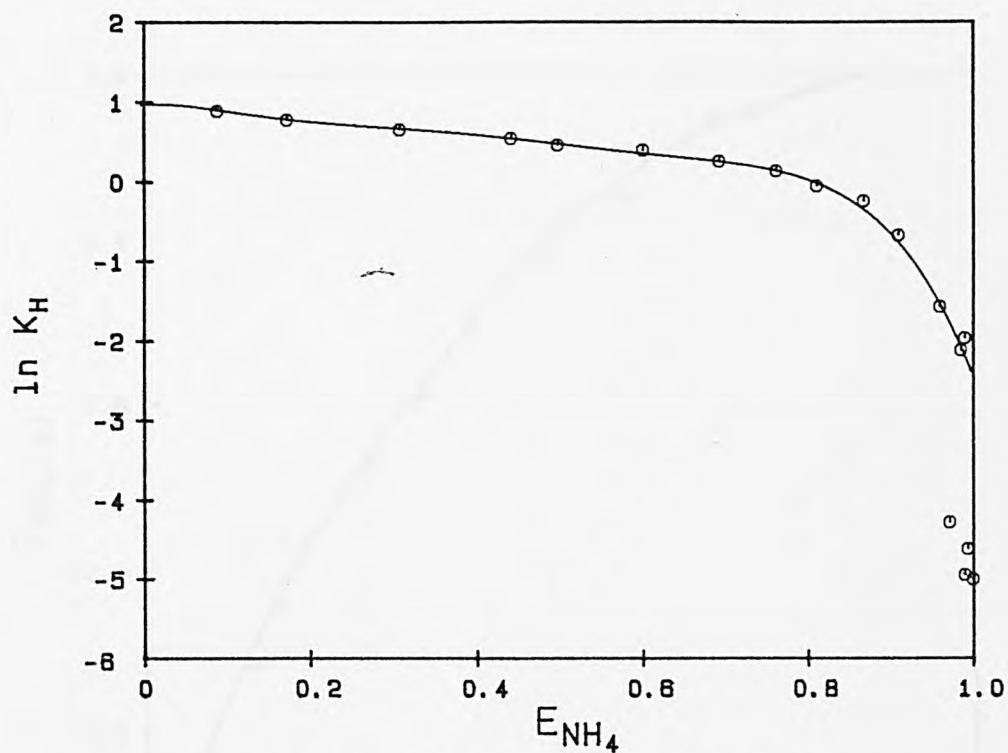


Figure 4.68: Corrected Selectivity Plot:
Na- NH_4 Exchange in Y (Grace).
Normalised Data.

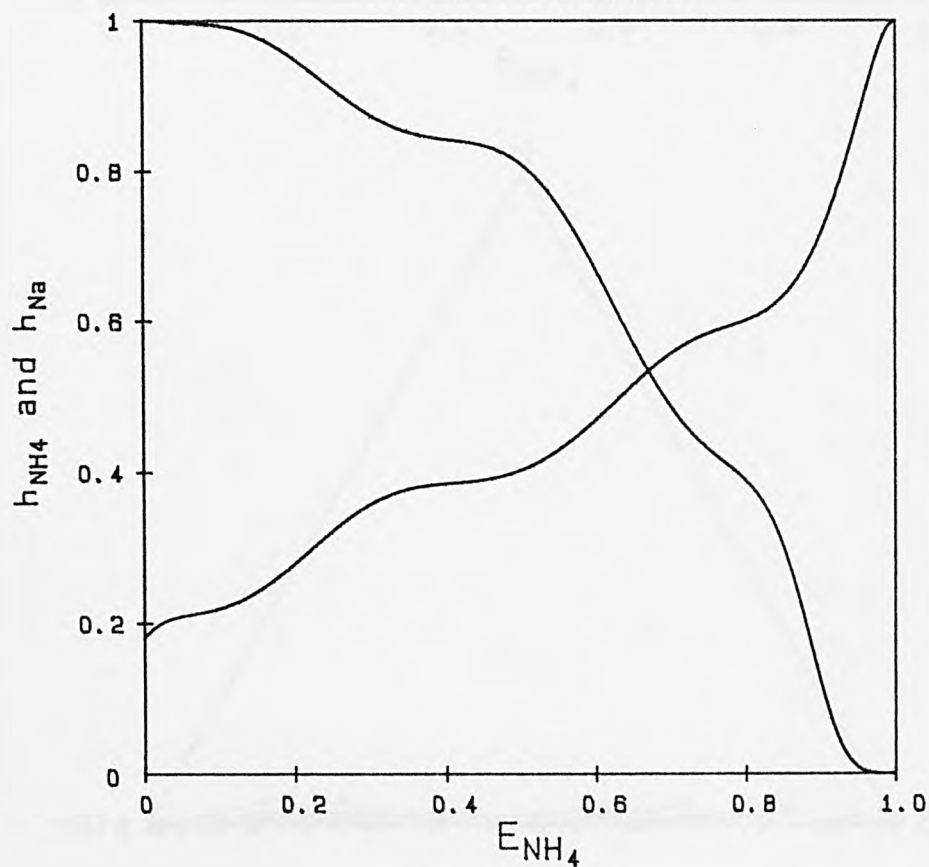


Figure 4.69: Zeolite Phase Activity Coefficients:
Na- NH_4 Exchange in Y (Grace).
Normalised Data.

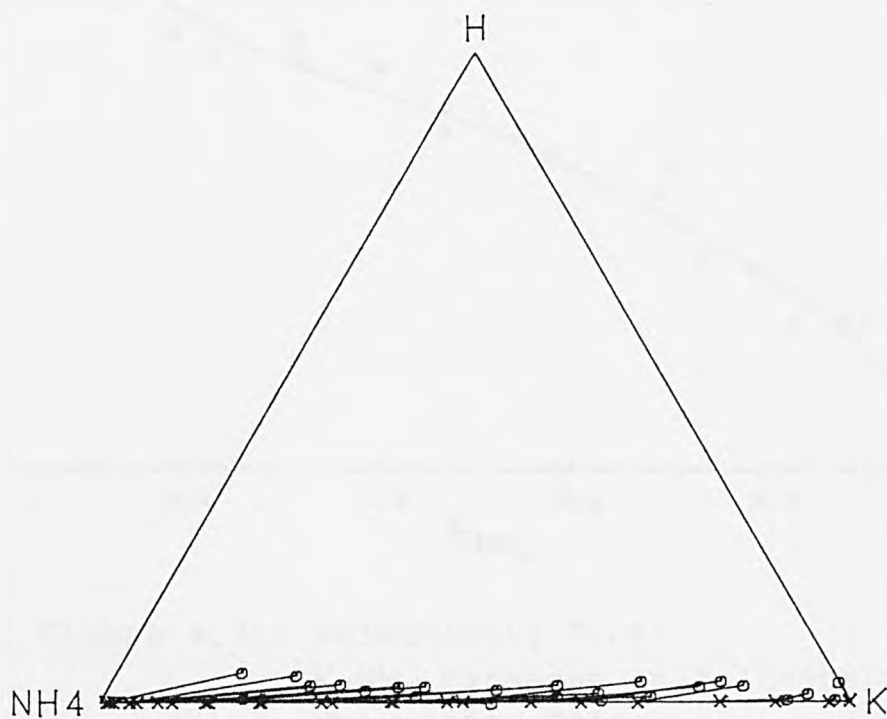
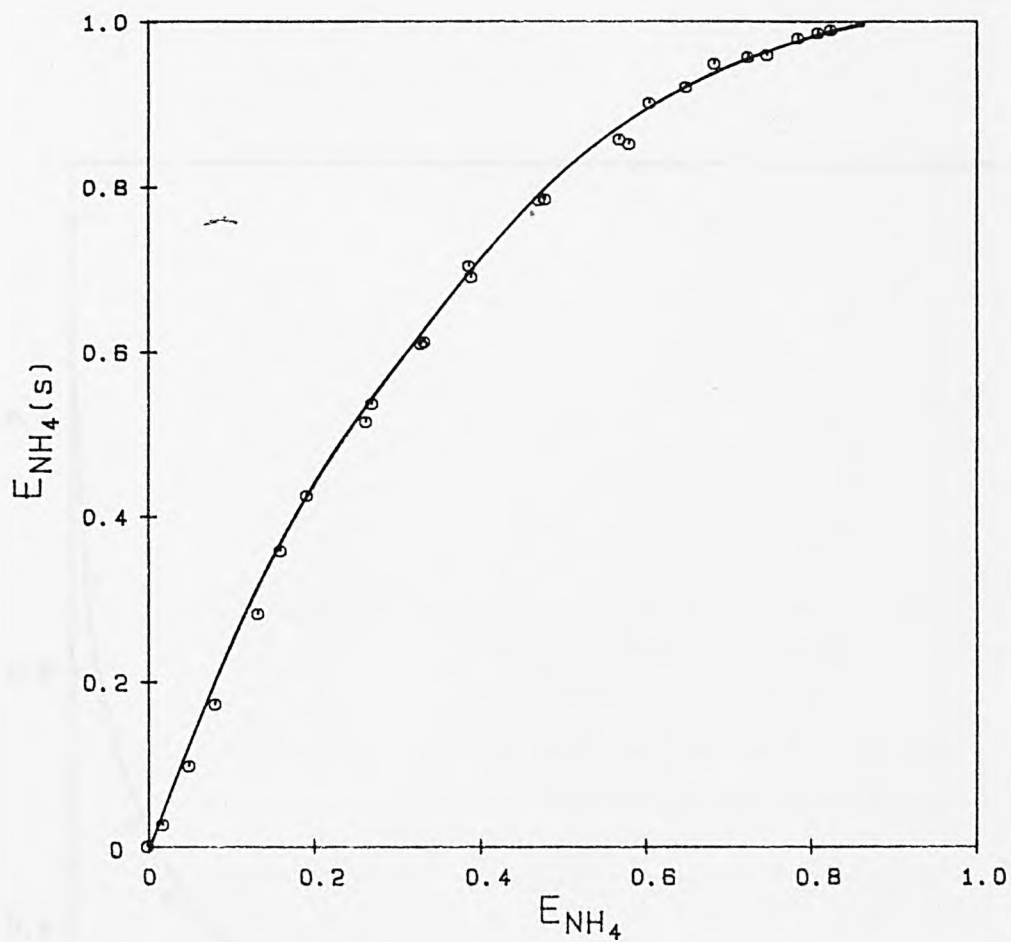


Figure 4.70: K-NH₄ Exchange in Y (Grace).

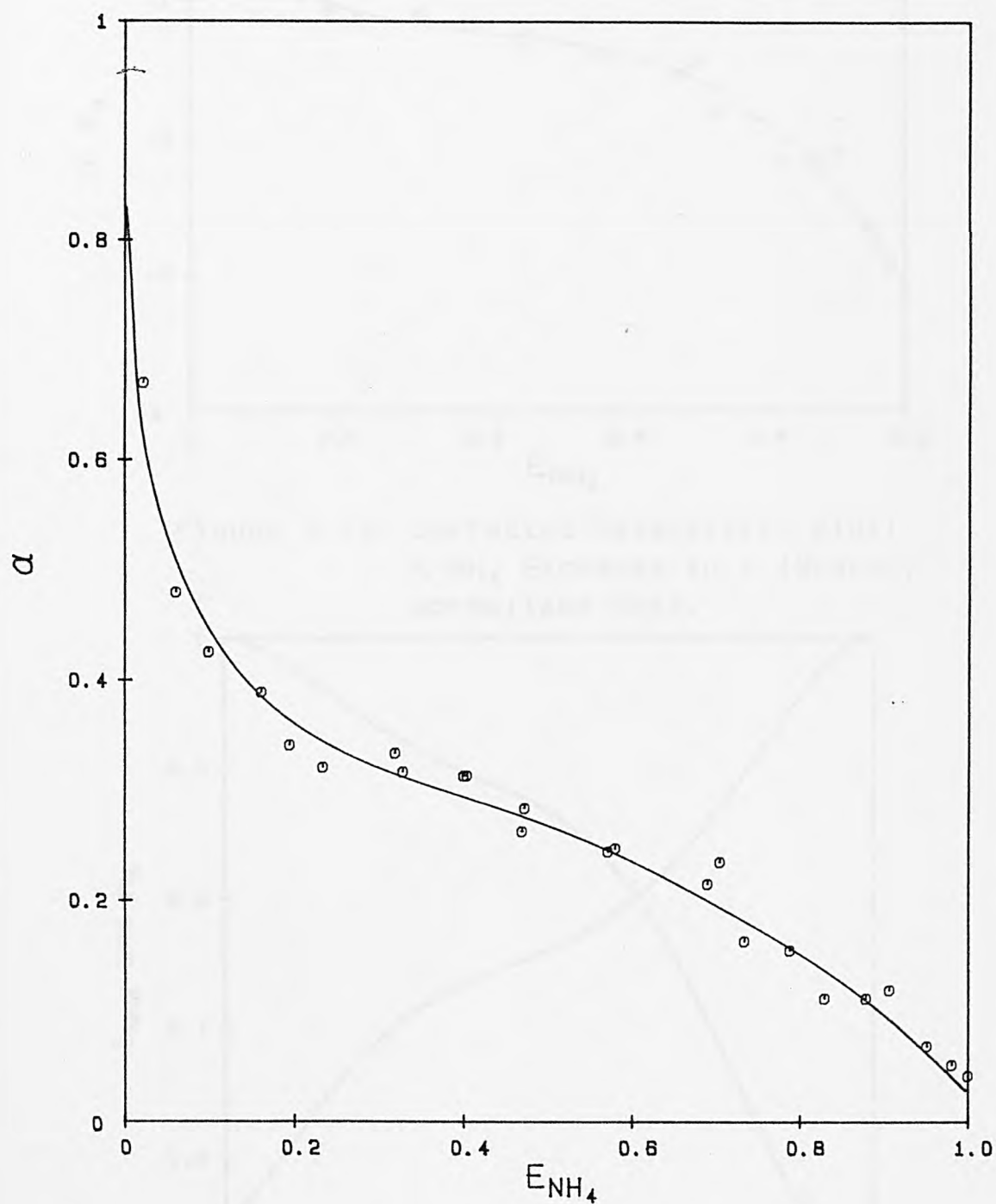


Figure 4.71: Selectivity Plot:
K-NH₄ Exchange in Y (Grace).
Normalised Data.

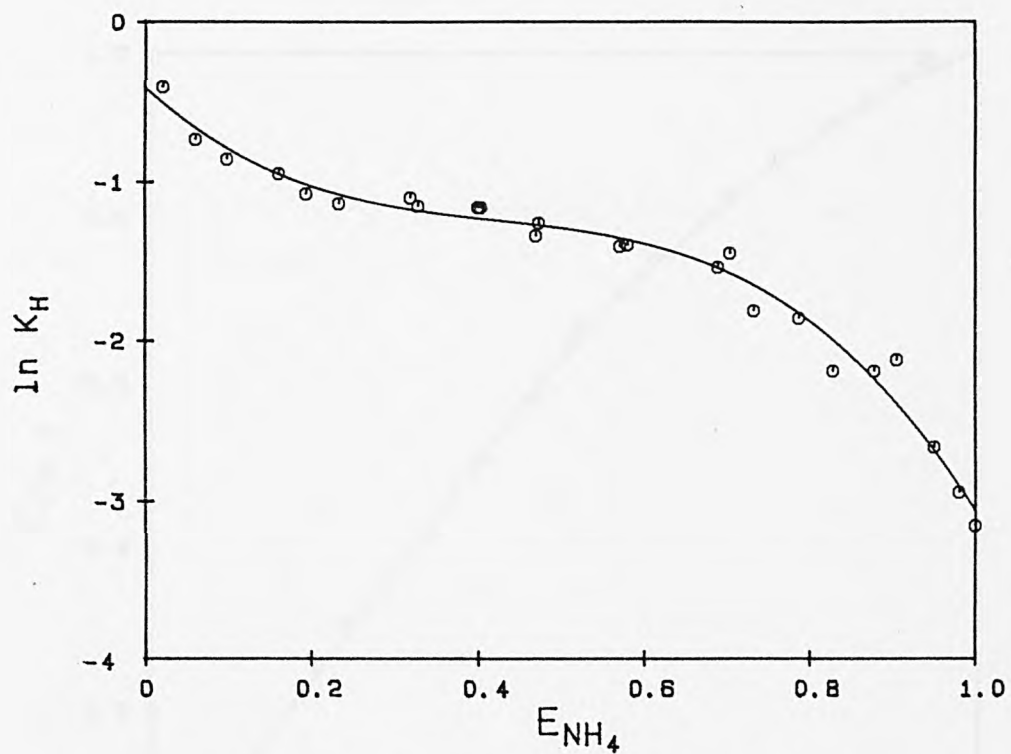


Figure 4.72: Corrected Selectivity Plot:
K- NH_4 Exchange in Y (Grace).
Normalised Data.

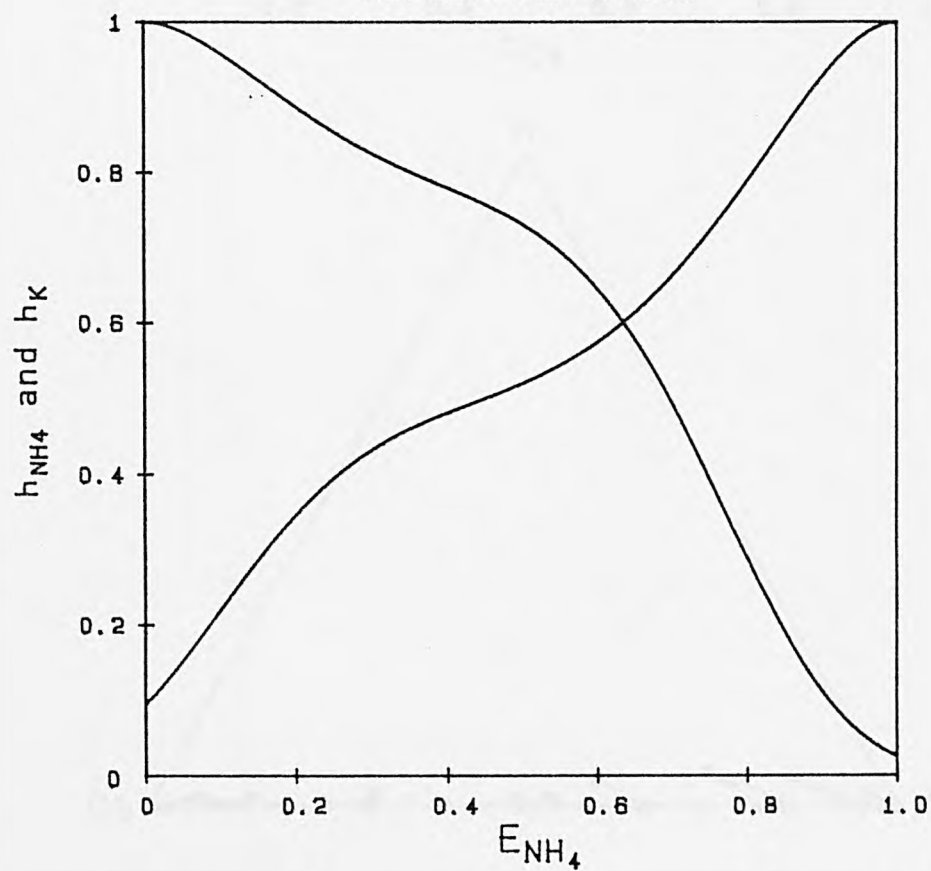


Figure 4.73: Zeolite Phase Activity Coefficients:
K- NH_4 Exchange in Y (Grace).
Normalised Data.

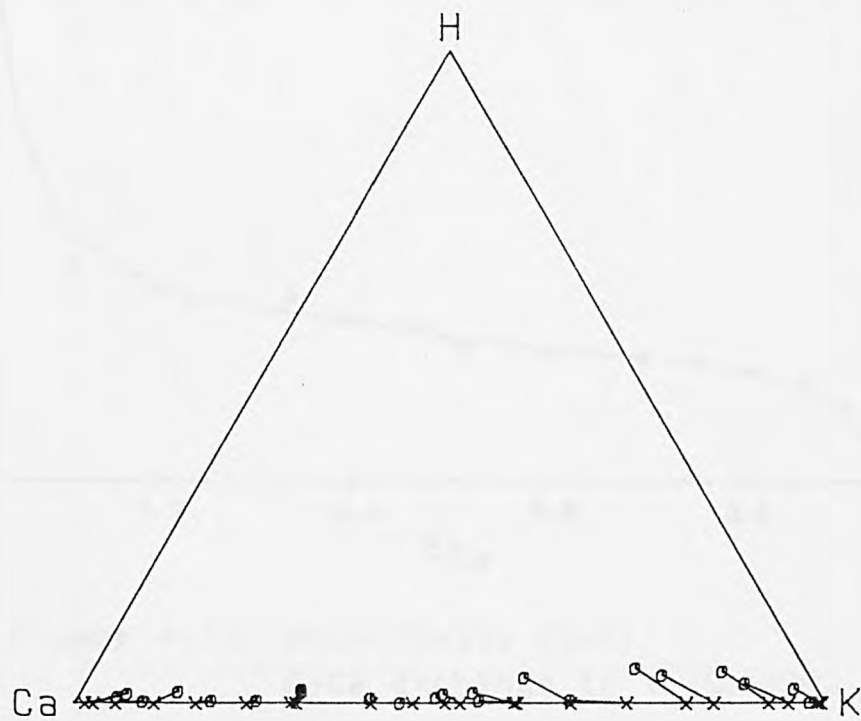
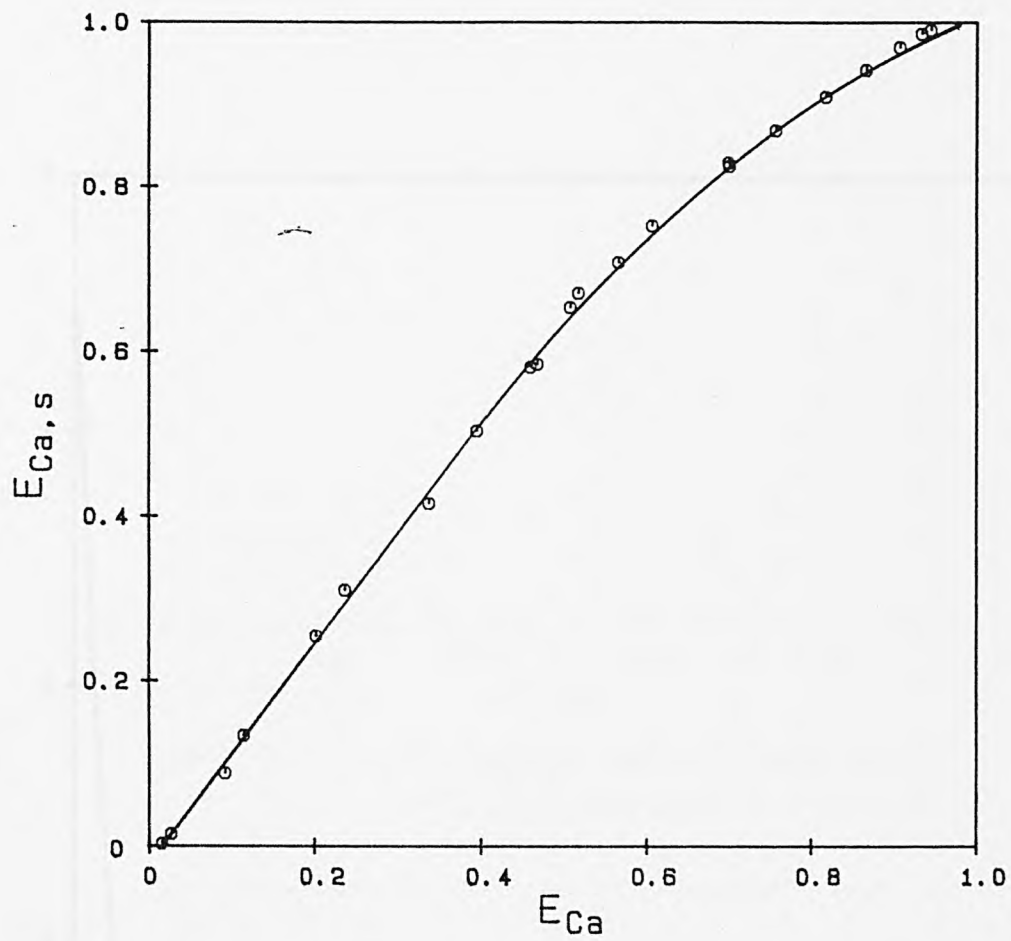


Figure 4.74: K-Ca Exchange in Y (Grace).

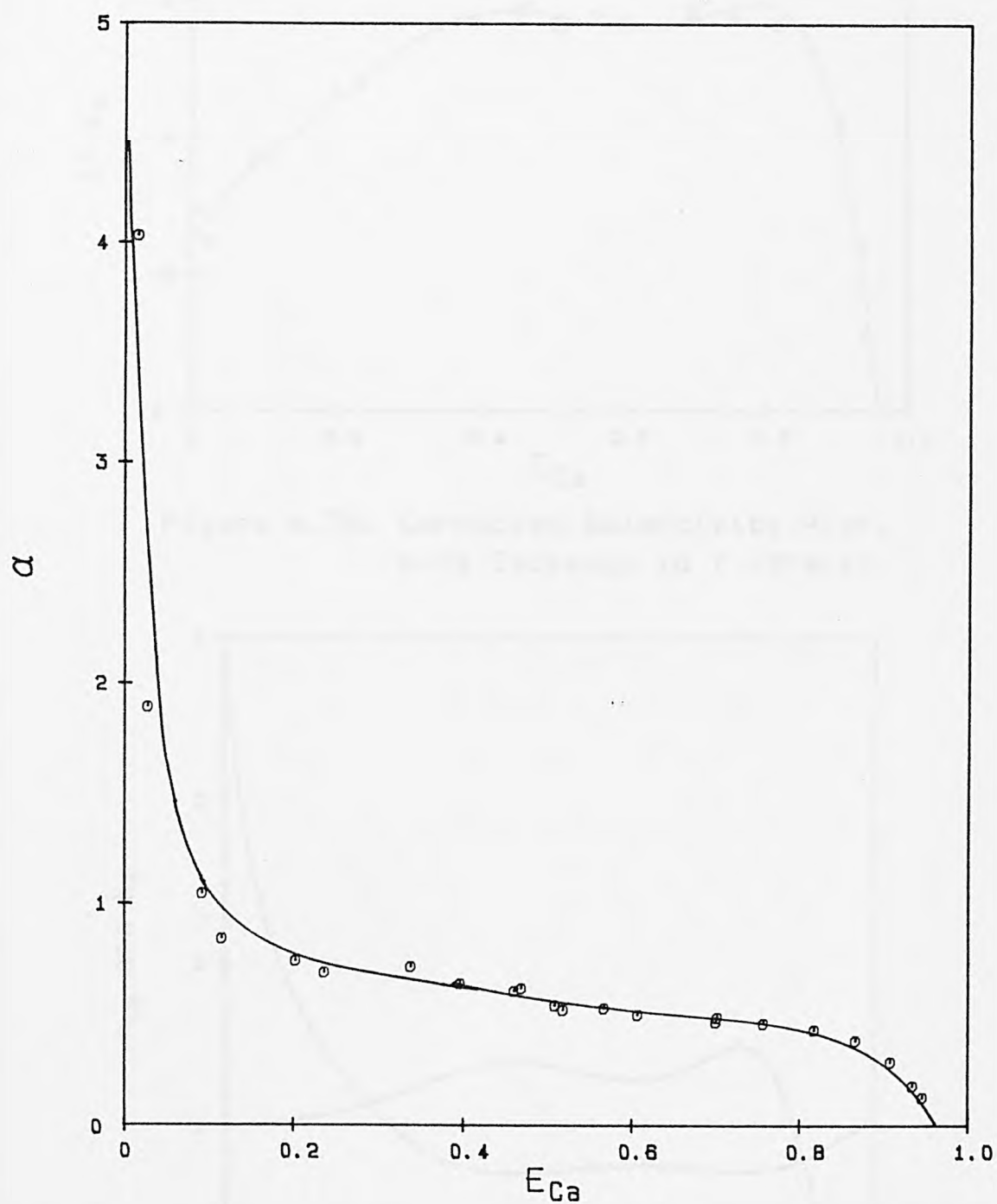


Figure 4.75: Selectivity Plot:
K-Ca Exchange in Y (Grace).

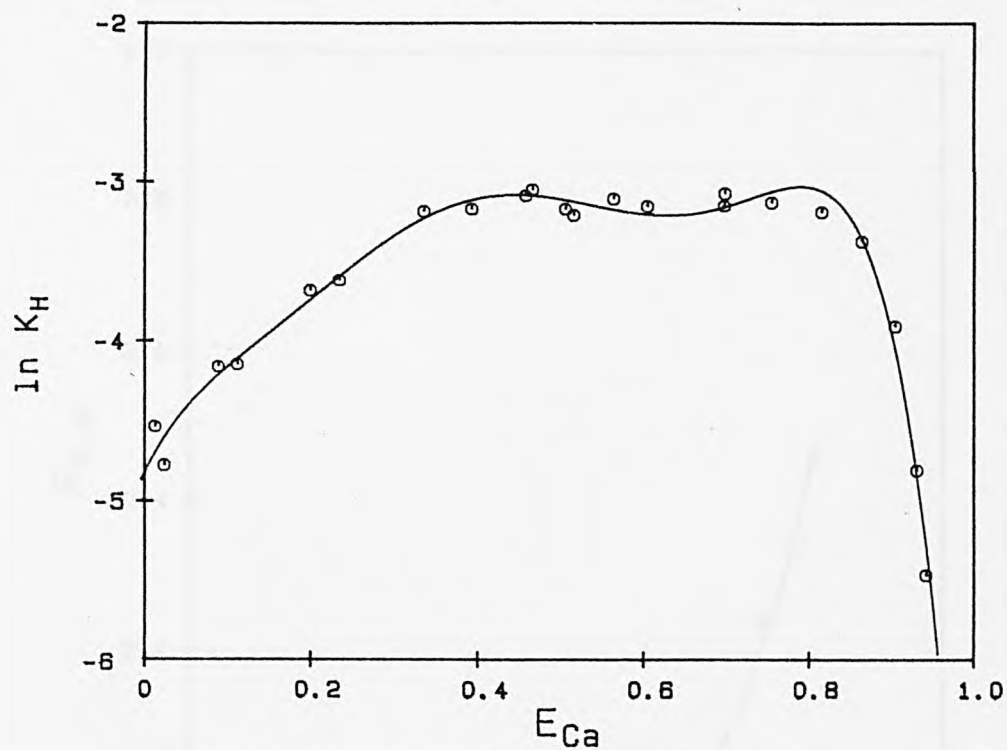


Figure 4.76: Corrected Selectivity Plot.
K-Ca Exchange in Y (Grace).

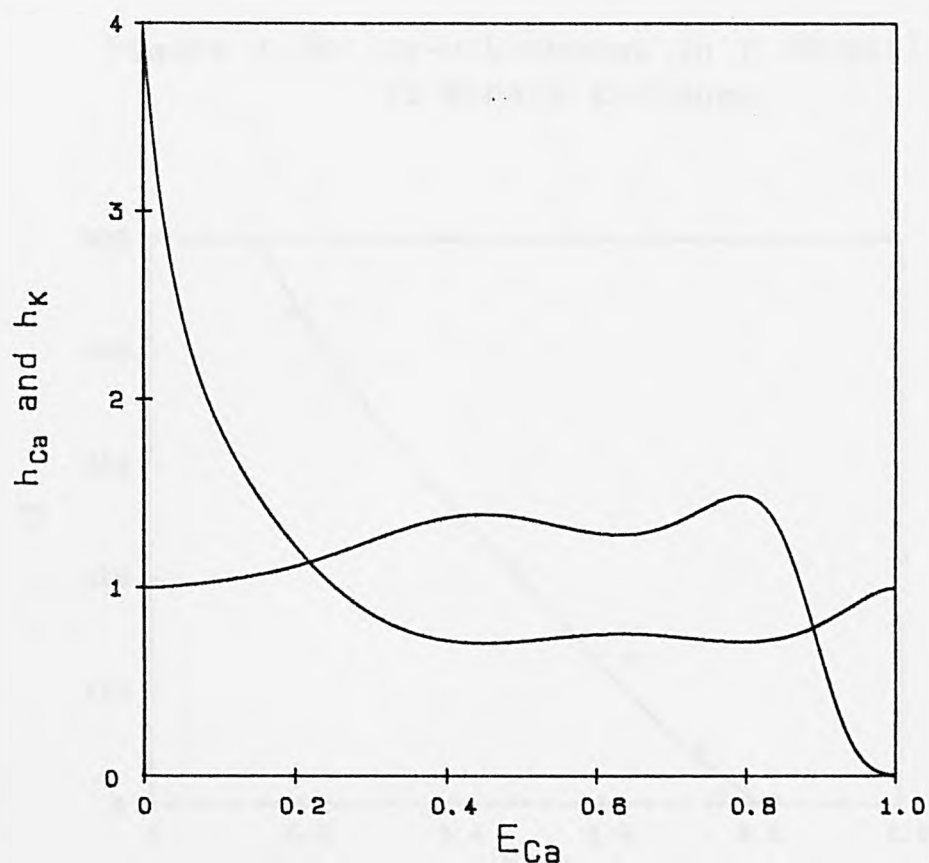


Figure 4.77: Zeolite Phase Activity Coefficients.
K-Ca Exchange in Y (Grace).

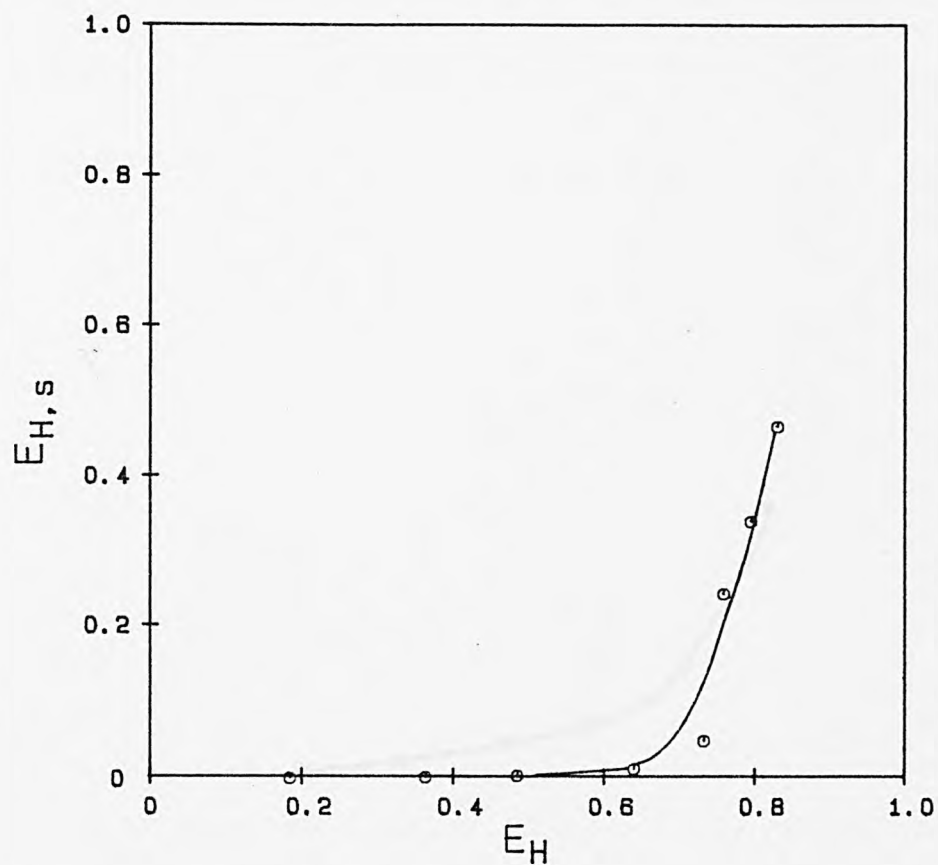


Figure 4.78: Na-H Exchange in Y (Grace).
..15 Minute Exchange.

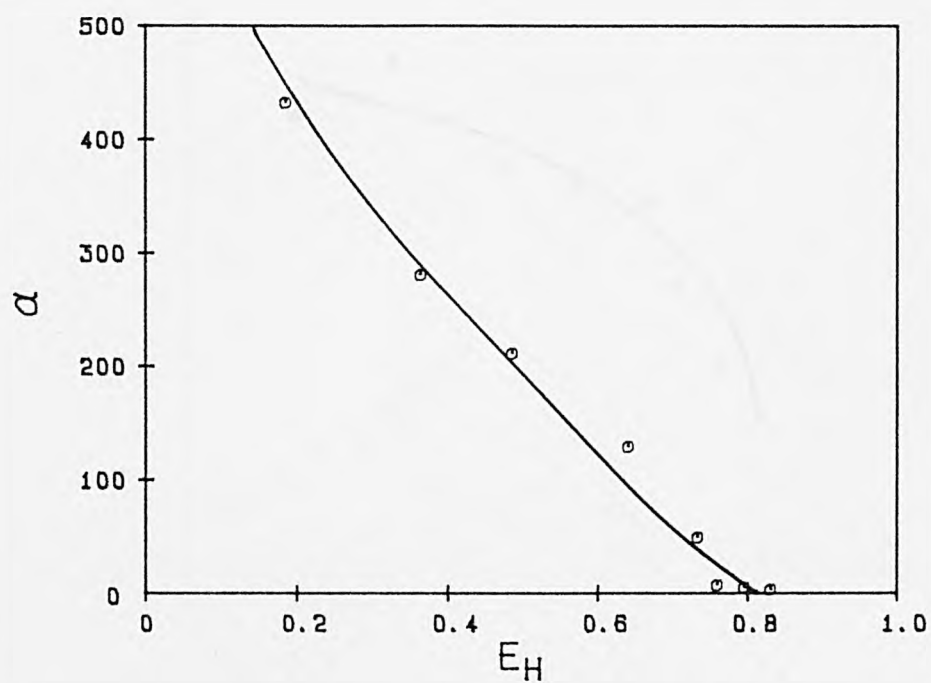


Figure 4.79: Selectivity Plot:
Na-H Exchange in Y (Grace).

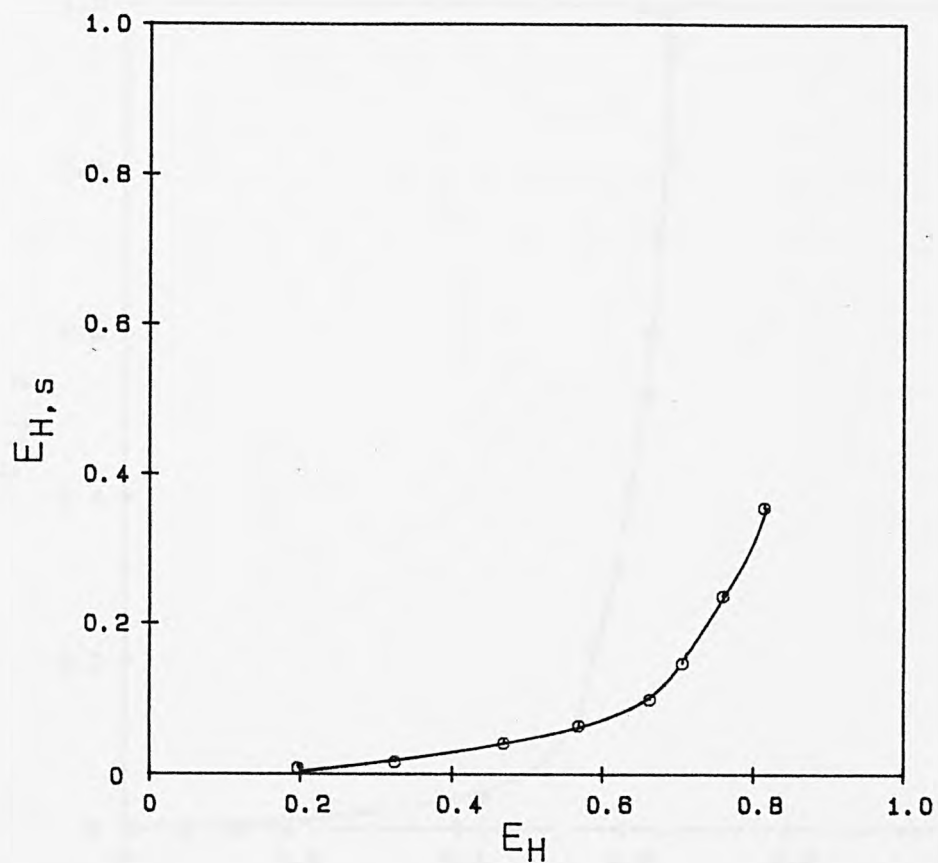


Figure 4.80: K-H Exchange in Y (Grace).
15 Minute Exchange.

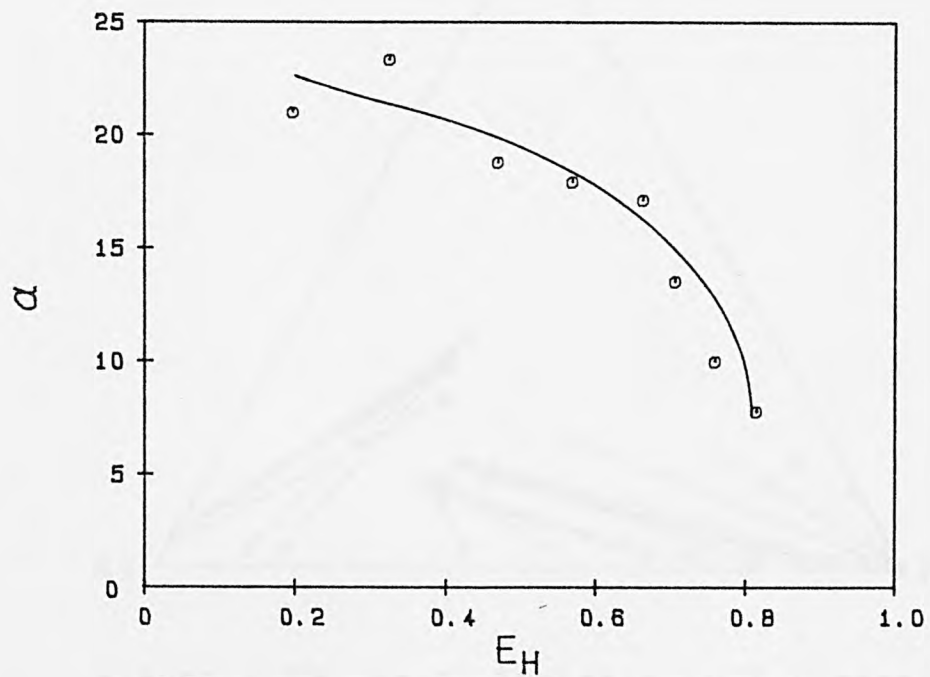


Figure 4.81: Selectivity Plot:
K-H Exchange in Y (Grace).

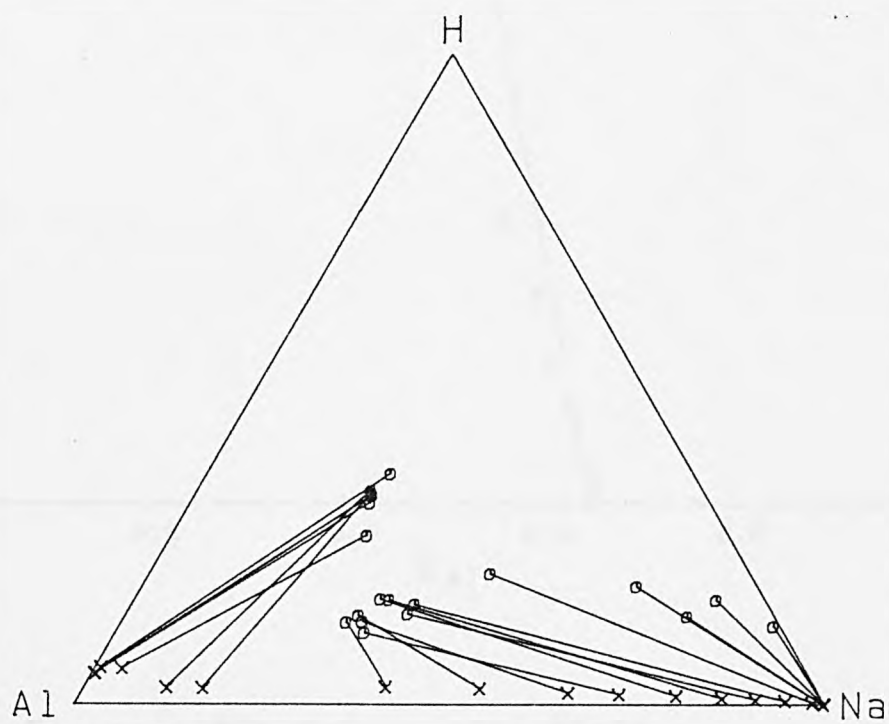
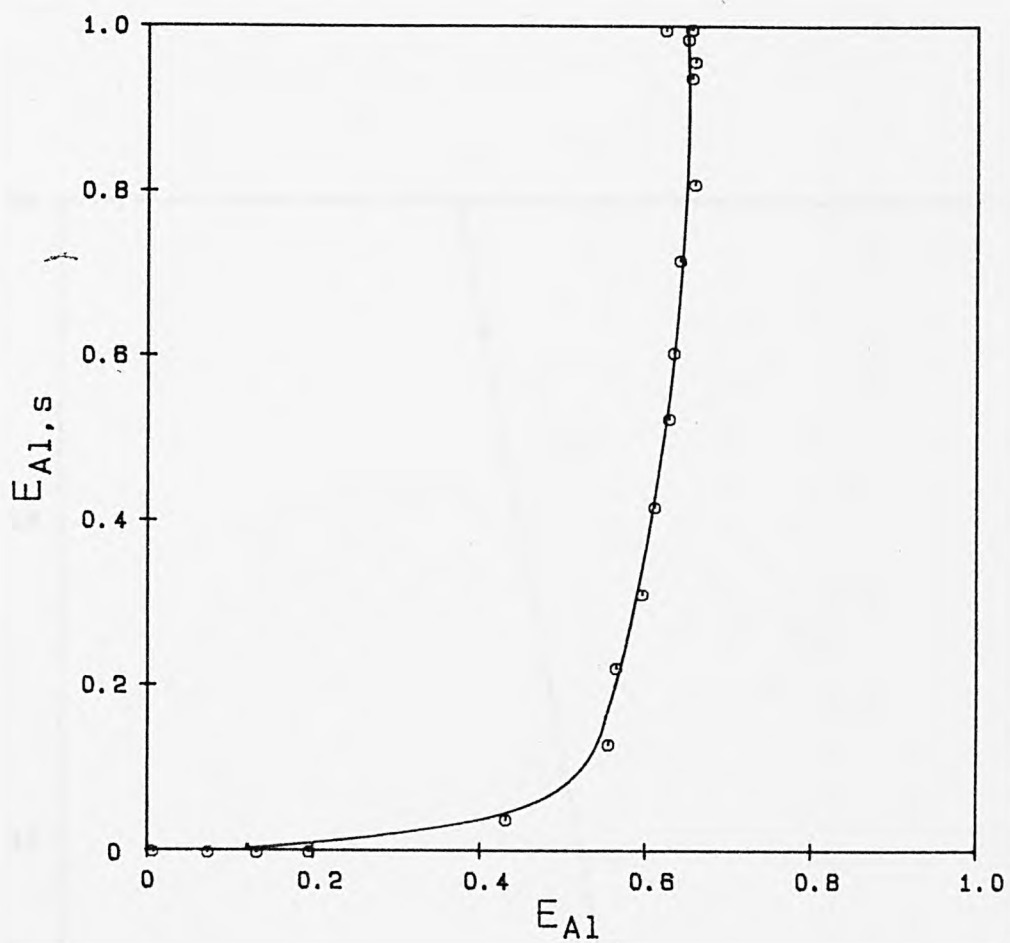


Figure 4.82: Na-Al Exchange in Y (Grace).

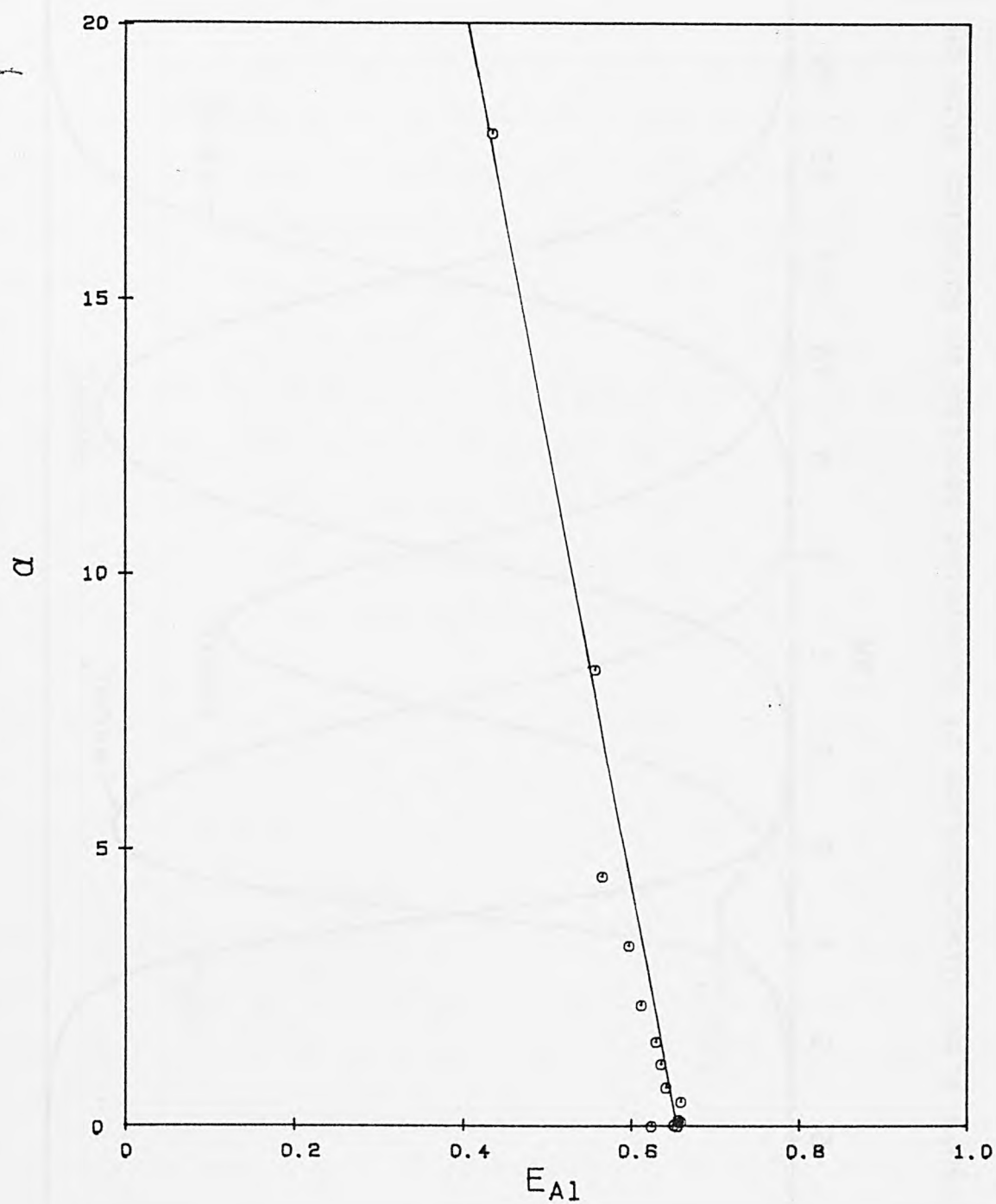


Figure 4.83: Selectivity Plot:
Na-Al Exchange in Y (Grace).

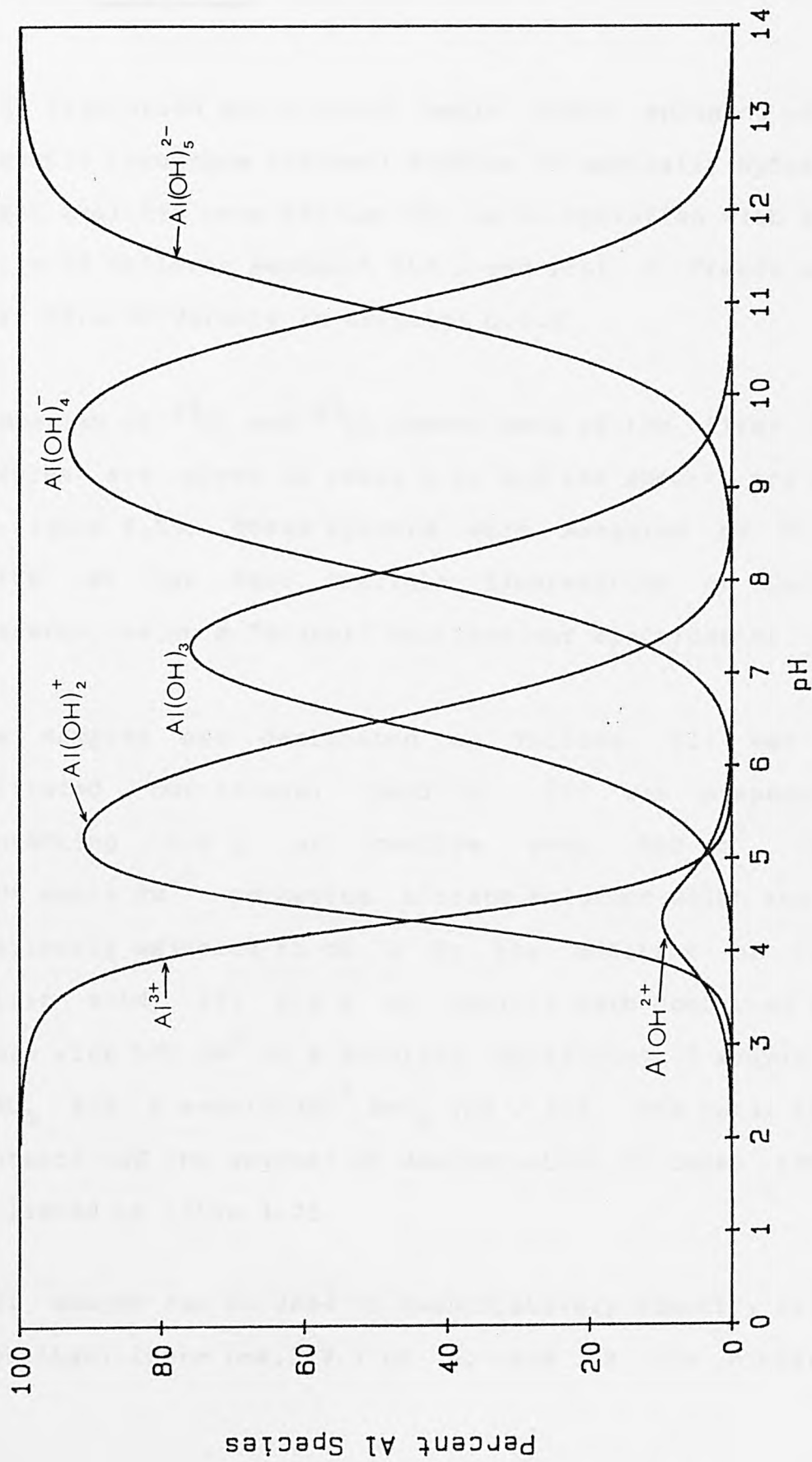


Figure 4.84: Distribution of Aluminium Species in Solution With pH.

4.4. ^{27}Al and ^{29}Si MASNMR Studies of Hydronium Exchange in Zeolite Y.

High resolution solid-state magic angle spinning nuclear magnetic resonance (masnmr) studies of partially hydrolysed NaK-Y zeolites were carried out in co-operation with [REDACTED] [REDACTED] of Unilever Research Ltd., and [REDACTED] [REDACTED] [REDACTED] at the Karl Marx University in Leipzig, G.D.R.

Summaries of ^{29}Si and ^{27}Al masnmr data of the first three samples are given in table 4.21 and the spectra are shown in figure 4.85. These spectra were measured by [REDACTED] [REDACTED] [REDACTED] at the Port Sunlight laboratories of Unilever Research, using a "Bruker" multinuclear spectrometer.

The samples are designated as follows: (1) was the untreated NaY (Grace) zeolite; (2) was prepared by contacting 2.0 g of zeolite with 500 cm³ of a 0.05 equiv dm⁻³ potassium nitrate solution which had been previously adjusted to pH 2 by the addition of dilute nitric acid; (3) 2.0 g of zeolite were contacted three times with 500 cm³ of a solution containing 2 mequiv dm⁻³ NaNO₃ and 8 mequiv dm⁻³ HNO₃ (pH 2.10). The total cation contents and the degrees of dealumination in these samples is listed in table 4.21.

^{29}Si masnmr can be used to quantitatively identify Si(nAl) groupings, where n=4,3,2,1 or 0, and is the number of

aluminium atoms linked tetrahedrally via oxygen bridges to the central silicon atom. The number of silicon atoms so bound is accordingly 4-n. Since the area under the nth ^{29}Si masnmr peak is directly proportional to the population of the $\text{Si}(\text{nAl})$ grouping, and Loewenstein's (1954) rule is obeyed, the Si/Al ratio of the framework can be calculated from the relative intensities, $I_{\text{Si}(\text{nAl})}$, of $\text{Si}(\text{nAl})$ signals using the formula:

$$(\text{Si/Al})_{\text{nmr}} = \sum_{n=0}^4 I_{\text{Si}(\text{nAl})} / \sum_{n=0}^4 \frac{n}{4} I_{\text{Si}(\text{nAl})} \quad \dots(4.1)$$

(Klinowski, Fyfe and Gobbi, 1985; Klinowski and Thomas, 1986).

^{27}Al masnmr can be used to distinguish between tetrahedrally and octahedrally coordinated aluminium in zeolites (Fyfe et al, 1982). The technique has found considerable application in determining the mechanism of hydrothermal dealumination and formation of extra-lattice aluminium in the preparation of ultra-stable zeolites (Flanigen, 1980; Freude et al, 1983).

Examination of the ^{29}Si masnmr data in table 4.21 shows that as the severity of the acid treatment is increased the Si/Al ratio increases. There is reasonably good agreement between the Si/Al ratio determined chemically and as determined from the masnmr spectra. The intensities of the $\text{Si}(3\text{Al})$ and $\text{Si}(2\text{Al})$ signals decrease with respect to

Si(1Al) and Si(0Al) with increasing dealumination, as would be expected (Klinowski et al, 1985; Freude et al, 1983).

Data from the ^{27}Al masnmr spectra (see table 4.21 and figure 4.85) show an increase in the amount of octahedrally coordinated aluminium with increasing dealumination. There is a discrepancy between the aluminium content of the zeolites determined chemically and that calculated from the masnmr spectra. This may be due in part to the calibration procedure. However, the percentage difference in these data is higher for the acid treated samples and may reflect the presence of species such as $\text{Al}(\text{OH})_3$ and $\text{Al}(\text{OH})_2^+$ which are not detected by ^{27}Al masnmr (Freude et al, 1983; Klinowski, Fyfe and Gobbi, 1985).

^{27}Al masnmr spectra of nine zeolite Y samples were measured at a frequency of 70 MHz using a "home-made" spectrometer at the Karl Marx University in Leipzig. The data are summarised in table 4.22. The framework Si/Al ratio was determined by comparing the intensity of the 50 ppm line in the ^{27}Al masnmr spectrum of the sample under study, with that of a reference material, after correcting for the cation and water content. The reference material used was a ZSM 5 zeolite which had a cation content of 2.3%, a water content of 4% and an Si/Al ratio of 15 (Freude, 1986).

Sample 1 was the untreated NaY (Grace) zeolite. The other samples were prepared by contacting 2 g of zeolite with

500 cm³ of a 0.05 equiv dm⁻³ solution of potassium nitrate, the pH of which had been adjusted to between 5.5 and 2.0 by the addition of dilute nitric acid. The exchange time was 24 hours and the zeolite was separated from the solution by centrifugation, washed with distilled water at pH 7, and dried under vacuum at room temperature. The data are summarised in table 4.22.

The Si/Al ratios of the zeolite samples (determined chemically) increased from 2.58 to 2.67 as aluminium was extracted from the framework. The Si/Al ratios calculated from the ²⁷Al spectra were significantly different. An initial increase in the Si/Al ratio was observed, to a maximum of 5.01 at pH 5.70, and then this was followed by a decrease as the pH fell to 3.52 (see figure 4.86). The data are very surprising and no adequate explanation can be given for them at present. The results will be discussed further at the end of the section.

²⁹Si masnmr spectra of zeolites contacted with solutions of nitric acid and potassium nitrate and nitric acid at various pH's, were measured at Unilever Research Ltd. The experimental details were the same as for the ²⁷Al masnmr study. The chemical analyses of these samples are given in table 4.23; (the prefix K refers to NaKH-Y samples, and H to NaH-Y). The ²⁹Si masnmr data is summarised in table 4.24 and the spectra are shown in figure 4.87. The intensities of the masnmr signals were re-calculated using

a Gaussian fitting routine written for a BBC microcomputer and kindly supplied by [REDACTED] of Cambridge University.

Si/Al ratios determined by chemical analysis and from ^{29}Si masnmr data compared very well for low hydronium-exchanged samples (NaY, K1, K2 and H1-H3). When dealumination occurred the $(\text{Si}/\text{Al})_{\text{nmr}}$ ratio was significantly greater than was the $(\text{Si}/\text{Al})_{\text{chem}}$ ratio. This is because the $(\text{Si}/\text{Al})_{\text{nmr}}$ value is the ratio of silicon to aluminium atoms in tetrahedral positions in the framework. As hydrolysis occurs, aluminium is removed from the framework but remains as octahedrally coordinated species in the channels and cages of the zeolite. The chemical analysis does not of course differentiate between framework and non-framework aluminium so the $(\text{Si}/\text{Al})_{\text{chem}}$ ratio only begins to increase as aluminium ions are extracted from the zeolite by acid solution. Again, the intensities of the Si(1Al) and Si(0Al) signals increased, at the expense of Si(2Al) and Si(3Al), with increasing dealumination.

A possible explanation for the unusual trend in the $(\text{Si}/\text{Al})_{\text{nmr}}$ ratios seen in the ^{27}Al masnmr data from Prof. Freude in Leipzig, is that the observation may be caused by an instrumental effect. As the cation and water content changes, the permittivity of the zeolite changes from sample to sample. This may result in the spectrometer instrumentation not remaining in tune with the masnmr

signal, causing errors in the measurement of the resonance peaks. However, the magnitude of the change in $(\text{Si}/\text{Al})_{\text{nmr}}$ ratios between samples is too large to be explained solely in these terms. At this stage, interpretation of the ^{27}Al masnmr data must be made with caution, but the results cannot be dismissed.

Tentative explanations for the discrepancy between the ^{27}Al and ^{29}Si masnmr data have been put forward and further work is suggested to examine these theories. These explanations are summarised below.

Acid attack of the zeolite will result in framework destruction, initially on the external surfaces of the crystallites. The effect of this will be to leave areas of crystalline material which are covered by amorphous silica. If ^{29}Si masnmr only detects signals from silicon atoms in those parts of the material which retain their crystalline integrity whereas ^{27}Al masnmr detects tetrahedrally coordinated aluminium atoms (not necessarily structural) throughout the structure, then this may explain the differences in the results obtained by the two techniques. To test this hypothesis, ^{29}Si masnmr spectra of acid treated zeolites should be measured using much longer times between pulses in order to detect amorphous silica, which may be formed in the samples. Klinowski, Carpenter and Thomas (1986) have shown recently that spin-lattice relaxation times of masnmr spectra of zeolites recorded

under oxygen are reduced by a factor of 100 in comparison with air. This method could be used to detect amorphous silica quantitatively, without greatly increasing the acquisition time of the spectra. ~

As aluminium is extracted from the zeolite lattice, "hydroxyl nests" will be formed in the vacancy positions in the framework. Corresponding ^{29}Si "vacancy peaks" occur at near identical chemical shifts in the masnmr spectra, i.e. they are to be found under existing $\text{Si}(\text{nAl})$ peaks. For example, a silicon atom joined via oxygen bridges to three silicon and one aluminium atom has almost the same chemical shift as a silicon atom where the $-\text{O}-\text{Al}$ linkage had been replaced by a hydroxyl group. $^1\text{H}-^{29}\text{Si}$ cross-polarisation techniques which allow the observation only of those silicon atoms which are close to a hydroxyl group (Klinowski, Fyfe and Gobbi, 1985) could be used to check out this possibility.

Careful studies of acid treated zeolites using both ^{27}Al and ^{29}Si masnmr and the techniques described above should be carried out to resolve this ambiguity.

sample meq.hg ⁻¹				measured signal intensities (%)		²⁹ Si chemical shifts (ppm)			
No.	Na	K	(Si/Al) _{chem}	(Si/Al) _{nmr}	Si(3Al)	Si(2Al)	Si(1Al)	Si(0Al)	Si(3Al) Si(2Al) Si(1Al) Si(0Al)
1	312	-	2.58	2.52	10.4	48.1	31.5	10.1	-88.9 -94.7 -100.6 -105.2
2	59	87	2.79	2.77	8.3	41.3	36.8	13.6	-89.2 -94.6 -100.3 -105.4
3	33	-	3.51	3.18	6.8	33.8	37.8	21.7	-89.2 -93.3 -101.8 -105.6

sample No.	Al (%)	Al removed p.u.c.	measured signal intensities (%)		%Al content		²⁷ Al chemical shift (ppm)	
			tetrahedral	octahedral	tet.	oct.	tot.	tetrahedral octahedral
1	8.41	-	100.0	0.0	6.1	0.0	6.1	60.3 0
2	7.73	3.1	87.6	12.4	4.5	0.64	5.1	60.6 0
3	5.30	11.2	82.9	17.1	3.1	0.63	3.7	60.8 0

Table 4.21: ²⁷Al and ²⁹Si masnmr data for acid treated Na-K Zeolite Y (Grace).
 Analysis courtesy of [REDACTED], Unilever Research.

sample No.	initial		final pH	% composition			Al removed		(Si/Al) _{chem}	(Si/Al) _{nmr}
	pH			H ₂ O	Na	K	p.u.c.			
1	-	-	-	26.08	9.42	-	-	2.58	-	-
2	5.5	6.73		23.01	2.02	8.59	0.0	2.58		4.24
3	4.0	6.60		22.75	2.05	8.75	0.0	2.58		4.38
4	3.0	5.70		23.20	1.89	8.14	0.0	2.58		5.01
5	2.6	4.43		23.62	1.93	7.58	<0.1	2.58		4.42
6	2.3	3.91		24.69	1.75	6.57	0.2	2.59		3.82
7	2.2	3.78		25.02	1.74	5.97	0.3	2.60		3.31
8	2.1	3.65		25.90	1.74	5.22	0.6	2.62		3.23
9	2.0	3.52		26.55	1.64	4.66	1.3	2.67		3.30

Table 4.22: Chemical and ²⁷Al masnmr data for acid treated Na-K Zeolite Y (Grace).
masnmr analysis courtesy of [REDACTED], Karl Marx University, Leipzig.

sample code	initial pH	final pH	% composition			Al removed p.u.c.	(Si/Al) _{chem}
			H ₂ O	Na	K		
NaY	-	-	26.08	9.42	-	-	2.58
K1	4.0	6.22	22.89	2.39	11.47	0.0	2.58
K2	3.0	4.44	22.61	2.31	11.04	0.0	2.58
K3	2.6	3.69	24.03	2.14	9.35	0.1	2.58
K4	2.2	3.34	25.76	2.18	7.14	1.0	2.65
K5	2.0	3.13	27.47	1.92	5.47	3.3	2.81
H1	4.0	5.49	25.13	9.40	-	0.0	2.58
H2	3.0	5.26	25.23	7.85	-	0.0	2.58
H3	2.6	5.26	26.31	7.85	-	0.0	2.58
H4	2.2	4.08	27.79	5.30	-	0.0	2.58
H5	2.0	2.78	29.48	3.25	-	1.0	2.65

Table 4.23: Chemical Analyses of Zeolite Y (Grace) ²⁹Si masnmr Samples.

sample code	<u>measured signal intensities (%)</u>				<u>²⁹Si chemical shifts (ppm)</u>					
	Si(3Al)	Si(2Al)	Si(1Al)	Si(0Al)	(Si/Al) _{chem}	(Si/Al) _{nmr}	Si(3Al)	Si(2Al)	Si(1Al)	Si(0Al)
NaY	12.0	40.1	38.8	9.1	2.58	2.58	-90.0	-95.0	-100.6	-106.0
K1	10.8	39.6	40.1	9.5	2.58	2.64	-89.9	-94.9	-100.4	-105.7
K2	10.2	40.8	39.1	9.9	2.58	2.64	-90.1	-95.1	-100.3	-105.5
K3	9.6	38.4	43.0	9.0	2.58	2.69	-89.3	-94.8	-100.4	-105.8
K4	6.7	37.9	42.6	12.9	2.65	2.89	-89.5	-94.9	-100.6	-105.0
K5	7.8	33.3	47.0	11.9	2.81	2.92	-89.4	-94.6	-100.0	-105.5
H1	12.9	38.2	41.3	7.5	2.58	2.55	-89.1	-94.3	-99.6	-105.3
H2	12.9	36.7	42.4	7.9	2.58	2.56	-89.1	-94.3	-99.8	-104.7
H3	11.7	38.3	41.6	7.3	2.58	2.61	-88.7	-94.1	-99.6	-104.8
H4	10.1	37.4	43.6	8.3	2.58	2.69	-89.1	-94.3	-99.8	-105.4
H5	8.6	35.0	44.3	8.9	2.65	2.85	-89.3	-94.4	-100.1	-105.4

Table 4.24: ²⁹Si masnmr data for acid treated Na-K zeolite Y (Grace); see also table 4.23.
Analyses courtesy of [REDACTED], Unilever Research.

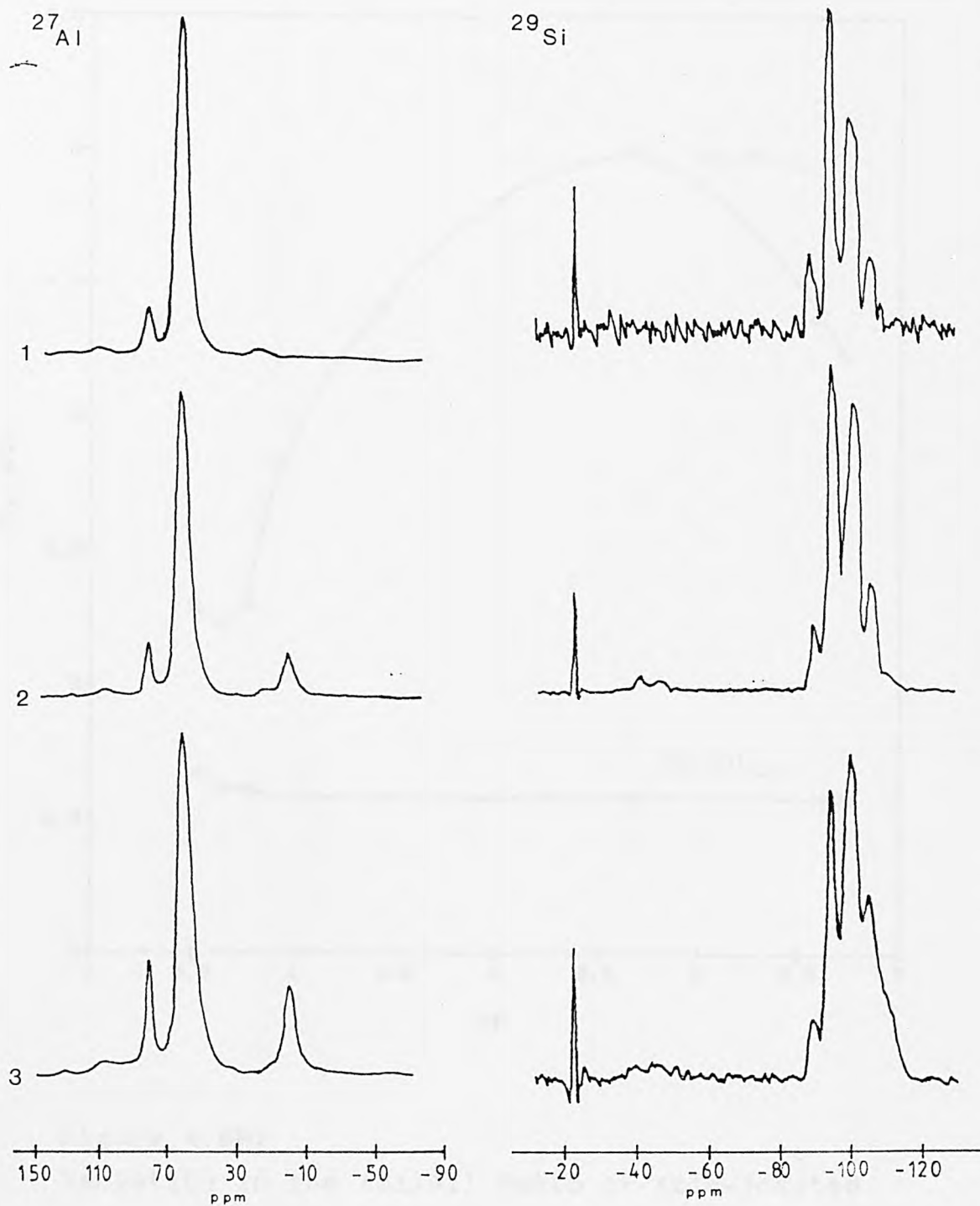


Figure 4.85:
 ^{27}Al & ^{29}Si MASNMR Spectra of Acid-Treated
 Zeolite Y (Grace) Samples.

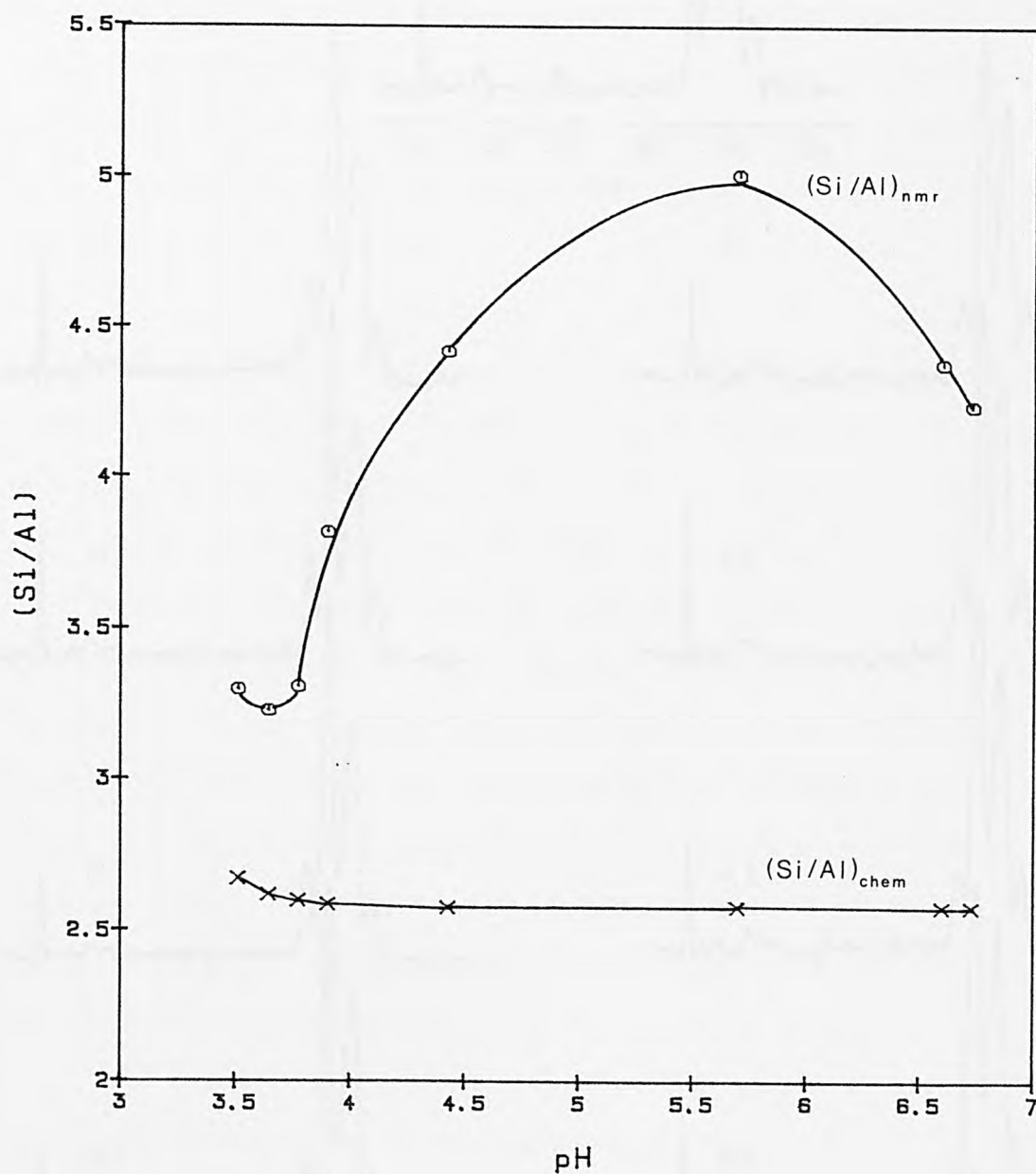


Figure 4.86:

Variation in the (Si/Al) Ratio of Acid-Treated Zeolite Y (Grace) Samples With Final Solution pH.



Figure 4.87:
 ^{29}Si MASNMR Spectra of NaH-Y & NaH-Y (Grace) Samples.

5. CONCLUSION.

The results of this study suggest that the ion-exchange properties of zeolites X and Y make these materials favourable as slow release ammonium and potassium fertilizers. However, several other factors must also be taken into consideration.

In a soil environment the release of ammonium and potassium from the zeolite would be controlled by exchange with ions already present in the soil solution, or introduced through irrigation water. The cations most likely to be involved in this process are sodium, calcium and magnesium. The results presented in this thesis have shown that the exchange of hydronium ions is also significant even in water with a neutral or only slightly acidic pH. This reaction would be of importance, for example, when using a growing medium composed of a soil-less compost, and irrigating with water largely free of cations, as would be the case with rain water.

The resistance of the zeolite to acid attack and hydrolysis in the soil is obviously also an important factor in determining its suitability as a fertilizer material. Breakdown of the zeolite would not only release the store of potassium and ammonium in an uncontrolled way, but the liberation of soluble aluminium species could have a catastrophic effect on plant growth. Aluminium in low

levels is thought to be harmless but at higher concentrations the element is toxic to higher plants. Excessive aluminium interferes with cell division in plant roots; fixes phosphorus in less available forms in soils and in plant roots; interferes with certain enzymes governing the deposition of polysaccharides in cell walls; increases cell wall rigidity by cross-linking with pectins; and interferes with the uptake, transport and assimilation of several elements (calcium, magnesium and phosphorus) and water by plants (Follet, Murphy and Donahue, 1981; Tisdale, Nelson and Beaton, 1984).

On a very large scale, the presence of aluminium in the environment is currently the cause of a great deal of concern. There is much documented evidence to show that the acidification of inland waters in Western Europe, Scandanavia and the United States has been progressing at an alarming rate over the last 120 years (Seip and Tollan, 1978). It is widely believed that acid precipitation, which is caused by the combustion of fossil fuels in power stations, factories and motor cars, is responsible for the acidification of rivers and lakes (Seip and Tollan, 1978; Cronan and Schofield, 1979). An alternative view was put forward by Rosenqvist (1978). Rosenqvist argued that acid rain is only a minor factor, the major cause of acidity in run-off waters being due to changes in land use, with increasing mechanisation and usage of chemical fertilizers in modern agricultural practice. [REDACTED] [REDACTED] and her

co-workers at Imperial College in London have even suggested recently (Pearce, 1986) that the formation of acid rain is accelerated by ammonia given off from animal wastes produced in intensive farming. High concentrations of ammonia in the air seem to speed up the rate of oxidation of sulphur dioxide given off by power stations burning fossil fuels. The gas oxidises to form sulphate ions which, it is thought, play a key role in acidifying soils and surface waters.

Whatever the ultimate source of the acidity, it is ion-exchange and chemical processes in the soil which are of upmost importance in determining the environmental effects. It is becoming clear that it is aluminium liberated from soils by acid waters which is the true toxin responsible for the wide scale destruction of trees in West Germany and Scandanavia, in much the same way as it is now known to poison fish (Noggle et al, 1984; Andelman and Miller, 1986; Tam and Williams, 1986).

This study has shown that zeolites X and Y are resistant to large scale destruction of the aluminosilicate framework at acid pH's which in a soil environment would be extreme. Any aluminium removed from the lattice appears to be retained within the channels and cages of the zeolite and is only released when the pH of the external solution falls to a relatively low value. The long term stability of zeolites X and Y in a mildly acidic environment has,

however, not been investigated. In view of the environmental problems of aluminium in soils outlined above, it is not envisaged that synthetic faujasite zeolite fertilizers would be appropriate for use in large scale agricultural situations; also this is not likely to be feasible economically. From a chemical point of view it is predicted that zeolites X and Y could find considerable potential as slow release ammonium and potassium fertilizers in other contexts. These contexts are likely to be in the production of high value greenhouse cash crops and in horticulture. Zeolites would seem to be ideally suited to provide a relatively long term nutritive reservoir in potting composts and for nursery-produced pot plants. Further evaluation of zeolites X and Y is now necessary through greenhouse experiments and it must be stressed that the economic value of these materials has yet to be determined.

6. REFERENCES.

- Alberti, A. (1975).
Min. Petr. Milt., 22, 25.
- Allen, H.E., Cho, S.H. & Neubecker, T.A. (1983).
Water Res., 17, 1871.
- Ames, L.L. (1960).
Am. Mineral., 45, 689.
- Andelman, J.B. & Miller, J.R. (1986).
Water Qual. Bull., 11, 19.
- Argesinger, J.W., Davidson, A.W. & Bonner, O.D. (1950).
Trans. Kansas. Acad. Sci., 53, 404.
- Arnon, D.I. & Stout, P.R. (1939).
Plant Physiol., 14, 371.
- Barbarick, K.A. & Pirela, H.J. (1984).
In "Zeo-Agriculture. Use of Natural Zeolites in Agriculture and Aquaculture." (Eds. Pond, W.G. & Mumpton, F.A.).
Westview Press, Boulder, Colorado.
- Barrer, R.M. (1978).
"Zeolites and Clay Minerals as Sorbents and Molecular Sieves." Academic Press, London.
- Barrer, R.M., Davies, J.A. & Rees, L.V.C. (1968).
J. Inorg. Nucl. Chem., 31, 2599.
- Barrer, R.M. & Falconer, J. (1956).
Proc. R. Soc. London, Ser. A., 236, 227.
- Barrer, R.M. & Klinowski, J. (1972).
J. Chem. Soc., Faraday Trans. 1., 68, 1956.
- Barrer, R.M. & Klinowski, J. (1974).
J. Chem. Soc., Faraday Trans. 1. 70, 2080.
- Barrer, R.M. & Klinowski, J. (1975).
J. Chem. Soc., Faraday Trans. 1., 71, 690.
- Barrer, R.M. & Klinowski, J. (1977).
Philos. Trans. R. Soc., London, 285, 637.
- Barrer, R.M. & Klinowski, J. & Sherry, H.S. (1973).
J. Chem. Soc., Faraday Trans. 2. 67, 1669.
- Barrer, R.M. & Munday, B.M. (1971).
J. Chem. Soc. (A), 2909.

- Barrer, R.M., Rees, L.V.C. & Shamsuzzoha, M. (1966).
J. Inorg. Nucl. Chem., 28, 629.
- Barrer, R.M. & Sammon, D.C. (1955).
J. Chem. Soc., 2838.
- Barrer, R.M. & Townsend, R.P. (1976).
J. Chem. Soc., Faraday Trans. 1., 72, 661.
- Barrer, R.M. & Townsend, R.P. (1984).
J. Chem. Soc., Faraday Trans. 2., 80, 629.
- Barri, S.A.I. & Rees, L.V.C. (1980).
J. Chromatogr., 201, 21.
- Barrow, G.M. (1973).
"Physical Chemistry."
McGraw-Hill Kagakosha Ltd., Tokyo.
- Bartz, J.K. & Jones, R.L. (1983).
Soil Sci. Soc., Am. J., 47, 259.
- Baur, W.H. (1964).
Amer. Mineral., 49, 697.
- Beagley, B., Dwyer, J. & Ibrahim, T.K. (1978).
J. Chem. Soc., Chem. Commun., 12, 493.
- Bell, P. & Coombe, D. (1965).
"Strasburger's Textbook of Botany."
Longman Group Ltd., London.
- Bonner, J. & Varner, J.E. (1976).
"Plant Biochemistry."
Academic Press Inc., London.
- Breck, D.W. (1974).
"Zeolite Molecular Sieves."
Wiley Interscience, New York.
- Breck, D.W., Eversole, W.G., Milton, R.M., Reed, T.B.
& Thomas, T.L. (1956). J. Am. Chem. Soc., 78, 5963.
- Broussard, L. & Shoemaker, D.P. (1960).
J. Am. Chem. Soc., 82, 1041.
- Burrisci, N., Valente, S., Ottana, R., Cimino, G.
& Zipelli, C. (1984). Zeolites, 4, 5.
- Charnell, J.F. (1971).
J. Crystal Growth., 8, 291.
- Chelischev, N.F., Martynova, N.S. (1974).
Dokl. Akad. Nauk. SSSR, 217, 1140.

- Chu, P. & Dwyer, F.G. (1983).
Zeolites, 3, 72.
- Cook, T.E., Cilley, W.A., Savitsky, A.C.
& Wiers, B.H. (1982). Environ. Sci. Technol., 16, 344.
- Cronan, C.S. & Schofield, C.L. (1979).
Science, 204, 304.
- Dempsey, E., Kuhl, G.H. & Olson, D.H. (1969).
J. Phys. Chem., 73, 387.
- Drummond, D., de Jong, A. & Rees, L.V.C. (1983).
J. Phys. Chem., 87, 1967.
- Dyer, A. (1984).
Chem. Ind. (London) 241.
- Flanigen, E.M. (1980).
In "Proc. 5th Int. Conf. Zeolites." (Ed. Rees, L.V.C.).
Heyden & Son Ltd., London.
- Fletcher, P. (1979).
Ph.D. Thesis. The City University, London.
- Fletcher, P. & Townsend, R.P. (1980).
J. Chromatogr., 201, 93.
- Fletcher, P. & Townsend, R.P. (1982).
J. Chem. Soc., Faraday Trans. 1, 78, 1741.
- Fletcher, P. & Townsend, R.P. (1985).
J. Chem. Soc., Faraday Trans. 1., 81, 1731.
- Follet, R.H., Murphy, L.S. & Donahue, R.L. (1981).
"Fertilizers and Soil Amendments."
Prentice-Hall Inc.
- Freude, D., Folich, T., Pfeifer, H. & Scheler, G. (1983).
Zeolites, 3, 171.
- Freude, D., Hasse, J., Pfeifer, H. & Prager, D. (1985).
Chem. Phys. Lett., 114, 143.
- Franklin, K.R. (1984).
PhD. Thesis. The City University, London.
- Franklin, K.R., Townsend, R.P., Whelan, S.J.
& Adams, C.J. (1986). In "Proc. 7th Int. Conf. Zeolites."
(Eds. Murakami, Y., Lijima, A. & Ward, J.W.).
Kodansha Ltd., Tokyo.
- Freude, D. (1986).
Private Communication.

- Fyfe, C.A., Gobbi, C.G., Hartman, J.S., Klinowski, J. & Thomas, J.M. (1982). J. Phys. Chem., 86, 1247.
- Gaines, G.L. & Thomas, H.G. (1953). J. Phys. Chem., 21, 714.
- Gapon, Y.N. (1933). J. Gen. Chem. (USSR), 3, 144.
- Glueckauf, E. (1949). Nature, 163, 414.
- Goldsberry, K.L. (1984). In "Zeo-Agriculture. Use of Natural Zeolites in Agriculture and Aquaculture." (Eds. Pond, W.G. & Mumpton, F.A.). Westview Press, Boulder, Colorado.
- Harned, H.S. & Davis, R. (1943). J. Am. Chem. Soc., 65, 2030.
- Harned, H.S. & Scholes, S.R. (1941). J. Am. Chem. Soc., 63, 1706.
- Hershey, D.R., Paul, J.L. & Carlson, R.M. (1980). Hort. Sci., 15, 87.
- Hirschfelder, J.O., Curtiss, C.F. & Bird, R.B. (1954). "Molecular Theory of Gases and Liquids." John Wiley and Sons, New York.
- Hogfeldt, E., Ekedahl, E. & Sillen, L.G. (1950). Acta Chem. Scand., 4, 828.
- Howery, D.G. & Thomas, H.C. (1965). J. Phys. Chem., 69, 531.
- Kanavirez, V. & Borisova, N. (1982). Zeolites, 2, 23.
- King, L.J., Campell, D.O., Collins, E.D., Knauer, J.B. & Wallace, R.M. (1984). In "Proc. 6th Int. Conf. Zeolites." (Eds. Olson, D. & Bisio, A.). Butterworths, London.
- Keller, I. & Jones, R.L. (1980). In "Adsorption and Ion-Exchange with Synthetic Zeolites." (Ed. Flank, W.H.). Washington: American Chemical Society, 135, 275.
- Kenney, C.N. & Kirkby, N.F. (1984). In "Zeolites: Science and Technology." (Eds. Ribeiro, F.R., Rodrigues, A.E., Rollman, L.D. & Naccache, C.). NATO ASI Series, Martinus Nijhoff, The Hague.

- Kent, J.A. (1983).
"Riegel's Handbook of Industrial Chemistry."
Van Nostrand Reinhold Co.
- Kerr, G.T. (1973).
in "Molecular Sieves." Advances in Chemistry Series, 121.
Am. Chem. Soc., Washington D.C.
- Klinowski, J., Carpenter, T.A. & Thomas, J.M. (1986).
J. Chem. Soc., Chem. Commun., 956.
- Klinowski, J., Fyfe, C.A. & Gobbi, G.C. (1985).
J. Chem. Soc., Faraday Trans 1., 81, 3003.
- Klinowski, J. & Thomas, J. (1986).
Endeavour, New Series, 10, 2.
- Klinowski, J., Ramdas, S., Thomas, J.M., Fyfe, C.A.
& Hartman, J.S. (1982).
J. Chem. Soc., Faraday Trans. 2., 78, 1025.
- Kroes, W.H. (1980).
Hydrobio. Bull., 14, 90.
- Kuhl, G.H. (1985).
Zeolites, 5, 4.
- Kuhl, G.H. & Sherry, H.S. (1980).
In "Proc. 5th Int. Conf. Zeolites."
(Ed. Rees, L.V.C.). Heyden, London.
- Lai, P.P. & Rees, L.V.C. (1976).
J. Chem. Soc., Faraday Trans. 1., 72, 1809.
- Lee, E.F.T. & Rees, L.V.C. (1986a).
Paper Submitted to J. Chem. Soc., Faraday Trans. 1.
Quoted with permission from the authors.
- Lee, E.F.T. & Rees, L.V.C. (1986b).
Paper Submitted to Zeolites.
Quoted with permission from the authors.
- Lewis, M.D., Moore, F.D. & Goldsberry, K.L. (1984).
In "Zeo-Agriculture. Use of Natural Zeolites in Agriculture
and Aquaculture." (Eds. Pond, W.G. & Mumpton, F.A.).
Westview Press, Boulder, Colorado.
- Li, C.Y. & Rees, L.V.C. (1986).
Zeolites, 6, 51.
- Loewenstein, W. (1954).
Am. Mineral, 39, 92.
- Loizidou, M. (1982).
PhD. Thesis. The City University, London.

- McDaniel, C.V. & Maher, P.K. (1976).
in "Zeolite Chemistry and Catalysis." (Ed. Rabo, J.A.)
A.C.S. Monograph, 171, 285.
- Maes, A., Verlinden, J. & Cremers, A. (1978).
J. Chem. Soc., Faraday Trans. 1., 73, 440.
- Magee, J.S. & Blazek, J.J. (1976).
In "Zeolite Chemistry and Catalysis." (Ed. Rabo, J.A.)
A.C.S. Monograph, 171, 285.
- Marion, G.M., Hendricks, D.M., Dutt, G.R.
& Fuller, W.H. (1976). Soil Sci., 121, 76.
- Marschner, H. (1983).
"Encyclopedia of Plant Physiology." (Eds. Lauchli, A. &
Bielski, R.L.). Springer-Verlag.
- Mortier, J.W. (1982).
"Compilation of Extra Framework Sites in Zeolites."
Butterworths, London.
- Mortier, J.W. & Bosmans, H.J. (1971).
J. Phys. Chem., 75, 3327.
- Muller, G. (1979).
Materialen, 4, 95.
- Mumpton, F.A. (1984).
In "Zeo-Agriculture. Use of Natural Zeolites in Agriculture
and Aquaculture." (Eds. Pond, W.G. & Mumpton, F.A.).
Westview Press, Boulder, Colorado.
- Murphy, C.B., Hyrck, O. & Gleason, W.T. (1978).
In "Natural Zeolites, Occurrence, Properties and Use."
Pergamon Press, Oxford.
- Nightingale, E.R. (1959).
J. Phys. Chem., 63, 1381.
- Nishita, H. & Haug, R.M. (1972).
Soil Sci., 114, 149.
- Noggle, J.C., Jones, H.C., Joslin, J.D., Garber, R.W.,
Kelley, J.M., Olem, H. & Brewer, P.F. (1984).
Proc.-APCA Annu. Meet., 77, 84.
Chem. Abs. 102, 154,432.
- O'Connor, J.F. & Townsend, R.P. (1985).
Zeolites, 5, 158.
- Olson, D.H. (1970).
J. Phys. Chem., 74, 2578.
- Parakrama, R. (1983).
PhD. Thesis. The City University, London.

- Pauling, L. (1960).
"The Nature of the Chemical Bond."
Cornell University Press.
- Pearce, F. (1986).
New Scientist, 23 October, p20.
- Pekarek, V. & Vesely, V. (1972).
Talanta, 19, 1245.
- Pirela, H., Westfall, D.G. & Barbarick, K.A. (1984).
In "Zeo-Agriculture. Use of Natural Zeolites in Agriculture
and Aquaculture." (Eds. Pond, W.G. & Mumpton, F.A.).
Westview Press, Boulder, Colorado.
- Rees, L.V.C. (1984).
Chem. Ind. (London) 252.
- Rees, L.V.C. & Zuyi, T. (1986).
Zeolites 6, 201.
- Reid, R.C. & Sherwood, T.K. (1958).
"Properties of Gases and Liquids."
McGraw-Hill, New York.
- Robinson, R.A. & Stokes, R.H. (1970).
"Electrolyte Solutions."
Butterworths, London.
- Rosengqvist, I., Th. (1978).
Sci. Total Environ., 10, 39.
- Sand, L.B. & Mumpton, F.A. (1978).
"Natural Zeolites, Occurrence, Properties and Use."
Pergamon Press, Oxford.
- Seip, H.M. & Tollen, A. (1978).
Sci. Total Environ., 10, 253.
- Semmens, M.J. (1980).
In "Proc. 5th Int. Conf. Zeolites."
(Ed. Rees, L.V.C.). Heyden, London.
- Schwuger, M.J. & Smolka, H.G. (1977).
Colloid, Polym. Sci., 254, 1062.
- Sherry, H.S. (1966).
J. Phys. Chem., 70, 1158.
- Sherry, H.S. (1968a).
J. Phys. Chem., 72, 4086.
- Sherry, H.S. (1968b).
J. Colloid Interface, Sci., 28, 288.

- Sherry, H.S. (1969).
In "Ion-Exchange: A Series of Advances."
Marcel-Dekker, New York, 2, 89.
- Sherry, H.S. (1976).
Colloid Interface Sci., 5, 321.
- Sherry, H.S. & Walton, H.F. (1967).
J. Phys. Chem., 71, 1457.
- Smith, J.V. (1963).
Amer. Mineral Soc., Spec. Paper 1, 281.
- Sposito, G. (1981).
A.S.A. Spec. Pub., 40, 13.
- Sposito, G., Holtzclaw, K.M., Charlet, L., Jouany, C.
& Page, A. (1983). Soil Sci. Soc., Am. J. 47, 51.
- Sposito, G., Holtzclaw, K.M., Johnston, C.T.
& Levesque-Madore, C.S. (1981).
Soil Sci. Soc., Am. J., 45, 1079.
- Sposito, G. & Mattigod, S.V. (1979).
Clays Clay Miner., 27, 125.
- Tam, S.C. & Williams, R.J.P. (1986).
J. Inorg. Biochem., 26, 35.
- Theng, B.K.G., Vansant, E. & Uytterhoeven, J.B. (1968).
Trans. Faraday Soc., 64, 3370.
- Tisdale, S.L., Nelson, W.L. & Beaton, J.D. (1985).
"Soil Fertility and Fertilizers."
Macmillan Publishing Company, New York.
- Torri, K. (1978).
in "Natural Zeolites, Occurrence, Properties and Use."
(Eds. Sand, L.B. & Mumpton, F.A.). Pergamon Press, Oxford.
- Townsend, R.P. (1977).
D.I.C. Thesis, Imperial College, London.
- Townsend, R.P. (1984).
Chem. Ind. (London) 246.
- Townsend, R.P. (1986).
In "Proc. 7th Int. Conf. Zeolites."
(Eds. Murakami, Y., Lijima, A. & Ward, J.W.).
Kodansha Ltd., Tokyo.
- Townsend, R.P., Franklin, K.R. & O'Connor, J.F. (1984).
Adsorption Sci. Technol., 1, 269.

Townsend, R.P. & Loizidou, M. (1984).
Zeolites, 4, 191.

Townsend, R.P.T., Fletcher, P. & Loizidou, M.
In "Proc. 6th Int. Conf. Zeolites." (Eds. Olson, D.
& Bisio, A.). Butterworths, London.

Valente, S., Burriesci, N., Cavallaro, S., Galvagno, S.
& Zipelli, C. (1982). Zeolites, 2, 271.

Vanselow, A.P. (1932).
J. Am. Chem. Soc., 54, 1307.

Vaughan, D.E.W. (1980).
In "Properties and Applications of Zeolites".
Special Publication No. 33, Chem. Soc., London.

Vogel, A. (1974).
"Textbook of Quantitative Inorganic Analysis."
Longmans, London.

Ward, J. (1983).
Paper Presented at B.Z.A. Annual Meeting, U.M.I.S.T.

APPENDIX 1.

Equilibrium Ion-Exchange Data.

Na - K Exchange in Y (Laporte) at 25°C. 1 Week Exchange, Normal pH.

Solution Total Normality = 0.050 mol dm⁻³

Exchange Capacity (in terms of Al) = 285.1 mequiv 100g⁻¹

	pH	m _K	m _{Na}	m _{K+mNa}	M _K	M _{Na}	M _{K+MNa}
1	6.59	0.00	50.29	50.29	0.0	250.9	250.9
2	6.45	0.00	50.94	50.94	0.0	251.4	251.4
3	6.55	1.61	48.52	50.13	26.4	232.5	258.9
4	6.39	1.66	49.01	50.67	26.4	233.2	259.6
5	6.50	3.14	46.91	50.05	45.7	218.4	264.1
6	6.45	3.20	48.38	51.58	44.3	212.5	256.8
7	6.58	4.84	45.94	50.78	64.1	200.9	265.0
8	6.42	4.90	45.98	50.88	62.5	184.9	247.4
9	6.43	6.50	43.51	50.01	76.5	192.2	268.7
10	6.54	6.64	43.87	50.51	75.5	192.2	267.7
11	6.49	8.51	41.86	50.37	95.8	176.8	272.6
12	6.39	8.53	41.23	49.76	91.7	174.2	265.9
13	6.35	11.97	37.18	49.15	119.7	155.8	275.5
14	6.43	12.20	36.09	48.29	117.0	153.8	270.8
15	6.34	10.72	39.10	49.82	114.9	164.8	279.7
16	6.43	10.62	39.14	49.76	114.8	166.3	281.1
17	6.40	14.48	32.49	46.97	125.4	141.4	266.8
18	6.26	14.64	35.33	49.97	130.2	149.0	279.2
19	6.28	17.06	33.72	50.78	134.3	133.9	268.2
20	6.31	17.06	33.34	50.40	132.7	136.3	269.0
21	6.30	18.58	30.77	49.35	145.6	127.8	273.4
22	6.18	18.99	31.36	50.35	150.3	130.9	281.2
23	6.19	20.80	30.13	50.93	161.5	125.2	286.7
24	6.24	21.28	30.06	51.34	145.6	112.2	257.8
25	6.45	23.53	27.61	51.14	162.2	113.9	276.1
26	6.19	23.70	27.52	51.22	168.4	116.7	285.1
27	6.32	24.83	24.70	49.53	171.0	107.8	278.8
28	6.14	26.23	24.28	50.51	173.9	100.1	274.0
29	6.30	26.31	24.06	50.37	174.7	100.5	275.2
30	6.24	26.41	24.70	51.11	169.2	107.8	277.0
31	6.27	29.95	22.09	52.04	184.4	90.0	274.4
32	6.23	30.29	22.58	52.87	177.4	90.0	267.4
33	6.40	32.37	20.05	52.42	195.1	89.3	284.4
34	6.16	33.76	17.41	51.17	202.2	79.8	282.0
35	6.32	33.97	17.27	51.24	188.9	79.8	268.7
36	6.19	33.97	20.05	54.02	186.3	86.2	272.5
37	6.24	35.79	16.23	52.02	203.8	76.9	280.7
38	6.24	36.23	16.18	52.41	201.6	71.5	273.1
39	6.20	38.71	14.14	52.85	212.2	67.2	279.4
40	6.31	35.46	14.54	50.00	214.8	71.5	286.3

m_K, m_{Na} solution phase concentration / mequiv dm⁻³

M_K, M_{Na} zeolite phase concentration / mequiv 100g⁻¹

	E_K	$K_{M,E}$	$\gamma_{\pm R\bar{R}}$	$\gamma_{\pm B\bar{B}}$	$\ln \Gamma$	$\ln K_H$
1	0.0000	—	0.8065	0.8129	0.0159	0.0159
2	0.0000	—	0.8065	0.8129	0.0157	0.0157
3	0.1020	3.4220	0.8062	0.8127	0.0160	1.2462
4	0.1017	3.3424	0.8063	0.8127	0.0158	1.2225
5	0.1730	3.1261	0.8060	0.8125	0.0160	1.1558
6	0.1726	3.1532	0.8062	0.8125	0.0155	1.1639
7	0.2419	3.0285	0.8059	0.8123	0.0157	1.1238
8	0.2525	3.1698	0.8059	0.8123	0.0157	1.1694
9	0.2847	2.6640	0.8056	0.8121	0.0160	0.9958
10	0.2820	2.5953	0.8056	0.8120	0.0158	0.9695
11	0.3514	2.6653	0.8054	0.8118	0.0159	0.9962
12	0.3449	2.5444	0.8053	0.8118	0.0161	0.9500
13	0.4345	2.3864	0.8048	0.8113	0.0163	0.8861
14	0.4321	2.2504	0.8046	0.8113	0.0165	0.8276
15	0.4108	2.5430	0.8050	0.8115	0.0161	0.9494
16	0.4084	2.5442	0.8050	0.8115	0.0161	0.9499
17	0.4700	1.9899	0.8042	0.8110	0.0170	0.7050
18	0.4663	2.1088	0.8045	0.8110	0.0160	0.7621
19	0.5007	1.9825	0.8043	0.8107	0.0157	0.7001
20	0.4933	1.9027	0.8043	0.8107	0.0159	0.6591
21	0.5326	1.8867	0.8039	0.8105	0.0162	0.6511
22	0.5345	1.8961	0.8040	0.8104	0.0159	0.6557
23	0.5633	1.8685	0.8039	0.8102	0.0157	0.6409
24	0.5648	1.8331	0.8039	0.8101	0.0156	0.6216
25	0.5875	1.6710	0.8035	0.8098	0.0156	0.5290
26	0.5907	1.6756	0.8035	0.8098	0.0156	0.5318
27	0.6133	1.5780	0.8032	0.8097	0.0161	0.4723
28	0.6347	1.6081	0.8031	0.8095	0.0158	0.4909
29	0.6348	1.5897	0.8031	0.8095	0.0159	0.4794
30	0.6108	1.4679	0.8032	0.8095	0.0156	0.3995
31	0.6719	1.5107	0.8028	0.8090	0.0153	0.4279
32	0.6634	1.4689	0.8029	0.8090	0.0151	0.3996
33	0.6860	1.3534	0.8026	0.8087	0.0152	0.3178
34	0.7170	1.3069	0.8022	0.8085	0.0156	0.2832
35	0.7030	1.2036	0.8022	0.8085	0.0156	0.2009
36	0.6837	1.2756	0.8026	0.8085	0.0147	0.2581
37	0.7260	1.2017	0.8021	0.8083	0.0154	0.1990
38	0.7381	1.2587	0.8021	0.8082	0.0152	0.2453
39	0.7594	1.1529	0.8018	0.8079	0.0151	0.1574
40	0.7503	1.2318	0.8019	0.8083	0.0160	0.2245

	$E_{K, \mu}$	$E_{N, \mu}$	E_K	E_N	α	$\%H_{\mu, \mu}$
1	0.0000	1.0000	0.0000	1.0000	—	12.00
2	0.0000	1.0000	0.0000	1.0000	—	11.82
3	0.0321	0.9679	0.1020	0.8980	3.4220	9.19
4	0.0328	0.9672	0.1017	0.8983	3.3424	8.94
5	0.0627	0.9373	0.1730	0.8270	3.1261	7.37
6	0.0620	0.9380	0.1726	0.8274	3.1532	9.92
7	0.0953	0.9047	0.2419	0.7581	3.0285	7.05
8	0.0963	0.9037	0.2525	0.7475	3.1698	13.24
9	0.1300	0.8700	0.2847	0.7153	2.6640	5.76
10	0.1315	0.8685	0.2820	0.7180	2.5953	6.10
11	0.1689	0.8311	0.3514	0.6486	2.6653	4.38
12	0.1714	0.8286	0.3449	0.6551	2.5444	6.73
13	0.2435	0.7565	0.4345	0.5655	2.3864	3.37
14	0.2526	0.7474	0.4321	0.5679	2.2504	5.02
15	0.2152	0.7848	0.4108	0.5892	2.5430	1.89
16	0.2134	0.7866	0.4084	0.5916	2.5442	1.40
17	0.3083	0.6917	0.4700	0.5300	1.9899	6.42
18	0.2930	0.7070	0.4663	0.5337	2.1088	2.07
19	0.3360	0.6640	0.5007	0.4993	1.9825	5.93
20	0.3385	0.6615	0.4933	0.5067	1.9027	5.65
21	0.3765	0.6235	0.5326	0.4674	1.8867	4.10
22	0.3772	0.6228	0.5345	0.4655	1.8961	1.37
23	0.4084	0.5916	0.5633	0.4367	1.8685	-0.56
24	0.4145	0.5855	0.5648	0.4352	1.8331	9.58
25	0.4601	0.5399	0.5875	0.4125	1.6710	3.16
26	0.4627	0.5373	0.5907	0.4093	1.6756	0.00
27	0.5013	0.4987	0.6133	0.3867	1.5780	2.21
28	0.5193	0.4807	0.6347	0.3653	1.6081	3.89
29	0.5223	0.4777	0.6348	0.3652	1.5897	3.47
30	0.5167	0.4833	0.6108	0.3892	1.4679	2.84
31	0.5755	0.4245	0.6719	0.3281	1.5107	3.74
32	0.5729	0.4271	0.6634	0.3366	1.4689	6.20
33	0.6175	0.3825	0.6860	0.3140	1.3534	0.25
34	0.6598	0.3402	0.7170	0.2830	1.3069	1.09
35	0.6630	0.3370	0.7030	0.2970	1.2036	5.76
36	0.6288	0.3712	0.6837	0.3163	1.2756	4.42
37	0.6880	0.3120	0.7260	0.2740	1.2017	1.54
38	0.6913	0.3087	0.7381	0.2619	1.2587	4.20
39	0.7325	0.2675	0.7594	0.2406	1.1529	1.99
40	0.7092	0.2908	0.7503	0.2497	1.2318	-0.42

Na - K Exchange in Y (Grace) at 25°C. 1 Week Exchange, Normal pH.

Solution Total Normality = 0.050 mol dm⁻³

Exchange Capacity (in terms of Al) = 311.8 mequiv 100g⁻¹

	pH	m _K	m _{Na}	m _K +m _{Na}	M _K	M _{Na}	M _K +M _{Na}
1	6.93	0.28	49.28	49.56	5.1	244.9	250.0
2	6.91	0.55	48.97	49.52	9.6	250.4	260.0
3	6.76	1.17	48.01	49.18	19.2	248.8	268.0
4	6.73	1.58	48.77	50.35	24.3	245.0	269.3
5	6.74	2.85	47.34	50.19	40.0	230.0	270.0
6	6.80	4.57	45.82	50.39	62.2	214.8	277.0
7	6.73	6.21	43.80	50.01	80.2	203.9	284.1
8	6.67	8.36	41.82	50.18	102.4	204.3	306.7
9	6.78	10.15	40.39	50.54	110.0	183.0	293.0
10	6.78	11.87	38.40	50.27	126.6	181.6	308.2
11	6.74	13.29	36.72	50.01	133.9	166.3	300.2
12	6.74	16.13	34.79	50.92	139.9	157.5	297.4
13	6.76	17.13	32.59	49.72	151.5	150.0	301.5
14	6.77	19.80	30.99	50.79	159.2	143.2	302.4
15	6.43	22.37	27.96	50.33	160.2	124.6	284.8
16	6.72	23.97	26.36	50.33	174.8	128.8	303.6
17	6.74	26.17	24.77	50.94	180.2	117.6	297.8
18	6.71	28.18	21.44	49.62	188.7	109.0	297.7
19	6.66	30.64	19.16	49.80	192.5	107.2	299.7
20	6.72	32.88	17.53	50.41	198.8	101.2	300.0
21	6.67	34.47	14.87	49.34	206.3	91.2	297.5
22	6.74	37.37	12.61	49.98	215.9	84.2	300.1
23	6.48	39.87	10.05	49.92	228.7	73.0	301.7
24	6.31	43.29	6.82	50.11	239.8	60.5	300.3
25	6.28	45.84	4.31	50.15	244.8	42.8	287.6
26	6.51	47.42	2.58	50.00	262.0	36.4	298.4
27	6.15	49.01	0.37	49.38	280.6	9.1	289.7
28	6.19	49.14	0.36	49.50	275.0	6.8	281.8
29	6.21	49.84	0.32	50.16	278.6	5.2	283.8

m_K, m_{Na} solution phase concentration / mequiv dm⁻³

M_K, M_{Na} zeolite phase concentration / mequiv 100g⁻¹

	$E_{K,s}$	$E_{Na,s}$	E_K	E_{Na}	α	$\%H_{\infty}$
1	0.0056	0.9944	0.0204	0.9796	3.6652	19.82
2	0.0111	0.9889	0.0369	0.9631	3.4135	16.61
3	0.0238	0.9762	0.0716	0.9284	3.1666	14.05
4	0.0314	0.9686	0.0902	0.9098	3.0615	13.63
5	0.0568	0.9432	0.1481	0.8519	2.8888	13.41
6	0.0908	0.9092	0.2245	0.7755	2.9008	11.16
7	0.1242	0.8758	0.2823	0.7177	2.7742	8.88
8	0.1666	0.8334	0.3339	0.6661	2.5073	1.64
9	0.2008	0.7992	0.3754	0.6246	2.3919	6.03
10	0.2361	0.7639	0.4108	0.5892	2.2553	1.15
11	0.2657	0.7343	0.4460	0.5540	2.2247	3.72
12	0.3168	0.6832	0.4704	0.5296	1.9158	4.62
13	0.3445	0.6555	0.5025	0.4975	1.9215	3.30
14	0.3898	0.6102	0.5265	0.4735	1.7400	3.01
15	0.4445	0.5555	0.5625	0.4375	1.6070	8.66
16	0.4763	0.5237	0.5758	0.4242	1.4925	2.63
17	0.5137	0.4863	0.6051	0.3949	1.4503	4.49
18	0.5679	0.4321	0.6339	0.3661	1.3171	4.52
19	0.6153	0.3847	0.6423	0.3577	1.1229	3.88
20	0.6523	0.3477	0.6627	0.3373	1.0473	3.78
21	0.6986	0.3014	0.6934	0.3066	0.9756	4.58
22	0.7477	0.2523	0.7195	0.2805	0.8655	3.76
23	0.7987	0.2013	0.7580	0.2420	0.7896	3.24
24	0.8639	0.1361	0.7985	0.2015	0.6242	3.68
25	0.9141	0.0859	0.8512	0.1488	0.5378	7.76
26	0.9484	0.0516	0.8780	0.1220	0.3916	4.30
27	0.9925	0.0075	0.9686	0.0314	0.2328	7.09
28	0.9927	0.0073	0.9759	0.0241	0.2963	9.62
29	0.9936	0.0064	0.9817	0.0183	0.3440	8.98

	E_K	$K_{H,E}$	$\gamma_{\pm B\bar{B}}$	$\gamma_{\pm B\bar{B}}$	$\ln \Gamma$	$\ln K_H$
1	0.0204	3.6652	0.8063	0.8129	0.0161	1.3150
2	0.0369	3.4135	0.8063	0.8128	0.0161	1.2439
3	0.0716	3.1666	0.8062	0.8127	0.0163	1.1689
4	0.0902	3.0615	0.8063	0.8127	0.0159	1.1348
5	0.1481	2.8888	0.8061	0.8125	0.0159	1.0768
6	0.2245	2.9008	0.8059	0.8123	0.0159	1.0809
7	0.2823	2.7742	0.8056	0.8121	0.0160	1.0364
8	0.3339	2.5073	0.8054	0.8118	0.0159	0.9352
9	0.3754	2.3919	0.8052	0.8116	0.0158	0.8879
10	0.4108	2.2553	0.8049	0.8114	0.0159	0.8292
11	0.4460	2.2247	0.8047	0.8112	0.0160	0.8156
12	0.4704	1.9158	0.8045	0.8108	0.0157	0.6659
13	0.5025	1.9215	0.8042	0.8107	0.0161	0.6692
14	0.5265	1.7400	0.8040	0.8103	0.0157	0.5696
15	0.5625	1.6070	0.8036	0.8100	0.0159	0.4903
16	0.5758	1.4925	0.8034	0.8098	0.0159	0.4163
17	0.6051	1.4503	0.8032	0.8095	0.0157	0.3875
18	0.6339	1.3171	0.8027	0.8092	0.0161	0.2916
19	0.6423	1.1229	0.8025	0.8089	0.0161	0.1320
20	0.6627	1.0473	0.8022	0.8086	0.0159	0.0621
21	0.6934	0.9756	0.8019	0.8084	0.0162	-0.0085
22	0.7195	0.8655	0.8016	0.8081	0.0160	-0.1284
23	0.7580	0.7896	0.8013	0.8077	0.0160	-0.2202
24	0.7985	0.6242	0.8009	0.8073	0.0160	-0.4553
25	0.8512	0.5378	0.8006	0.8070	0.0159	-0.6044
26	0.8780	0.3916	0.8003	0.8068	0.0160	-0.9215
27	0.9686	0.2328	0.8000	0.8066	0.0162	-1.4414
28	0.9759	0.2963	0.8000	0.8065	0.0162	-1.2003
29	0.9817	0.3440	0.8000	0.8064	0.0159	-1.0512

Na - K Exchange in Y (Grace) at 25°C. 24 Hr. Exchange, Normal pH.

Solution Total Normality = 0.050 mol dm⁻³

Exchange Capacity (in terms of Al) = 311.8 mequiv 100g⁻¹

	pH	m _K	m _{Na}	m _{K+mNa}	M _K	M _{Na}	M _{K+MNa}
1	7.16	0.28	49.28	49.56	6.1	294.5	300.6
2	7.15	0.55	48.97	49.53	10.7	278.0	288.7
3	7.09	1.17	48.91	50.08	21.3	275.4	296.7
4	7.01	3.15	46.41	49.56	47.9	250.9	298.8
5	6.98	4.59	45.26	49.85	62.8	233.0	295.8
6	7.00	6.48	44.03	50.51	78.4	218.6	297.0
7	6.89	10.37	39.46	49.83	114.0	199.7	313.7
8	6.94	12.68	37.31	49.99	129.1	184.3	313.4
9	6.90	16.01	33.92	49.93	141.8	169.7	311.5
10	6.80	18.08	32.05	50.13	151.5	160.0	311.5
11	6.86	22.48	27.42	49.90	167.2	145.7	312.9
12	6.86	26.83	23.48	50.31	184.0	125.0	309.0
13	6.73	31.08	19.04	50.12	199.1	108.0	307.1
14	6.84	36.08	14.48	50.56	213.9	99.1	313.0
15	6.85	39.60	10.36	49.96	230.0	83.9	313.9
16	6.79	42.28	7.47	49.75	235.1	62.8	297.9
17	6.81	47.30	2.58	49.88	260.8	36.5	297.3
18	6.75	48.64	0.37	49.01	292.4	9.4	301.8
19	6.63	48.80	0.32	49.12	301.0	6.8	307.8
20	6.74	49.76	0.11	49.88	299.0	4.2	303.2

m_K, m_{Na} solution phase concentration / mequiv dm⁻³

M_K, M_{Na} zeolite phase concentration / mequiv 100g⁻¹

	$E_{K, \infty}$	$E_{Na, \infty}$	E_K	E_{Na}	α	$\%H_{\infty}$
1	0.0057	0.9943	0.0204	0.9796	3.6548	3.59
2	0.0112	0.9888	0.0369	0.9631	3.3834	7.42
3	0.0234	0.9766	0.0718	0.9282	3.2284	4.84
4	0.0635	0.9365	0.1603	0.8397	2.8146	4.17
5	0.0921	0.9079	0.2123	0.7877	2.6577	5.13
6	0.1283	0.8717	0.2640	0.7360	2.4365	4.75
7	0.2081	0.7919	0.3634	0.6366	2.1722	-0.61
8	0.2537	0.7463	0.4119	0.5881	2.0611	-0.51
9	0.3206	0.6794	0.4552	0.5448	1.7703	0.10
10	0.3607	0.6393	0.4864	0.5136	1.6785	0.10
11	0.4505	0.5495	0.5344	0.4656	1.3997	-0.35
12	0.5333	0.4667	0.5955	0.4045	1.2882	0.90
13	0.6201	0.3799	0.6483	0.3517	1.1294	1.51
14	0.7136	0.2864	0.6833	0.3167	0.8661	-0.39
15	0.7926	0.2074	0.7328	0.2672	0.7174	-0.66
16	0.8498	0.1502	0.7893	0.2107	0.6618	4.47
17	0.9483	0.0517	0.8772	0.1228	0.3896	4.65
18	0.9925	0.0075	0.9690	0.0310	0.2376	3.22
19	0.9935	0.0065	0.9780	0.0220	0.2920	1.30
20	0.9977	0.0023	0.9861	0.0139	0.1641	2.75

	E_K	$K_{M, E}$	γ_{K}	γ_{Na}	$\ln \Gamma$	$\ln K_H$
1	0.0204	3.6548	0.8063	0.8129	0.0161	1.3122
2	0.0369	3.3834	0.8063	0.8128	0.0161	1.2350
3	0.0718	3.2284	0.8063	0.8127	0.0160	1.1880
4	0.1603	2.8146	0.8060	0.8125	0.0161	1.0509
5	0.2123	2.6577	0.8058	0.8123	0.0160	0.9935
6	0.2640	2.4365	0.8057	0.8121	0.0158	0.9064
7	0.3634	2.1722	0.8051	0.8116	0.0161	0.7918
8	0.4119	2.0611	0.8048	0.8113	0.0160	0.7393
9	0.4552	1.7703	0.8044	0.8108	0.0160	0.5872
10	0.4864	1.6785	0.8041	0.8106	0.0160	0.5339
11	0.5344	1.3997	0.8035	0.8100	0.0160	0.3523
12	0.5955	1.2882	0.8030	0.8094	0.0159	0.2691
13	0.6483	1.1294	0.8024	0.8089	0.0160	0.1376
14	0.6833	0.8661	0.8019	0.8082	0.0158	-0.1280
15	0.7328	0.7174	0.8013	0.8078	0.0160	-0.3161
16	0.7893	0.6618	0.8010	0.8074	0.0161	-0.3966
17	0.8772	0.3896	0.8003	0.8068	0.0160	-0.9265
18	0.9690	0.2376	0.8000	0.8066	0.0163	-1.4207
19	0.9780	0.2920	0.8000	0.8066	0.0163	-1.2148
20	0.9861	0.1641	0.8000	0.8065	0.0160	-1.7910

Na - K Exchange in Y (Grace) at 25°C. Background pH=4.

Solution Total Normality = 0.050 mol dm⁻³

Exchange Capacity (in terms of Al) = 311.8 mequiv 100g⁻¹

	pH	m _K	m _{Na}	m _{K+mNa}	M _K	M _{Na}	M _{K+MNa}
1	4.88	3.00	47.47	50.47	45.1	245.5	290.6
2	4.86	6.69	44.27	50.96	77.9	211.7	289.6
3	4.74	14.76	36.53	51.29	125.3	163.2	288.5
4	4.61	23.43	27.96	51.39	161.4	136.1	297.5
5	4.58	32.62	20.49	53.11	183.5	105.8	289.3
6	4.60	41.77	10.51	52.28	212.5	80.1	292.6
7	4.07	45.67	5.78	51.45	218.2	56.3	274.5
8	3.82	47.11	3.46	50.57	207.2	41.7	248.9

m_K, m_{Na} solution phase concentration / mequiv dm⁻³

M_K, M_{Na} zeolite phase concentration / mequiv 100g⁻¹

	E _{K,s}	E _{Na,s}	E _K	E _{Na}	α	%H _{ex}
1	0.0594	0.9406	0.1552	0.8448	2.9088	6.80
2	0.1313	0.8687	0.2691	0.7309	2.4366	7.10
3	0.2878	0.7122	0.4343	0.5657	1.9002	7.47
4	0.4559	0.5441	0.5425	0.4575	1.4152	4.59
5	0.6142	0.3858	0.6343	0.3657	1.0895	7.22
6	0.7990	0.2010	0.7262	0.2738	0.6674	6.15
7	0.8876	0.1124	0.7948	0.2052	0.4906	11.95
8	0.9316	0.0684	0.8324	0.1676	0.3648	20.17

	E _K	K _{M,E}	γ _{±KX}	γ _{±NaX}	lnΓ	lnK _M
1	0.1552	2.9088	0.8061	0.8125	0.0158	1.0836
2	0.2691	2.4366	0.8057	0.8120	0.0157	0.9063
3	0.4343	1.9002	0.8047	0.8110	0.0156	0.6575
4	0.5425	1.4152	0.8036	0.8099	0.0156	0.3628
5	0.6343	1.0895	0.8026	0.8087	0.0150	0.1007
6	0.7262	0.6674	0.8013	0.8075	0.0153	-0.3892
7	0.7948	0.4906	0.8007	0.8070	0.0155	-0.6966
8	0.8324	0.3648	0.8004	0.8068	0.0158	-0.9927

Na - K Exchange in Y (Grace) at 25°C. Background pH=3.

Solution Total Normality = 0.050 mol dm⁻³

Exchange Capacity (in terms of Al) = 311.8 mequiv 100g⁻¹

	pH	m _K	m _{Na}	m _{K+m_{Na}}	M _K	M _{Na}	M _{K+M_{Na}}
1	4.88	3.00	47.47	50.47	45.1	245.5	290.6
2	4.86	6.69	44.27	50.96	77.9	211.7	289.6
3	4.61	23.43	27.96	51.39	161.4	136.1	297.5
4	4.74	14.76	36.53	51.29	125.3	163.2	288.5
5	4.58	32.62	20.49	53.11	183.5	105.8	289.3
6	4.60	41.77	10.51	52.28	212.5	80.1	292.6
7	4.07	45.67	5.78	51.45	218.2	56.3	274.5
8	3.82	47.11	3.46	50.57	207.2	41.7	248.9

m_K, m_{Na} solution phase concentration / mequiv dm⁻³

M_K, M_{Na} zeolite phase concentration / mequiv 100g⁻¹

	E _{K,s}	E _{Na,s}	E _K	E _{Na}	α	%H _{ex}
1	0.0594	0.9406	0.1552	0.8448	2.9088	6.80
2	0.1313	0.8687	0.2691	0.7309	2.4366	7.10
3	0.4559	0.5441	0.5425	0.4575	1.4152	4.59
4	0.2878	0.7122	0.4343	0.5657	1.9002	7.47
5	0.6142	0.3858	0.6343	0.3657	1.0895	7.22
6	0.7990	0.2010	0.7262	0.2738	0.6674	6.15
7	0.8876	0.1124	0.7948	0.2052	0.4906	11.95
8	0.9316	0.0684	0.8324	0.1676	0.3648	20.17

	E _K	K _{H,E}	γ _{±BX}	γ _{±BX}	ln Γ	ln K _H
1	0.1552	2.9088	0.8061	0.8125	0.0158	1.0836
2	0.2691	2.4366	0.8057	0.8120	0.0157	0.9063
3	0.5425	1.4152	0.8036	0.8099	0.0156	0.3628
4	0.4343	1.9002	0.8047	0.8110	0.0156	0.6575
5	0.6343	1.0895	0.8026	0.8087	0.0150	0.1007
6	0.7262	0.6674	0.8013	0.8075	0.0153	-0.3892
7	0.7948	0.4906	0.8007	0.8070	0.0155	-0.6966
8	0.8324	0.3648	0.8004	0.8068	0.0158	-0.9927

Na - K Exchange in Y (Grace) at 25°C. Background pH=2.3.

Solution Total Normality = 0.050 mol dm⁻³

Exchange Capacity (in terms of Al) = 311.8 mequiv 100g⁻¹

	pH	m _K	m _{Na}	m _{K+mNa}	M _K	M _{Na}	M _{K+MNa}
1	3.94	4.01	51.89	55.90	28.5	171.9	200.4
2	3.75	7.81	46.79	54.60	44.0	147.8	191.7
3	3.74	16.51	39.25	55.76	73.4	126.4	199.8
4	3.75	26.00	29.13	55.13	92.5	105.0	197.5
5	3.62	35.05	20.68	55.73	105.0	86.3	191.3
6	3.65	42.98	11.01	53.99	132.9	70.5	203.4
7	3.43	47.26	5.96	53.22	98.8	41.9	140.7
8	3.32	49.67	2.83	52.51	88.7	16.7	105.4

m_K, m_{Na} solution phase concentration / mequiv dm⁻³

M_K, M_{Na} zeolite phase concentration / mequiv 100g⁻¹

	E _{K,s}	E _{Na,s}	E _K	E _{Na}	α	%H _{ex}
1	0.0718	0.9282	0.1422	0.8578	2.1449	35.73
2	0.1430	0.8570	0.2292	0.7708	1.7820	38.50
3	0.2961	0.7039	0.3673	0.6327	1.3800	35.93
4	0.4716	0.5284	0.4683	0.5317	0.9868	36.66
5	0.6289	0.3711	0.5488	0.4512	0.7178	38.64
6	0.7961	0.2039	0.6533	0.3467	0.4826	34.75
7	0.8881	0.1119	0.7022	0.2978	0.2971	54.87
8	0.9460	0.0540	0.8415	0.1585	0.3031	66.21

	E _K	K _{M,E}	γ _K	γ _{Na}	lnΓ	lnK _H
1	0.1422	2.1449	0.8067	0.8124	0.0141	0.7772
2	0.2292	1.7820	0.8060	0.8119	0.0145	0.5922
3	0.3673	1.3800	0.8050	0.8108	0.0142	0.3362
4	0.4683	0.9868	0.8037	0.8095	0.0144	0.0011
5	0.5488	0.7178	0.8027	0.8084	0.0142	-0.3174
6	0.6533	0.4826	0.8014	0.8073	0.0147	-0.7138
7	0.7022	0.2971	0.8008	0.8068	0.0150	-1.1986
8	0.8415	0.3031	0.8004	0.8065	0.0152	-1.1787

Na - K Exchange in Y (Grace) at 25°C. Background pH=2.

Solution Total Normality = 0.050 mol dm⁻³

Exchange Capacity (in terms of Al) = 311.8 mequiv 100g⁻¹

	pH	m _K	m _{Na}	m _{K+Na}	M _K	M _{Na}	M _{K+Na}
1	3.28	0.00	58.07	58.07	0.0	122.6	122.6
2	3.30	4.28	53.78	58.06	12.9	106.0	118.9
3	3.25	8.58	48.54	57.12	24.5	106.0	130.6
4	3.23	13.19	44.97	58.16	34.7	94.1	128.8
5	3.27	17.41	40.10	57.51	42.3	97.3	139.7
6	3.29	22.45	35.23	57.68	50.0	89.1	139.1
7	3.27	26.82	30.09	56.91	55.1	82.3	137.4
8	3.27	31.44	25.62	57.06	62.2	78.2	140.4
9	3.27	36.00	20.83	56.83	70.3	74.5	144.7
10	3.32	41.14	15.99	57.13	77.8	67.7	145.4
11	3.33	44.57	13.76	58.33	86.4	58.1	144.5

m_K, m_{Na} solution phase concentration / mequiv dm⁻³

M_K, M_{Na} zeolite phase concentration / mequiv 100g⁻¹

	E _{K,s}	E _{Na,s}	E _K	E _{Na}	α	%H _{ex}
1	0.0000	1.0000	0.0000	1.0000	—	60.68
2	0.0737	0.9263	0.1087	0.8913	1.5324	61.86
3	0.1503	0.8497	0.1881	0.8119	1.3098	58.13
4	0.2268	0.7732	0.2696	0.7304	1.2582	58.69
5	0.3027	0.6973	0.3032	0.6968	1.0022	55.21
6	0.3892	0.6108	0.3594	0.6406	0.8806	55.38
7	0.4713	0.5287	0.4009	0.5991	0.7507	55.93
8	0.5510	0.4490	0.4431	0.5569	0.6485	54.96
9	0.6335	0.3665	0.4855	0.5145	0.5459	53.58
10	0.7201	0.2799	0.5348	0.4652	0.4468	53.36
11	0.7641	0.2359	0.5980	0.4020	0.4593	53.67

	E _K	K _{M,E}	γ _K	γ _{Na}	ln Γ	ln K _H
1	0.0000	—	0.8075	0.8129	0.0134	0.0134
2	0.1087	1.5324	0.8069	0.8123	0.0134	0.4402
3	0.1881	1.3098	0.8062	0.8118	0.0137	0.2836
4	0.2696	1.2582	0.8058	0.8112	0.0134	0.2431
5	0.3032	1.0022	0.8051	0.8106	0.0136	0.0158
6	0.3594	0.8806	0.8045	0.8100	0.0135	-0.1136
7	0.4009	0.7507	0.8039	0.8094	0.0138	-0.2730
8	0.4431	0.6485	0.8033	0.8088	0.0137	-0.4194
9	0.4855	0.5459	0.8027	0.8082	0.0138	-0.5915
10	0.5348	0.4468	0.8020	0.8076	0.0137	-0.7920
11	0.5980	0.4593	0.8018	0.8071	0.0133	-0.7647

Na - K Exchange in Y (Grace) at 2°C.

Solution Total Normality = 0.050 mol dm⁻³

Exchange Capacity (in terms of Al) = 311.8 mequiv 100g⁻¹

	pH	m _K	m _{Na}	m _{K+mNa}	M _K	M _{Na}	M _{K+MNa}
1	6.60	0.23	49.33	49.56	6.2	280.5	286.7
2	6.77	0.50	48.64	49.14	12.0	280.9	292.9
3	6.84	1.02	48.82	49.84	21.8	277.2	299.0
4	6.04	3.11	46.87	49.98	52.7	258.2	310.9
5	6.13	6.74	43.38	50.12	93.2	219.7	312.9
6	5.84	10.72	40.49	51.21	119.9	191.6	311.5
7	6.21	14.92	35.65	50.57	142.4	167.6	310.0
8	6.16	19.21	30.80	50.01	155.3	154.6	309.9
9	6.20	22.98	28.21	51.19	168.2	140.7	308.9
10	6.26	27.79	23.15	50.94	185.8	124.7	310.5
11	6.33	31.91	18.62	50.53	194.5	114.7	309.2
12	6.28	36.13	14.79	50.92	204.8	103.1	307.9
13	6.85	40.78	9.40	50.18	219.8	82.2	302.0
14	6.60	47.13	3.85	50.98	238.6	60.7	299.3
15	6.59	47.74	2.30	50.04	250.1	49.4	299.5
16	6.79	48.02	2.53	50.55	250.1	53.4	303.5
17	6.44	48.89	1.30	50.19	262.5	39.6	302.1
18	6.53	49.06	0.76	49.82	275.7	28.8	304.5
19	6.46	49.68	0.05	49.73	299.0	3.2	302.2

m_K, m_{Na} solution phase concentration / mequiv dm⁻³

M_K, M_{Na} zeolite phase concentration / mequiv 100g⁻¹

	$E_{K, \pm}$	$E_{Na, \pm}$	E_K	E_{Na}	α	$\%H_{\pm}$
1	0.0047	0.9953	0.0216	0.9784	4.6398	8.05
2	0.0102	0.9898	0.0410	0.9590	4.1558	6.06
3	0.0205	0.9795	0.0729	0.9271	3.7641	4.11
4	0.0622	0.9378	0.1695	0.8305	3.0760	0.29
5	0.1346	0.8654	0.2979	0.7021	2.7295	-0.37
6	0.2093	0.7907	0.3849	0.6151	2.3636	0.10
7	0.2950	0.7050	0.4594	0.5406	2.0301	0.58
8	0.3841	0.6159	0.5011	0.4989	1.6106	0.61
9	0.4489	0.5511	0.5445	0.4555	1.4675	0.93
10	0.5455	0.4545	0.5984	0.4016	1.2412	0.42
11	0.6315	0.3685	0.6290	0.3710	0.9895	0.83
12	0.7095	0.2905	0.6652	0.3348	0.8132	1.25
13	0.8127	0.1873	0.7278	0.2722	0.6164	3.14
14	0.9245	0.0755	0.7972	0.2028	0.3211	4.01
15	0.9540	0.0460	0.8351	0.1649	0.2439	3.94
16	0.9500	0.0500	0.8241	0.1759	0.2468	2.66
17	0.9741	0.0259	0.8690	0.1310	0.1767	3.11
18	0.9848	0.0152	0.9055	0.0945	0.1484	2.34
19	0.9989	0.0011	0.9894	0.0106	0.1021	3.08

	E_K	$K_{H, E}$	$\gamma_{\pm K \pm}$	$\gamma_{\pm Na \pm}$	$\ln \Gamma$	$\ln K_H$
1	0.0216	4.6398	0.8063	0.8129	0.0161	1.5508
2	0.0410	4.1558	0.8062	0.8128	0.0163	1.4408
3	0.0729	3.7641	0.8063	0.8128	0.0160	1.3416
4	0.1695	3.0760	0.8060	0.8125	0.0160	1.1396
5	0.2979	2.7295	0.8056	0.8120	0.0160	1.0201
6	0.3849	2.3636	0.8052	0.8115	0.0156	0.8758
7	0.4594	2.0301	0.8046	0.8110	0.0158	0.7239
8	0.5011	1.6106	0.8040	0.8104	0.0160	0.4926
9	0.5445	1.4675	0.8036	0.8099	0.0156	0.3992
10	0.5984	1.2412	0.8030	0.8093	0.0157	0.2318
11	0.6290	0.9895	0.8024	0.8088	0.0158	0.0053
12	0.6652	0.8132	0.8019	0.8082	0.0157	-0.1911
13	0.7278	0.6164	0.8012	0.8076	0.0159	-0.4680
14	0.7972	0.3211	0.8005	0.8068	0.0157	-1.1203
15	0.8351	0.2439	0.8003	0.8067	0.0160	-1.3950
16	0.8241	0.2468	0.8003	0.8067	0.0158	-1.3835
17	0.8690	0.1767	0.8002	0.8066	0.0159	-1.7172
18	0.9055	0.1484	0.8001	0.8065	0.0161	-1.8917
19	0.9894	0.1021	0.8000	0.8065	0.0161	-2.2655

Na - K Exchange in X (Laporte) at 25°C. Normal pH.

Solution Total Normality = 0.050 mol dm⁻³

Exchange Capacity (in terms of Al) = 455.9 mequiv 100g⁻¹

	pH	m _K	m _{Na}	m _{K+m_{Na}}	M _K	M _{Na}	M _{K+M_{Na}}
1	9.10	0.24	49.62	49.86	7.0	420.8	427.8
2	9.33	0.49	49.32	49.81	13.4	416.3	429.7
3	9.80	1.04	48.72	49.76	25.3	406.7	432.0
4	6.50	2.66	46.69	49.35	48.3	385.4	433.7
5	8.94	5.97	43.64	49.61	79.9	353.1	433.0
6	9.15	9.36	40.27	49.63	113.2	328.1	441.3
7	9.54	13.14	36.76	49.90	144.6	304.1	448.7
8	9.24	17.41	32.21	49.62	165.4	277.8	443.2
9	9.50	21.40	28.44	49.84	188.5	263.8	452.3
10	9.40	24.16	25.61	49.77	200.9	237.6	438.5
11	9.56	28.64	20.62	49.26	232.5	213.2	445.7
12	9.53	33.98	16.21	50.19	262.8	194.1	456.9
13	9.27	42.81	7.08	49.89	328.2	115.2	443.4
14	8.16	45.70	4.36	50.05	368.0	71.2	439.1
15	6.64	45.76	4.12	49.88	365.9	73.8	439.7
16	6.48	47.45	2.42	49.87	383.7	42.5	426.2
17	6.10	48.71	1.07	49.78	417.5	20.2	437.7
18	6.38	49.27	0.59	49.86	419.5	12.5	432.0

m_K, m_{Na} solution phase concentration / mequiv dm⁻³

M_K, M_{Na} zeolite phase concentration / mequiv 100g⁻¹

	$E_{K, \mu}$	$E_{N, \mu}$	E_K	$E_{N, \mu}$	α	$\%H_{\mu, x}$
1	0.0048	0.9952	0.0164	0.9836	3.4828	6.16
2	0.0098	0.9902	0.0312	0.9688	3.2399	5.75
3	0.0209	0.9791	0.0586	0.9414	2.9177	5.24
4	0.0540	0.9460	0.1114	0.8886	2.1984	4.86
5	0.1203	0.8797	0.1845	0.8155	1.6541	5.02
6	0.1886	0.8114	0.2565	0.7435	1.4844	3.20
7	0.2633	0.7367	0.3223	0.6777	1.3302	1.58
8	0.3509	0.6491	0.3732	0.6268	1.1015	2.79
9	0.4294	0.5706	0.4168	0.5832	0.9496	0.79
10	0.4854	0.5146	0.4582	0.5418	0.8963	3.82
11	0.5814	0.4186	0.5217	0.4783	0.7851	2.24
12	0.6770	0.3230	0.5752	0.4248	0.6459	-0.22
13	0.8580	0.1420	0.7402	0.2598	0.4714	2.74
14	0.9130	0.0870	0.8380	0.1620	0.4929	3.67
15	0.9174	0.0826	0.8322	0.1678	0.4466	3.56
16	0.9515	0.0485	0.9003	0.0997	0.4604	6.51
17	0.9785	0.0215	0.9538	0.0462	0.4529	3.99
18	0.9882	0.0118	0.9710	0.0290	0.4002	5.24

	E_K	$K_{H, E}$	$\gamma_{\pm 0.5}$	$\gamma_{\pm 0.5}$	$\ln \Gamma$	$\ln K_H$
1	0.0164	3.4828	0.8064	0.8129	0.0160	1.2639
2	0.0312	3.2399	0.8063	0.8128	0.0161	1.1916
3	0.0586	2.9177	0.8063	0.8128	0.0161	1.0869
4	0.1114	2.1984	0.8060	0.8126	0.0162	0.8039
5	0.1845	1.6541	0.8056	0.8121	0.0161	0.5194
6	0.2565	1.4844	0.8052	0.8117	0.0161	0.4111
7	0.3223	1.3302	0.8047	0.8112	0.0160	0.3014
8	0.3732	1.1015	0.8041	0.8106	0.0161	0.1128
9	0.4168	0.9496	0.8036	0.8101	0.0160	-0.0356
10	0.4582	0.8963	0.8033	0.8098	0.0161	-0.0934
11	0.5217	0.7851	0.8026	0.8092	0.0162	-0.2257
12	0.5752	0.6459	0.8021	0.8085	0.0159	-0.4212
13	0.7402	0.4714	0.8009	0.8074	0.0160	-0.7359
14	0.8380	0.4929	0.8006	0.8070	0.0160	-0.6915
15	0.8322	0.4466	0.8005	0.8070	0.0160	-0.7900
16	0.9003	0.4604	0.8003	0.8068	0.0160	-0.7595
17	0.9538	0.4529	0.8001	0.8066	0.0161	-0.7760
18	0.9710	0.4002	0.8001	0.8065	0.0160	-0.8998

Na - K Exchange in X (Laporte) at 25°C. Background pH=2.3.

Solution Total Normality = 0.050 mol dm⁻³

Exchange Capacity (in terms of Al) = 458.2 mequiv 100g⁻¹

	pH	m _K	m _{Na}	m _{K+mNa}	M _K	M _{Na}	M _{K+MNa}
1	6.18	3.07	50.48	53.55	45.2	292.1	337.3
2	6.03	6.62	47.72	54.34	75.1	261.9	337.0
3	5.58	14.78	41.33	56.11	117.9	215.3	333.2
4	6.22	23.42	32.11	55.53	149.3	195.1	344.4
5	6.07	32.56	23.55	56.11	175.0	166.5	341.5
6	5.19	41.22	14.60	55.82	198.7	133.1	331.8
7	5.79	44.59	8.64	53.23	173.6	72.1	245.7
8	4.23	46.77	3.91	50.68	55.7	18.9	74.5

m_K, m_{Na} solution phase concentration / mequiv dm⁻³

M_K, M_{Na} zeolite phase concentration / mequiv 100g⁻¹

	E _{K,s}	E _{Na,s}	E _K	E _{Na}	α	%H _{ex}
1	0.0574	0.9426	0.1340	0.8660	2.5416	26.39
2	0.1218	0.8782	0.2229	0.7771	2.0679	26.44
3	0.2634	0.7366	0.3538	0.6462	1.5313	27.28
4	0.4218	0.5782	0.4335	0.5665	1.0492	24.84
5	0.5803	0.4197	0.5124	0.4876	0.7602	25.47
6	0.7384	0.2616	0.5989	0.4011	0.5288	27.59
7	0.8377	0.1623	0.7065	0.2935	0.4665	46.37
8	0.9229	0.0771	0.7467	0.2533	0.2463	83.73

Na - NH₄ Exchange in Y (Grace) at 25°C.

Solution Total Normality = 0.050 mol dm⁻³

Exchange Capacity (in terms of Al) = 311.8 mequiv 100g⁻¹

	pH	m _{NH4}	m _{Na}	m _{NH4+mNa}	M _{NH4}	M _{Na}	M _{NH4+MNa}
1	6.95	1.47	48.38	49.85	20.9	278.4	299.3
2	6.87	3.36	47.64	51.00	40.1	257.7	297.8
3	6.81	6.86	42.88	49.74	71.2	227.5	298.7
4	6.77	11.36	38.36	49.72	105.2	203.2	308.4
5	6.76	13.73	35.13	48.86	115.2	184.0	299.2
6	6.56	18.34	31.84	50.18	140.3	162.0	302.3
7	6.51	23.45	26.47	49.92	162.5	141.3	303.8
8	6.69	27.56	22.27	49.83	177.6	124.3	301.9
9	6.57	31.77	18.14	49.91	192.9	115.2	308.1
10	6.48	35.79	13.89	49.68	204.3	100.5	304.8
11	6.54	41.21	8.91	50.12	210.4	89.0	299.4
12	6.34	46.81	3.41	50.22	225.4	78.7	304.2
13	6.26	47.93	2.08	50.02	230.5	71.1	301.6
14	6.38	48.26	1.83	50.09	225.4	70.8	296.2
15	6.20	49.80	0.11	49.91	228.0	70.2	298.2
16	6.29	49.84	0.23	50.07	227.4	75.5	302.9
17	6.47	49.93	0.15	50.08	226.2	68.5	294.7
18	6.04	50.03	0.10	50.13	232.2	68.6	300.8

m_{NH4}, m_{Na} solution phase concentration / mequiv dm⁻³

M_{NH4}, M_{Na} zeolite phase concentration / mequiv 100g⁻¹

	$E_{NH_4, s}$	$E_{Na, s}$	E_{NH_4}	E_{Na}	α	$\chi_{H_{2x}}$
1	0.0295	0.9705	0.0698	0.9302	2.4685	4.01
2	0.0658	0.9342	0.1346	0.8654	2.2072	4.50
3	0.1379	0.8621	0.2384	0.7616	1.9563	4.20
4	0.2285	0.7715	0.3411	0.6589	1.7484	1.09
5	0.2810	0.7190	0.3851	0.6149	1.6023	4.03
6	0.3655	0.6345	0.4641	0.5359	1.5033	3.05
7	0.4698	0.5302	0.5349	0.4651	1.2981	2.57
8	0.5531	0.4469	0.5883	0.4117	1.1546	3.18
9	0.6365	0.3635	0.6261	0.3739	0.9561	1.19
10	0.7204	0.2796	0.6703	0.3297	0.7889	2.25
11	0.8222	0.1778	0.7027	0.2973	0.5111	3.98
12	0.9321	0.0679	0.7411	0.2589	0.2087	2.44
13	0.9583	0.0417	0.7642	0.2358	0.1410	3.28
14	0.9634	0.0366	0.7611	0.2389	0.1211	5.00
15	0.9978	0.0022	0.7645	0.2355	0.0071	4.35
16	0.9954	0.0046	0.7507	0.2493	0.0139	2.84
17	0.9970	0.0030	0.7675	0.2325	0.0099	5.48
18	0.9980	0.0020	0.7719	0.2281	0.0068	3.53

	E_{NH_4}	$K_{H, E}$	$\gamma_{\pm NH_4}$	$\gamma_{\pm Na}$	$\ln \Gamma$	$\ln K_H$
1	0.0904	2.4685	0.8048	0.8127	0.0194	0.9231
2	0.1744	2.2072	0.8047	0.8124	0.0190	0.8107
3	0.3088	1.9563	0.8040	0.8118	0.0195	0.6905
4	0.4419	1.7484	0.8032	0.8111	0.0195	0.5782
5	0.4989	1.6023	0.8027	0.8107	0.0198	0.4913
6	0.6012	1.5033	0.8022	0.8100	0.0193	0.4270
7	0.6930	1.2981	0.8014	0.8092	0.0194	0.2803
8	0.7621	1.1546	0.8007	0.8086	0.0194	0.1632
9	0.8111	0.9561	0.8001	0.8079	0.0194	-0.0255
10	0.8683	0.7889	0.7994	0.8073	0.0195	-0.2176
11	0.9104	0.5111	0.7987	0.8064	0.0193	-0.6518
12	0.9602	0.2087	0.7978	0.8056	0.0193	-1.5476
13	0.9901	0.1410	0.7976	0.8054	0.0194	-1.9396
14	0.9860	0.1211	0.7976	0.8053	0.0193	-2.0921
15	0.9904	0.0071	0.7973	0.8051	0.0194	-4.9231
16	0.9725	0.0139	0.7973	0.8051	0.0194	-4.2583
17	0.9943	0.0099	0.7973	0.8051	0.0193	-4.5966
18	1.0001	0.0068	0.7973	0.8051	0.0193	-4.9766

K - NH₄ Exchange in Y (Grace) at 25°C.

Solution Total Normality = 0.050 mol dm⁻³

Exchange Capacity (in terms of Al) = 304.9 m equiv 100g⁻¹

	pH	m _{NH4}	m _K	m _{NH4+K}	M _{NH4}	M _K	M _{NH4+K}
1	6.25	1.41	50.03	51.44	5.6	298.0	303.6
2	6.50	5.00	45.12	50.12	15.2	285.6	300.8
3	6.46	8.50	40.44	48.94	25.0	278.8	303.8
4	6.46	14.21	35.95	50.16	39.7	257.4	297.1
5	6.33	17.50	31.24	48.74	47.5	247.4	294.9
6	6.44	21.15	28.44	49.59	57.5	239.7	297.2
7	6.05	25.89	24.18	50.07	79.9	222.5	302.4
8	6.36	26.50	22.67	49.17	80.0	214.7	294.7
9	6.34	30.20	18.99	49.19	100.3	200.2	300.5
10	5.97	30.25	19.27	49.52	100.4	203.1	303.5
11	6.03	34.07	15.18	49.25	118.1	184.3	302.4
12	6.39	35.40	14.75	50.15	115.1	181.5	296.6
13	6.39	38.50	10.60	49.10	141.1	157.7	298.8
14	6.07	38.69	10.47	49.16	146.4	159.2	305.6
15	6.40	42.20	6.91	49.11	169.5	128.0	297.5
16	6.44	42.48	7.24	49.72	175.6	126.3	301.9
17	6.24	44.81	4.81	49.62	180.2	117.3	297.5
18	6.24	45.92	3.87	49.79	194.6	104.5	299.1
19	6.10	47.16	2.45	49.61	203.1	93.3	296.4
20	6.34	47.89	2.05	49.94	215.4	81.2	296.7
21	6.07	47.96	1.95	49.91	218.6	73.4	292.0
22	6.17	48.90	0.60	49.51	245.5	57.4	302.9
23	6.24	49.30	0.94	50.24	238.0	64.8	302.8
24	5.98	49.50	0.45	49.95	240.2	50.6	290.8

m_{NH4}, m_K solution phase concentration / m equiv dm⁻³

M_{NH4}, M_K zeolite phase concentration / m equiv 100g⁻¹

	$E_{NH_4, s}$	$E_{K, s}$	E_{NH_4}	E_K	α	$\%H_{sx}$
1	0.0000	1.0000	0.0000	1.0000	1.0000	3.02
2	0.0274	0.9726	0.0185	0.9815	0.6711	0.42
3	0.0998	0.9002	0.0506	0.9494	0.4806	1.34
4	0.1737	0.8263	0.0823	0.9177	0.4266	0.36
5	0.2833	0.7167	0.1336	0.8664	0.3902	2.56
6	0.3590	0.6410	0.1611	0.8389	0.3427	3.28
7	0.4265	0.5735	0.1935	0.8065	0.3226	2.53
8	0.5171	0.4829	0.2643	0.7357	0.3355	0.81
9	0.5389	0.4611	0.2715	0.7285	0.3188	3.35
10	0.6139	0.3861	0.3338	0.6662	0.3150	1.44
11	0.6109	0.3891	0.3308	0.6692	0.3149	0.46
12	0.6918	0.3082	0.3905	0.6095	0.2855	0.82
13	0.7059	0.2941	0.3881	0.6119	0.2642	2.72
14	0.7841	0.2159	0.4722	0.5278	0.2463	2.00
15	0.7870	0.2130	0.4791	0.5209	0.2489	-0.23
16	0.8594	0.1406	0.5697	0.4303	0.2167	2.43
17	0.8544	0.1456	0.5817	0.4183	0.2370	0.97
18	0.9031	0.0969	0.6057	0.3943	0.1649	2.43
19	0.9223	0.0777	0.6506	0.3494	0.1569	1.90
20	0.9506	0.0494	0.6853	0.3147	0.1132	2.80
21	0.9590	0.0410	0.7261	0.2739	0.1133	2.70
22	0.9609	0.0391	0.7486	0.2514	0.1211	4.23
23	0.9878	0.0122	0.8105	0.1895	0.0529	0.66
24	0.9812	0.0188	0.7859	0.2141	0.0703	0.68
25	0.9910	0.0090	0.8260	0.1740	0.0430	4.63

	E_{NH_4}	$K_{M, E}$	$\gamma_{\pm BX}^{\circ}$	$\gamma_{\pm BX}^{\circ}$	$\ln \Gamma$	$\ln K_H$
1	0.0000	1.0000	0.7986	0.8000	0.0035	0.0035
2	0.0224	0.6711	0.7986	0.8000	0.0033	-0.3956
3	0.0612	0.4806	0.7985	0.7999	0.0034	-0.7294
4	0.0996	0.4266	0.7984	0.7998	0.0035	-0.8484
5	0.1618	0.3902	0.7983	0.7996	0.0034	-0.9377
6	0.1950	0.3427	0.7981	0.7995	0.0035	-1.0673
7	0.2342	0.3226	0.7981	0.7994	0.0034	-1.1280
8	0.3199	0.3355	0.7980	0.7993	0.0034	-1.0889
9	0.3286	0.3188	0.7979	0.7993	0.0034	-1.1399
10	0.4041	0.3150	0.7978	0.7992	0.0034	-1.1516
11	0.4005	0.3149	0.7978	0.7992	0.0034	-1.1521
12	0.4728	0.2855	0.7977	0.7991	0.0034	-1.2500
13	0.4698	0.2642	0.7977	0.7990	0.0034	-1.3276
14	0.5717	0.2463	0.7976	0.7990	0.0034	-1.3976
15	0.5800	0.2489	0.7976	0.7990	0.0034	-1.3874
16	0.6898	0.2167	0.7975	0.7989	0.0034	-1.5258
17	0.7042	0.2370	0.7975	0.7989	0.0034	-1.4363
18	0.7333	0.1649	0.7974	0.7988	0.0034	-1.7992
19	0.7877	0.1569	0.7974	0.7988	0.0034	-1.8488
20	0.8297	0.1132	0.7974	0.7987	0.0034	-2.1749
21	0.8791	0.1133	0.7974	0.7987	0.0034	-2.1745
22	0.9063	0.1211	0.7974	0.7987	0.0034	-2.1078
23	0.9812	0.0529	0.7973	0.7987	0.0034	-2.9356
24	0.9514	0.0703	0.7973	0.7987	0.0034	-2.6518
25	1.0000	0.0430	0.7973	0.7987	0.0034	-3.1438

K-Ca Exchange in Y (Grace) at 25°C.

Solution Total Normality = 0.050 mol dm⁻³

Exchange Capacity (in terms of Al) = 304.8 mequiv 100g⁻¹

	pH	m _{Ca}	m _K	m _{Ca} +m _K	M _{Ca}	M _K	M _{Ca} +M _K
1	6.17	0.22	50.09	50.31	5.3	298.9	304.2
2	6.23	0.78	49.83	50.61	8.6	289.2	297.8
3	6.47	4.46	45.29	49.75	27.7	267.9	295.6
4	6.31	6.73	43.22	49.95	33.8	256.0	289.8
5	6.28	12.79	37.35	50.14	59.5	232.1	291.6
6	5.84	15.24	33.90	49.14	68.7	219.7	288.4
7	6.10	20.66	28.92	49.58	103.1	200.2	303.3
8	6.14	25.23	24.69	49.92	116.3	176.5	292.8
9	6.27	29.25	20.68	49.93	140.7	159.1	299.8
10	5.93	29.19	20.95	50.14	140.0	163.6	303.6
11	5.64	32.71	17.26	49.97	153.1	147.4	300.5
12	5.96	33.77	16.48	50.25	157.0	145.1	302.1
13	6.11	37.63	12.26	49.89	184.0	118.5	302.5
14	5.85	35.53	14.55	50.08	173.0	131.7	304.7
15	6.03	41.55	8.43	49.98	210.0	89.6	299.6
16	6.01	41.68	8.73	50.41	209.6	88.8	298.4
17	5.97	43.37	6.46	49.83	230.1	73.3	303.4
18	5.68	45.31	4.41	49.72	248.7	54.9	303.6
19	6.17	47.14	2.80	49.94	260.0	39.4	299.4
20	6.11	48.64	1.42	50.06	276.5	27.4	303.9
21	6.04	49.16	0.63	49.79	281.2	19.3	300.5
22	6.03	49.58	0.37	49.95	285.9	16.0	301.9

m_{Ca}, m_K solution phase concentration / mequiv dm⁻³

M_{Ca}, M_K zeolite phase concentration / mequiv 100g⁻¹

	$E_{Ca, \mu}$	$E_{K, \mu}$	E_{Ca}	E_K	α	$\%H_{\mu x}$
1	0.0044	0.9956	0.0172	0.9828	3.9729	-0.41
2	0.0151	0.9849	0.0287	0.9713	1.9334	2.34
3	0.0897	0.9103	0.0938	0.9062	1.0502	3.04
4	0.1252	0.8748	0.1166	0.8834	0.9219	4.96
5	0.2837	0.7163	0.1901	0.8099	0.5927	6.01
6	0.3101	0.6899	0.1984	0.8016	0.5507	10.56
7	0.4167	0.5833	0.2263	0.7737	0.4096	15.13
8	0.5054	0.4946	0.2813	0.7187	0.3830	16.12
9	0.5939	0.4061	0.3930	0.6070	0.4428	12.89
10	0.5982	0.4018	0.4740	0.5260	0.6054	-2.33
11	0.6772	0.3228	0.3896	0.6104	0.3042	19.72
12	0.6745	0.3255	0.5438	0.4562	0.5753	-5.12
13	0.7408	0.2592	0.5160	0.4840	0.3730	19.03
14	0.7717	0.2283	0.5984	0.4016	0.4407	-7.54
15	0.8435	0.1565	0.5928	0.4072	0.2701	26.70
16	0.8283	0.1717	0.7089	0.2911	0.5049	-1.82
17	0.9196	0.0804	0.6485	0.3515	0.1612	31.62
18	0.9557	0.0443	0.7289	0.2711	0.1248	33.61
19	0.9450	0.0550	0.8736	0.1264	0.4022	-2.20
20	0.9719	0.0281	0.9116	0.0884	0.2982	-1.89
21	0.9875	0.0125	0.9390	0.0610	0.1944	-3.91
22	0.9926	0.0074	0.9485	0.0515	0.1364	-1.87

	E_{Ca}	$K_{M, E}$	$\gamma_{\pm \text{BZ}}$	$\gamma_{\pm \text{BZ}}$	$\ln \Gamma$	$\ln K_M$
1	0.0172	0.0070	0.6495	0.8000	0.4024	-4.5655
2	0.0287	0.0058	0.6505	0.8001	0.3980	-4.7469
3	0.0938	0.0098	0.6360	0.8007	0.4689	-4.1515
4	0.1166	0.0114	0.6372	0.8010	0.4648	-4.0056
5	0.1901	0.0104	0.6146	0.8020	0.5777	-3.9889
6	0.1984	0.0092	0.6087	0.8020	0.6066	-4.0775
7	0.2263	0.0069	0.5985	0.8025	0.6597	-4.3120
8	0.2813	0.0074	0.5907	0.8028	0.7006	-4.2052
9	0.3930	0.0119	0.5838	0.8030	0.7373	-3.6974
10	0.4740	0.0229	0.5839	0.8031	0.7368	-3.0415
11	0.3896	0.0062	0.5769	0.8032	0.7734	-4.3075
12	0.5438	0.0226	0.5774	0.8032	0.7708	-3.0186
13	0.5160	0.0098	0.5719	0.8032	0.7999	-3.8305
14	0.5984	0.0153	0.5706	0.8033	0.8072	-3.3721
15	0.5928	0.0060	0.5656	0.8034	0.8338	-4.2751
16	0.7089	0.0215	0.5668	0.8034	0.8275	-3.0135
17	0.6485	0.0023	0.5610	0.8034	0.8584	-5.1959
18	0.7289	0.0014	0.5589	0.8034	0.8697	-5.6772
19	0.8736	0.0155	0.5596	0.8034	0.8660	-3.2980
20	0.9116	0.0087	0.5581	0.8034	0.8744	-3.8697
21	0.9390	0.0037	0.5572	0.8034	0.8791	-4.7079
22	0.9485	0.0019	0.5569	0.8034	0.8807	-5.4064

K - H Exchange in Y (Grace) at 25°C. 15 Minute Exchange.

Solution Total Normality = $0.010 \text{ mol dm}^{-3}$

Exchange Capacity (in terms of Al) = $304.9 \text{ mequiv } 100\text{g}^{-1}$

	pH	m_H	m_K	m_H+m_K	M_H	M_K	M_H+M_K
1	3.95	0.11	9.50	9.61	60.7	244.2	304.9
2	3.71	0.19	9.29	9.48	99.9	205.0	304.9
3	3.37	0.43	9.05	9.48	143.7	161.2	304.9
4	3.21	0.62	8.34	8.96	174.3	130.6	304.9
5	3.08	0.82	7.16	7.98	202.8	102.1	304.9
6	2.96	1.09	6.14	7.23	216.0	88.9	304.9
7	2.81	1.55	4.90	6.45	232.3	72.7	305.0
8	2.61	2.46	4.38	6.84	248.9	56.0	304.9

m_H, m_K solution phase concentration / mequiv dm^{-3}

M_H, M_K zeolite phase concentration / $\text{mequiv } 100\text{g}^{-1}$

	$E_{H,s}$	$E_{K,s}$	E_H	E_K	α
1	0.0117	0.9883	0.1991	0.8009	21.082
2	0.0204	0.9796	0.3276	0.6724	23.444
3	0.0450	0.9550	0.4713	0.5287	18.904
4	0.0689	0.9311	0.5717	0.4283	18.046
5	0.1032	0.8968	0.6651	0.3349	17.262
6	0.1513	0.8487	0.7085	0.2915	13.638
7	0.2402	0.7598	0.7618	0.2382	10.117
8	0.3599	0.6401	0.8164	0.1836	7.9106

Na - H Exchange in Y (Grace) at 25°C. 15 Minute Exchange.

Solution Total Normality = 0.010 mol dm⁻³

Exchange Capacity (in terms of Al) = 311.8 mequiv 100g⁻¹

	pH	m _H	m _{Na}	m _{H+m_{Na}}	M _H	M _{Na}	M _{H+M_{Na}}
1	5.27	0.01	10.18	10.19	58.4	253.4	311.8
2	4.68	0.02	10.23	10.25	114.2	197.6	311.8
3	4.35	0.05	10.14	10.19	152.1	159.7	311.8
4	3.86	0.14	10.11	10.25	200.2	111.6	311.8
5	3.29	0.51	9.47	9.98	229.3	82.5	311.8
6	2.65	2.24	6.92	9.16	237.6	74.2	311.9
7	2.54	2.87	5.54	8.41	248.8	63.0	311.8
8	2.40	3.99	4.53	8.52	259.5	52.3	311.8

m_H, m_{Na} solution phase concentration / mequiv dm⁻³

M_H, M_{Na} zeolite phase concentration / mequiv 100g⁻¹

	E _{H,s}	E _{Na,s}	E _H	E _{Na}	α
1	0.0005	0.9995	0.1873	0.8127	434.47
2	0.0020	0.9980	0.3663	0.6337	282.88
3	0.0044	0.9956	0.4878	0.5122	213.66
4	0.0135	0.9865	0.6421	0.3579	131.42
5	0.0509	0.9491	0.7354	0.2646	51.803
6	0.2445	0.7555	0.7619	0.2381	9.8887
7	0.3414	0.6586	0.7979	0.2021	7.6178
8	0.4681	0.5319	0.8323	0.1677	5.6415

Na - Al Exchange in Y (Grace) at 25°C.

Solution Total Normality = 0.050 mol dm⁻³

Exchange Capacity (in terms of Al) = 311.8 mequiv 100g⁻¹

	pH	m _{Al}	m _{Na}	m _{Al} +m _{Na}	M _{Al}	M _{Na}	M _{Al} +M _{Na}
1	5.86	0.00	49.64	49.64	2.5	271.3	273.8
2	5.73	0.00	49.20	49.20	19.9	241.2	261.1
3	4.78	0.00	50.22	50.22	36.4	232.9	269.3
4	4.80	0.05	49.16	49.21	50.2	204.4	254.6
5	3.74	2.07	48.62	50.69	107.9	140.7	248.6
6	3.53	6.69	43.98	50.67	146.8	116.6	263.4
7	3.40	11.31	39.07	50.38	151.8	116.1	267.9
8	3.35	15.57	34.14	49.71	156.3	105.0	261.3
9	3.29	21.07	29.21	50.28	160.0	101.0	261.0
10	3.25	27.02	24.28	51.30	174.5	102.4	276.9
11	3.23	30.78	19.97	50.75	172.8	98.8	271.6
12	3.17	35.26	13.82	49.08	172.9	96.0	268.9
13	3.18	39.91	9.30	49.21	179.5	92.4	271.9
14	3.31	47.57	2.03	49.60	138.2	71.2	209.4
15	3.30	47.83	3.09	50.92	138.6	72.3	210.9
16	3.00	48.23	0.65	48.88	150.3	80.2	230.5
17	3.00	49.42	0.14	49.56	125.6	75.4	201.1
18	3.08	49.76	0.09	49.85	138.7	72.8	211.5
19	3.06	49.84	0.09	49.93	141.2	73.8	215.0

m_{Al}, m_{Na} solution phase concentration / mequiv dm⁻³

M_{Al}, M_{Na} zeolite phase concentration / mequiv 100g⁻¹

	E _{Al,s}	E _{Na,s}	E _{Al}	E _{Na}	α	%H _{ex}
1	0.0000	1.0000	0.0091	0.9909	—	12.19
2	0.0000	1.0000	0.0762	0.9238	—	16.26
3	0.0000	1.0000	0.1352	0.8648	—	13.63
4	0.0010	0.9990	0.1973	0.8027	241.66	18.33
5	0.0408	0.9592	0.4340	0.5660	18.012	20.27
6	0.1320	0.8680	0.5573	0.4427	8.2761	15.53
7	0.2245	0.7755	0.5666	0.4334	4.5167	14.08
8	0.3132	0.6868	0.5982	0.4018	3.2640	16.20
9	0.4191	0.5809	0.6130	0.3870	2.1962	16.29
10	0.5267	0.4733	0.6302	0.3698	1.5316	11.18
11	0.6065	0.3935	0.6362	0.3638	1.1347	12.89
12	0.7184	0.2816	0.6430	0.3570	0.7059	13.76
13	0.8110	0.1890	0.6602	0.3398	0.4527	12.80
14	0.9591	0.0409	0.6600	0.3400	0.0828	32.84
15	0.9393	0.0607	0.6572	0.3428	0.1238	32.36
16	0.9867	0.0133	0.6521	0.3479	0.0253	26.07
17	0.9972	0.0028	0.6247	0.3753	0.0046	35.52
18	0.9982	0.0018	0.6557	0.3443	0.0035	32.16
19	0.9983	0.0017	0.6566	0.3434	0.0033	31.03

APPENDIX 2.

Computer Programs.

**Computer programs
(p.299-305) have been
removed for copyright
reasons**